ENERGY EFFICIENT RADIO FREQUENCY SYSTEM DESIGN FOR GREEN MOBILE WIMAX APPLICATIONS

A S HUSSAINI

Ph.D.

2012

ENERGY EFFICIENT RADIO FREQUENCY SYSTEM DESIGN FOR MOBILE WIMAX APPLICATIONS

Modelling, optimisation and measurement of Radio Frequency Power Amplifier covering WiMAX bandwidth based on the combination of Class AB, Class B, and C operations.

ABUBAKAR SADIQ HUSSAINI

HNDip., PGDip., M.Sc., M.Phil.

Submitted for the Degree of

Doctor of Philosophy

School of Engineering, Design and Technology

University of Bradford

2012

Abstract

ENERGY EFFICIENT RADIO FREQUENCY SYSTEM DESIGN FOR MOBILE WIMAX APPLICATIONS

Modelling, optimisation and measurement of Radio Frequency Power Amplifier covering WiMAX bandwidth based on the combination of Class AB, Class B, and C operations.

Keywords

Radio Frequency; Power Amplifier; Doherty Technique; Modulation; Matching Network; Power Added Efficiency (PAE); Non-linearity; Orthogonal Frequency Division Multiplexing (OFDM); WiMAX.

In today´s digital world, information and communication technology accounts for 3% and 2% of the global power consumption and CO_2 emissions respectively. This alarming figure is on an upward trend, as future telecommunications systems and handsets will become even more power hungry since new services with higher bandwidth requirements emerge as part of the so called "future internet" paradigm. In addition, the mobile handset industry is tightly coupled to the consumer need for more sophisticated handsets with greater battery lifetime. If we cannot make any significant step to reducing the energy gap between the power hungry requirements of future handsets, and what battery technology can deliver, then market penetration for 4G handsets can be at risk. Therefore, energy conservation must be a design objective at the forefront of any system design from the network layer, to the physical and the microelectronic counterparts. In fact, the energy distribution of a handset device is dominated by the energy consumption of the RF hardware, and in particular the power amplifier design. Power amplifier design is a traditional topic that addresses the design challenge of how to obtain a trade-off between linearity and efficiency in order to avoid the introduction of signal distortion, whilst making best use of the available power resources for amplification. However, the present work goes beyond this by investigating a new line of amplifiers that address the green initiatives, namely green power amplifiers. This research work explores how to use the Doherty technique to promote efficiency enhancement and thus energy saving. Five different topologies of RF power amplifiers have been designed with custom-made signal splitters. The design core of the Doherty technique is based on the combination of a class B, class AB and a class C power amplifier working in synergy; which includes 90-degree 2-way power splitter at the input, quarter wavelength transformer at the output, and a new output power combiner. The frequency range for the amplifiers was designed to operate in the 3.4 - 3.6 GHz frequency band of Europe mobile WiMAX. The experimental results show that 30dBm output power can be achieved with 67% power added efficiency (PAE) for the user terminal, and 45dBm with 66% power added efficiency (PAE) for base stations which marks a 14% and 11% respective improvement over current state-of-the-art, while meeting the power output requirements for mobile WiMAX applications.

Acknowledgements

First, I wish to express my gratitude to Almighty ALLAH for His guidance and support. I wish to express my sincere appreciation in respect to the support, pointing out useful resources, corrections, and assistances, I enjoyed from my supervisors, ***Prof. Raed Abd-Alhameed***, ***Dr. Jonathan Rodriquez***, and ***Dr. Neil J. McEwan.***

I am deeply grateful and indebted to ***Prof. Raed Abd-Alhameed***, Director Mobile and Satellite Communications Research Centre (MSCRC), University of Bradford, UK and ***Dr. Jonathan Rodriquez***, Leader 4Tell Research Group, Instituto de Telecomunicações – Aveiro, Portugal and ***Dr. Bashir A. L. Gwandu***, Executive Commissioner (Technical Services) Nigerian Communications Commission (NCC), for their outstanding support, strength, and encouragement.

I wish to acknowledged ***C2POWER*** project; this work has been performed in the framework of the cognitive radio and cooperative strategies for power saving in multi-standard wireless devices (***C2POWER***) project (FP7/2007-2013) under the European Community (project n. 248577).

I wish to recognise in a very special way the assistance both moral, support and concern rendered to me by ***Hajia Halita Aliyu*** Chairman Akkaim Telecomms, my father ***Alhaji Musa Hussaini***, and my mother ***Hajia Hafsat Hussaini*** and also to my father ***Alhaji Hussaini Hassan*** and my father ***Alhaji Muhammadu Hussaini***, may their soul rest in peace in Aljanna Fildausi, whose exemplary leadership and good parental upbringing will continue to be the source of inspiration to me and to all of us.

I am profoundly grateful to my Uncles ***Dr. Sabo A. Albasu, Alhaji Jibril Khalid, Alhaji Bappa Tiyal,*** and ***Alhaji Abubakar Dawaki Dukku,*** for their marvellous support, strength, and encouragement.

Many thanks go to people in the research laboratories in Bradford University, many thanks go to the man ***Issa Elfergani,*** whose help and co-operation in connection with this thesis cannot be underestimated, and many thanks go to ***Paulo Gonçalves,*** Instituto de Telecomunicações - Aveiro, Portugal whose co-operation in connection with the practical aspect of this work cannot be underestimated.

Finally my whole families, my Sisters, my Brothers, my Sons, my Daughters, my well-wishers, and my friends love, care and assistance rendered to me throughout my period of study is really appreciated. Together we will win at all the time In Shaa ALLAH. Amin.

Table of Contents

List of Figures

List of Tables

The Acronyms

ACPR	Adjacent Channel Power Ratio
ADS	Advanced Design System
AM-AM	Amplitude-to-Amplitude Distortion
AM-PM	Amplitude-to-Phase Distortion
AMPS	Advanced Mobile Phone Service
BER	Bit Error Rate
BJT	Bipolar Junction Transistor
CDMA	Code Division Multiple Access
CW	Sinusoidal Carriers
DSP	Digital Signal Processing
DVB	Digital Video Broadcasting
EDGE	Enhanced Data Rates for Global Evolution
EER	Envelope Elimination and Restoration
ET	Envelope Tracking
EVM	Error Vector Magnitude
FDM	Frequency Division Multiplexing
FET	Field Effect Transistor
FM	Frequency Modulation
GaAs	Gallium Arsenide
GMSK	Gaussian Minimum shift keying
GSM	Global System for Mobile Communications
HBT	Heterojunction Bipolar Transistor

HPA	High Power Amplifier
IBO	Input Power Back-Off
ICI	Inter Carrier Interference
ICT	Information and Communications Technology
IIP3	Third Order Intercept Point
IM	Intermodulation
IMD3	Third Order Intermodulation Distortion
IMD5	Fifth Order Intermodulation Distortion
IMP	Intermodulation Product
LDMOS	Laterally Diffused Metal Oxide Semiconductor
LINC	Linear Amplification with Nonlinear Components
LNA	Low-Noise-Amplifier
LTE	Long Term Evolution
MEMS	Microelectromechanical Systems
MESFET	Metal-epitaxial Semiconductor FET
MOSFET	Metal-oxide Semiconductor FET
NMT	Nordic Mobile Telephone
OBO	Output Power Back-Off
OFDM	Orthogonal Frequency Division Multiplexing
P1dB	1dB Compression Point
PA	Power Amplifier
PAE	Power Added Efficiency
PAPR	Peak to Average Power Ratio
PAVG	Average Output Power
PDF	Probability Density Function

PHEMT Pseudomorphic High Electron Mobility Transistor

POUT Output Power

QAM Quadrature Amplitude Modulation

QPSK Quadrature Phase Shift Keying

RF Radio Frequency

RMS Root Mean Square

SM Spectral Mask

SNR Signal to Noise Ratio

SSPA Solid-state Power Amplifiers

TDD Telecommunications Device for the Deaf

TDMA Time Domain Multiple Address

TDMA Time Division Multiple Access

TETRA Terrestrial Trunked Radio

TV Television

TWT Travelling-wave-tube

TWTA Travelling Wave Tube Amplifier

UMTS Universal Mobile Telecommunications System

WCDMA Wideband Code Division Multiple Access

WiMAX Worldwide Interoperability For Microwave Access

CHAPTER ONE

1. Introduction

1.1 Background and Motivation

The future accelerated growth of mobile traffic coupled with the need for broadband applications have increased the complexity and design requirements of Radio Frequency (RF) front end, especially the RF power amplifier design. The beyond 3G communication paradigm envisages the end user living in a pervasive and ubiquitous wireless world having the freedom of access to internet services on any device or any network at anytime. The flexibility to be connected to any network implies that future handsets will become fully virtualised and support multiple air-interfaces using reconfigurable hardware and software defined radio.

These two enabling technologies will interact in synergy to allow the mobile device to scan and synchronise to the available radios, and to connect in a seamless fashion to the best available network. This means that the power amplifier needs to effectively support a whole host of modulation schemes, and frequencies [1-3]. The most commonly used modulation technique in legacy and future emerging technologies is OFDM [4-9]. This is a multicarrier modulation technique that can provide high data rate and significantly overcome multipath interference that leads to signal degradation. However, this modulation technique, unlike in legacy 2G modulation techniques, has a high crest

factor enforcing linear amplification over a large dynamic range [4-9]. If this were to be done with existing power amplifier techniques, this would result in poor efficiency and output power [1-4].

A rising concern in today´s green society is the energy consumption and the carbon footprint emitted by ICT devices. In fact, the whole ICT sector has been estimated to account for only 2 percent of global CO2 emissions, this percentage is comparable to the emissions due to global aviation [10-13]. Therefore energy saving should be at the forefront any communication system design. Moreover, there is a continuously increasing gap between the energy requirements of power hungry radio devices, and what can actually be delivered by new battery technology. Without new approaches to energy saving, there is significant concern that future mobile users will be searching for power outlets rather than for network access which stands in a complete irony to the beyond 3G philosophy.

In typical mobile terminals for cellular systems up to half of the power consumptions come from communications-related functions, such as baseband processing, RF, and connectivity functions. Therefore any reduction in the power consumption of the power amplifier device will have a substantial impact on carbon footprint and prolong battery lifetime [14-59]. As you can see in Figure 1.1, Figure 1.2 and Figure 1.3, that the power consumption growth in ICT and the power consumption of power amplifier in particular is unsustainable.

We have highlighted energy consumption and linearity as two important design requirements that should be addressed if we are to have effective RF power amplification in tomorrow´s handsets.

The state-of-the-art on energy efficient RF power amplifier design techniques include the Chireix out-phasing [60], Doherty configuration [61], Kahn EER [62], and ET [63], and that involve complex circuit design and require the use of external circuit control and signal processing making their practical implementation challenging. However, the Doherty amplifier, which has self-managing characteristics is considered to be the most attractive design and is considered here as the baseline for the proposed three stage design.

The proposed Doherty configuration will be designed for the mobile WiMAX frequency band, where we focus on the 3.4 – 3.6 GHz range which is the band being utilised in Europe.

After improving the RF power amplifier transceiver's performance in term of battery lifetime/talk time of battery-powered devices and energy consumptions of base station, with the aim to prolong their operational time and avoid active cooling in the base station, which is the key objective of the present work. However, we have suggested and highlighted a recommendation for the future work.

The future work is designing a frequency reconfigurable RF front ends (multi-standard) by using RF MEMS technology to be able to frequency reconfigure the efficient RF power amplifier.

The first part of the design should be the design RF MEMS matching network for the reconfiguration of RF power amplifier to cover more than six frequency bands (a tunable RF power amplifier). And the second part of the design should address the RF MEMS Filters.

The RF MEMS is a key enabling technology for reconfigurable radio front ends that promises to enable new paradigms in RF systems since it will enable superior functionality, integration and performance, and will also play a role in size reduction (miniaturisation). It also provides very good linearity, low power consumption and potential low cost manufacturing into a variety of substrates. The multiband mobile transceiver will be capable of operating in 2G, 3G and 4G radios and will rely on high-Q technology that must interface with the PA at circuit level with the reduction in area.

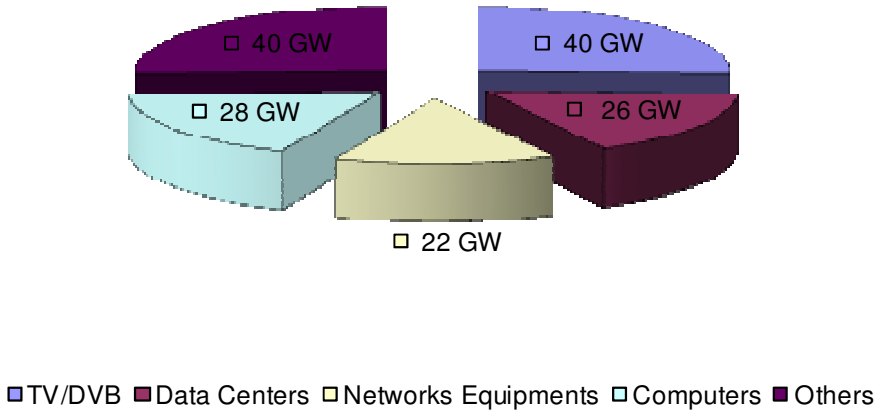

Figure 1.1: ICT Power Consumption in GigaWatts [10-11].

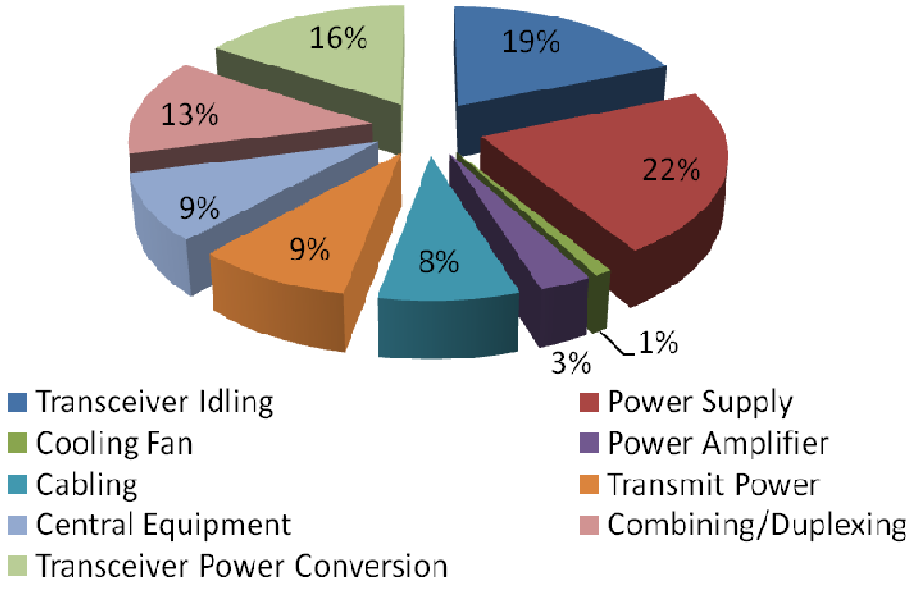

Figure 1.2: Base station power consumption breakdown [12].

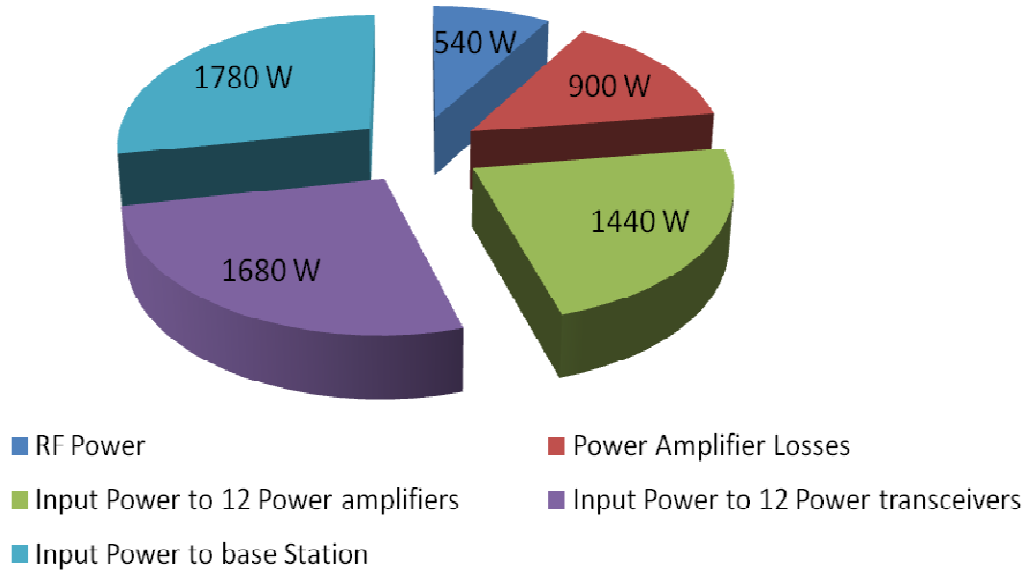

Figure 1.3: Power amplifier energy consumption breakdown within the network [12].

1.2 Wireless Applications

The specifications of unlicensed and licensed frequency bands of interest of wireless standards within and outside Europe are shown in a Table 1.1.

Table 1.1: Frequency bands of interest.

Standard	**Up Link**	**Down Link**
TETRA2 (TEDS) & LTE	700-800MHz (TBC)	
GSM -900, UMTS BANDE VIII	880-915MHz	925-960MHz
DCS - 1800	1710-1785MHz	1805-1880MHz
UMTS TDD	1900-1920MHz	
UMTS	1920-1980MHz	2110-2170MHz
UMTS TDD	2010-2025MHz	
Wi-Fi 802.11 b/g/n	2400-2483MHz	
LTE (38)	2570-2620MHz	
LTE (7)	2500-2570MHz	2620-2690MHz
Mobile WiMAX	3400-3600MHz	
Wi-Fi 802.11 a/n	5180-5700MHz	

The technical specifications in the amplifier design are tied to mobile WiMAX requirements. This band has a frequency range from 3.4GHz to 3.6GHz. The uplink

band (3400-3500 MHz) and downlink band (3500-3600 MHz) approximately. The mobile Wimax base stations transmit at power level of approximately 43dBm (20W) and LTE user terminals typically transmit at 30 dBm (1W). These values depend on modulation (QPSK, 16QAM, 64QAM), because in each case the back-off must be different according to modulation level.

1.3 Target Objectives

Research related to the RF System Design, whereby focus will be on practical issues of designing a linear RF Doherty power amplifier with high efficiency, for the implementation in Mobile WiMAX RF transmitter frontend. This technique (Advance design method of Doherty amplifier) should allow the design of RF power amplifier, which will meet the output power and linearity requirements of European mobile WiMAX systems that has high efficiency, and gain.

We have highlighted energy consumption and linearity as two important design requirements that should be addressed if we are to have effective RF power amplification in tomorrow´s handsets and base stations.

This research work explores the emerging area of optimising efficiency as well as linearity in RF power amplifier design, as part of the green RF front end. In fact, the energy bills of a handset device and base station are dominated by the energy consumption of the RF hardware, and in particular the power amplifier design.

Power amplifier design is a traditional topic that namely addresses the design challenge of how to obtain a trade-off between linearity and efficiency in order to avoid the introduction of signal distortion, whilst making best use of the available power resources for amplification. However, the present work goes beyond this by investigating a new line of amplifiers that address the green initiatives, namely green power amplifiers.

1.4 Outline of this Report

Chapter 1 gives an introduction and aims of this novel research and discuss the problems that are going to be tackled, which is the prime challenge for future wireless systems and the need to limit the energy consumptions of battery-powered devices and base station, with the aim to prolong their operational time and avoid active cooling.

Method of signal amplification and feature of power amplifiers will be reviewed in chapter 2, amplifiers are classified according to their circuit configurations and methods of operation into different classes, such of these are A, B, AB, C, and F. These classes are based on conduction angle (2θc). And also its presented a widely used figures of merit to evaluate the linearity or the impact of nonlinearity.

Chapter 3 describes the characterisation and design of energy efficient user terminal transceiver power amplifier. This design comprised several design steps for which the optimisation is applied to each in order to obtain global high performances of the entire system. Initially, the design of carrier and peak amplifiers, input signal 3dB 90-degree

hybrid coupler designs, Output 90 degree offset line and impedance transformer designs were performed.

Chapter 4 covers the proposed base stations efficient RF power amplifiers design and its implementations. The aim of this chapter was the design process of the base station load modulation RF power amplifier and balance RF power amplifier. The conventional balance amplifier was first proposed to improve power efficiency of 3G base station, is designed to work over a given dynamic range where the amplifier should work linearly. Conventional balanced amplifier was a commercially successful to 2G/3G base station front end power amplifier. However, there are some problems that limit the balanced amplifier for use as power amplifier for 4G communications.

Chapter 5 describes the proposed Multi-stage Load Modulation circuit architecture; in which section 5.1 explains the current drive analysis for the three stage load modulation circuit; circuit prototype and results are given by section 5.2.

And finally a summarised conclusions and future work are stated in chapter 6.

References

[1] S.C. Cripps Advanced Techniques in RF Power Amplifier Design, Norwood, MA: Artech House, 2002.

[2] Raab, F.H.; Asbeck, P.; Cripps, S.; Kenington, P.B.; Popovic, Z.B.; Pothecary, N.; Sevic, J.F.; Sokal, N.O.;,"Power amplifiers and transmitters for RF and microwave", IEEE Transactions on Microwave Theory and Techniques, Vol. 50, No 3, PP. 814 – 826, March, 2002

[3] J. Vuolevi and T. Rahkonen, "Distortion in RF Power Amplifiers," Artech House Inc., 2003

[4] R. Baxley and G. Zhou, "Power savings analysis of peak-to-average power ratio in OFDM," Consumer Electronics, IEEE Transactions on, vol. 50, no. 3, pp. 792 – 798, 2004

[5] S. Muller and J. Huber, "OFDM with reduced peak-to-average power ratio by optimum combination of partial transmit sequences," Electronics Letters, vol. 33, no.5, pp. 368 –369, Feb. 1997.

[6] R. van Nee and A. de Wild, "Reducing the peak-to-average power ratio of OFDM," in Vehicular Technology Conference, 1998. VTC 98. 48th IEEE, vol. 3, May 1998, pp. 2072 –2076 vol.3

[7] J. Tellado and J. M. Cioffi, "Peak power reduction for multicarrier transmission," 1999

[8] N. Chen, G. T. Zhou, and H. Qian, "Power efficiency improvements through peak-to- average power ratio reduction and power amplifier linearization," EURASIP J. Appl. Signal Process., vol. 2007, pp. 9-9, 2007.

[9] H. Zhang, "Cognitive Radio for Green Communications and Green Spectrum," in Chinacom, Hangzhou, China, 2008.

[10] IBCN “Energy Efficient Communication” www.ibcn.intec.ugent.be

[11] www.itu.int/dms_pub/itu-t/oth/33/.../T33040000020004PDFE.pdf

[12] www.ist-emobility.org/WorkingGroups/.../2008.../WVereecken.pdf

[13] "Green Base Station - The Benefits of Going Green," Mobile Europe, 2008. Huawei, "Improving energy efficiency, Lower CO2 emmision and TCO," 2009

[14] J. Rowley and D. Haig-Thomas, "Unwiring the Planet - Wireless Communications and Climate Change," in ITU International Symposiums ICT's and Climate Change, London, UK, 2008.

[15] C. Lamour, "Energy Consumption of Mobile Networks," in The Base station e-Newsletter, 2008.

[16] Ericsson, "Green Power to Bring Mobile Telephony to Billions of People," 2008.

[17] "Core 5 - Green Radio: Programme Objectives and Overview," Presentation from Mobile VCE.

[18] www.huawei.com/en/static/hw-076768.pdf

[19] www.trai.gov.in/WriteReadData/.../Green_Telecom-12.04.2011.pdf

[20] www.mobileeurope.co.uk/news/features/7603-7641

[21] www.broadcast.harris.com/.../ComparisonRFPowerAmplifiers_25-17...

[22] wwwen.zte.com.cn/en/about/.../P020110808574801953436.pdf

[23] www.wireie.com/pdfs/energy_emissions_cell_sites_ver.3.2.pdf

[24] H. Sistek, "Green-tech base stations cut diesel usage by 80 percent," 2008.

[25] T. Haynes, "Designing energy-smart 3G base stations," RF Design, 2007. R. Min and A. Chandrakasan, "A framework for energy-scalable communication in high-density wireless networks," in ISLPED International Symposium on Low Power Electronics and Design, Montery, CA, 2002, pp. 36- 41.

[26] H. Karl, “An overview of energy-efficiency techniques for mobile communication

systems," Telecommunication Networks Group Technical University Berlin, Germany Tech Rep TKN03017, 2003.

[27] L. M. Correia, D. Zeller, O. Blume, D. Ferling, Y. Jading, I. Gdor, G. Auer, and L. V. Der Perre, "Challenges and enabling technologies for energy aware mobile radio networks," Communications Magazine, IEEE, vol. 48, no. 11, pp. 66 –72, 2010.

[28] http://www.tkn.tu-berlin.de/publications/papers/TechReport 03 017.pdf

[29] H. Sistek, "Green-tech base stations cut diesel usage by 80 percent," in CNET News Green Tech, 2008.

[30] Ericsson, "Sustainable Energy Use in Mobile Communications-Whitepaper," 2007.

[31] S. M. Betz and H. V. Poor, "Energy Efficient Communications in CDMA Networks: A Game Theoretic Analysis Considering Operating Costs," Signal Processing, IEEE Transactions on, vol. 56, pp. 5181-5190, 2008.

[32] R. Grigonis, "ATIS Announces Three New Energy Efficiency Standards for Telecom," Green News, 2009.

[33] M. Ajmone Marsan, L. Chiaraviglio, D. Ciullo, M. Meo, "Optimal Energy Savings in Cellular Access Networks," International Workshop on Green Communications (Green Comm), Dresden, 2009.

[34] E. Kudoh, F. Adachi, "Power and frequency efficient virtual cellular networks," Proc. IEEE VTC, pp. 2485-2489, 2003.

[35] How green is your network? The Economist, Dec2008. Saving RF power in cellular base stations, E&T magazine, IET, vol. 4, issue. 5, pp: 74-75, Apr, 2009.

[36] K. Li, "Green Thinking Beyond TCO Consideration," in-stat, whitepaper, May, 2008.

[37] S. Lee, L. Kim, H. Kim, "MIPv6 –based power saving scheme in integrated

WLAN and cellular networks," IEICE Trans. Commun., vol. E90-B, no. 10, Oct. 2007.

[38] F. Richter, A. J. Fehske, G. P. Fettweis, "Energy efficiency aspects of base station deployments strategies for cellular networks," in Proc. IEEE Vehicular Technology Conference, 2009.

[39] U.S Environmental Protection Agency ENERGY STAR Program, Report to Congress on Server and Data Center Energy Efficiency, Public Law 109-431, page 94, August 2007.

[40] G. Koutitas, "Low carbon network planning," in Proc.European Wireless Conf., Aprl. 2010.

[41] K. Schwieger, A. Kumar, G. Fettweis, "On the impact of physical layer to energy consumption in sensor networks," Proc. IEEE, 2005.

[42] Gartner, "Forecast: Mobile Services, Worldwide, 2004– 2013, 4Q09 Update," by Jessica Ekholm, et al., 2 Dec. 2009, Chart created by NEC based on Gartner's data.

[43] Study on Energy Efficient Radio Access Network (EERAN) Technologies, 2009 Project Report of Technical University of Dresden, Vodafone Chair Mobile Communication Systems.

[44] GSMA, "Mobile's Green Manifesto," November 2009. NEC, White Paper: Self Organizing Network, http ://www.nec.com/lte/son/index.html

[45] M. Gupta and S. Singh, "Greening of the Internet," Proc. ACM SIGCOMM, August 2003.

[46] H. Karl (Ed.), "An Overview of Energy-Efficiency Techniques for Mobile Communication Systems," Technical Report TKN-03-017, Telecommunication Networks Group, Technical University Berlin, 2003.

[47] 3GPP TR 32.826, Telecommunication Management; Study on Energy Savings Management (ESM), (Release 9), December 2009.

[48] "Verizon NEBS Compliance: Energy Efficiency Requirements for Telecommunications Equipment " Verizon, VZ.TPR.9205, 2008.

[49] Commission of the European Communities, "Addressing the challenges for energy efficiency through ICTs," Report, Brussels 2008.

[50] J. Selwyn, S. Craven, "A Review of Sustainable development policy and practice in the English regions and developed administrations," report, Sustain IT Program, UK CEED, Aug. 2008.

[51] H. Scheck, "Power consumption and energy efficiency of fixed and mobile telecom networks," ITU-T, Kyoto, 2008.

[52] Document on, "Green Power for Mobile: Top ten findings," GSM Association 2009 (www.gsmworld.com/greenpower).

[53] A. Gladisch, C. Lange, R. Leppla, "Power efficiency of optical versus electronic access networks," Proc. European Conference and Exhibition on optical communications, Brussels, 2008.

[54] Ericsson, "Sustainable energy use in mobile communications," whitepaper, August 2007.

[55] Report to Congress, "Server and data center energy efficiency," U.S Environmental Protection Agency, Energy Star Program, Aug. 2007.

[56] L. A. Barroso, U. Holzle, The data center as a computer: An introduction to the design of warehouse-scale machines, Morgan and Claypool, ISBN: 9781599295573, 2009.

[57] N. Rasmussen, "Allocating data center energy costs and carbon to IT users," APC White Paper, 2009.

[58] M. Deruyck, et. al., “Power consumption in wireless access networks,” in Proc. European Wireless Conf., Aprl. 2010.

[59] U. Insider, “Mobile networks go green,” Report Huawei, issue 45, Dec 2008. E. Hwang, K. Kim, J. Son, B. Choi, “The power saving mechanism with periodic traffic indications in the IEEE 802.16e/m,” IEEE Trans. Veh. Technol., vol. 59, no. 1, 2010.

[60] H. Chireix, “High Power Outphasing Modulation”, Proceedings of the IRE, Vol. 23, No 11, PP. 1370– 1392, November, 1935.

[61] W. H. Doherty, “A New High Efficiency Power Amplifier for Modulated Wave”, Proc. IRE, Vol. 24, No. 9, PP. 1163 – 1182, September, 1936.

[62] Kahn, L.R.;, “Comparison of Linear Single-Sideband Transmitters with Envelope Elimination and Restoration Single Sideband Transmitters”, Proceedings of the IRE, Vol. 44, No 12, PP. 1706 - 1712, December, 1956.

[63] Kimball, D.F.; Jeong, J.; Hsia, C.; Draxler, P.; Lanfranco, S.; Nagy, W.; Linthicum, K.; Larson, L.E.; Asbeck, P.M.; “High- Efficiency Envelope-Tracking W-CDMA Base-Station Amplifier Using GaN HFETs”, IEEE Transactions on Microwave Theory and Techniques, Vol. 54, No. 11 PP. 3848 – 3856, November, 2006.

CHAPTER TWO

2. Method of Amplification

2.1 Amplifiers

Amplifiers are classified according to their circuit configurations and methods of operation into different classes, which include A, B, AB, C, and F [1-3]. These classes are based on the conduction angle ($2\theta_c$). The conduction angle is the portion of RF cycle the device spends in its active region (behaves as a current-controlled source). Moreover, these classes range from entirely linear with low efficiency to entirely non-linear with high efficiency. The choice of the quiescent point for gate and drain voltage, as shown in Figure 2.1, will determined by the operation class and certainly, the linearity and efficiency.

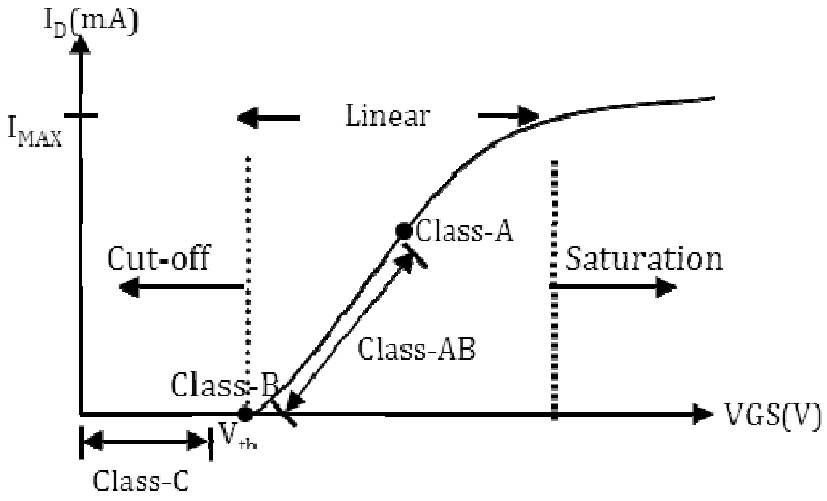

Figure 2.1: Quiescent point of class A, B, AB, and C amplifiers.

2.1.1 Class A

This amplifier has the highest linearity relative the other classes particularly when in force in backed off mode from full power. It operates in a linear region of its operating mode and is corresponding to a current source (current-controlled-current). The configurations of class-A, B, and C amplifiers can be either a push–pull or a single ended tuned version [1-3]. However, to attain high linearity, the amplifier's gate DC voltage and the amplifier's drain DC voltage should be selected properly so that the amplifier operates in the linear region. Class A amplifier operate over the whole 360^0 conduction angle ($2\theta_c = 360^0$) of the input signal, as shown in Figure 2.2, and the efficiency is less than 50% [1-3].

According to Mihai Albulet ref. [2], a simplified analysis of the single-ended Class A amplifier is based on the following assumptions: The RF choke is ideal. It has no series resistance, and its reactance at the operating frequency is infinite. Consequently, the RF choke allows only a constant (DC) input current, I_{dc}, whose value is determined by the bias circuit. There are also DC-blocking capacitors (short circuit at the operating frequency). For this simplified the transfer characteristic of the active device is assumed to be perfectly linear, i.e., a sinusoidal drive signal determines a sinusoidal collector current [2].

CLASS -A

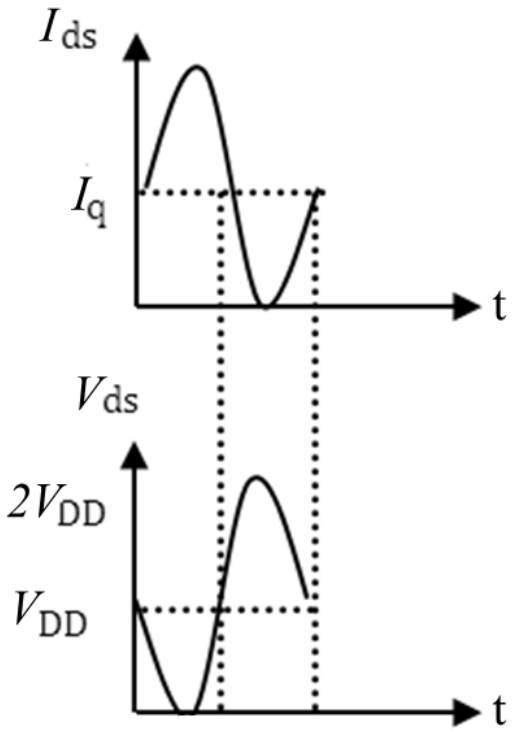

Figure 2.2: Voltage and current waveforms of class A operation.

2.1.2 Class B

The class B amplifier operate over 180^0 ($2\theta_c = 180^0$) as shown in

Figure 2.3, which means amplify only half of the input signal, therefore suffers from large amount of distortion (crossover distortion). The theoretical efficiency is around 79% [1-3].

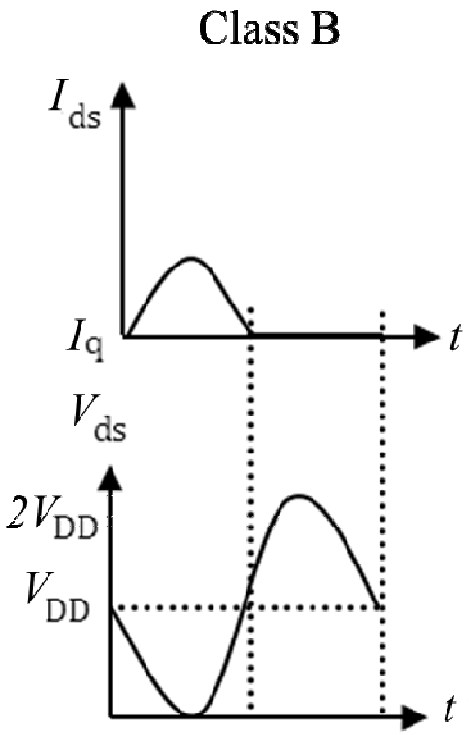

Figure 2.3: Voltage and current waveforms of class B operation.

2.1.3 Class AB

This amplifier is a compromise between class A and class B in terms of efficiency and linearity. The class AB amplifier is biased as close to pinch-off as possible [1-3]. In this situation, the class AB amplifier will operate more than 180^0 ($2\theta_c > 180^0$), but less than 360^0 of the input signal ($180^0 < 2\theta_c < 360^0$) as shown in Figure 2.4.

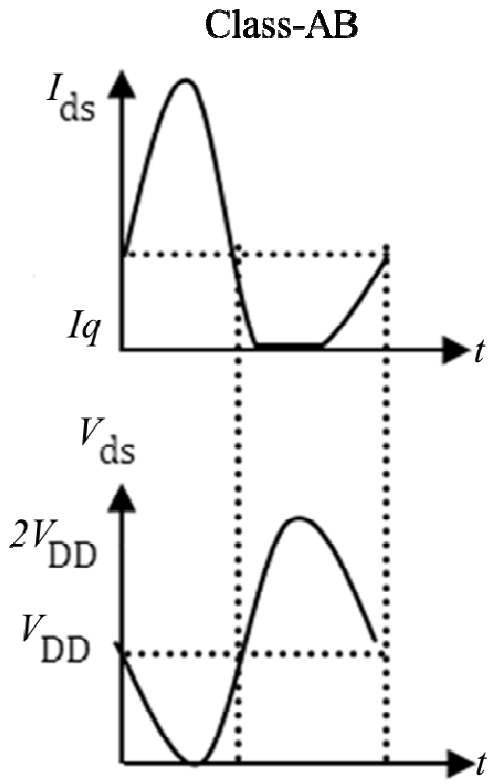

Figure 2.4: Voltage and current waveforms of class AB operation.

2.1.4 Class C

This is a completely non-linear and high efficient amplifier and is applicable in circumstances where efficiency is an essential concern. The class C amplifier operate less than 180^0 ($2\theta_c < 180^0$) of the input signal, as shown in Figure 2.5 [1-3].

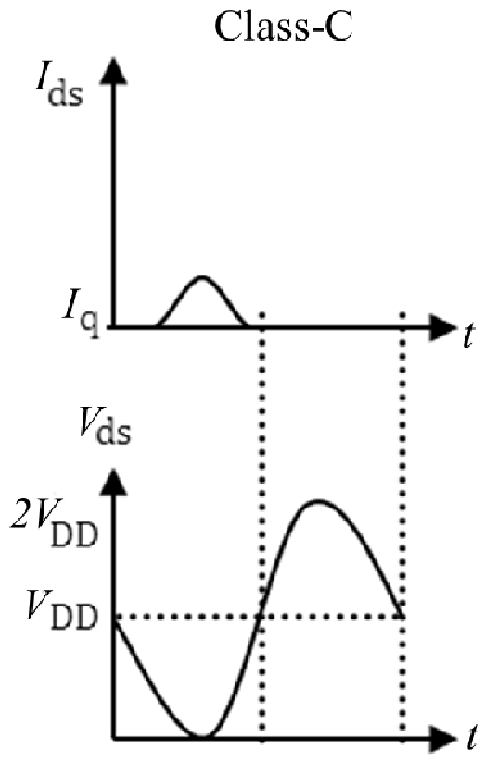

Figure 2.5: Voltage and current waveforms of class C operation.

2.1.5 Class F

Class F amplifier is one of the highest efficiency amplifiers with zero linearity performance, is based on switched mode transistor circuits [1], [4-7]. The switched mode amplifiers can achieve better efficiency than the conduction angle based amplifiers. It uses harmonic resonators to control the harmonic content of its both drain current and voltage waveforms, in order to achieve high efficiency, which results from a low dc voltage current product. In other words, the both drain voltage and current are shaped to reduce their overlap region [1], [4-7].

To design class F amplifier, one have to start by designing a proper matching network at a given fundamental frequency follow by the designing of harmonic tuning network at a definite order of harmonics. Normally, short circuit are present at even harmonics, while open circuit at odd harmonic [1], [4-7].

Figure 2.6 shows the example of class F power amplifier.

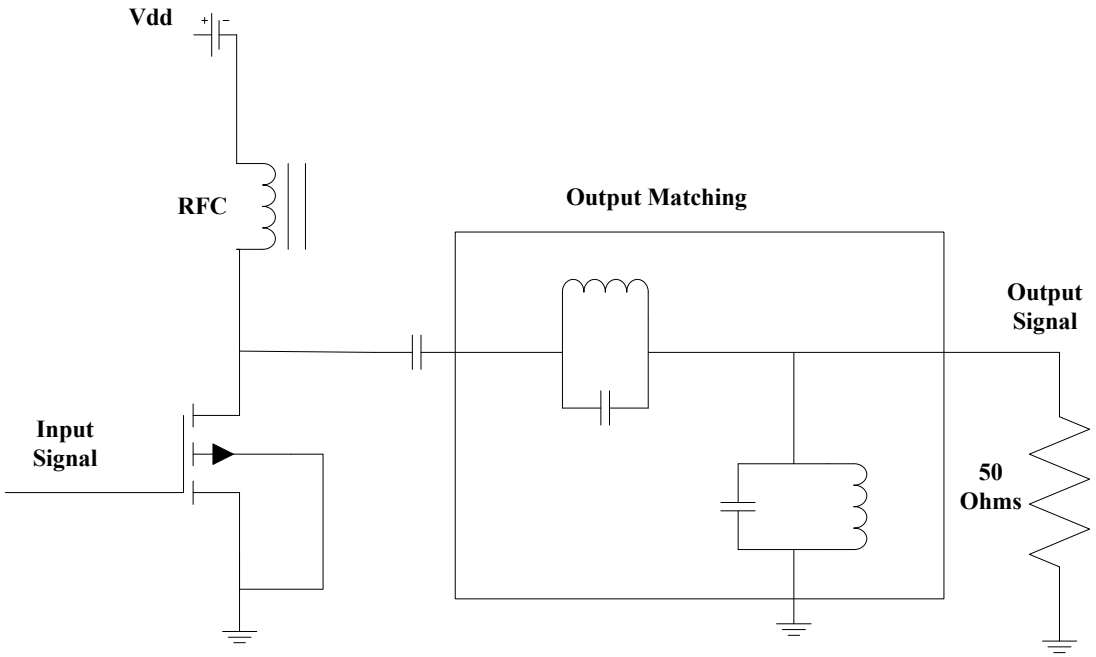

Figure 2.6: Example of class F power amplifier.

2.2 Features of RF power amplifiers

2.2.1 Linearity

Non-linearity is an impending cause of interference and system performance deprivation. The RF power amplifier can distort the transmitted signal due to their nonlinearities [1-3]. Therefore, signal should be amplified linearly in order to transmit faithfully. High data transfer leads to the development of multilevel modulations, which causes non-constant envelope and wide envelope frequency, and are considerably sensitive to nonlinear distortion, usually caused by RF power amplifier. Therefore, linear or linearisation of RF power amplifier is needed for high data transfer [1-3], [8-20].

The widely used figures of merit to evaluate the linearity or the impact of nonlinearity of RF power amplifier to transmitted signal are;

a) 1dB compression point (1dB)

b) 3rd order intermodulation distortion (IMD3)

c) Adjacent channel power ratio (ACPR)

d) Error vector magnitude (EVM)

2.2.1.1 1dB compression point

This is output power at which the gain compresses by 1dB from its linear region, or can be defined as the input power that causes a 1dB drop in the linear gain due to device saturation [1], [3]. The 1dB compression point is a power amplifier performance metric

which is not defined in standards. Figure 2.7 shows the relationship between input power versus output power and 1dB compression point. The Pin is related to corresponding Pout at 1dB compression point as:

$$Pin\ (dBm) = Pout\ (dBm) + G\ (dB) \quad (2.1)$$

Where G is the gain

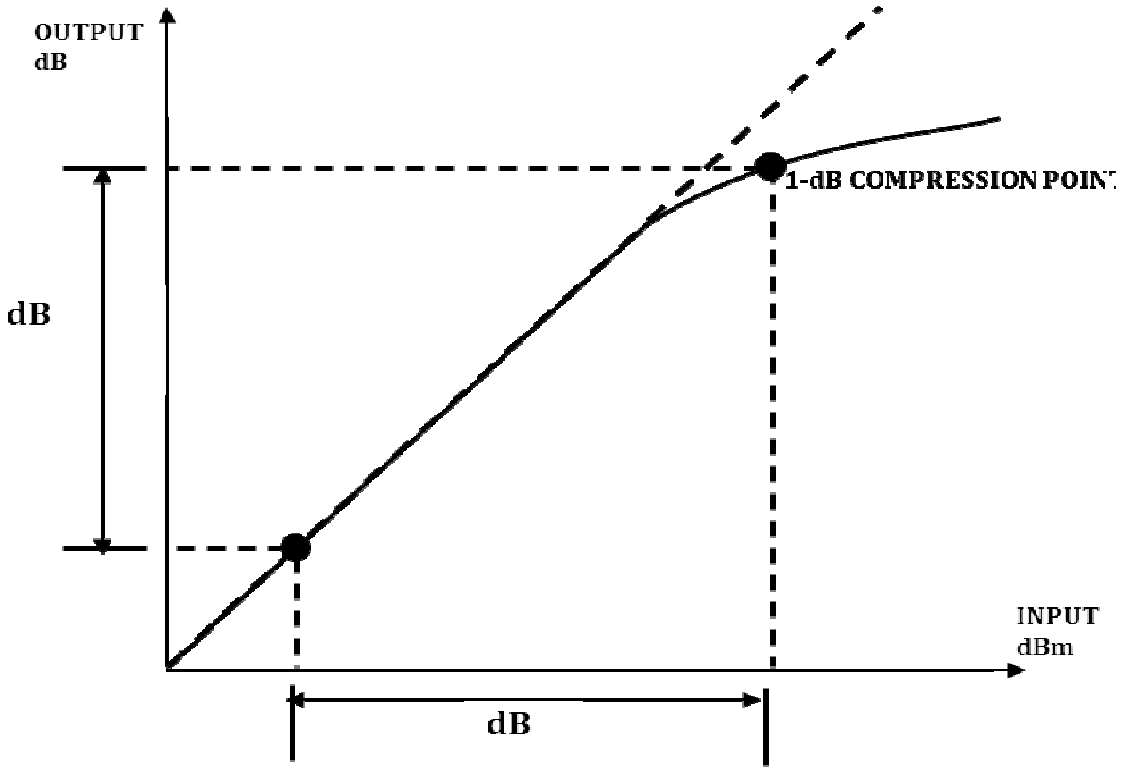

Figure 2.7: Input power Vs Output power showing 1dB compression point.

2.2.1.2 3rd order intermodulation distortion (IMD3)

Intermodulation component occurs when the inputs to the non-linear device or system is composed with two or more frequencies, the third, and the fifth intermodulation

products are caused by the sum and difference products of each fundamental and their harmonic input signals [1], [3]. The IMD3 has serious effect on the signal because is very close to the fundamental signal which is very hard to filtered it out as shown in Figure 2.8. The IMD3 is a power amplifier performance metric which is defined in standards.

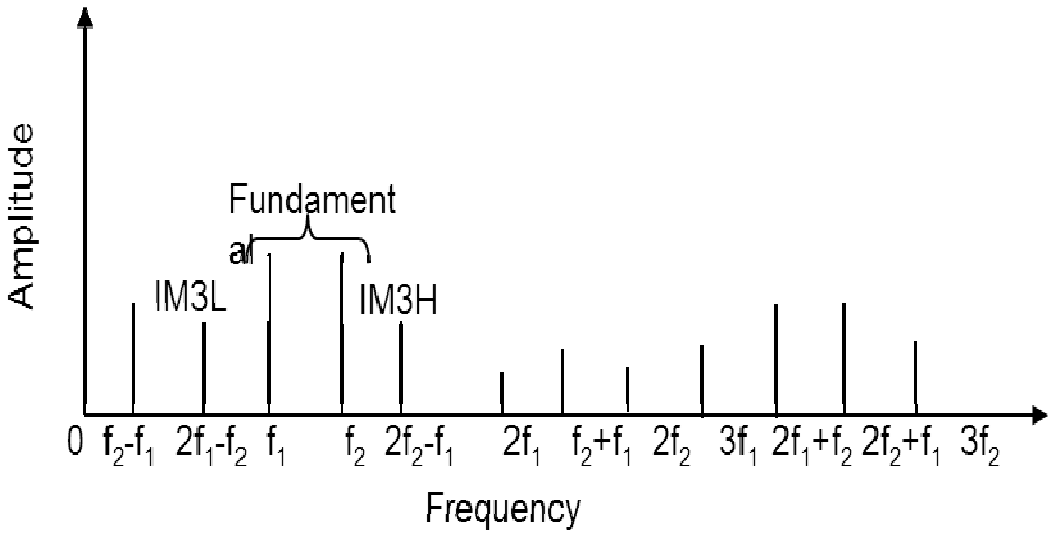

Figure 2.8: Third order intermodulation distortion (Showing lower and higher intermodulation).

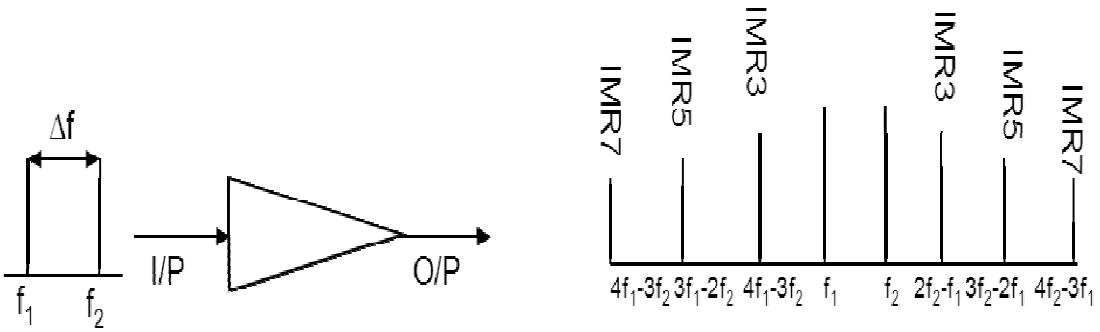

Figure 2.9: Intermodulation distortion for a nonlinear power amplifier.

2.2.1.3 Adjacent channel power ratio (ACPR)

This is the parameter that describes the degree of the spectral re-growth into adjacent channel and is defined as the ratio of the total power of the adjacent channels to the signal power in the main channel [1-3]. Moreover this is one of the main parameters that frequency regulatory bodies use to characterise the interferences with other adjacent channel. The ACPR is a power amplifier performance metric which is defined in standards Figure 2.10 shows the adjacent channel power ratio based on the adjacent bandwidth and main bandwidth.

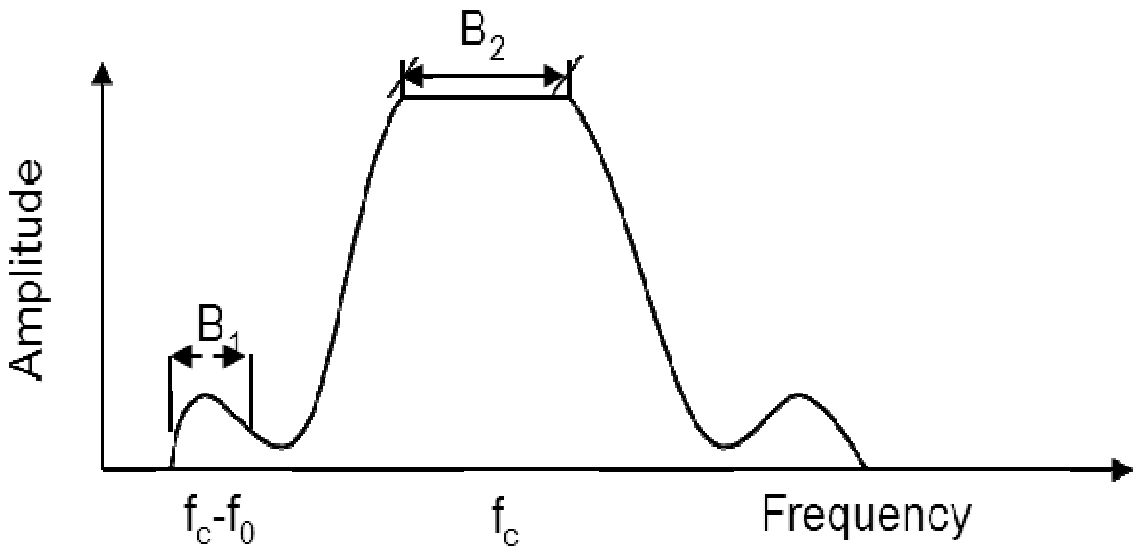

Figure 2.10: Adjacent Channel Power Ratio (B1 = Adjacent bandwidth, B2 = Main bandwidth).

2.2.1.4 Error vector magnitude (EVM)

This describes the blemish of the constellation after receptions. The error vector (E(s)) is the difference between the actual transmitted (A(s)) and ideal (H(s)) constellation point [3], [8], [12]. EVM is specified after reception and demodulation by an ideal

receiver and ensures a correct transmission within the channel. The EVM is a power amplifier performance metric which is defined in standards.

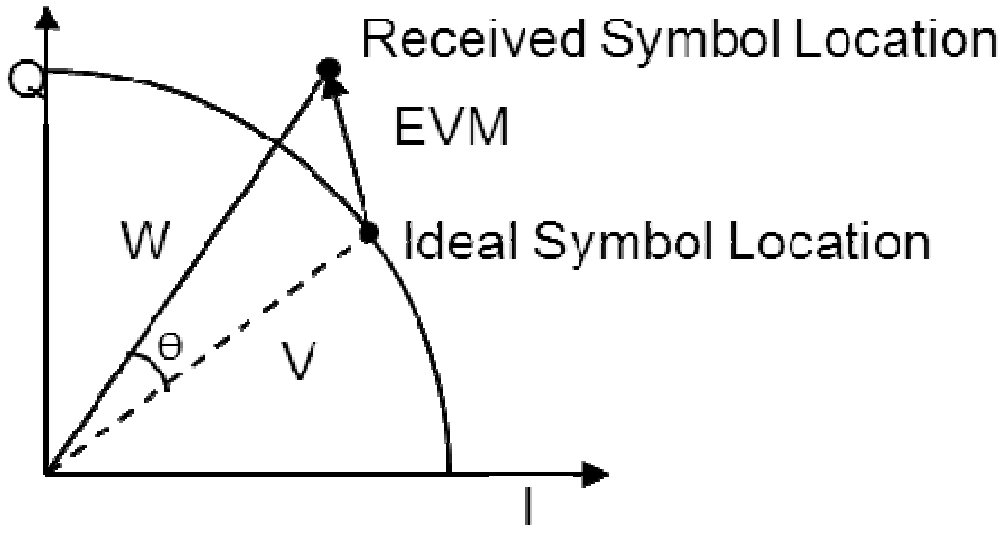

Figure 2.11: Error vector magnitude.

2.2.2 Power Efficiency

Power efficiency of the user terminal power amplifier is an important attribute that leads to increase talk time and battery lifetime, whilst efficiency at the base station leads to reduced power consumption and avoid the need for active cooling. Therefore this is a vital parameter for power amplifier, a value which quantifies the portion of the supplied DC power converted to RF power by the amplifier, and takes on added importance when the available input power is limited, such as in battery-powered mobile terminals [3].

The power efficiency is a power amplifier performance metric which is not defined in standards, and there are two most common power efficiency metrics that are used in RF power amplifier design: Drain efficiency and PAE.

Drain efficiency is defined as the ratio of RF output power delivered to the load (P_{out}), to the power supplied by the DC (P_{DC}) [1-3].

$$\eta = \frac{P_{out}}{P_{DC}} \times 100\% \tag{2.2}$$

The drain efficiency does not includes the effect of the input power (drive signal), therefore cannot deeply show the overall power efficiency of the RF power amplifiers.

PAE includes the effect of the input power (drive signal) and shows how efficiently can convert DC supply to RF power. PAE can be defined as ratio of RF output power (P_{out}) minus RF input power (P_{in}), to the DC power (P_{DC}) [1-3].

$$\eta_{PAE} = \frac{P_{out} - P_{in}}{P_{DC}} \times 100\% \tag{2.3}$$

To sum up, power efficiency of RF power amplifiers can significantly influence the global power efficiency of the transceiver. Unlike linearity (ACPR) which is defined in standards, power efficiency is a performance metric which is not defined in standards. RF power amplifier nonlinearity and efficiency are in direct conflict- improves one and you degrade the other.

2.3 Trade-off between Efficiency and Linearity

The goal of designing efficient power amplifiers with good linearity is therefore to obtain a system that maintains high efficiency over a wide range of input powers. But achieving high efficiency and high linearity simultaneously in power amplifiers design is the most challenging task [8-20]. However, to obtain linearity and efficiency simultaneously, some linearisation or efficiency enhancement techniques have to be employed. The efficiency enhancement technique in the linear region of operations of power amplifier will be implemented which can be used to achieve higher efficiency at a low-level output power.

Generally, the maximum efficiency is achieved at maximum output power of the amplifier, usually close to saturation point (1dB compression point). And forcing it into saturation results in severe distortion, efficiency degrades dramatically as output power decreases. As you can see in Figure 2.12 the maximum output power (V_{load}) of this amplifier is 38.709dBm at input power of 26dBm, any increase in input power will force the amplifier into saturation. The maximum efficiency is 42.503% and is obtained exactly at the point of maximum output power (V_{load}), as the output power decreases, efficiency drops dramatically as shown in Figure 2.13.

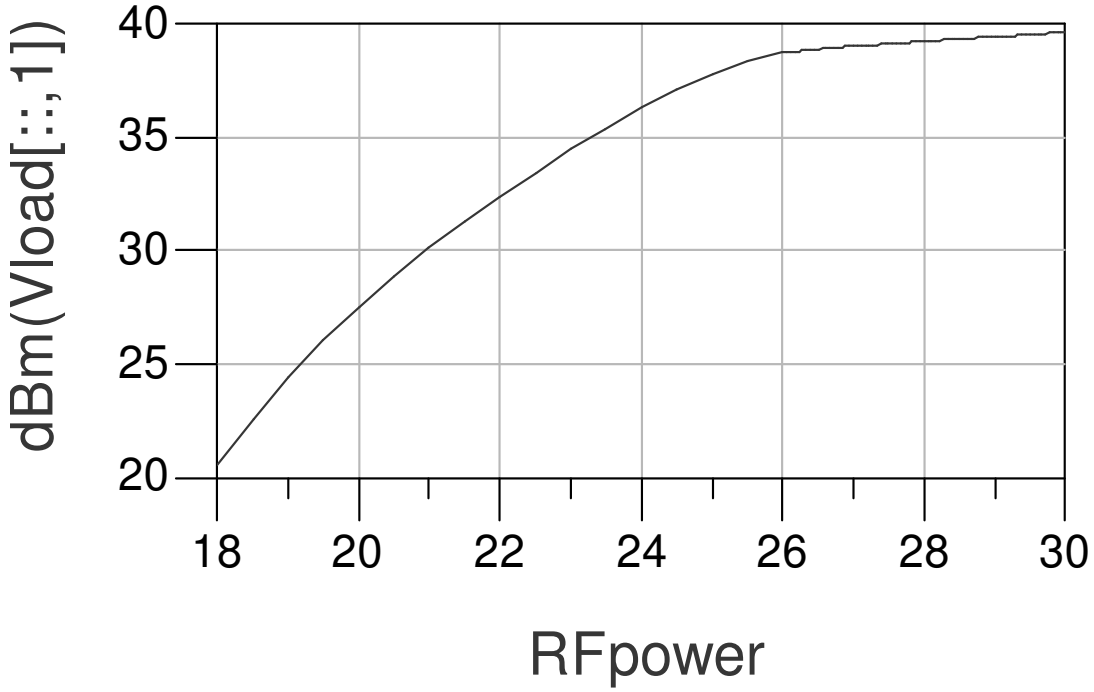

Figure 2.12: Input power (dBm) versus output power (dBm).

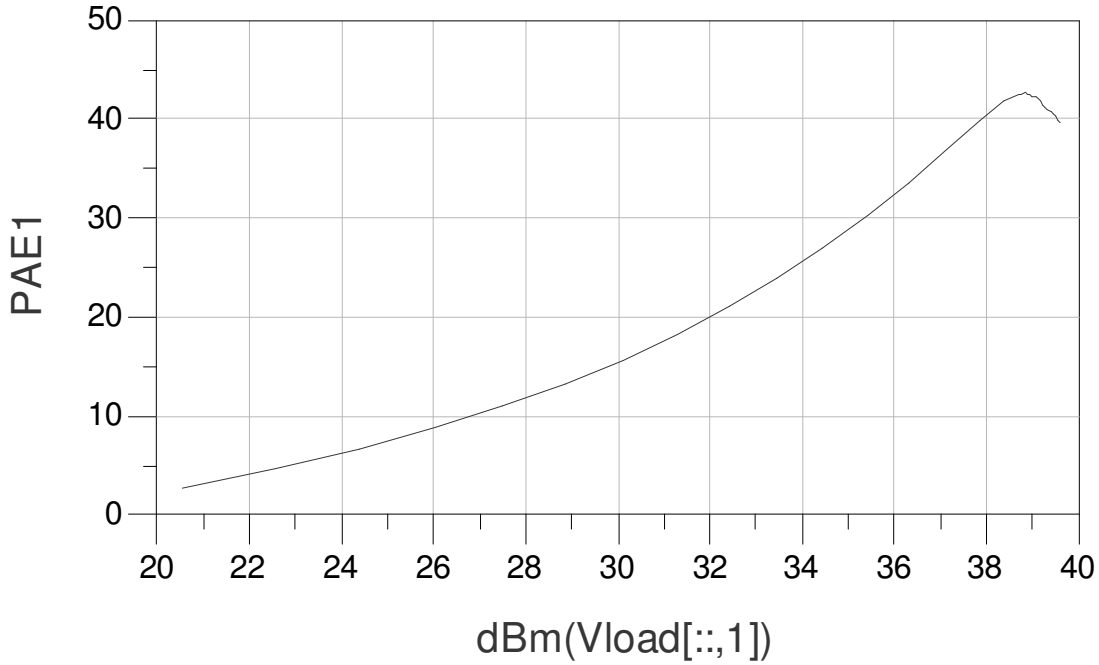

Figure 2.13: Output power (dBm) versus efficiency (%).

2.4 RF power amplifier's linearity and output power requirements

The envelope variation of an OFDM signal clearly requires a linear RFPA. It should be noted that the IEEE 802.16e/Mobile WiMAX standard doesn't specify the minimal required IMD of the user terminal PA, but it uses system level requirement to describe the maximal allowable distortion. These system level requirements are: SM and EVM [3], [8], [12]. The spectral mask is specified at the PA output, and ensures that the user terminal transmitter does not corrupt or block the spectrum from adjacent channels. The error vector (E(s)) is the difference between the actual transmitted (A(s)) and ideal (H(s)) constellation point. EVM is specified after reception and demodulation by an ideal receiver and ensures a correct transmission within the channel. The EVM of a symbol S is defined as,

$$\text{EVM} = \sqrt{\frac{|E(s)|^2}{\frac{1}{N}\sum_s |H(s)|^2}} \tag{2.4}$$

To obtain EVM as a percentage, the RMS value is used; this is a useful systems level figure of merit for the accuracy of the OFDM signal,

$$\text{EVM}\ (\%) = \sqrt{\frac{P_{error}}{P_{ref}}} \times 100\% \tag{2.5}$$

And can also be measured in (dB)

$$\text{EVM (dB)} = 10\log_{10}\left(\frac{P_{error}}{P_{reference}}\right) \quad (2.6)$$

Where P_{error} is the RMS power of the error vector, and P_{ref} is the power of the outermost point in the reference constellation. The SM and EVM targets for mobile WiMAX are comparatively rigorous among existing standards.

2.5 Conclusion

This chapter has shown the classes of RF power amplifier from highly linear to the less linear. It is well known that power amplifiers cannot operate efficiently when used for linear amplification. The classes A, B and AB are considered linear amplifiers and have been used for GSM and AM broadcasting. High data transfer leads to the development of multilevel modulations which causes non-constant envelope and wide envelope frequency and hence significantly sensitive to nonlinear distortion caused by RF power amplifier. Therefore, linear or linearisation of RF power amplifier is needed for high data transfer.

References

[1] S.C.Cripps, RF Power Amplifier for Wireless Communications, Norwood, MA: Artech House, 1999.

[2] Mi Albulet, RF Power Amplifiers, Atlanta, GA: Noble Publishing Corporation, 2001.

[3] P. B. Kenington, High- Linearity RF Amplifier Design, Norwood, MA: Artech House, 2000.

[4] Raab, F., "Class-F power amplifier with maximally flat waveforms," IEEE Tran. MTT, Vol. 45, No. 11, 2007–2012, 1997.

[5] Gao, S., "High-efficiency class F RF/microwave power amplifiers," IEEE Microwave Mag., Vol. 7, No. 1, 40–48, 2006.

[6] Woo, Y. Y., Y. Yang, I. Kim and B. Kim, "Efficiency comparison between highly efficient Class-F and inverse Class-F power amplifiers," IEEE Microwave Mag., Vol. 8, No. 3, 100–110, 2007

[7] Schmelzer, D. and S. Long, "A GaN HEMT class F amplifier at 2 GHz with 80% PAE," IEEE Compound Semiconductor IC Symposium, 96–99, San Antonio, USA, November 2006.

[8] S.C. Cripps Advanced Techniques in RF Power Amplifier Design, Norwood, MA: Artech House, 2002.

[9] Raab, F, "Efficiency of Outphasing RF Power-Amplifier Systems", IEEE Transactions on Communications, Vol. 33, No 10, PP. 1094– 1099, October, 1985.

[10] F. H. Raab, "Efficiency of Doherty RF Power Amplifier System", IEEE Trans. Broadcasting, Vol. BC-33, No 3, PP. 77-83, September, 1987.

[11] Raab, F.H.; Asbeck, P.; Cripps, S.; Kenington, P.B.; Popovic, Z.B.; Pothecary, N.; Sevic, J.F.; Sokal, N.O.;,"Power amplifiers and transmitters for RF and microwave", IEEE Transactions on Microwave Theory and Techniques, Vol. 50, No 3, PP. 814 – 826, March, 2002.

[12] J. Groe, "Polar transmitters for wireless communications", IEEE Communications Mag.,Vol. 45, No 9, PP. 58 – 63, Sept. 2007.

[13] W. H. Doherty, "A New High Efficiency Power Amplifier for Modulated Wave", Proc. IRE, Vol. 24, No. 9, PP. 1163– 1182, September, 1936.

[14] C. T. Burns, A. Chang, and D. W. Runton, "A 900 MHz, 500 W Doherty power amplifier using optimized output matched Si LDMOS power transistors", IEEE MTT-S Int. Microw. Theory Tech., Symp. Dig., PP. 1557 – 1580, June, 2007.

[15] A. S. Huusaini, R. Abd-Alhameed, J. Rodriguez, "Implementation of Efficiency Enhancement Techniques in the Linear Region of Operations of Power Amplifier", IT 7th Conference on Telecommunications, No 103, PP. 105 – 108, May, 2009.

[16] A. N. Rudiakova and V. G. Krizhanovski, "Driving waveforms for Class-F power amplifiers, " IEEE MTT-S Dig., pp. 473-476, 2000.

[17] F. H. Raab, "Class-E, Class-C, and Class-F power amplifiers based upon a finite number of harmonics," IEEE Trans. on Microwave Theory and Techniques, Vol. 49, No. 8, pp. 1462-1468, Aug. 2001.

[18] Gary Hau, Takeshi B. Nishimura, Naotaka Iwata, "High efficiency, wide dynamic range variable gain and power amplifier MMICs for wide-band CDMA handsets,"

IEEE Microwave and Wireless Components Letters, Vol. 11, No. 1, pp. 13-15, Jan. 2001.

[19] F. H. Raab, “An introduction to Class-F power amplifies,” RF Design, Vol. 19, No. 5, pp. 79-84, May 1996.

[20] Thomas H. Lee, The Design of CMOS Radio-Frequency Integrated Circuits, Cambridge, 1999.

CHAPTER THREE

3. User Terminal Efficient RF Power Amplifiers Design

3.1 Even load modulation RF power amplifier

This work describes the characterisation and design of energy efficient user terminal transceiver power amplifier. The design core is based on the combination of Class B and Class C that includes quarter wavelength transformer at the output to perform the load modulation [1-15]. This power amplifier is designed to operate over the frequency range of 3.4GHz to 3.6GHz mobile WiMAX band. The performances of load modulation RF power amplifier are compared with conventional Class B amplifier. The results of 30dBm output power and 53% power added efficiency are achieved.

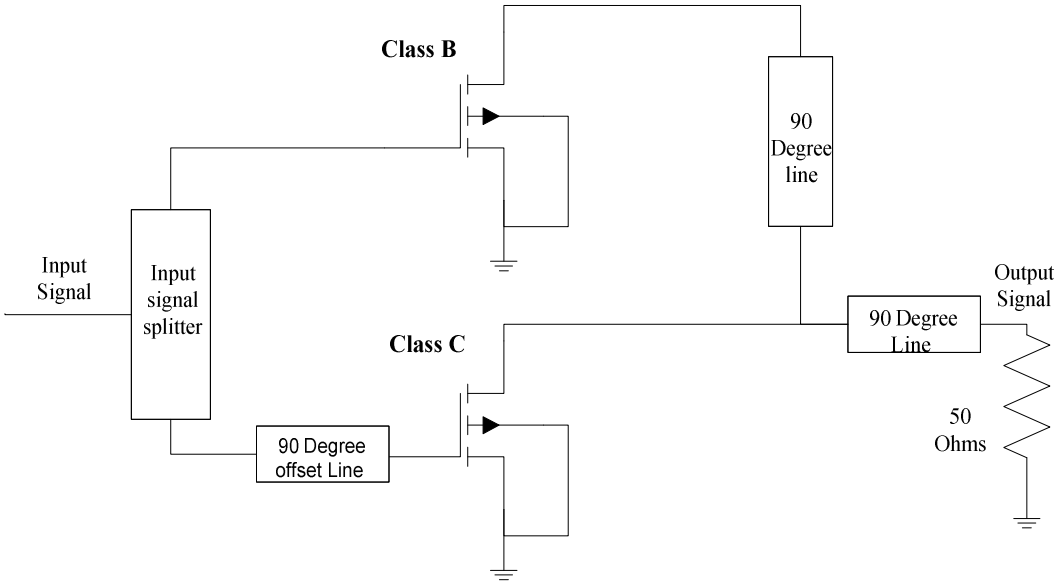

Figure 3.1 : The schematic diagram of the user terminal load modulation RF power amplifier.

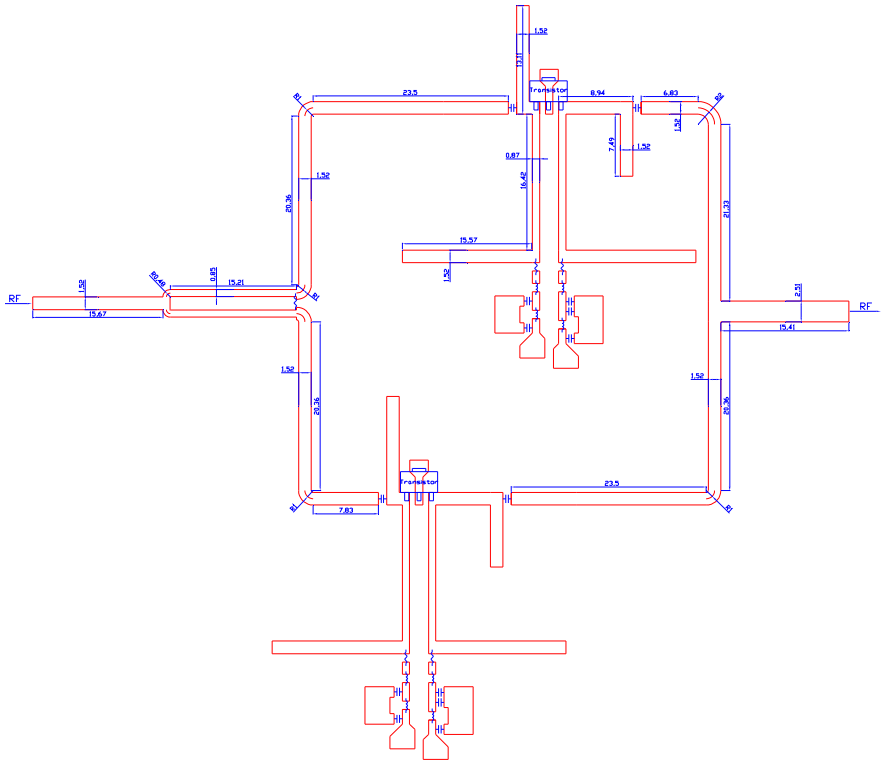

Figure 3.2: The scale design diagram of the user terminal load modulation RF power amplifier.

In this work, the efficiency and the output power of the load modulation RF power amplifier has been achieved by 1) Proposed additional of 32mm offset lines at the output and input matching network for which it prevents power leakage at the output junction between the output impedance transformer and peaking Class C amplifier, 2) The optimum design of Class B amplifier with proposed circuitry increases the quiescent current to an order of 8% of the peak drain current of the transistor, 3) The optimum design of 3dB 90 degree input splitter, and a transmission-line choke and RF short-circuit used to de-couple the DC supply. The proposed schematic diagram of this kind of amplifier is presented in Figure 3.2.

3.2 Circuit Design

A 3.5GHz, 30dBm Mobile WiMAX handset load modulation RF power amplifier, has been designed using the TOM3 large signal model and FPD1500 transistor. The FPD1500SOT89 is a packaged depletion model AIGaAs/InGaAs pseudomorphic pHEMT. It contains double recessed gate structure, which minimises parasitic and optimise performance.

This design comprised several design steps for which the optimisation is applied to each in order to obtain global high performances of the entire system. Initially, the design of carrier and peak amplifiers, input signal 3dB 90-degree hybrid coupler designs, Output 90 degree offset line and impedance transformer designs were performed.

However, it is important to note that in the design of carrier and peak amplifiers, the DC simulation should be done first in order to find the optimal bias point and bias network

based on the class of operation and power requirements. In this work, the bias circuit was designed based on Class B and Class C for carrier peak respectively. We decided to use class B to improve the efficiency and linearity instead of Class AB, which is widely used in the combination of Doherty amplifier.

The DC quiescent current for Class B is at threshold while for Class C is below the threshold. In theory the quiescent current of Class B is zero but for the current work, we increased the quiescent current to an order of 8% of the peak drain current that is resulting in 0.046mA. The reason for this is to minimise crossover distortion and increases the efficiency. The peak drain current is 0.587mA when the VGS is at 0V and VDS is 5V. 5V was chosen for VDS since it is located between cut-off and saturation of the transistor. 0.046mA is 8% of the peaks drain current, which gave the VGS of -0.9V as shown in Figure 3.3, while the overall power consumption is 0.228W. The thresholds of class B drain current for this work was shown in Figure 3.4. Moreover, the same supply power applied to class C but with drain current of 0.004mA and the power consumption is 0.019W.

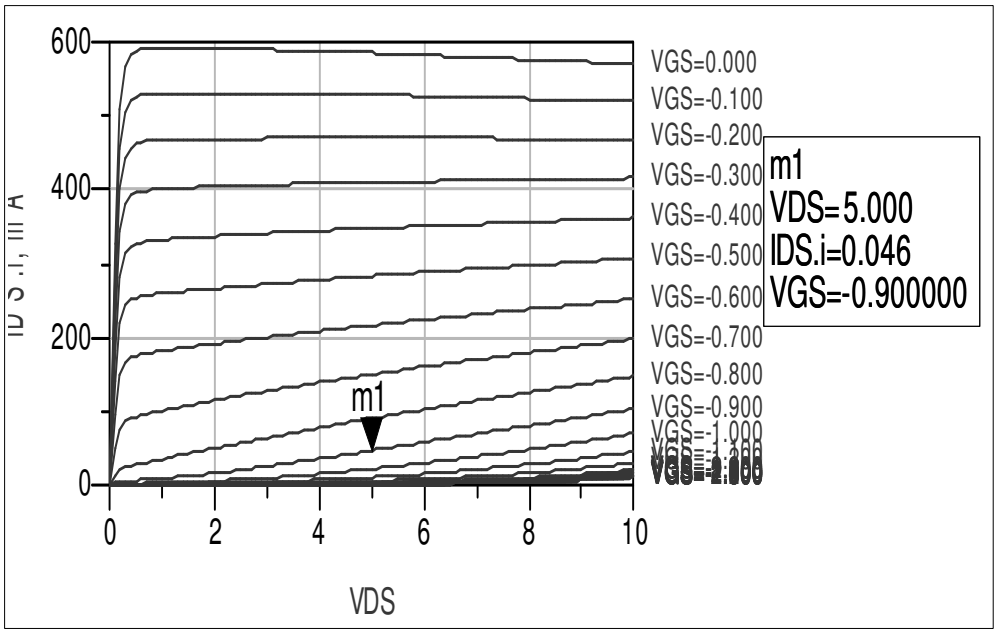

Figure 3.3: Current and voltage drain-source curve.

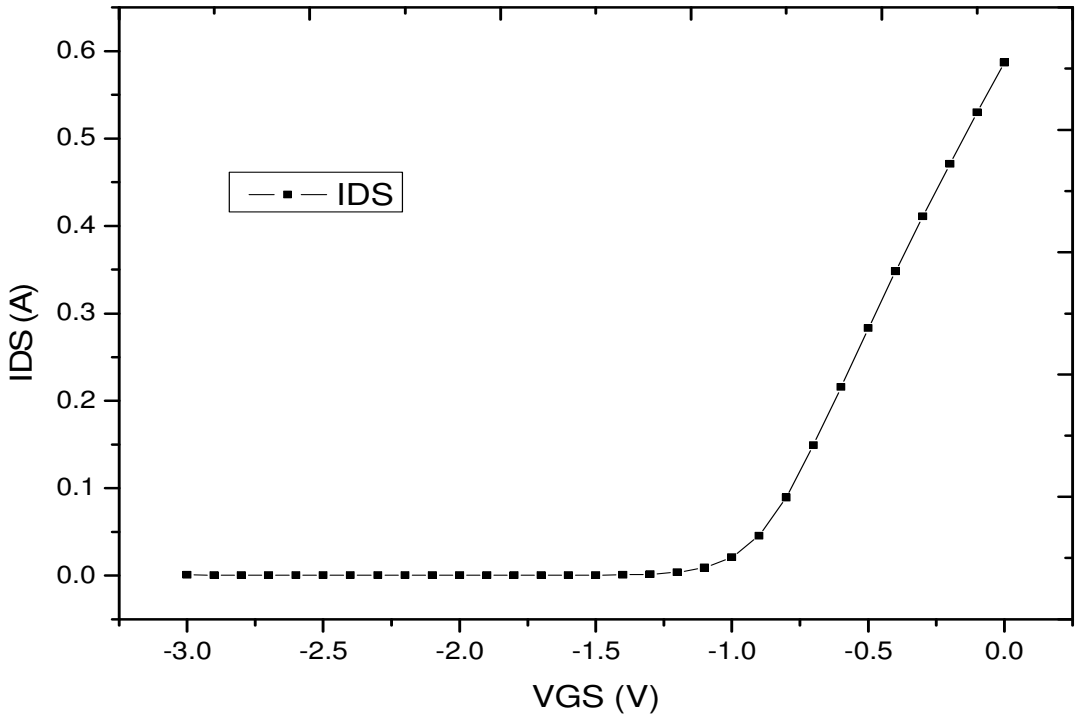

Figure 3.4: The threshold of the drain current of class B.

Having obtained the DC quiescent current, the next step is to determine the load line impedance to design the output and input matching networks of Class B power amplifier and to obtain the performance regarding the output power and efficiency. The output-matching network was designed for optimum output power performance with load pull technique and the input matching network was based on S-parameters.

The transistor is a package form; Figure 3.5 shows transistor with external parasitic and the parasitic elements are included in the load-pull analysis in order to optimise the output-matching network. The results obtained from the load pull simulation showed that the transistor needs to see an impedance of 20.492 + j3.775Ω at the output.

Therefore the target of the matching network was to transform the impedance from 49.393 – j1.776 to 20.492 + j3.775Ω. This impedance was the optimal load value, which compromised the 40.39% efficiency and 27.05dBm output power at 1dB compression point of single Class B alone, Figure 3.6. The load reflection coefficient was used to design the output matching network while for the input matching network S-parameter was employed and conjugated the input reflection coefficient for maximum power transfer. Figure 3.7 shows the linear results obtained from the matched Class B power amplifier, the gain is flat over the range of 3.4GHz to 3.6GHz with excellent matching at the input and output return losses.

The non-linear simulation of Class B was performed and the performance of the design in terms of output power and efficiency was observed. The 26.98dBm output power was achieved at 1dB compression point and 39% efficiency. From this nonlinear simulation,

the result shows a clear compromise with the load pull measurement values. The same was applied to Class C but with different bias point.

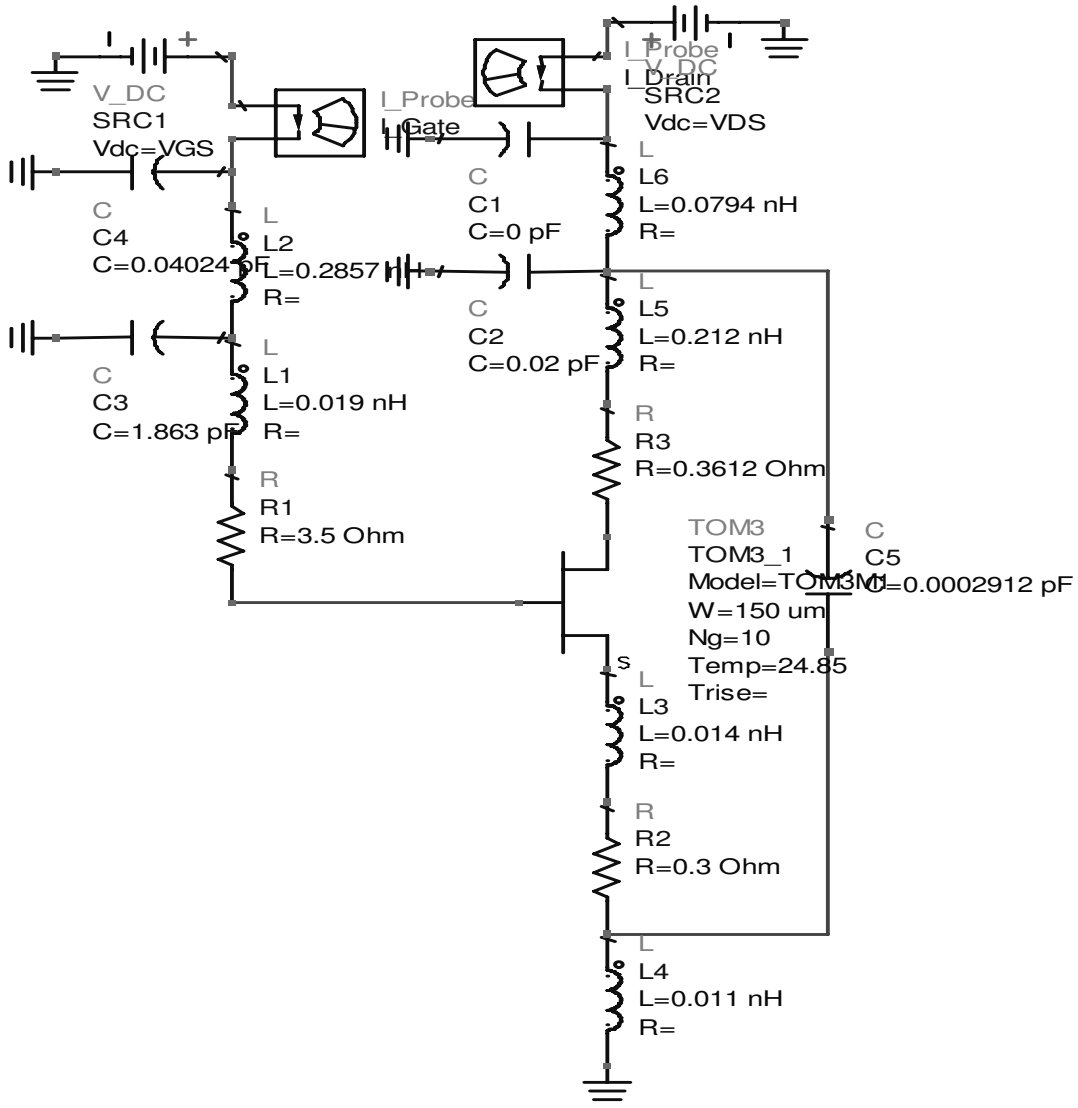

Figure 3.5: Transistor with external parasitic.

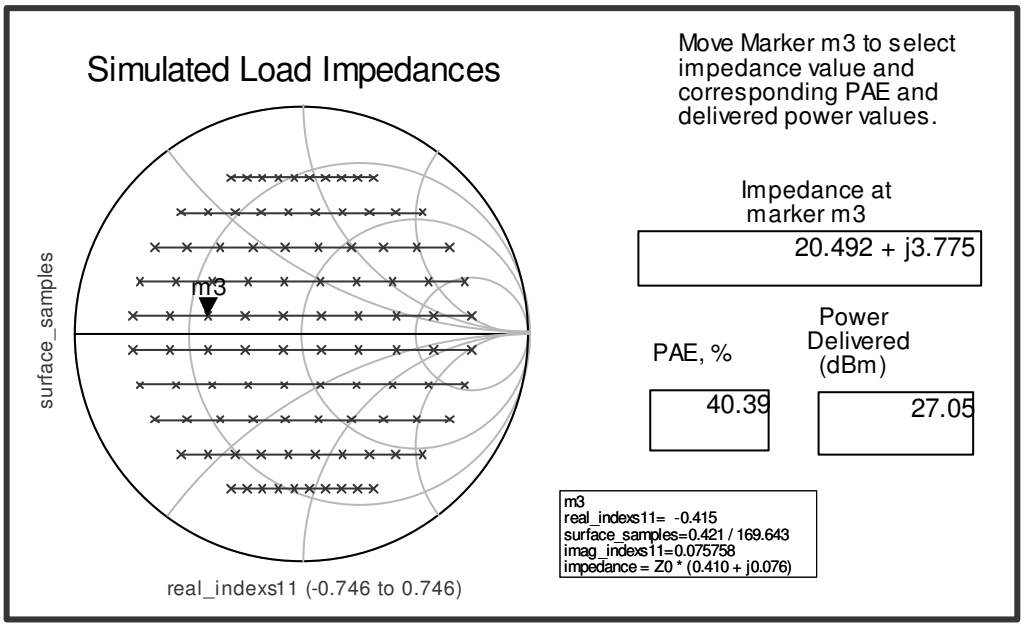

Figure 3.6: Compromise between 40.39% efficiency and 27.05dBm output power at 1dB compression point.

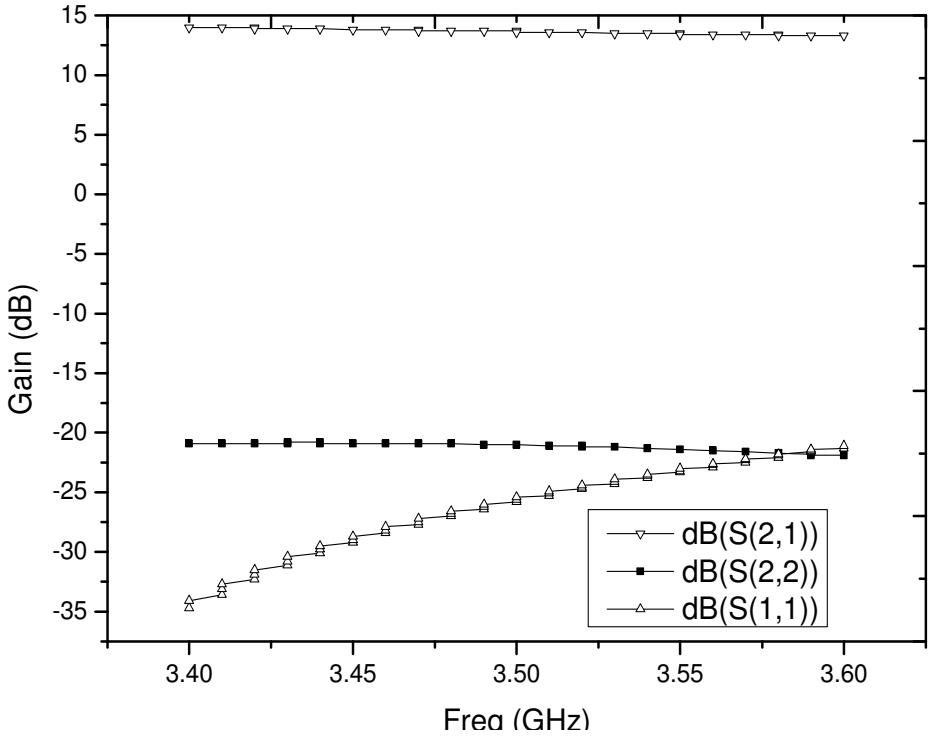

Figure 3.7: Linear simulation: Flat gain & return loss.

A 3dB quadrature splitter is part of load modulation and if design properly can contribute a lot to the total efficiency of the system. Our investigation shows that the operation of this technique is strongly influenced by the coupling factor of the input splitter. In fact, in this work 3dB quadrature splitter have been designed (Figure 3.8) and tested in terms of operating frequency and bandwidth, and this showed good results as appeared in Figure 3.9, and Figure 3.10. It should be noted that, the splitter is at the input of amplifier and divides the input signal equally between the carrier and peaking amplifiers. The splitter, the Carrier Class B, the peaking Class C, and impedance transformer at the output are combined to form a Doherty RF power amplifier.

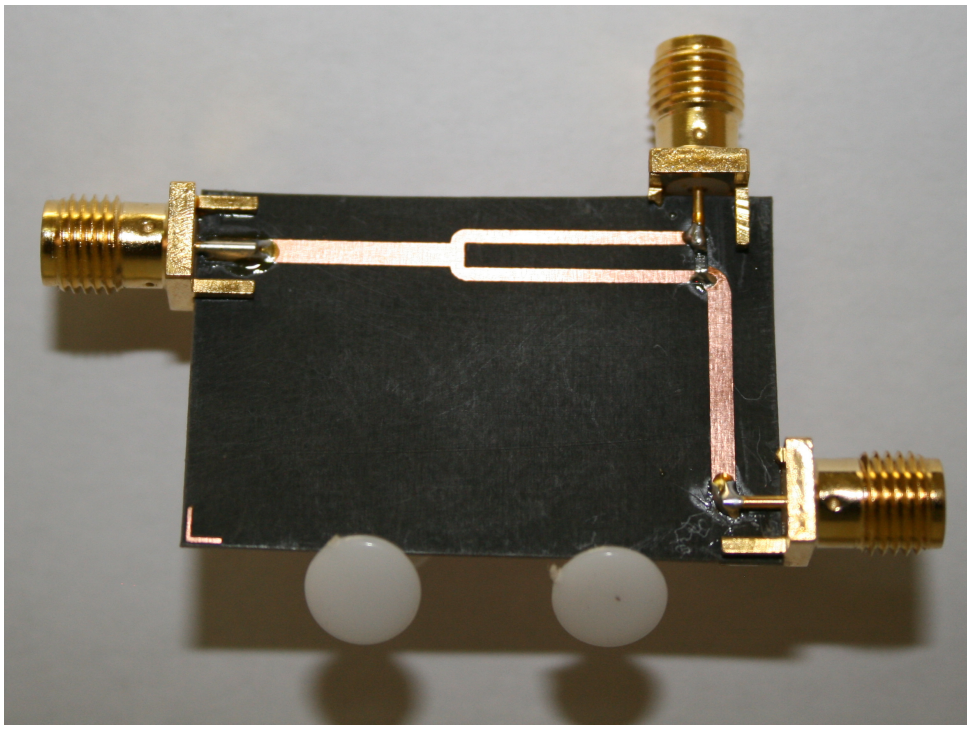

Figure 3.8: Power splitter.

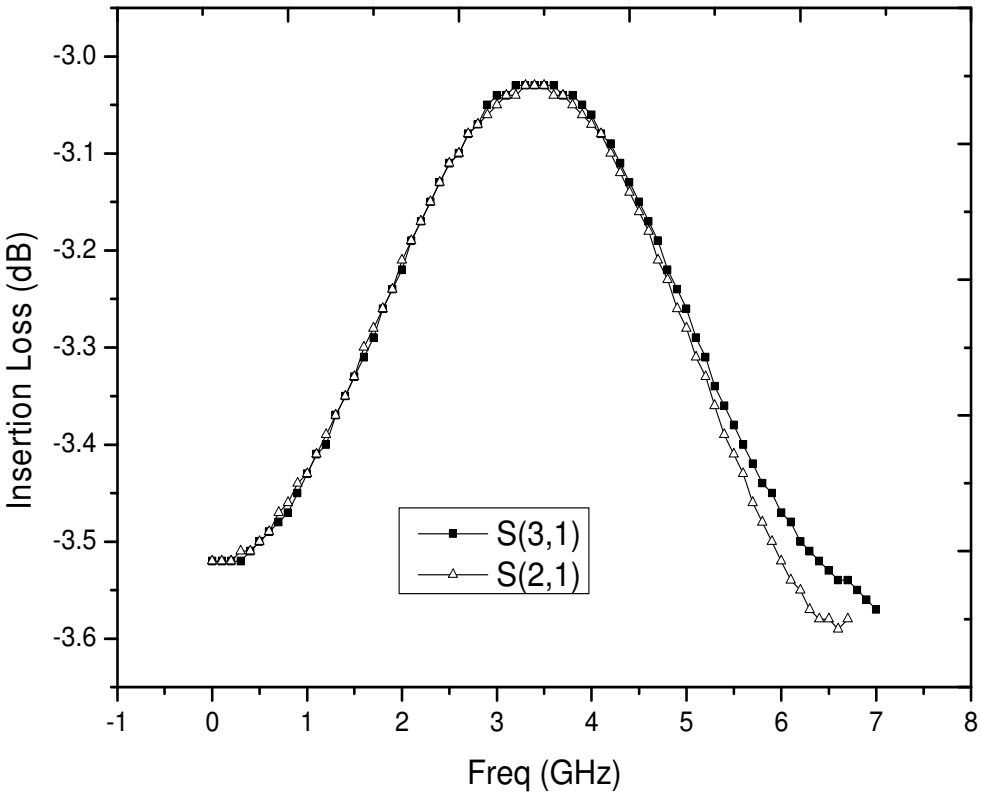

Figure 3.9: Insertion loss of S21 and S31.

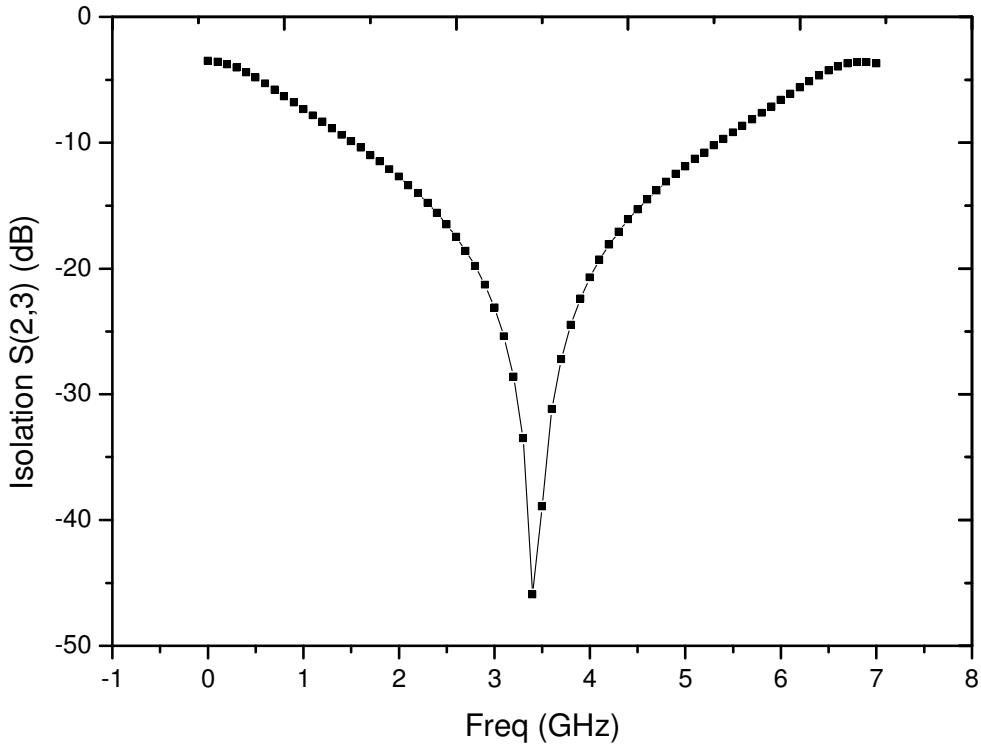

Figure 3.10: Isolation between the ports 2 and 3.

3.3 Implementation & Results

Figure 3.11, shows the prototype diagram of the proposed load modulation RF power amplifier with offset transmission line at both output and input circuit which, maximise the overall system's efficiency with the configuration of Class B amplifier. The FPD1500SOT89 transistor with 27.5dBm output power was used for both Class B and Class C amplifiers and produces a Doherty power amplifier with 30dBm output power and efficiency of 53%. The bias condition for the Class B carrier amplifier are Vgs = -0.9V (Ids = 46 mA), and for the Class C peaking amplifier, Vgs = -1.1V (Ids = 4 mA). Both of the amplifiers use the same drain voltage (5V). Table 3.1 summarises the recommended bias setting.

The load modulation RF power amplifier initially characterised for AM-AM and AM-PM responses as well as output power and efficiency. The performance comparisons between the Doherty amplifier and Class B amplifier are performed and the output power increased to 30dBm at 1dB compression point while the efficiency increased to 53%. Figure 3.12 represent the variation of the input power versus output power of the load modulation RF power amplifier. It clearly shows that 30dBm output power is at linear region of the amplifier and this was achieved due to the characteristic of gain compression and expression of the load modulation. The peaking amplifier Class C late gain expansion can compensate the carrier Class B amplifier gain compression. Figure 3.13, Figure 3.14 represent the gain characteristic versus output power, the graph shows the power gain of load modulation amplifier is degraded drastically compared to Class B due to the arrangement of lower biasing.

Figure 3.15 shows the power added efficiency versus output power. The Doherty amplifier have higher efficiency over the range of wide output power levels compared to Class B amplifier.

Table 3.1: Bias point setting for load modulation.

Drain Voltage (V)	**Carrier VGS (V)**	**Peaking VGS (V)**
5	-0.9	-1.1

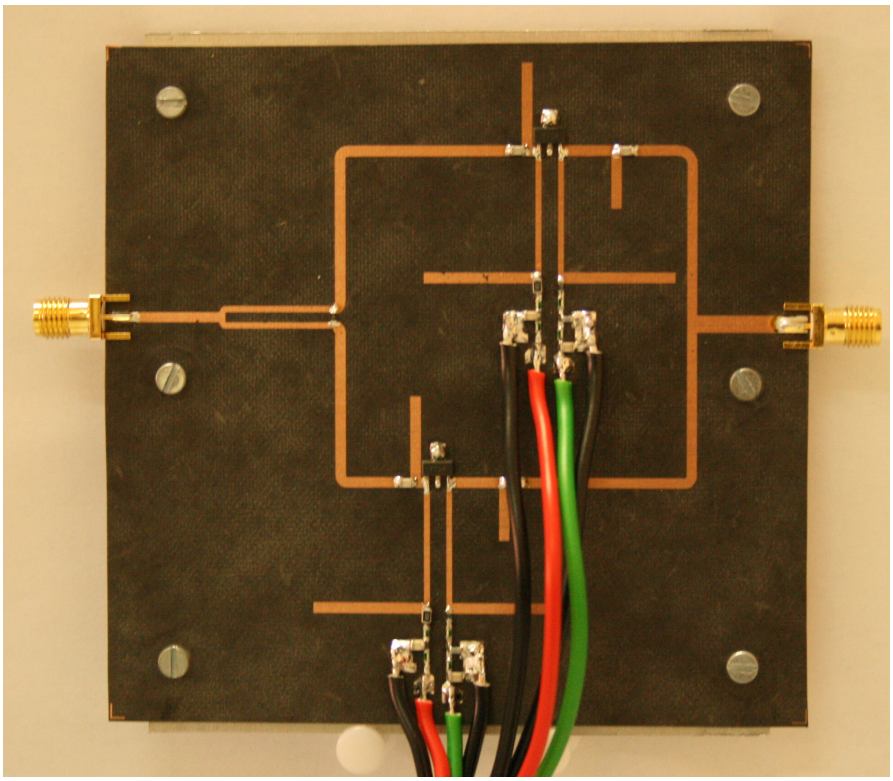

Figure 3.11: Implemented prototype of load modulation RF power amplifier.

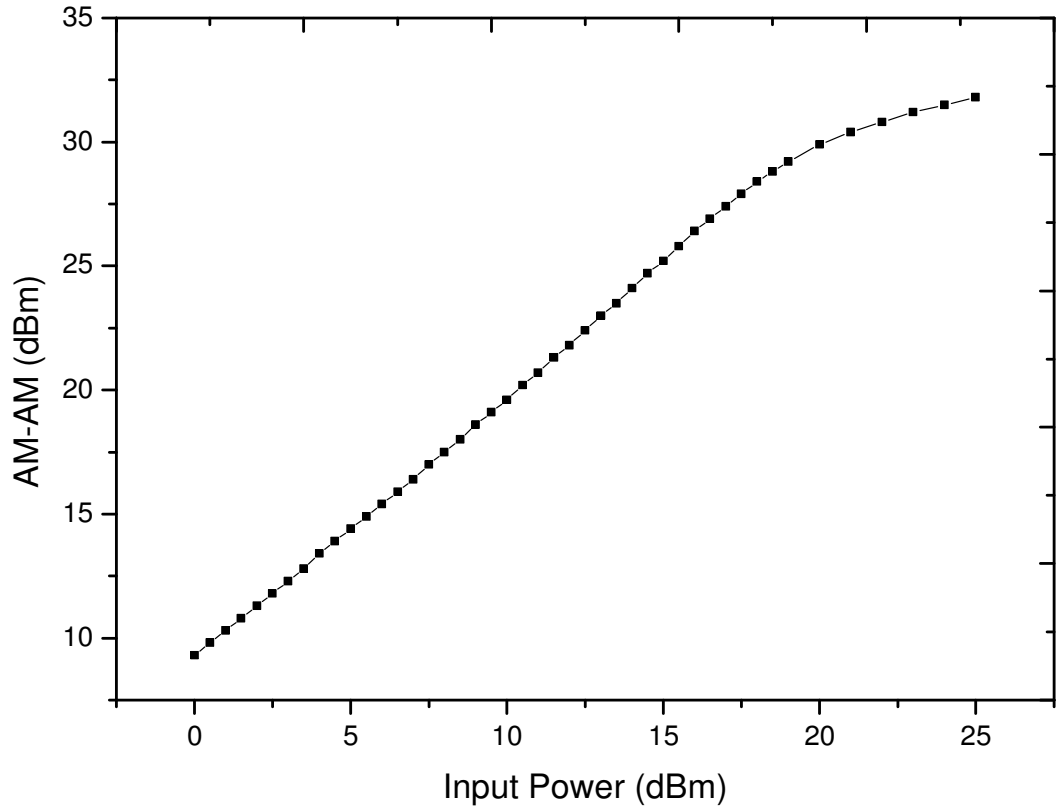

Figure 3.12: AM-AM characteristics of load modulation RF power amplifier.

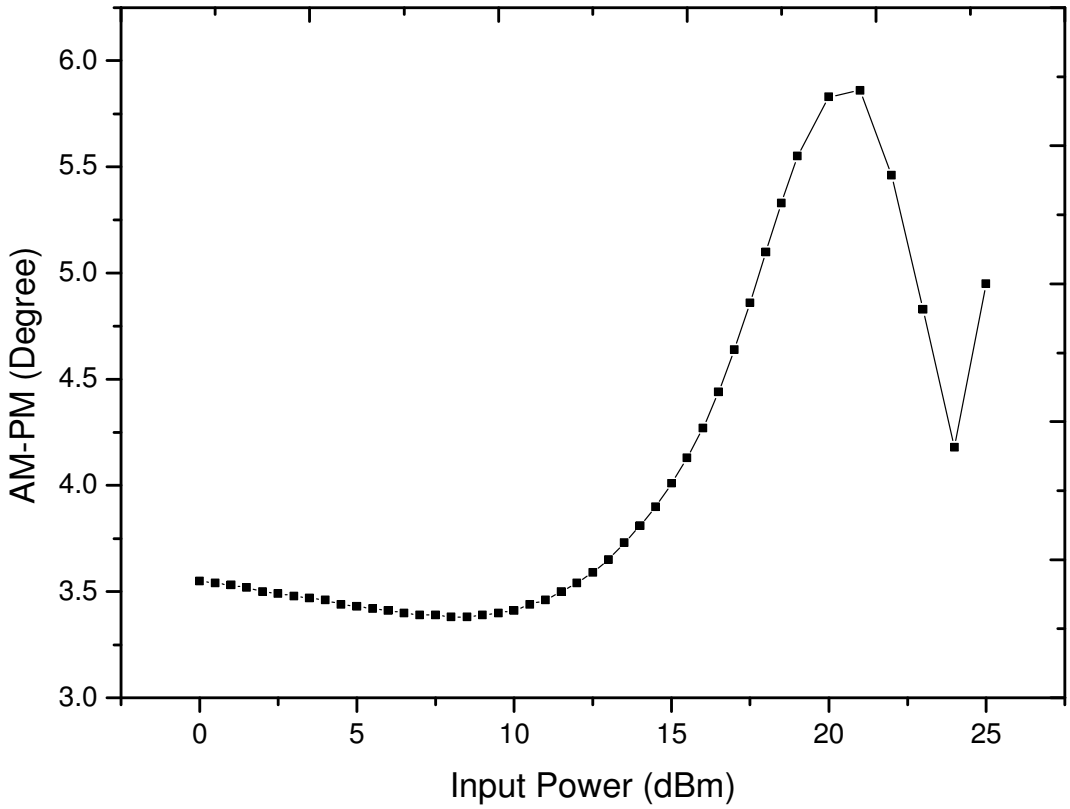

Figure 3.13: AM-PM characteristics of load modulation RF power amplifier.

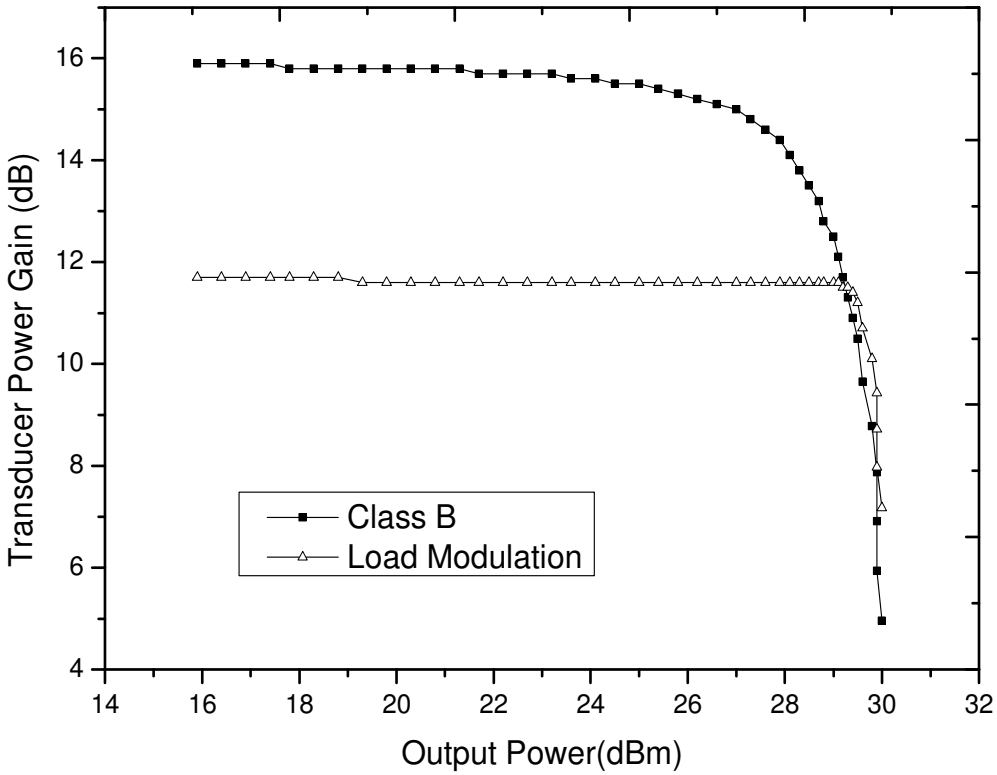

Figure 3.14: Gain characteristics.

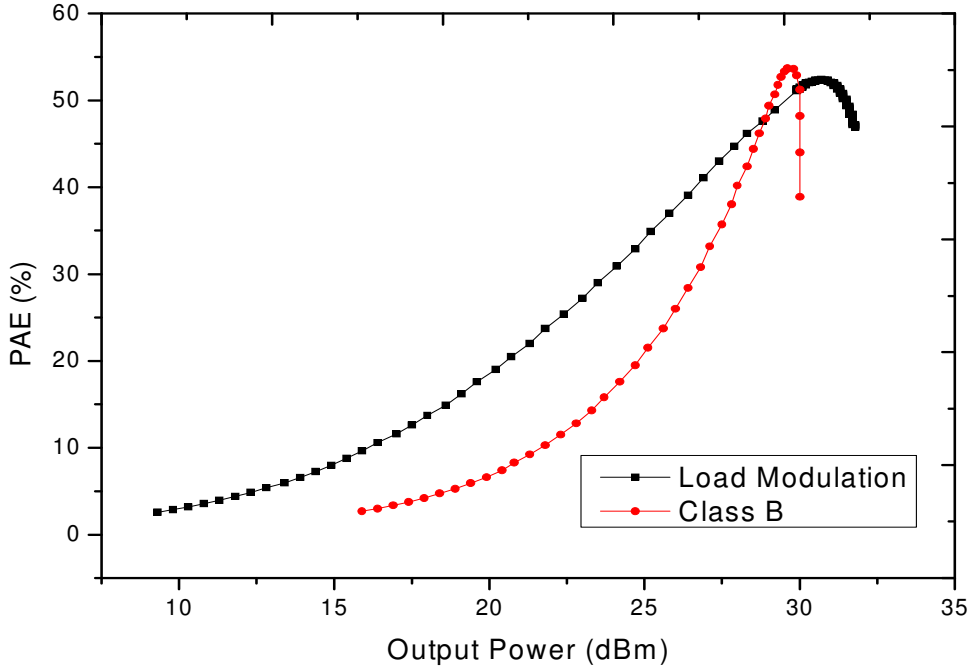

Figure 3.15: Power-Added Efficiency.

Table 3.2: Comparison performance of class B and load modulation at Pout 1dB compression point.

Amplifier	**Gain (dB)**	**Pout (dBm) at 1dB**	**PAE (%) at P1dB**	**Pavg (dBm)**	**PAE (%) at Pavg**
Class B amplifier	15.4	27.5	37	23	11
Load modulation	11.8	30	53	23	26

3.4 Uneven Doherty RF power amplifier

This work is the improvement of Doherty RF power amplifier which uses identical transistors but different only in biasing. Doherty techniques are based on load modulation and when using two transistors, the second transistor should be able to pull the load presented to the first transistor for high efficiency. However, it is impossible for Class C to deliver the same output power as Class B because, Class C used part of the input signal to turn on and for this reason Class C will never pull the load presented to Class B for peak efficiency.

To solve this problem, uneven Doherty RF power amplifier with uneven signal splitter at the input has been designed, which is to allow more input signal to Class C amplifier than Class B amplifier. An uneven Doherty technique with new offset lines was

employed and has been designed to operate over the frequency range of 3.4GHz to 3.6GHz band. The proposed schematic diagram of this kind of amplifier is presented in Figure 3.16. The performances of Uneven Doherty power amplifier are compared with Doherty power amplifier. The results of 30dBm output power and 62% power added efficiency are achieved.

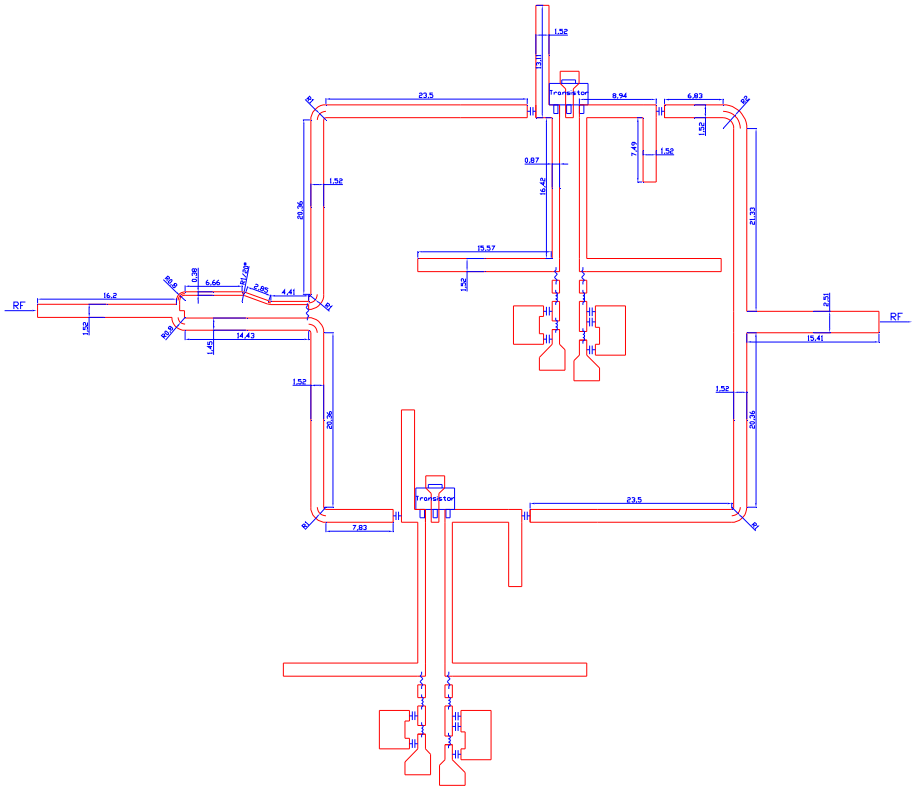

Figure 3.16: The proposed schematic diagram of Uneven Doherty power amplifier.

3.5 Uneven circuit design

The large signal model, the design tools and the procedure that were used in the first design (Doherty power amplifier) have also been followed in this design to optimise the performance.

This design comprised several design steps for which the optimisation is applied to each in order to obtain global high performances of the entire Uneven RF power amplifier. Initially, the design of carrier and peak amplifiers, unequal input signal 90-degree hybrid coupler designs, output 90 degree offset line, and impedance transformer designs were performed.

A 3dB quadrature unequal splitter is part of uneven Doherty power amplifier and if design properly can contribute a lot to the total efficiency of the system. Our investigation shows that the operation of this technique is strongly influenced by the coupling factor of the input splitter. In fact, in this work the quadrature unequal splitter have been designed (Figure 3.17) and tested in terms of operating frequency and bandwidth, and this showed good results as appeared in Figure 3., and Figure 3.. It should be noted that, the unequal splitter is at the input of amplifier and divides the input signal unequally between the carrier and peaking amplifiers. The unequal splitter, the Carrier Class B, the peaking Class C, and impedance transformer at the output are combined to form an uneven Doherty RF power amplifier**.**

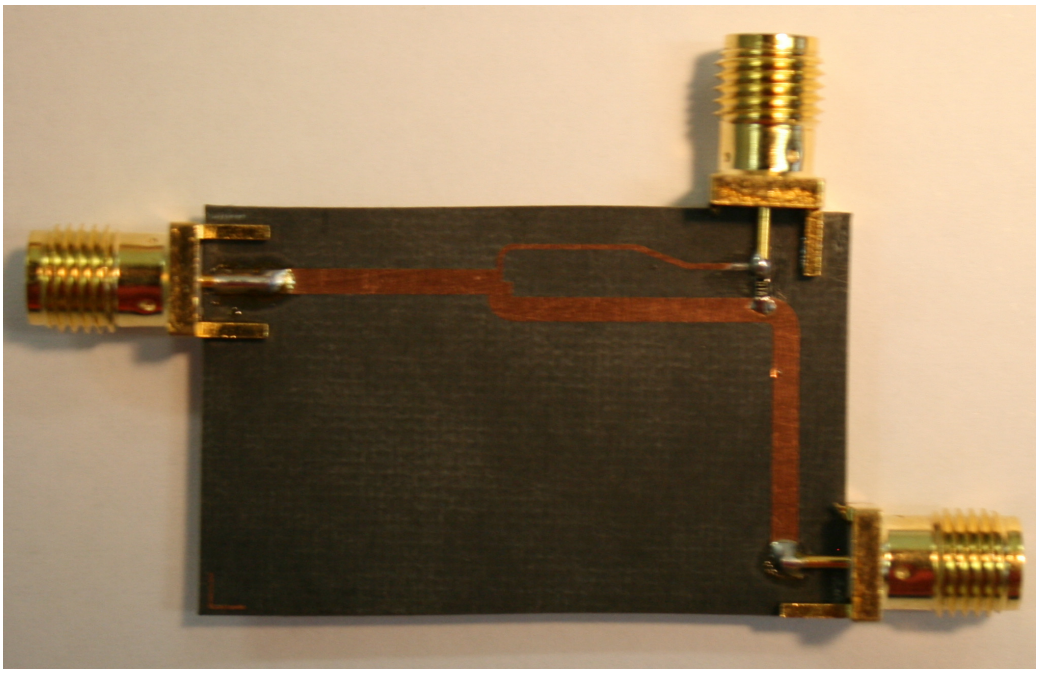

Figure 3.18: Unequal power splitters.

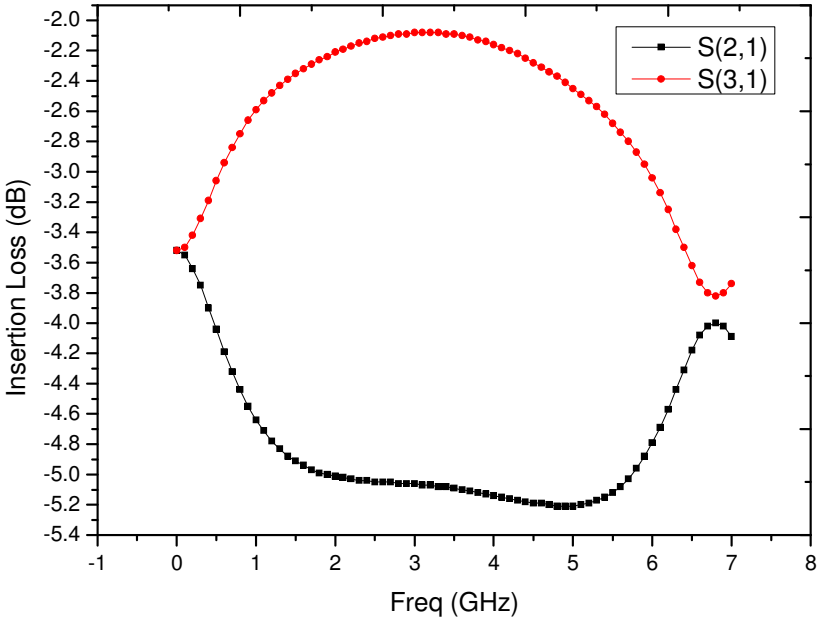

Figure 3.19: Insertion loss of S21 and S31.

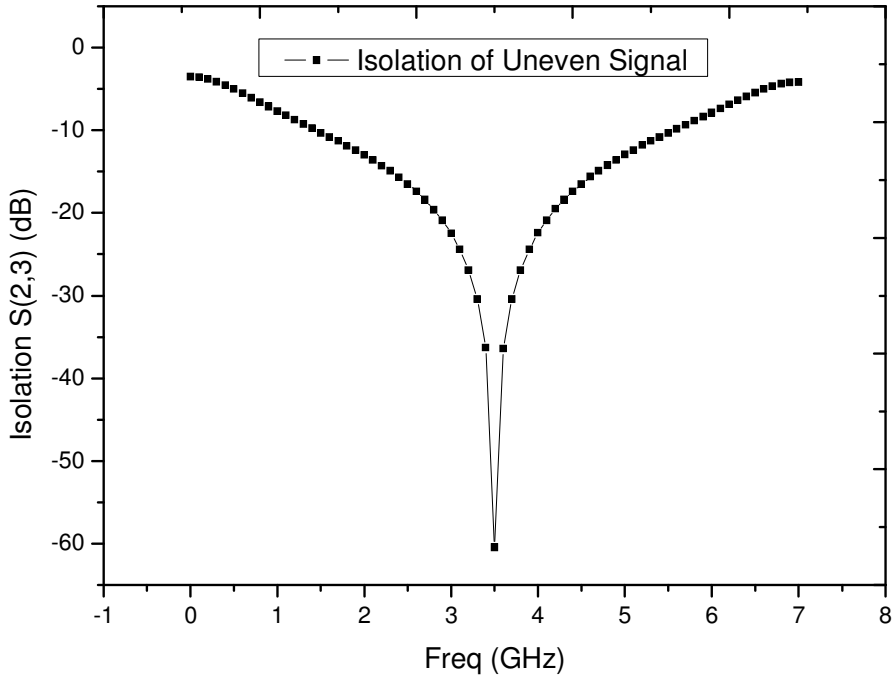

Figure 3.19: Isolation between the ports 2 and 3.

3.6 **Uneven implementation & results**

Figure 3.20, shows the prototype diagram of the proposed uneven Doherty RF power amplifier with offset transmission line at both output and input circuit which maximise the overall system's efficiency with the configuration of Class B amplifier. The FPD1500SOT89 transistors with 27.5dBm output power was used for both Class B and Class C amplifiers and produce an uneven Doherty RF power amplifier with 30dBm and Efficiency of 62%. The bias condition for the Class B carrier amplifier are Vgs = -0.9V (Ids = 46 mA), and for the Class C peaking amplifier, Vgs = -1.1V (Ids = 4 mA). Both of the amplifiers use the same drain voltage (5V).

The uneven Doherty initially characterised for AM-AM and AM-PM responses as well as output power and efficiency. The performance comparisons between uneven Doherty

amplifier and Doherty amplifier are performed and the output power increased to 30dBm at 1dB compression point while the efficiency increased to 62%. Figure 3.21 represent the variation of the input power versus output power of the uneven Doherty amplifier. It clearly shows that 30dBm output power is at linear region of the amplifier and this was achieved due to the characteristic of gain compression and expression of the uneven Doherty. The peaking amplifier Class C late gain expansion can compensate the carrier Class B amplifier gain compression. Figure 3.23 represent the gain characteristic versus output power, the graph shows the power gain of uneven Doherty amplifier is a little more increase compare to Doherty amplifier and this is due to the arrangement of lower biasing. Figure 3.24 shows the power added efficiency versus output power. The uneven Doherty amplifier have higher efficiency over the range of wide output power levels compared to Doherty amplifier.

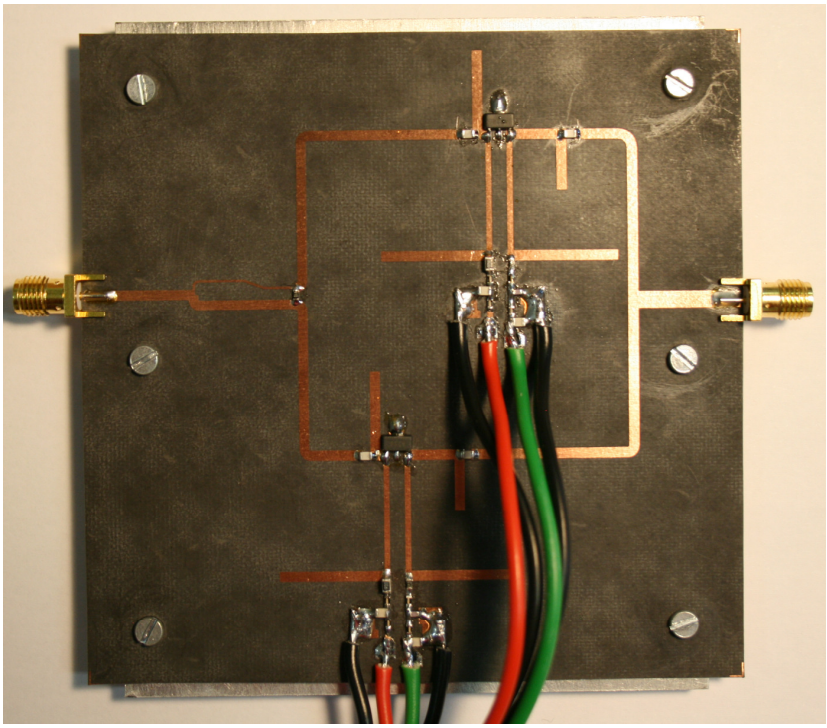

Figure 3.20: Implemented prototype of uneven Doherty power amplifier.

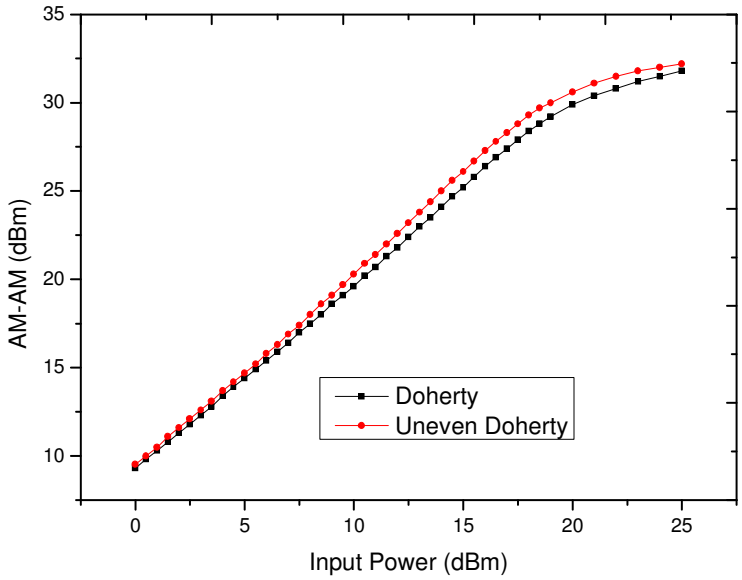

Figure 3.21: Comparison of AM-AM Characteristics for uneven Doherty amplifier and Doherty amplifier.

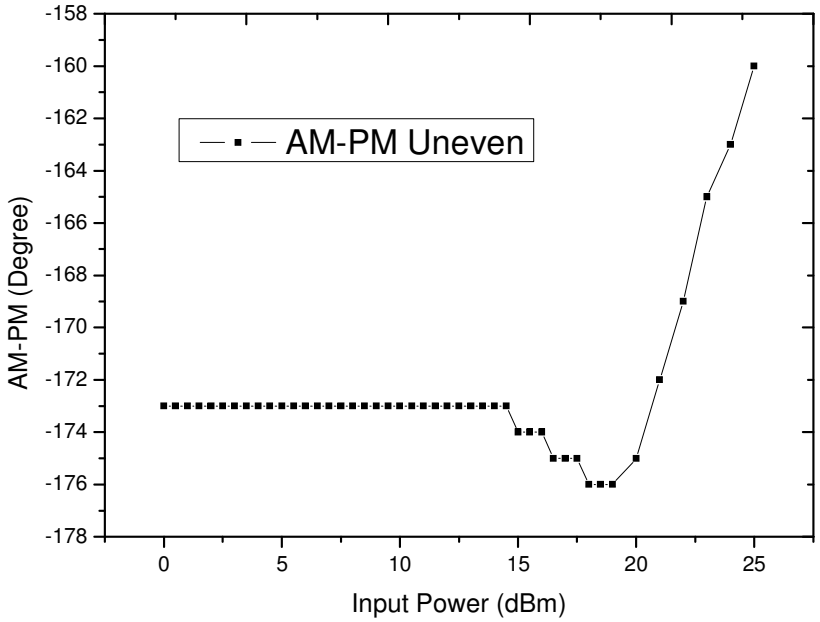

Figure 3.22: AM-PM characteristics of Uneven Doherty amplifier.

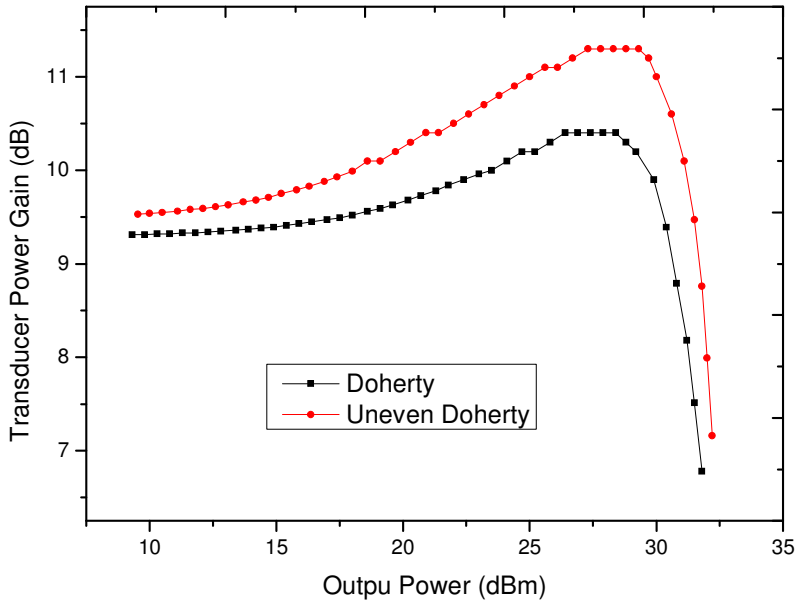

Figure 3.23: Gain characteristics.

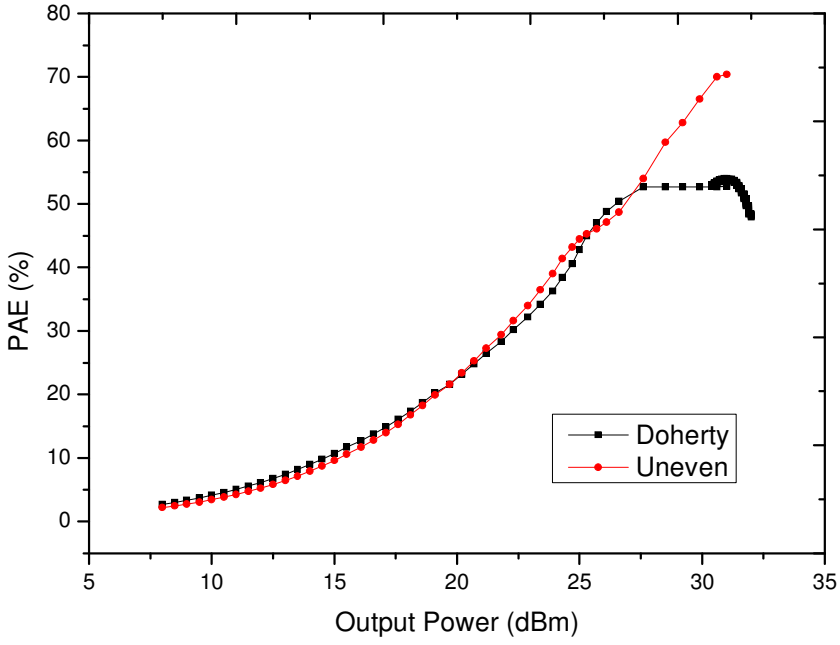

Figure 3.24: Power-Added Efficiency.

Table 3.3: Comparison performance of uneven Doherty power amplifer and Doherty power amplifier at Pout 1dB compression point.

Amplifier	**Gain (dB)**	**Pout (dBm) at 1dB**	**PAE (%) at P1dB**	**Pavg (dBm)**	**PAE (%) at Pavg**
Doherty amplifier	11.8	30	53	23	26
UnevenDoherty amplifier	9.7	32	62	23	26

3.7 Conclusion

This chapter has presented two different topologies. Topology one (combination of class B and class C) is even Doherty in which the results are compared with classical class B. The even Doherty has better efficiency and output power than class B but still it has some limitation, which does not allow utilising all the efficiency. Doherty techniques are based on load modulation and when using two transistors, the second transistor should be able to pull the load presented to the first transistor for high efficiency. However, it is impossible for class C to deliver the same output power as class B because, class C used part of the input signal to turn on and for this reason class C will never pull the load presented to class B for peak efficiency. With this reason we decided to designed uneven Doherty RF power amplifier with uneven signal splitter, which is to allow more input signal to class C amplifier than class B amplifier. The trade-off between efficiency and linearity in load modulation power amplifier has been presented. The achieved results of the proposed design process have shown an excellent efficiency and power performances. The proper phasing of 3dB quadrature splitter effectively contributed to the total efficiency of the system. The operation of this design was strongly influenced by the coupling factor of the splitter, biasing of class B and C amplifiers. In addition, the turn–on of the class C amplifier was dependent on the gate bias voltage and the input signal. The self-managing characteristic of the load modulation amplifier has made its implementation more attractive.

References

[1] W. H. Doherty, "A New High Efficiency Power Amplifier for Modulated Wave", Proc. IRE, Vol. 24, No. 9, PP. 1163– 1182, September, 1936.

[2] A. S. Huusaini, R. Abd-Alhameed, J. Rodriguez, "Implementation of Efficiency Enhancem-ent Techniques in the Linear Region of Operations of Power Amplifier", IT 7th Conference on Telecommunications, No 103, PP. 105 – 108, May, 2009.

[3] F. H. Raab, "Efficiency of Doherty RF Power Amplifier System", IEEE Trans. Broadcasting, Vol. BC-33, No 3, PP. 77-83, September, 1987.

[4] S .C. Cripps, RF Power Amplifier for Wireless Communications, Norwood, MA: Artech House, 1999.

[5] F. H., Asbeck P., Cripps S., Kenington P.B., Popovic Z.B., Pothecary N., Sevic J.F., Sokal N.O., "Power amplifiers and transmitters for RF and microwave", IEEE Transactions on Microwave Theory and Techniques, Vol. 50, No 3, PP. 814 – 826, March, 2002.

[6] J. Groe, "Polar transmitters for wireless communications", IEEE Communications Mag.,Vol. 45, No 9, PP. 58 – 63, Sept. 2007.

[7] J. Cha, J. Kim, B. Kim, J. S. Lee, and S. H. Kim, "Highly Efficient Power Amplifier for CDMA Base Stations Using Doherty Configuration," IEEE MTT-S int. Microwave Sympo., pp. 553-556, June 2004.

[8] B. Shin, J. Cha, J. Kim, Y. Y. Woo, J. Yi, and B. Kim, "Linear Power Amplifier based on 3-Way Doherty Amplifier with Predistorter," IEEE MTT-S Int.mn Microwave Sympo., pp. 2027-2030, June 2004.

[9] Y. Yang, J. Yi, Y. Y. Woo, and B. Kim, "Optimum Design for Linearity and Efficiency of Microwave Doherty Amplifier Using a New Load Matching Technique," Microwave Journal, Vol. 44, No. 12, pp. 20-36, Dec. 2001.

[10] S. M. Wood, R. S. Pengelly, and M. Suto, “A High Power High Efficiency UMTS Amplifier using a Novel Doherty Configuration,” RAWCON’03 proceedings, pp.329-332, Aug. 10-13, 2003.

[11] H. Sano, N. Ui, and S. Sano, "A 40W GaN HEMT Doherty Power Amplifier with 48% Efficiency for WiMAX Applications," in Compound Semiconductor Integrated Circuit Symposium, 2007. CSIC 2007. IEEE, 2007, pp. 1-4.

[12] S. Kwon, "Inverted Load network for high power Doherty amplifier," IEEE Microwave Magazine, vol. 10, February 2009.

[13] P. B. Kenington, High- Linearity RF Amplifier Design, Norwood, MA: Artech House, 2000.

[14] D. M. Upton and P. R. Massey, “A New Circuit Topology to Realize High Efficiency, High Linearity and High Power Microwave Amplifiers”, RAWCON ’98 Proceedings, PP. 317– 320, August, 1998.

[15] C. T. Burns, A. Chang, and D. W. Runton, “A 900 MHz, 500 W Doherty power amplifier using optimized output matched Si LDMOS power transistors”, IEEE MTT-S Int. Microw. Theory Tech., Symp. Dig., PP. 1557 – 1580, June, 2007.

CHAPTER FOUR

4. Base Station Efficient RF Power Amplifiers Design

4.1 Efficient mobile WiMAX base station RF power amplifier

The B3G base station transceiver Doherty power amplifier was designed to operate over the frequency range of 3.47GHz to 3.53GHz mobile WiMAX band using Freescale's N-Channel Enhancement-Mode Lateral MOSFET Transistor, MRF7S38010HR3; The performances of the Doherty amplifier are compared with that of the conventional Class AB amplifier [1-13]. The results of 43dBm output power and 66% power added efficiency were achieved.

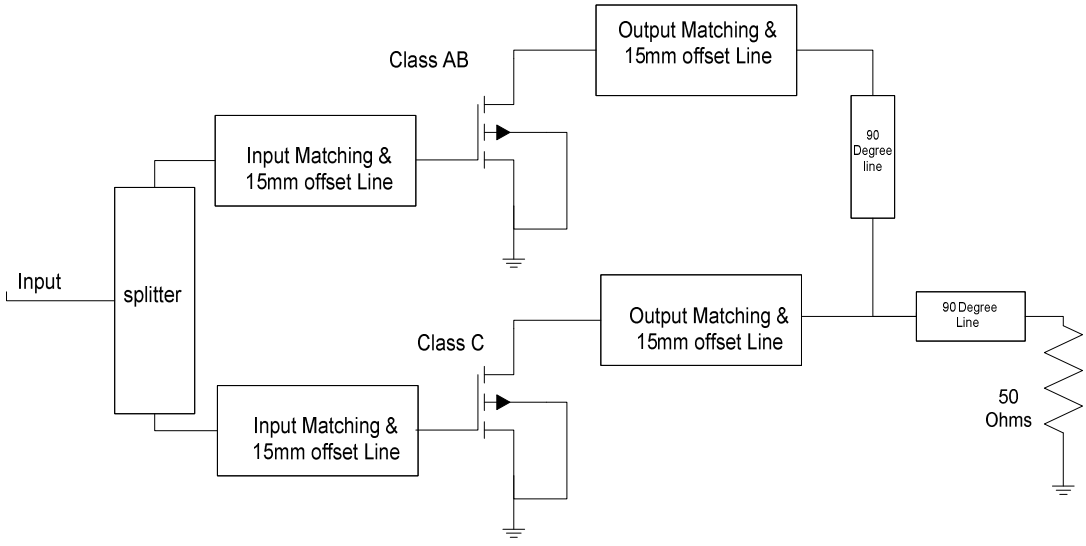

Figure 4.1: The proposed block diagram of Doherty RF power amplifier.

The efficiency and the output power of the Doherty RF power amplifier has been achieved by two identical 38dBm, 15dB gain, 30V devices for 3400 – 3600MHz configured as Class AB and Class C respectively, with the proposed additional of 15mm offset lines at the output matching to adopt to the Doherty configuration and prevents the power leakage at the output junction between the output impedance transformer and peaking Class C amplifier. The 15mm length of micro strip line was obtained by using "LineCalc" from ADS simulator with RT 5880 substrates' parameters Er = 2.2, H= 0.5mm, Zo = 50 Ω, T= 35um, TanD= 0.017. The 50 Ω 90 degree open circuits were added to right angle of the RF blocking transmission lines. The proposed schematic diagram of this kind of amplifier is presented in Figure 4.1.

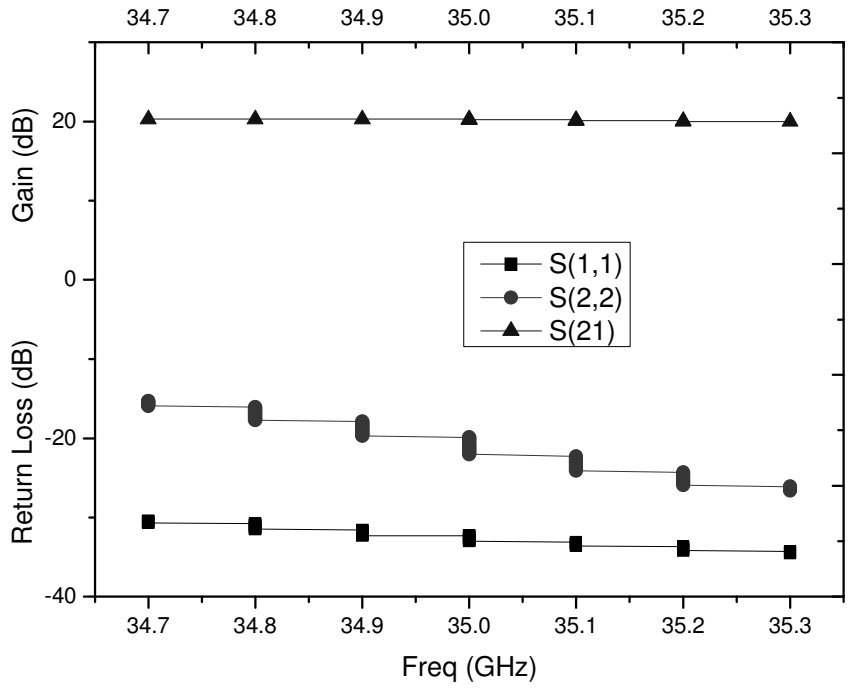

Figure 4.2: Linear simulation: Flat gain & return loss.

4.2 Circuit design

A 43dBm output power beyond 3G base station Doherty RF power amplifier have been designed using Freescale N-Channel Enhancement-Mode Lateral MOSFET MRF7S38010HR3. The 50Ω quarter wavelength transmission line impedance inverter is used to provide a dynamic load adaptation. This also includes the optimised biases, and operation classes of carrier and peaking amplifier using a large signal harmonic balance simulation to offer improvements in efficiency. The design comprises several design steps for which the optimisation is applied to each in order to obtain high performances of the entire Doherty RF power amplifier.

However, it is important to note that in the design of the Doherty RF power amplifier, the DC simulation should be carried out first in order to find the optimal bias point and bias network based on the class of operation and power requirements. In this paper the bias circuit was designed based on Class AB carrier and Class C peaking amplifiers. In Class AB, the transistor is biased just at the start of conduction, about 300mA while Class C is biased in the pinch off region and conducts as the input signal increases.

Having obtained the selected DC quiescent current to maximally cancel the signal distortions, the next step is to determine the design of Class AB amplifier and to obtain the performance regarding the output power and efficiency before incorporating into Doherty design. The output and input impedance was internally matched to 50 Ω impedance microstrip transmission lines, the 15mm offset lines is added to the input side before the input matching network and another 15mm offset line was added to the output side after the output matching network. The Class AB in this design will serve as a carrier amplifier in which the Doherty configuration and the quarter wavelength line

will enable it to see high output impedance which leads to its saturation and keeps it maximum voltage at constant condition.

Figure 4.2 shows the linear results obtained from the matched Class AB power amplifier, the gain is flat in the range of 3.47 to 3.6 GHz with excellent matching at the input and output return losses.

The non-linear simulation of Class AB was performed and the performance of the design in terms of output power and efficiency was observed. The 38dBm output power was achieved at 1dB compression point and 32% efficiency. The same was applied to Class C, but with different bias point.

3dB quadrature splitters in the past were very expensive and difficult to design for wide bandwidths and at low frequencies are bulky in nature. The power input splitter is part of the Doherty configurations and if properly designed can contribute to the total efficiency of the system. Our investigation shows that the operation of this technique is strongly influenced by the coupling factor of the input splitter. In fact, in this research the splitters have been designed and tested in terms of operation frequency and bandwidth, and showed good results as seen in Figure 4.3, Figure 4.4, and Figure 4.5. It should be noted that this splitter, at the input of amplifier, divides the input signal equally, but 90-degree phase difference between the carrier and peaking amplifiers. The splitter, the Carrier Class AB, the peaking Class C, and impedance transformer at the output are combined to form the Doherty RF power amplifier.

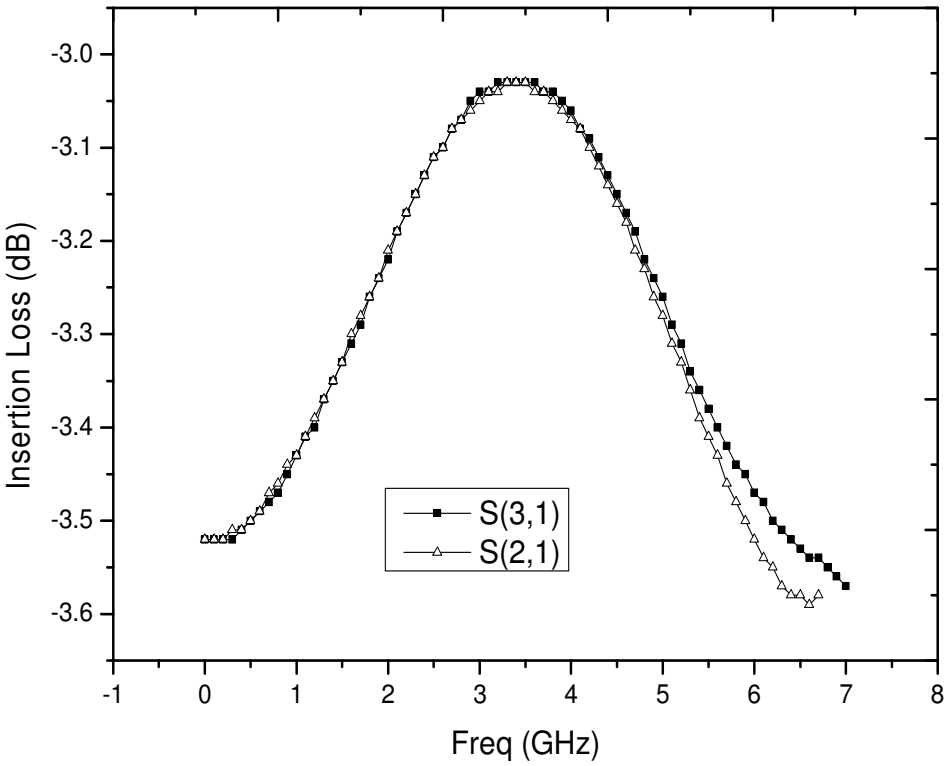

Figure 4.3: Insertion loss of S21 and S31 in dB.

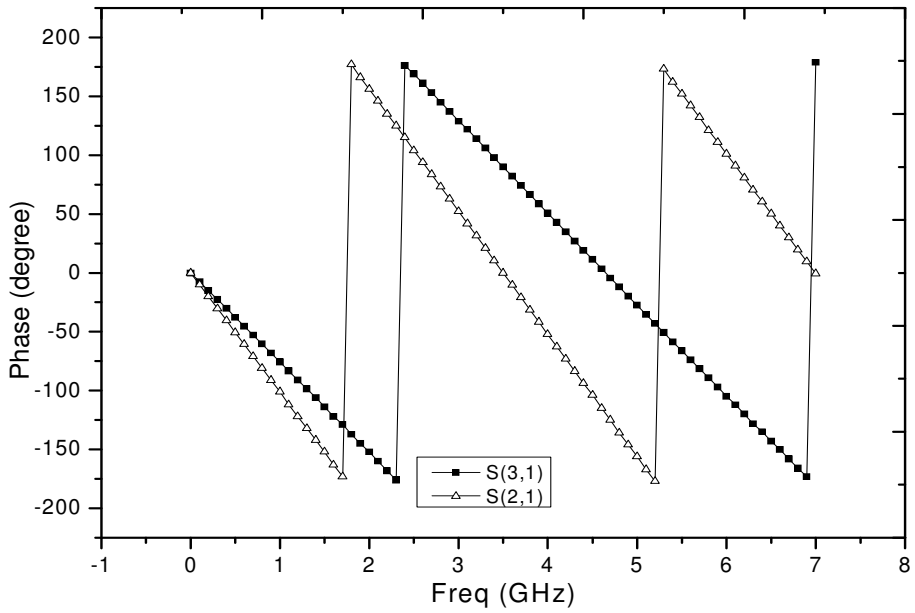

Figure 4.4: The phase variations of S21 and S31 in degrees.

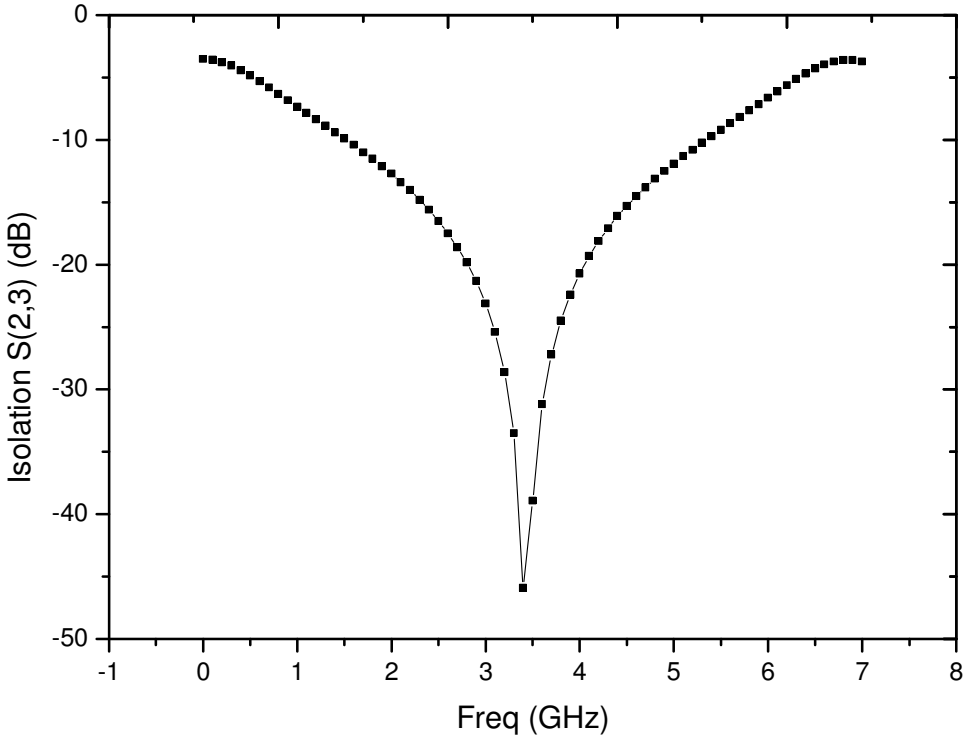

Figure 4.5: Isolation between the ports 2 and 3.

4.3 Implementation & results

Figure 4.6, shows the prototype diagram of the proposed Doherty RF power amplifier with offset transmission lines at both output and input circuit which maximise the overall system's efficiency with the configuration of Class AB and Class C amplifiers. The Freescale N-Channel Enhancement-Mode Lateral MOSFET, MRF7S38010HR3 transistor with 33dBm output power was used for both Class AB and Class C amplifiers and produces a Doherty RF power amplifier with 43dBm output power and efficiency of 66%. The bias conditions used in this experiment are: class AB as carrier amplifier was set at Vgs = 3.0V (Ids =300 mA) and class C as the peaking amplifier was set at Vgs = 2.4V (Ids = 1 mA). Both amplifiers use the same drain voltage (30V).

The non-linear simulation of Doherty RF power amplifier was achieved through the ADS simulator. The following results are based on simulations and were initially characterised for AM-AM and AM-PM responses, as well as output power and efficiency. The performance comparisons between the Doherty amplifier and Class AB amplifier were performed. The output power of Class AB power amplifier standalone was 37.5dBm and with Doherty configuration, the output power was increased to 43dBm at 1dB compression point, while the efficiency increased to 66%.

Figure 4.7 represent the variation of the input power in relation to output power of the Doherty amplifier. It clearly shows that 43dBm output power is achieved at linear region of the amplifier, and this was achieved due to the characteristic of gain compression and expression of the Doherty amplifier. The peaking amplifier Class C late gain expansion compensated the carrier Class AB amplifier gain compression. Figure 4.8 represent the AM-PM data and the graph shows the phase can vary approximately 40 to 47 degree at the 1dB compression point. Figure 4.9 represent the gain in relation to output power, the graph shows the power gain of Doherty amplifier degraded severely compared to Class AB amplifier due to the arrangement of lower biasing.

Figure 4.10 shows the power added efficiency versus output power. The Doherty RF power amplifier has higher efficiency over the range of wide output power levels compared to Class AB RF power amplifier.

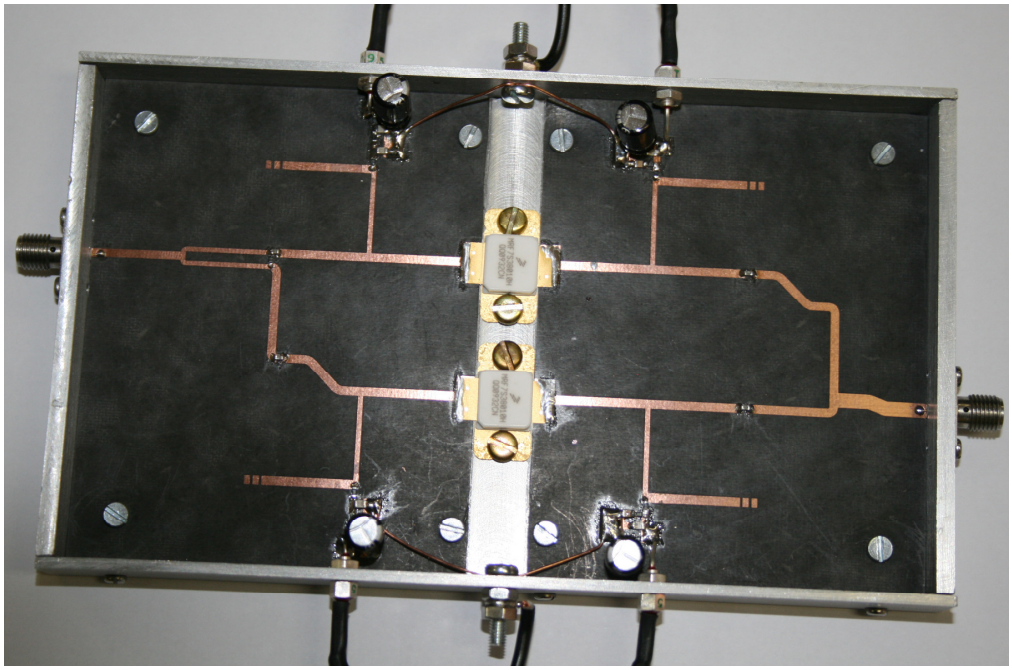

Figure 4.6**:** Implemented prototype of proposed power efficient power amplifier.

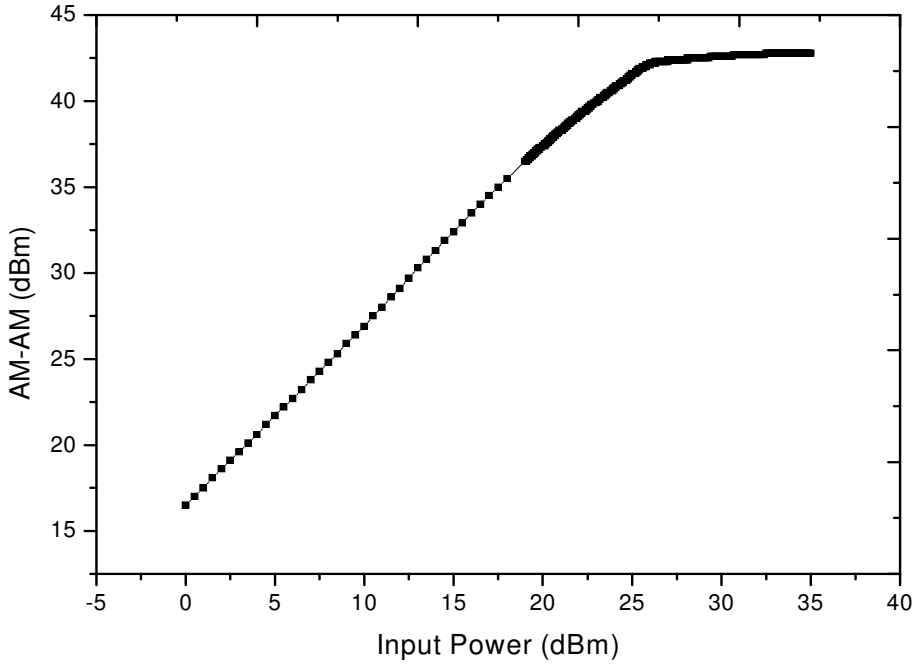

Figure 4.7: AM-AM characteristics of load modulation amplifier.

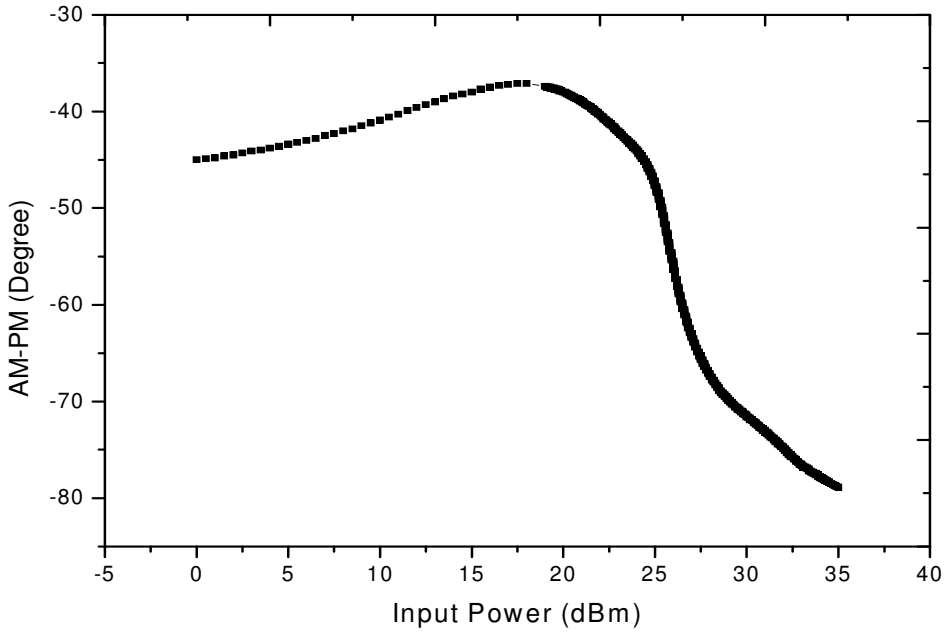

Figure 4.8: AM-PM characteristics of load modulation amplifier.

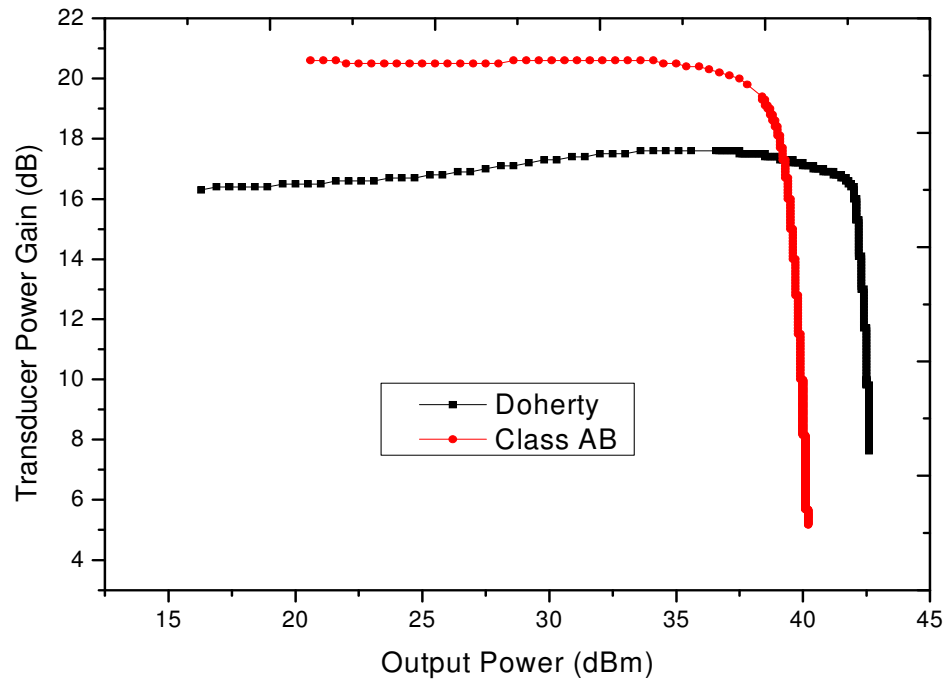

Figure 4.9: Gain characteristics.

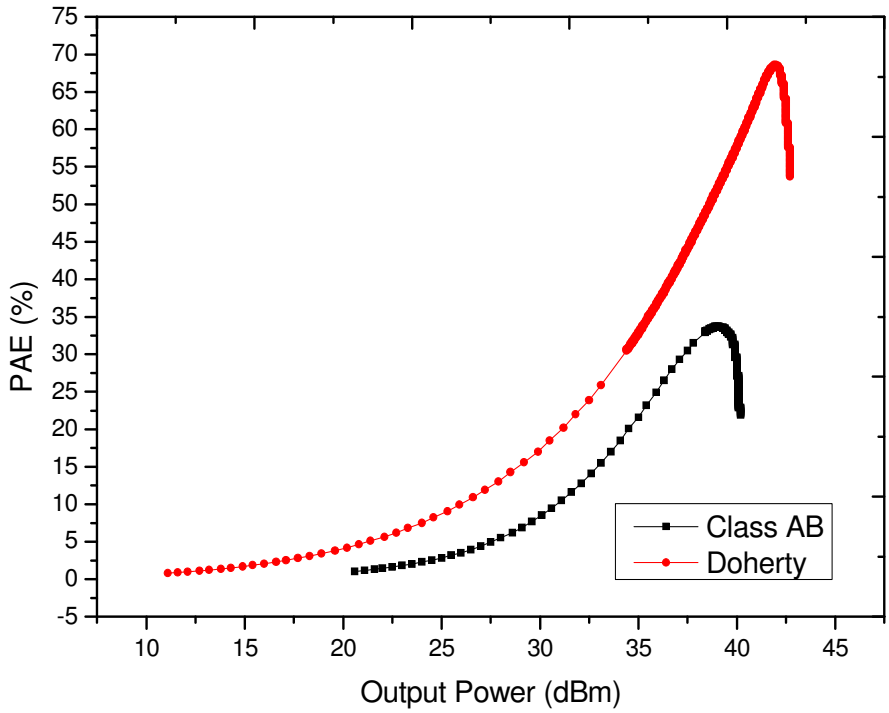

Figure 4.10: Power-Added Efficiency.

4.4 Conventional balanced and load modulation circuit architectures

The conventional balance and load modulation amplifiers exploit the Freescale N-Channel Enhancement-Mode Lateral MOSFET MRF7S38010HR3 transistors. The balanced amplifier was first proposed to improve efficiency of 3G base station, is designed to work over a given dynamic range where the amplifier should behave linearly. Conventional balanced amplifier was a commercially successful 2G/3G base station amplifier. However, there are some problems that limit the balanced amplifier for use as power amplifier for 4G communications.

The balanced amplifier can be realised by combining two class AB amplifiers as shown in Figure 4.11. The splitter divides the input signal equally with 90-degree phase-shift, after the input matching circuitry the signals are fed to the transistors' gates. With the proper biasing of VGS both class AB amplifiers are set to conduct in the positive cycles, the signals from the drain of the transistors are also 90 degree in phase and feed into the combiner and at the output, combiner combines the signals with 90 degree phase differences, and full sine wave. While by combining the carrier class AB and the peaking class C amplifiers can realise load modulation RF power amplifier as shown in Figure 4.12. The splitter divides the input signal into two equal magnitude but 90-degree phase difference. At the output a microstrip quarter wave impedance inverter combines the signals.

The concept of load modulation technique has been fully explained in chapter two. The load modulation RF power amplifier improves the efficiency and the linearity by complementing the saturation class AB amplifier with the turn on characteristic of class C amplifier. The design comprises of step-by-step procedure for the optimum design of energy efficient power amplifier, the proposed additional of 90 degree offset lines at the output and input matching network for which will prevent power leakage at the output junction between the output impedance transformer and peaking class C amplifier. The gate biases and the individually matching of class AB and class C amplifiers are further optimised to achieve high efficiency, linearity and wideband characteristics. The peaking amplifier allows the load modulation amplifier to respond to the high input levels of short duration, by amplifying the signal peaks, and to dynamically change the load impedance of the main class AB amplifier.

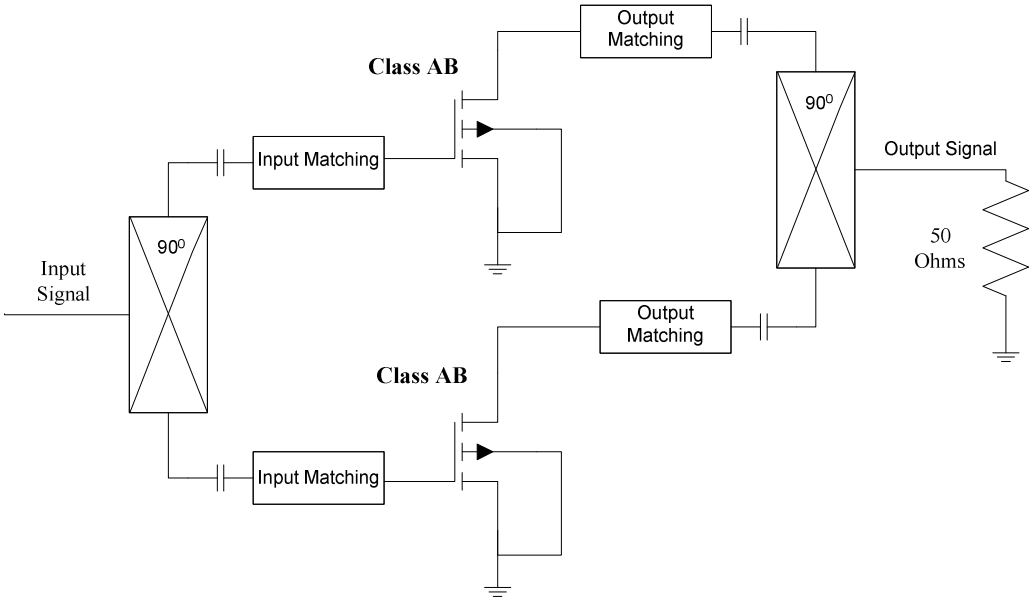

Figure 4.11: Balanced amplifier configuration.

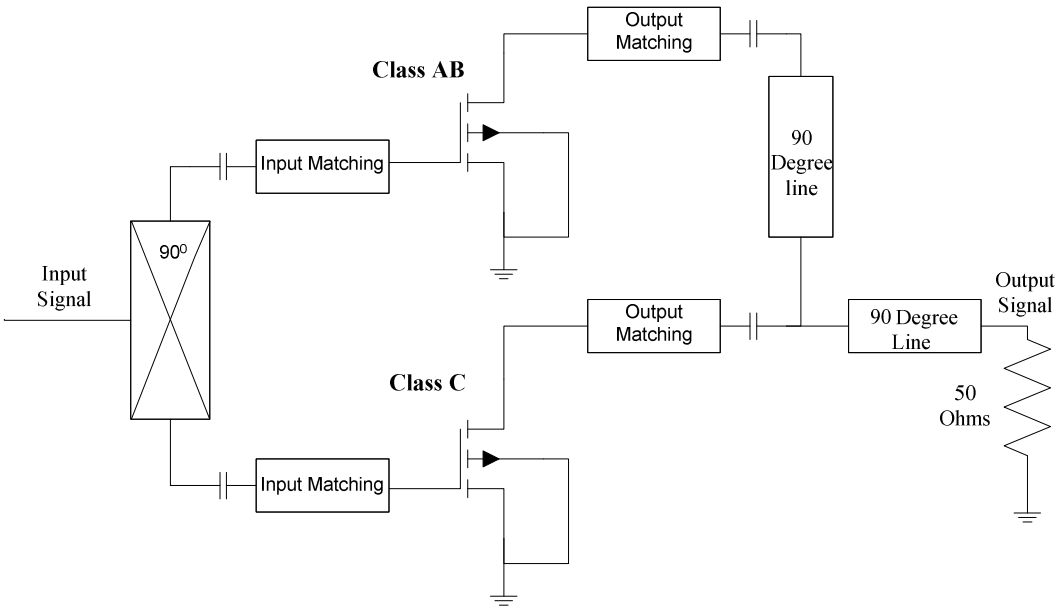

Figure 4.12: load modulation amplifier configuration.

4.5 Design layout and results

The conventional balanced and load modulation amplifiers are fabricated with RT 5880 substrates, H=0.5mm and relative permittivity of 2.2. In Figure 4.13 and

Figure 4.14 shows the layout of conventional balanced amplifier and load modulation amplifiers respectively.

Figure 4.15 and Figure 4.6 in chapter 4 Page 70 shows the implemented prototype of conventional balanced and load modulation amplifiers respectively. In Figure 4.16 and Figure 4.17 shows the simulated linear performance of the balance and load modulation amplifier respectively, the gain is flat in the range of 3.47 to 3.53 GHz with excellent input and output return losses.

The non-linear simulations and the comparisons of conventional balanced and load modulation amplifiers are performed. The bias conditions used in this experiment those shown in Table 4.1, for balanced amplifier while in Table 4.2; represent that of load modulation amplifier. The drain bias voltage VDS = 30V for both two transistors of balanced and their gate voltage is VGS = 3V. The drain bias voltage of load modulation amplifier is VDS = 30V for both carrier and the peak transistors, while their respective gate bias voltages are VGS (Carrier) = 3V and VGS (Peaking) = 2.2V. Figure 4.18 represent the comparison of the variation of the input power versus output power of both balanced and load modulation amplifiers. It clearly shows that 43dBm output power is achieved at the linear region of both amplifiers. Figure 4.20 represent the transducer power gain versus output power. The load modulation has less gain

compared to balanced amplifier; this is due to the fact that the peaking amplifier of load modulation is biased in Class C mode. Figure 4.21 shows the PAE versus output power of balanced and load modulation amplifier. From the graph one can be seen that the load modulation amplifier has a higher efficiency over the wide range of output power than conventional balanced amplifier. The PAE of 66% is obtained at 1dB compression point of 42 dBm output power of load modulation amplifier while the PAE of 50% is obtained at 1dB compression point of 42 dBm output power of conventional balanced amplifier.

The load modulation offers improved efficiency at the whole range of output power compared to conventional balanced amplifier. The heart of the load modulation is the load modulation output combiner and that is the fascinating part of the design, while the input behaves the same as a conventional balanced amplifier.

Table 4.1: Bias point setting for balanced amplifier.

Drain Voltage (V)	Class AB1 VGS (V)	Class AB2 VGS (V)
30	3.0	3.0

Table 4.2: Bias point setting for load modulation.

Drain Voltage (V)	Carrier VGS (V)	Peaking VGS (V)
30	3.0	2.2

Table 4.3: Performances of load modulation and balanced amplifiers.

	Gain (dB)	PAE (%)
Balanced	19.5	50
Load Modulation	16.5	66

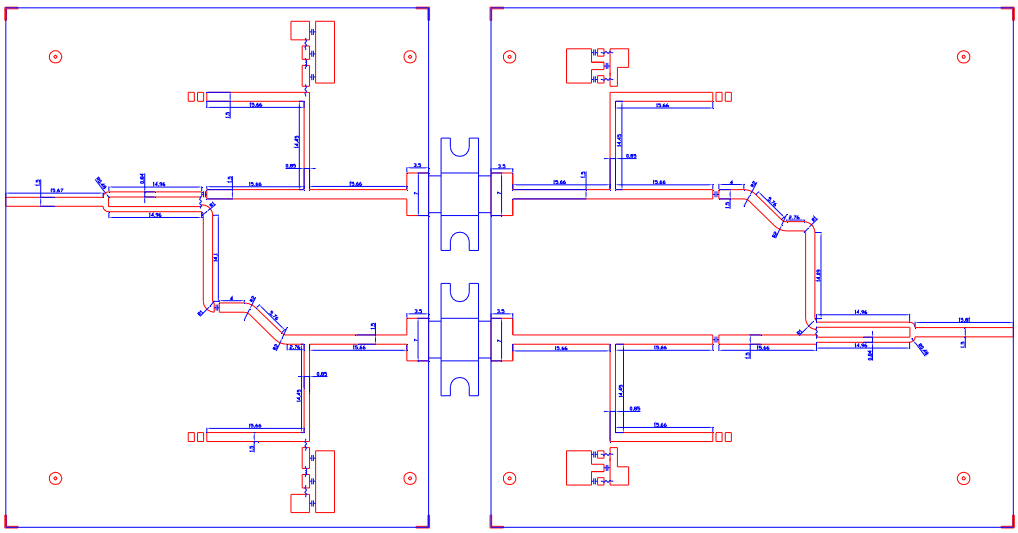

Figure 4.13: Design layout of Balanced amplifier.

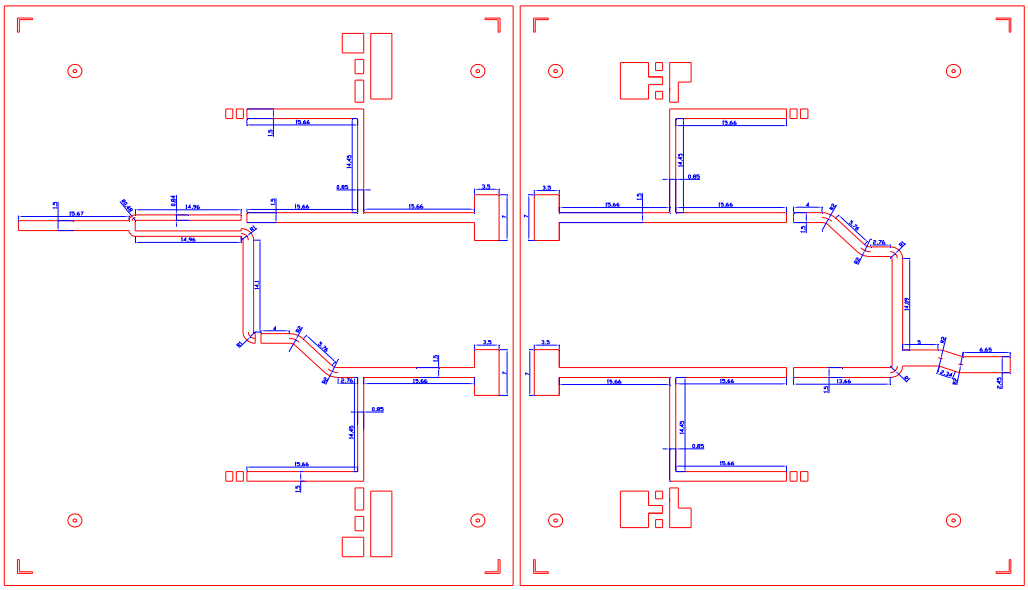

Figure 4.14: Design layout of load modulation amplifier.

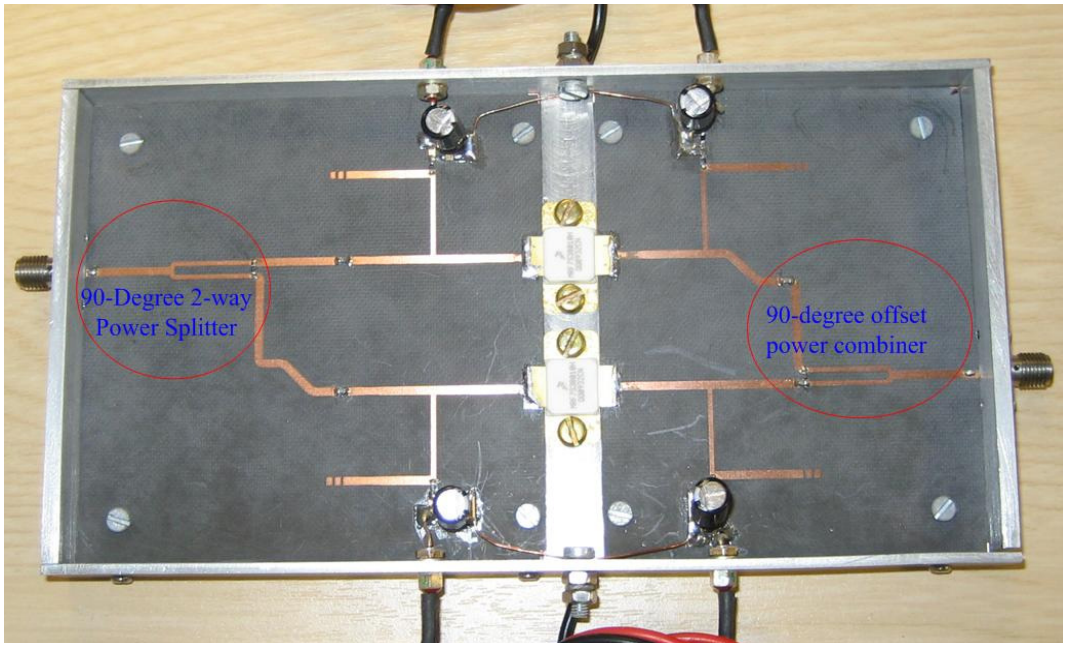

Figure 4.15: Implemented prototype of Balanced amplifier.

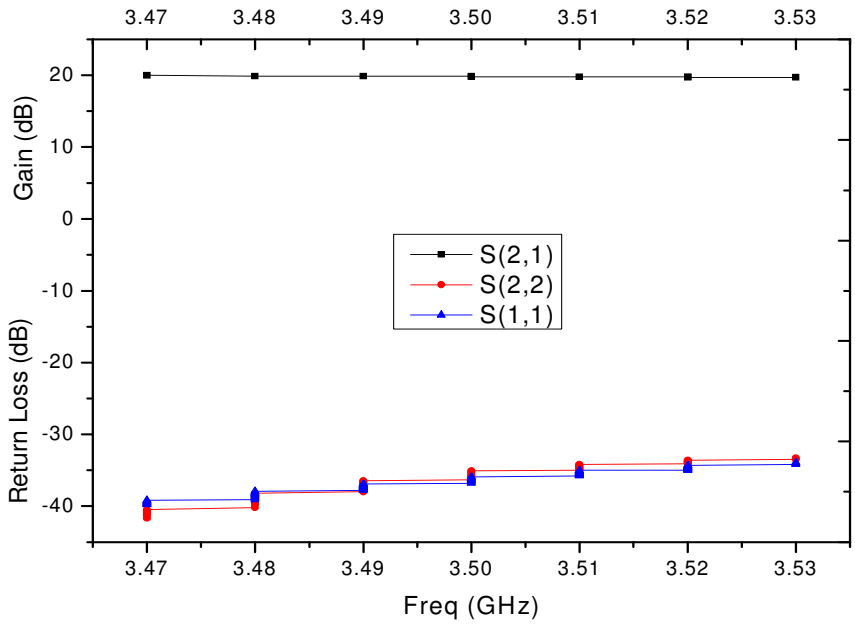

Figure 4.16: Linear simulation of Balance amplifier.

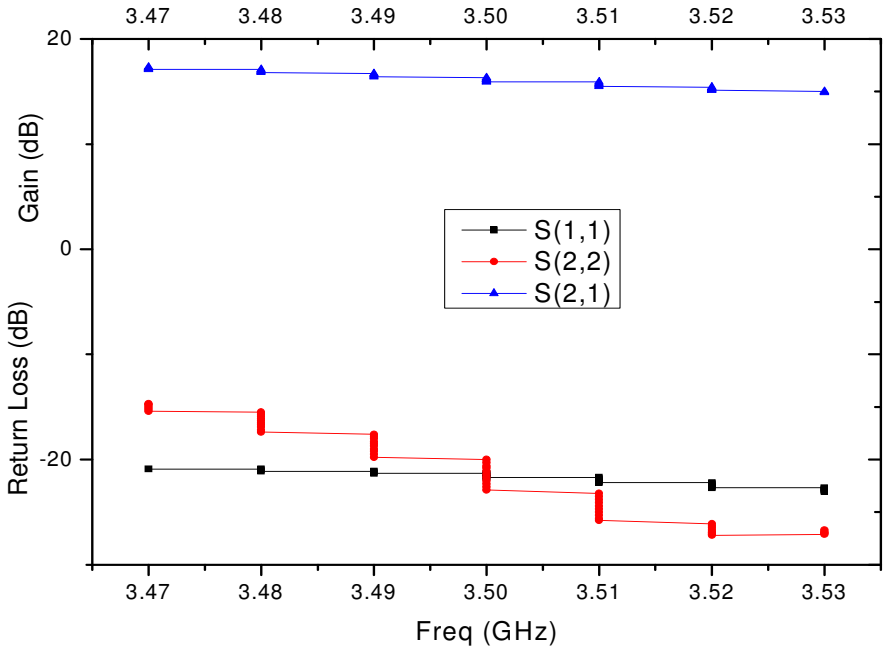

Figure 4.17: Linear simulation of load modulation amplifier.

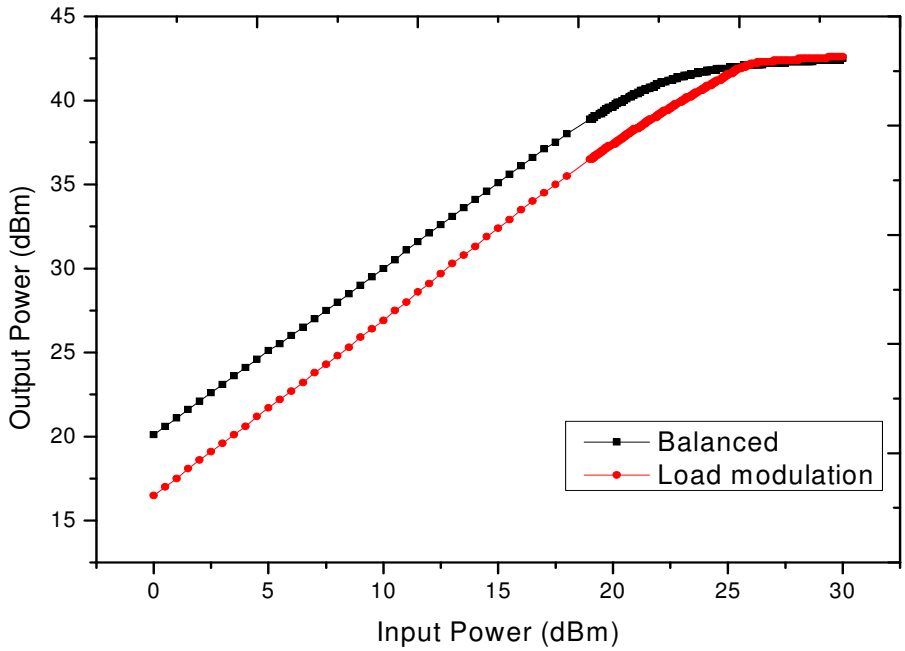

Figure 4.18: AM-AM responses.

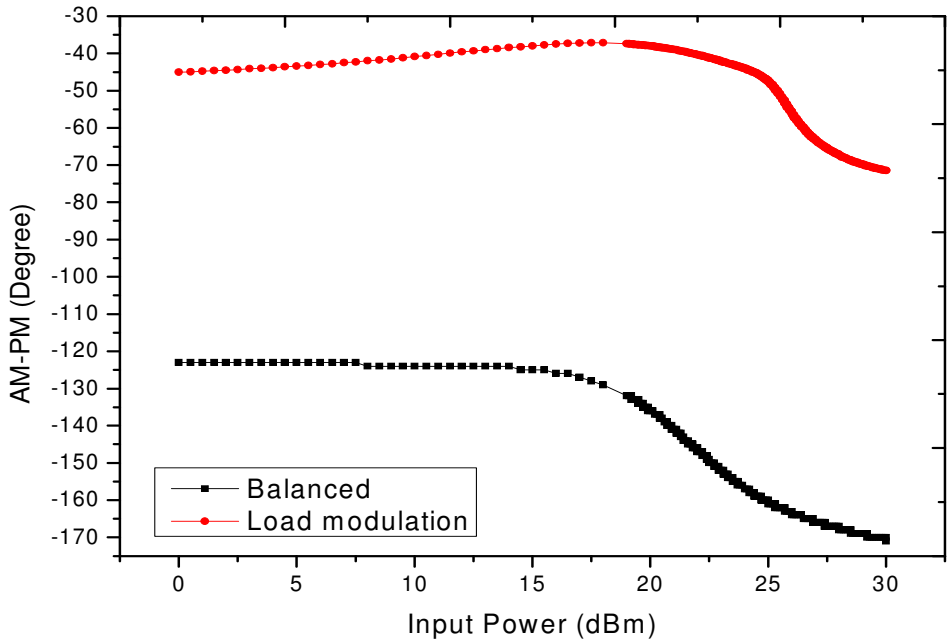

Figure 4.19: AM-PM responses.

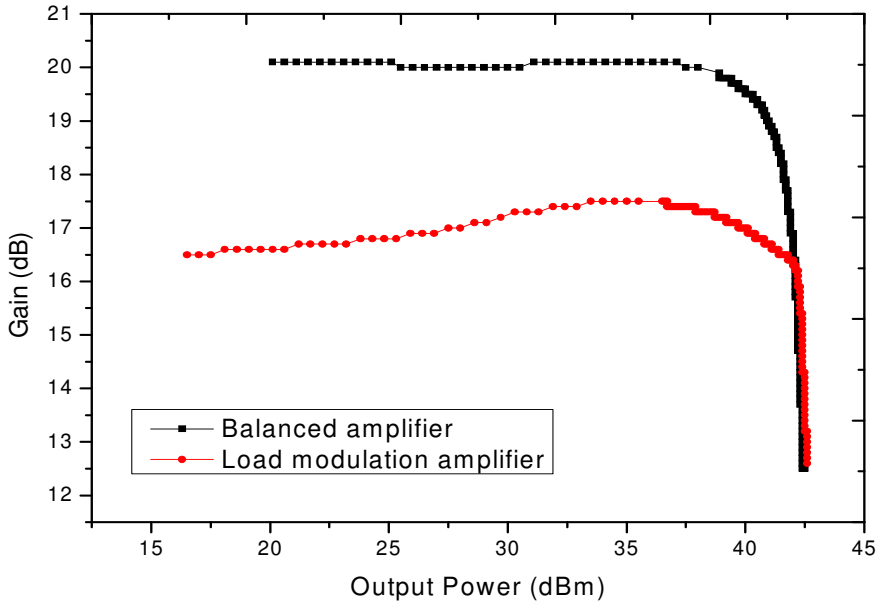

Figure 4.20: Transducer power gain.

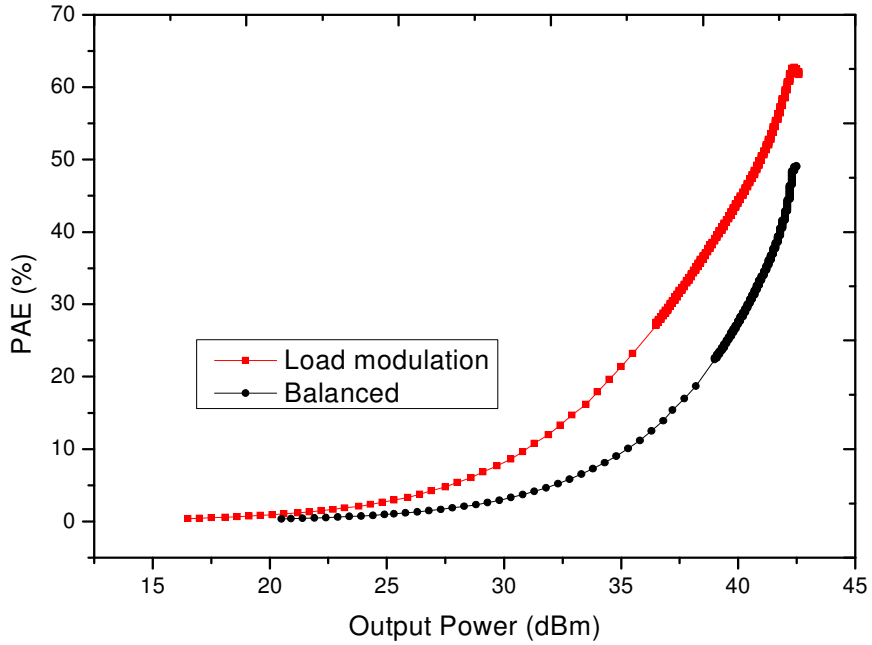

Figure 4.21: Power-Added Efficiency.

4.6 Uneven load modulation circuit design for base station

In this section, the author presents an innovative uneven load modulation RF power amplifier for the applications of B3G base station whose operating frequency covers 3.4GHz to 3.6GHz band [1-13]. The performances of uneven load modulation RF power amplifier have been compared with the load modulation RF power amplifier. The results of 45dBm output power and 66% power added efficiency have been achieved.

Load modulation RF power amplifiers are based on load modulation techniques and when using two transistors, the second transistor should be able to pull the load presented to the first transistor for high output power and efficiency. However, it is impossible for Class C to deliver the same output power as Class AB because, Class C used part of the input signal to turn on and for this reason Class C will never pull out the

load presented to Class AB for peak efficiency. Therefore, to solve this problem, uneven load modulation RF power amplifier with uneven signal splitter at the input has been designed, and this will allow more input signal to pass through Class C amplifier than Class AB amplifier for peak efficiency. The proposed diagram of this kind of amplifier is presented in Figure 4.22.

The bias and biasing networks are very important in controlling bias current and voltage for the operation of uneven load modulation RF power amplifier. The DC quiescent current for Class AB is in the region between the cut-off point/pinch-off and the Class A bias point, typically at 10 to 15 percent of I_{ds} while for Class C is below the threshold. With this arrangement, and at the low level of input signal looking at Figure 4.23, the Class C will act as open circuit, because at low level input signal, the signal is too small to turn on the Class C amplifier and as a result of this, the quarter wavelength transmission line present in front of Class AB will enable Class AB amplifier to see high output impedance which leads to its saturation and keeps it at maximum voltage constant condition.

The transformation of input, output and characteristic impedance of a quarter wave transmission line is given as:

$$Z_1 = Z_O^2 / Z_2 \tag{4.1}$$

Z_1 and Z_2 are the input and output impedance respectively and Z_o is the characteristic impedance of the transmission line. However, with the increased of input signal and the saturation of Class AB, the suitable bias of Class C will enable it to turn on

automatically and start sending current and the same time increasing the impedance of Z_O. With the increase of impedance of Z_O results in decrease of impedance of Z_1, which is the impedance seen by Class AB. At this stage, both Class AB and Class C amplifiers will see a terminating impedance of $2R_L$, while Class C amplifier also reaches its saturation. This means that both Class AB and Class C amplifiers contributed the same amount of power to the load, Figure 4.22 i.e $I_0 = I_2$, and Z_1 and Z_2 becomes:

$$Z_1 = Z_O^2 / 2R_L \quad (4.2)$$

$$Z_2 = 2R_L \quad (4.3)$$

As we have seen, the operation of the second amplifier has been forced to operate in Class C, and as we all know that, the DC quiescent current of Class C amplifier is below the threshold, typically have lower gain than Class AB amplifier. Therefore to achieve the maximum output power and overall performance, one solution is to supply more input power to Class C amplifier than Class AB amplifier. With this solution, one should be able to achieve maximum output power without creating AM-AM distortion.

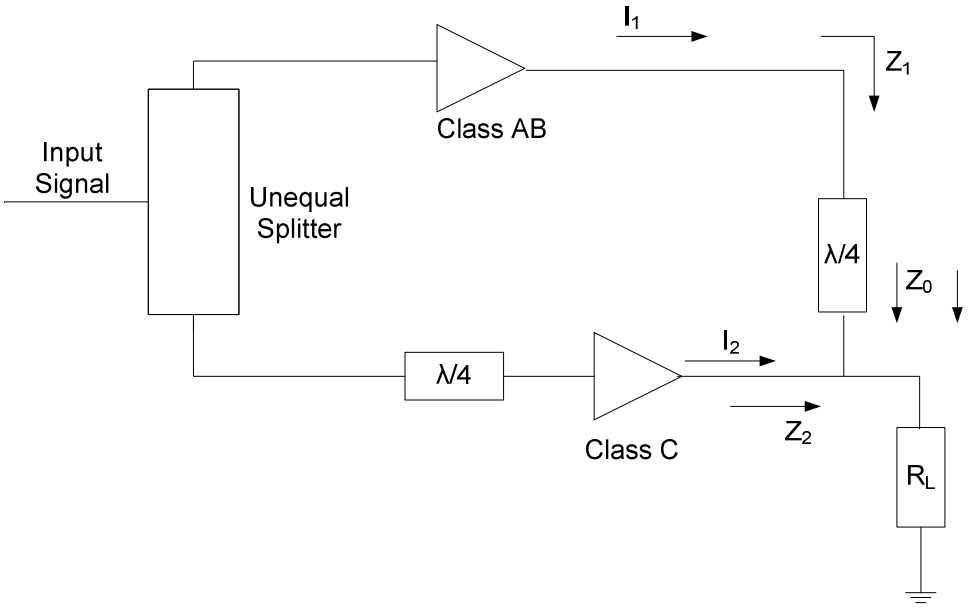

Figure 4.22: Uneven load modulation at high level input signal.

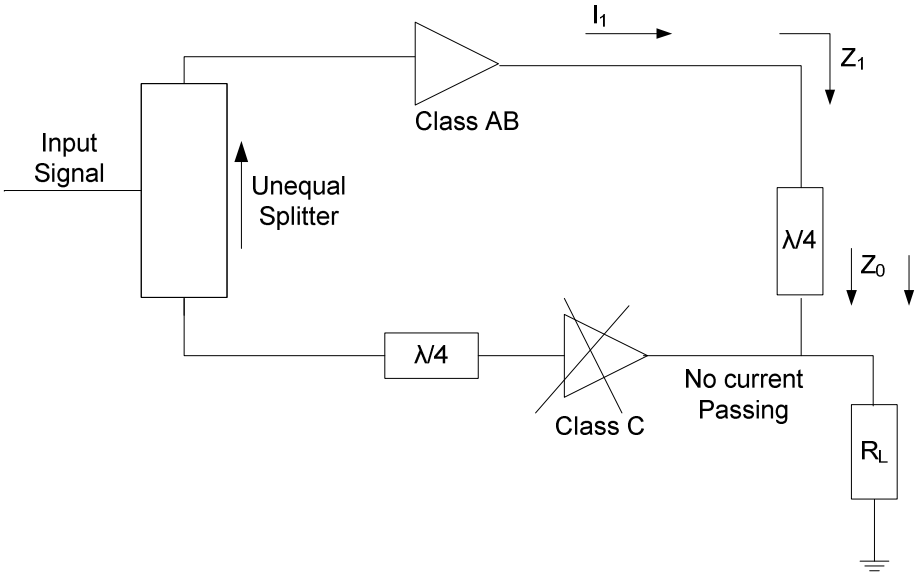

Figure 4.23: Uneven load modulation at low level input signal.

4.7 Design prototype and results

An unequal splitter is part of an uneven load modulation RF power amplifier and if design properly can contribute a lot to the total efficiency of the system. An unequal splitter, the Carrier Class AB, the peaking Class C, and impedance transformer at the output are combined to form an uneven load modulation RF power amplifier.

Figure 4.24 shows the implemented prototype of uneven load modulation RF power amplifier which fabricated with RT 5880 substrates, H=0.5mm and relative permittivity of 2.2 and covers the range of frequency from 3.4GHz to 3.6GHz, with excellent input and output return losses.

The comparisons of uneven load modulation RF power amplifier and load modulation RF amplifier have been performed. The bias conditions used in this experiment are: The drain bias voltage VDS for all transistors is 30V and the gate bias voltage VGS for both Class AB is 3.0V and for Class C is 2.4V. Figure 4.25 represent the comparison of the variation of the input power versus output power for both uneven load modulation RF power amplifier and load modulation RF power amplifier. It clearly shows that there's an increase of 2dB more in compared with load modulation, this shows that with uneven splitter you can able to pull more output power than with equal splitter. The 45dBm output power was achieved at the linear region of uneven load modulation. Figure 4.26 represent the transducer power gain versus output power. The uneven load modulation has more gain compared to load modulation; this is due to the fact that we provided more input power to Class C than Class AB in the uneven configuration, while in the load modulation configuration, the input signal are equally divided. Figure 4.27 shows the power added efficiency (PAE) versus output power of uneven load modulation RF power amplifier and load modulation amplifier. From the graph one can be seen that

uneven load modulation amplifier has a higher efficiency. The PAE of 66% is obtained at 1dB compression point of 45dBm output power of uneven load modulation RF power amplifier while the PAE of 62% is obtained at 1dB compression point of 42dBm output power of load modulation RF power amplifier. The heart of uneven load modulation and the load modulation is the load modulation output combiner, and that is the fascinating part of the design.

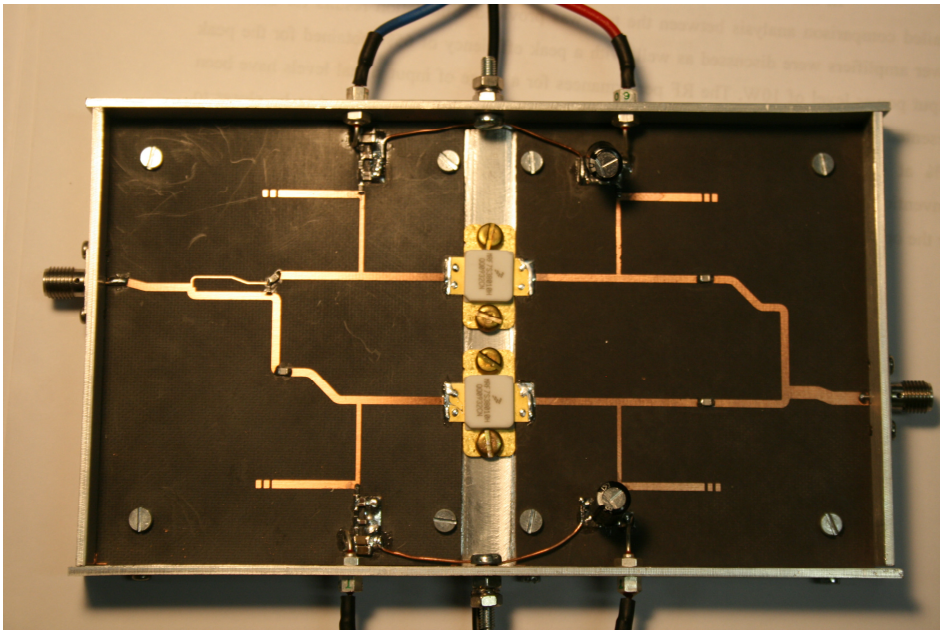

Figure 4.24: Prototype of uneven load modulation RF power amplifier.

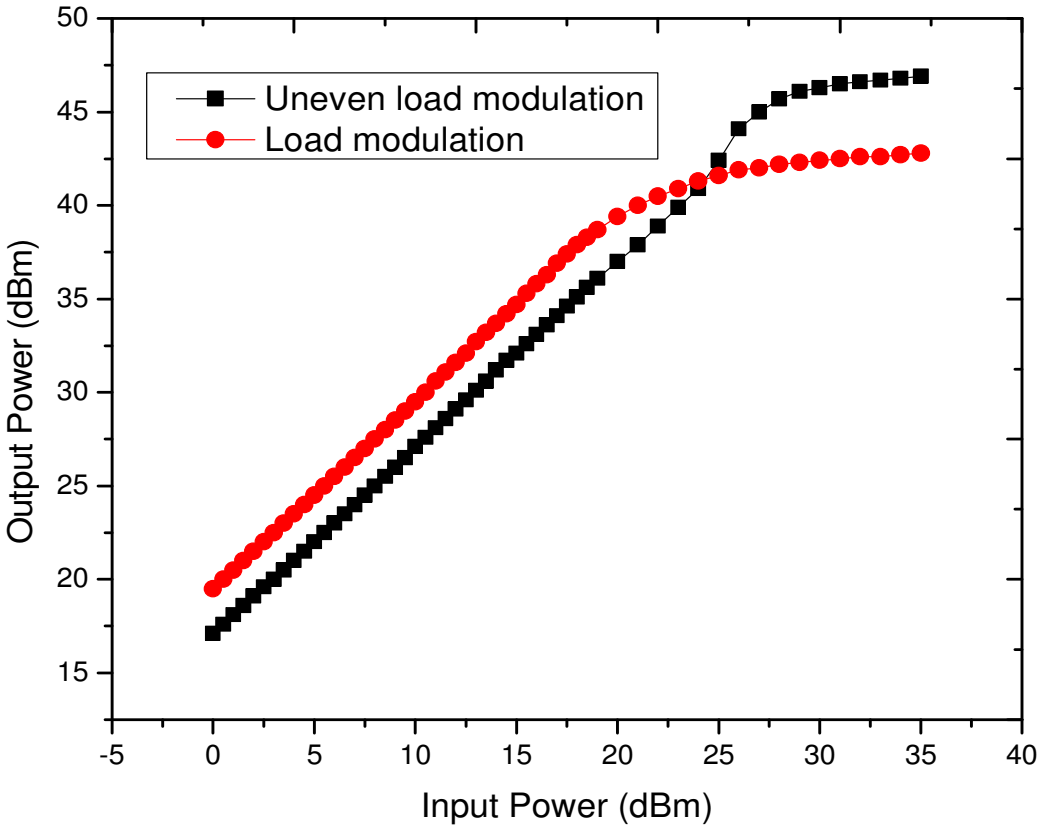

Figure 4.25: AM-AM responses.

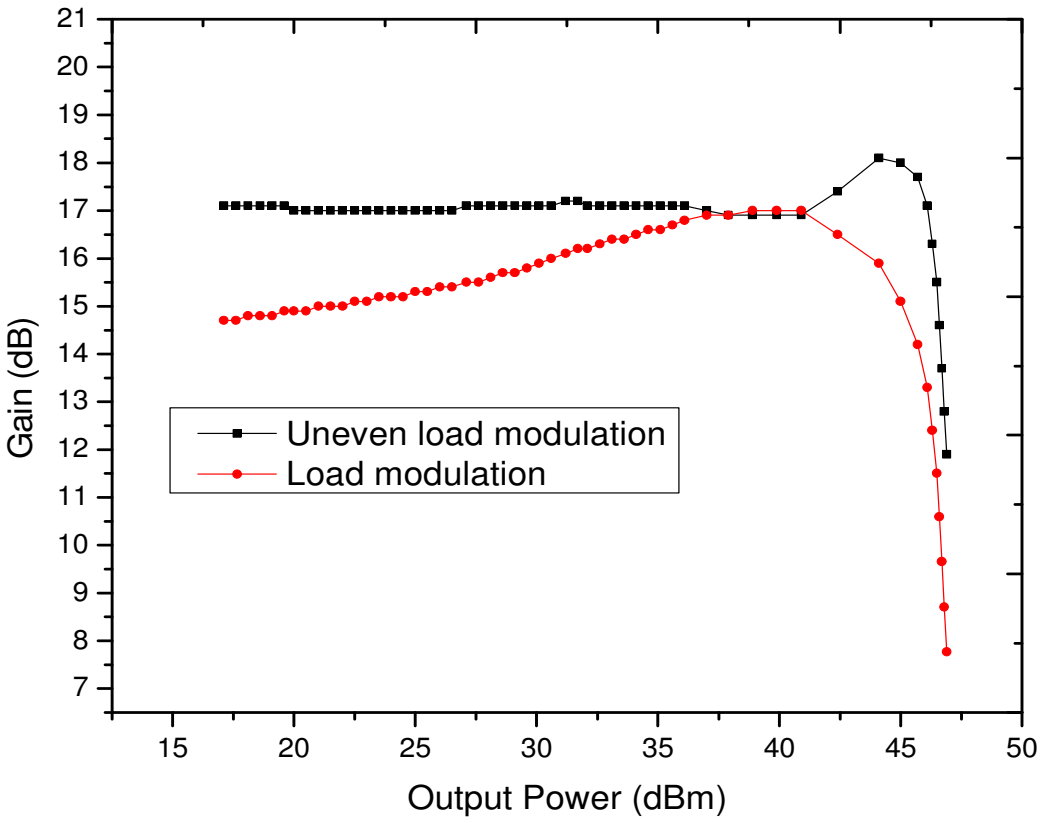

Figure 4.26: Transducer power gain.

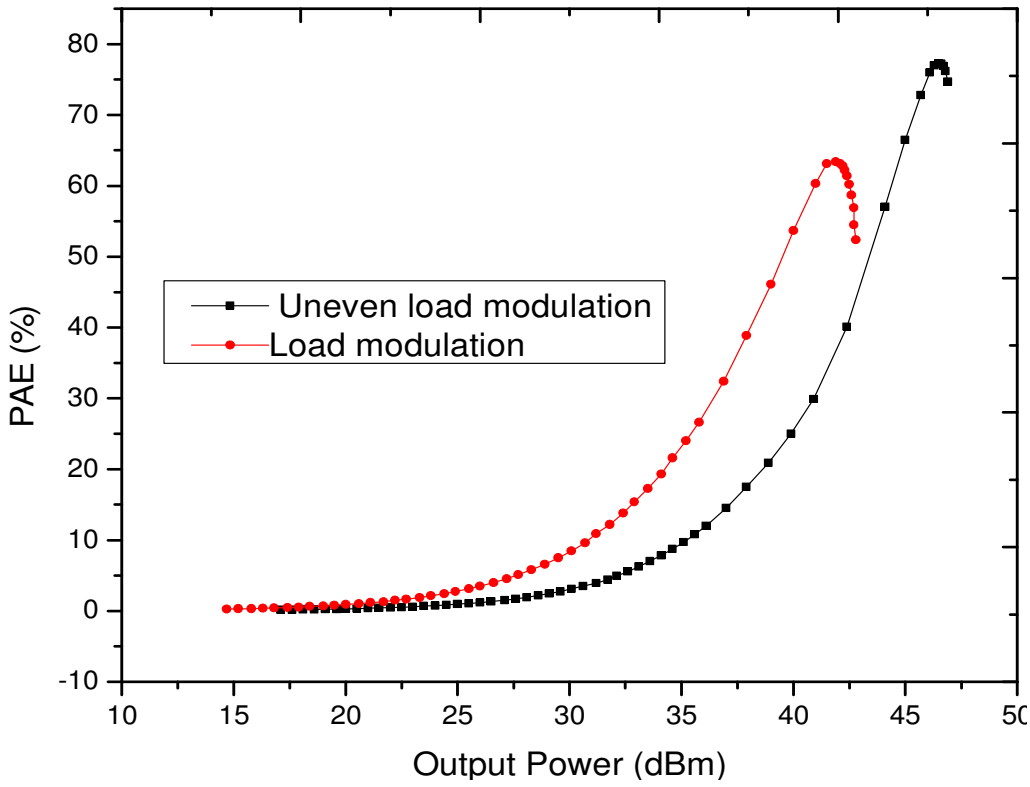

Figure 4.27: Power-Added Efficiency.

4.8 Conclusion

Three different topologies of RF power amplifiers (Doherty, Conventional Balanced, and Uneven Load modulation) have been designed with custom-made even and uneven signal splitters that have been tested and compared, for base station applications. The presented designs can be summarised separately as follows:

In section 4.1, the Doherty RF power amplifier was designed using Freescale N-Channel Enhancement-Mode Lateral MOSFET transistor, the achieved results of the Doherty were compared with conventional Class AB amplifier, and Doherty exhibited a PAE of 66% at peak output power of 43 dBm close to 1dB compression point. And exhibited a PAE of 40% at average output power of 37 dBm back off. The Class AB, Class C, input signal splitter and output transformer were adjusted to optimise the design under Doherty operation. The Doherty RF power amplifier has demonstrated good concession between the cost, linearity, efficiency, and output power. The proper phasing of 3dB quadrature splitter effectively contributed to the total efficiency of the system. In addition, the turn–on of the class C amplifier was dependent on the gate bias voltage and the input signal.

Section 4.4 presents the performance comparisons between load modulation power amplifier and conventional balanced power amplifier. The achieved results of the proposed design process have shown an excellent efficiency and power performances. Load modulation achieved a PAE of 66% at peak output power of 43 dBm close to 1dB compression point. And exhibited a PAE of 40% at average output power of 37 dBm back off., while conventional balanced achieved a PAE of 50% at peak output power of 42 dBm and achieved a PAE of 15% at average output power of 37 dBm back off .

Load modulation has 16% peak PAE achievement over conventional balanced RF power amplifier.

The proper phasing of input signal splitter effectively contributed to the total efficiency of the system. The load modulation amplifier improved the efficiency over a wide range of output power compared to conventional balanced amplifier. The load modulation has less gain compared to balanced amplifier due the arrangement of lower biasing of Class C peaking transistor of load modulation. The operation of this design was strongly influenced by the coupling factor of the splitter, biasing of class AB and C amplifiers.

In section 4.6 the performance comparisons between uneven load modulation RF power amplifier and load modulation RF power amplifier are presented. As can be seen, the operation of the second amplifier has been forced to operate in Class C, (typically Class C have lower gain than Class AB amplifier), and hence, it is impracticable for Class C to deliver the same output power as Class AB. This is because the Class C used part of the input signal to turn on the active device and for this reason Class C will never pull out the load presented by Class AB for peak efficiency. To achieve the maximum output power and overall performance, one solution is to supply more input power to Class C amplifier than Class AB. With this method one should be able to achieve maximum output power without creating AM-AM distortion. The operation of this design was strongly influenced by the coupling factor of the splitter, biasing of class AB and C amplifiers. The achieved results of the proposed design process have shown an excellent efficiency and power performances. The uneven load modulation RF power amplifier achieved a PAE of 66% at peak output power of 45 dBm close to 1dB compression point. And exhibited a PAE of 25% at average output power of 39 dBm back off.

References

[1] The W. H. Doherty, “A New High Efficiency Power Amplifier for Modulated Wave”, Proc. IRE, Vol. 24, No. 9, PP. 1163– 1182, September, 1936.

[2] F. H. Raab, “Efficiency of Doherty RF Power Amplifier System”, IEEE Trans. Broadcasting, Vol. BC-33, No 3, PP. 77-83, September, 1987.

[3] S.C. Cripps, Advanced Techniques in RF Power Amplifier Design,Norwood, MA: Artech House, 2002.

[4] S.C.Cripps, RF Power Amplifier for Wireless Communications, Norwood, MA: Artech House, 1999.

[5] A. S. Huusaini, R. Abd-Alhameed, J. Rodriguez, “Implementation of Efficiency Enhancement Techniques in the Linear Region of Operations of Power Amplifier”, IT 7th Conference on Telecommunications, No 103, PP. 105 – 108, May, 2009.

[6] Abubakar Sadiq Hussaini, Bashir A. L. Gwandu, Raed Abd-Alhameed, Jonathan Rodriguez, "Design of Power Efficient Power Amplifier for B3G Base Stations", 9th International Symposium on Electronics and Telecommunications (ISETC 2010) , Timisoara, Romania 11-12 November 2010, Paper No. 103, pp. 89-92, ISBN: 978-1-4244-8458-4

[7] Abubakar Sadiq Hussaini, R. Abd-Alhameed, J. Rodriguez, “Green Radio: Approach Towards Energy Efficient Power Amplifier for 4G Communications”, Proc. of the 25th WWRF Meeting, Kingston-upon-Thames, UK, 16th-18th November 2010.

[8] Abubakar Sadiq Hussaini, Raed Abd-Alhameed, Jonathan Rodriguez, "Design of Energy Efficient Power Amplifier for 4G User Terminals", 17th IEEE International Conference on Electronics, Circuits, and Systems (ICECS 2010), Athens, Greece 12-15 December 2010, Paper No. 533, pp. 617-620, ISBN: 978-1-4244-8156-9

[9] C. T. Burns, A. Chang, D. W. Runton, “A 900 MHz, 500 W Doherty power amplifier using optimised output matched Si LDMOS power transistors”, IEEE MTT-S Int. Microw. Theory Tech., Symp. Dig., PP. 1557 – 1580, June, 2007.

[10] Raab F.H., Asbeck P., Cripps S., Kenington P.B., Popovic Z.B., Pothecary N., Sevic J.F., Sokal N.O., “Power amplifiers and transmitters for RF and microwave”, IEEE Transactions on Microwave Theory and Techniques, Vol. 50, No 3, PP. 814 – 826, March, 2002.

[11] K. J. Cho, J-H. Kim, and S. P. Stapleton, “A Highly Efficient Doherty Feed-Forward Linear Power Amplifier for W-CDMA Base-Station Applications,” IEEE Trans. on MTT, Vol. 53, pp. 292 - 300, Jan. 2005.J. Groe, “Polar transmitters for wireless communications”, IEEE Communications Mag., Vol. 45, No 9, PP. 58 – 63, Sept. 2007.

[12] P. B. Kenington, High- Linearity RF Amplifier Design, Norwood, MA: Artech House, 2000.

[13] C. F. Campbell, “A fully integrated Ku-band Doherty amplifier MMIC,” IEEE Microw. Wireless Compon. Lett., vol. 9, no. 3, pp. 114–116, Mar. 1999.

CHAPTER FIVE

5. Multi-Stage Load Modulation RF Power Amplifier Design

5.1 Multi-stage load modulation circuit architecture

The classical load modulation RF power amplifier, shown in Figure 5.1, has two amplifiers with the same output power capability arranged in parallel, but different in biasing. The two amplifiers are the carrier amplifier stage, which operates in class AB and the peaking amplifier stage that operates in class C. The input signal is divided equally in amplitude by splitter with 90-degree phase difference, so as to drive the class AB carrier amplifier stage and the class C peaking amplifier stage, and their outputs are connected by a transformer coupler which combines the output signals [1-18].

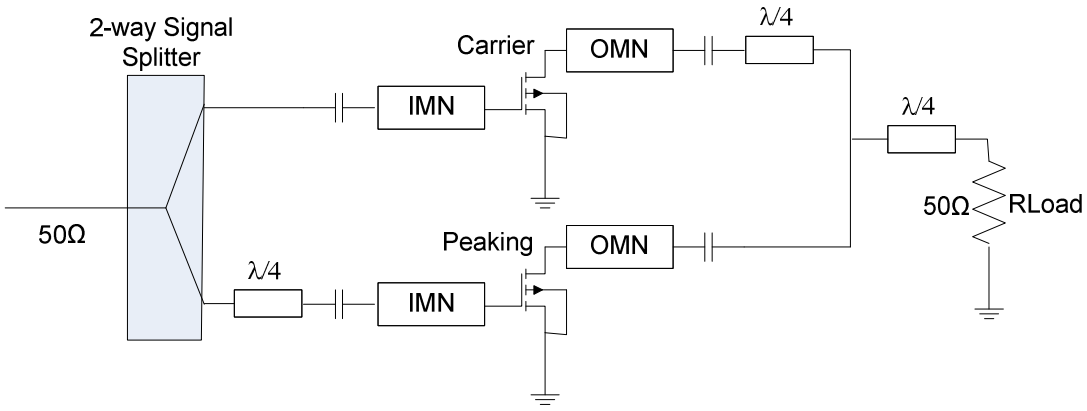

Figure 5.1. Schematic diagram of classical load modulation power amplifier

The classical load modulation RF power amplifier achieves a significantly higher efficiency at some point of output power back-off over the traditional stand-alone RF power amplifier. However, with OFDM wireless signals that have high peak-to-average power ratios, the efficiency of the classical load modulation RF power amplifier can be improved further by extending configuration to a three-stage design.

The proposed three-stage load modulation RF power amplifier shown in Figure 5.3, has three power amplifiers with the same out power capability and are arranged in parallel; two have the same bias point whereas the other has its own different bias point. The three amplifiers are carrier amplifier stage, which operates in class B mode while the two peaking amplifiers operate in class C mode. Furthermore, for proper load modulation, the input signal is divided equally in amplitude, but with phase differences. The phase difference between carrier amplifier and peaking1 amplifier is 90-degree, and the phase difference between carrier amplifier and peaking 2 amplifiers is 180-degree. The signal splitter was designed independently and tested in terms of the frequency response and the operational bandwidth, before integrated it into the whole design. This was done due to the fact that the operation is strongly influenced by the coupling factor of the input splitter.

In this design, the class B mode was chosen to act as the carrier amplifier stage, instead of class AB mode which is widely used in the classical load modulation power amplifier design. The selection of class B mode as carrier amplifier stage would significantly increase the efficiency of the whole design.

According to reference [6] and Figure 5.2, the output of the carrier amplifier and the output of the peaking 1 amplifier require a quarter wavelength transmission line, which is also applied to the output of peaking1 amplifier and the output of peaking 2 amplifier. Obviously, this will increase the complexity of the design and increase the circuit space, and if not properly designed can significantly reduce the efficiency and linearity of the whole design.

In this chapter, as shown in Figure 5.3, we considered a simple summing network at the output of the three-stage load modulation power amplifier. The summing network also acts as a phase difference compensator which adds the signal from each amplifier to the output load constructively. The quarter-wave length transmission line was implemented between the output of the carrier amplifier and the output of the peaking 1 amplifier; then the output of the peaking 2 amplifier was directly connected to the output of the peaking 1 amplifier without adding any quarter-wave length transmission line. This summing network will allow a proper load modulation operation. The operation is also strongly influenced by the quarter-wave length at the output of the carrier amplifier. However, the peaking1 and the peaking2 amplifiers can pull out the load presented to the carrier amplifier for peak efficiency and output power.

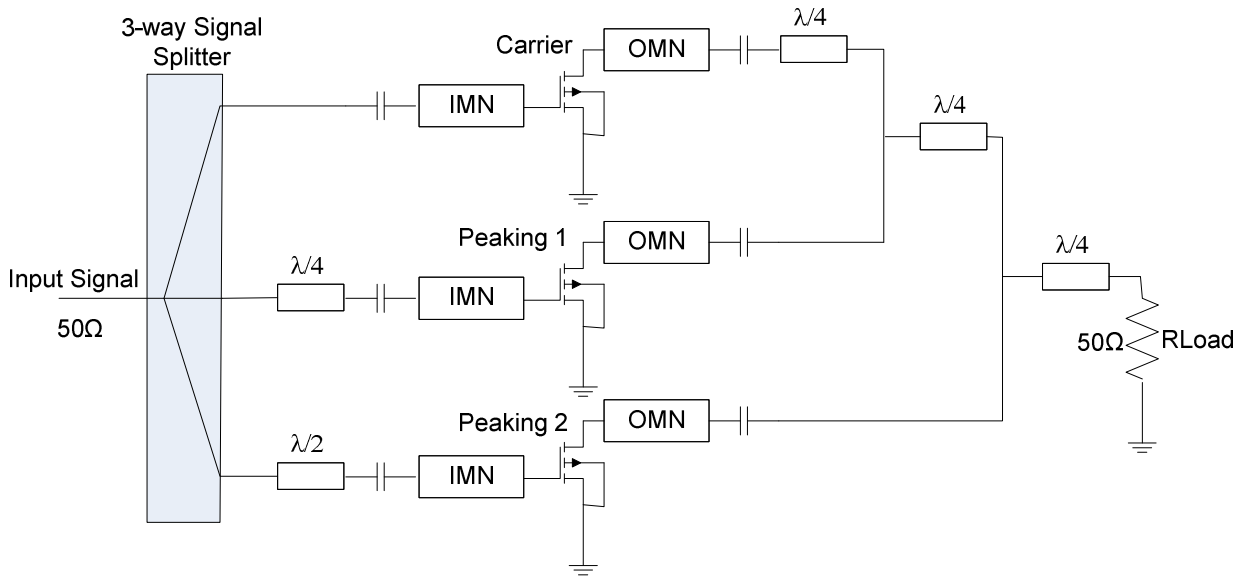

Figure 5.2. Schematic diagram of three-stage load modulation power amplifier

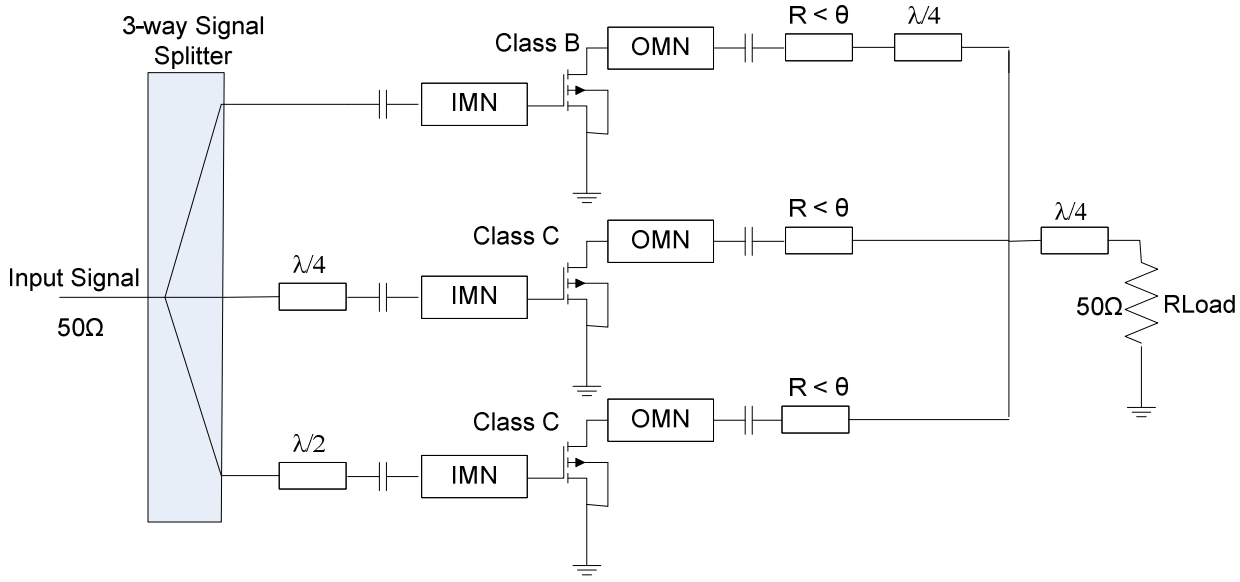

Figure 5.3. Schematic diagram of proposed three-stage load modulation power amplifier

5.2 Current Drive Analysis of Three-Stage Load Modulation Circuit

For the transmission line, the relationship between input voltage V_{in} and input current I_{in} to the output voltage V_{out} and output current I_{out} is given by matrix form [4-5]

$$\begin{bmatrix} V_{in} \\ I_{in} \end{bmatrix} = \begin{bmatrix} \cos\pi/2 & jZ_o \sin\pi/2 \\ jY_o \sin\pi/2 & \cos\pi/2 \end{bmatrix} \begin{bmatrix} V_{out} \\ I_{out} \end{bmatrix} \tag{5.1}$$

$Z_{in} = V_{in} / I_{in}$ is the source impedance, Z_o is the characteristic impedance of the transmission line, and Z_L is the load impedance and is given as $Z_L = V_{out} / I_{out.}$

Z_{in} becomes

$$Z_{in} = \frac{Z_L \cos\pi/2 + jZ_0 \sin\pi/2}{j(Z_L / Z_0)\sin\pi/2 + \cos\pi/2} \tag{5.2}$$

For the quarter-wavelength transmission line, $\cos \pi/2 = 0$, and $\sin \pi/2 = 1$, then Z_{in} will becomes

$$Z_{in} = \frac{Z_0}{Z_L / Z_0}, \qquad Z_{in} = \frac{Z_0^{\,2}}{Z_L} \tag{5.3}$$

Figure 5.4, shows the analysis diagram for a three-stage current. The quarter wavelength at the output of carrier amplifier acts as a load modulation coupler which causes the

resistive impedance seen by the carrier amplifier to go high when two peaking amplifiers are in off-state and to go low when the two peaking amplifiers are in on-state.

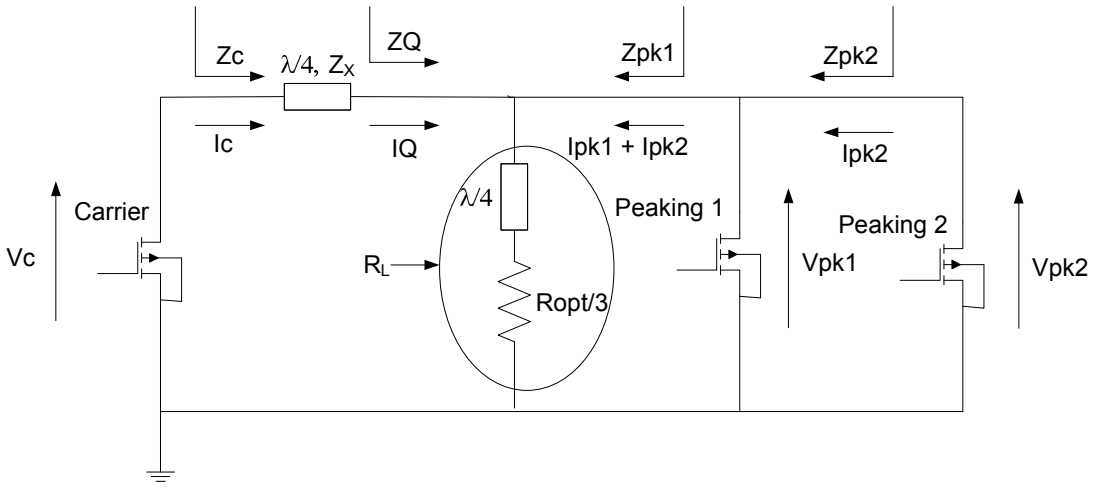

Figure 5.4. Analysis diagram for three-stage current

The phase output current of carrier amplifier (I_c) must lead that of the output current of peaking1 and peaking2 amplifiers (I_{pk1}, I_{pk2}) by 90-degree and 180-degree respectively. However, the operational principle of a three-stage load modulation RF power amplifier can be best described by dividing the level of input drive into low level drive (carrier is turned ON and peaking1 and peaking2 are turned OFF), medium level drive (carrier and peaking1 are turned ON and peaking2 is turned OFF) and high level drive (where both amplifiers are turned ON). At high input signal, both the carrier and the two peaking amplifiers are in on-state and their RF current envelopes can be written as follow:

$$I_C = \frac{I_{\max}}{6}(1+x) \tag{5.4}$$

$$I_{PK1} = \frac{I_{\max}}{3} x \tag{5.5}$$

$$I_{PK2} = \frac{I_{\max}}{3} x(x - 0.5) \tag{5.6}$$

Where x has a value of 0 at low level drive, has a value of 0.5 at medium level drive, and 1 value at high level drive.

The effective impedance with load pulling effect, on each amplifier can be given by:

$$Z_Q = R_L \left(1 + \frac{I_{PK1} + I_{PK2}}{I_Q} \right) \tag{5.7}$$

$$Z_{PK1} = R_L \left(1 + \frac{I_Q}{I_{PK1} + I_{PK2}} \right) \tag{5.8}$$

$$Z_{PK2} = R_L \left(1 + \frac{I_Q + I_{PK1}}{I_{PK2}} \right) \tag{5.9}$$

From equation 5.1, and in Figure 5.5, the quarter wavelength at the output of the carrier amplifier acts as a load modulation coupler where the resistive impedance seen by the carrier amplifier goes high when the two peaking amplifiers are in off-state and goes low when they are in on-state.

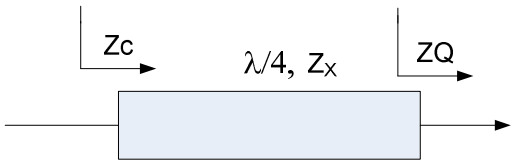

Figure 5.5. Quarter wavelength transmission line

The transformation of the input, output and characteristic impedance of a quarter-wave length transmission line is given as

$$Z_C = \frac{Z_X{}^2}{Z_Q} \tag{5.10}$$

Equation 5.10 is the output impedance seen by the carrier amplifier and when substituting Z_Q in the equation 5.10, the output impedance, becomes:

$$Z_C = \frac{Z_X^2}{Z_Q} = \frac{Z_X^2}{R_L\left(1+\frac{I_{PK1}+I_{PK2}}{I_Q}\right)} \tag{5.11}$$

V_c is the output voltage of carrier amplifier and is given as

$$V_C = Z_C * I_C = \frac{Z_X^2}{R_L\left(1+\frac{I_{PK1}+I_{PK2}}{I_Q}\right)} * I_C \tag{5.12}$$

$$I_Q = \frac{V_C}{Z_X}$$

$$V_C = \frac{Z_X^2 * I_C}{R_L\left(1+\frac{I_{PK1}+I_{PK2}}{V_C / Z_X}\right)} \tag{5.13}$$

After substituting $I_{C,}$ $I_{PK1,}$ and $I_{PK1,}$ into Z_C, it yields the following,

$$V_C = \left(\frac{Z_X}{6R_L}\right)(I_{MAX})\left(Z_X(1+X) - 4R_L X^2 + 2R_L X\right) \tag{5.14}$$

$$R_L = \frac{R_{opt}}{3}$$

$$V_C = \frac{Z_X}{R_{opt}}\left(\frac{I_{\max}}{2}\right)\left(Z_X(1+X) - 4\frac{R_{opt}}{3}X^2 + 2\frac{R_{opt}}{3}X\right) \quad (5.15)$$

$Z_X = R_{opt}$

$$V_C = \frac{R_{opt} + I_{\max}}{2}\left(-\frac{4}{3}X^2 + \frac{5}{3}X + 1\right) \quad (5.16)$$

From the above equation, the output voltage remains approximately constant only at low level drive where only the carrier is in on-state and high level drive (where both amplifiers are on-state), at medium level drive, the output voltage of the carrier amplifier increases by the factor 3/2 (1.5). Figure 5.6 and Figure 5.7 shows the input voltage versus output voltage of classical and three-stage load modulation respectively.

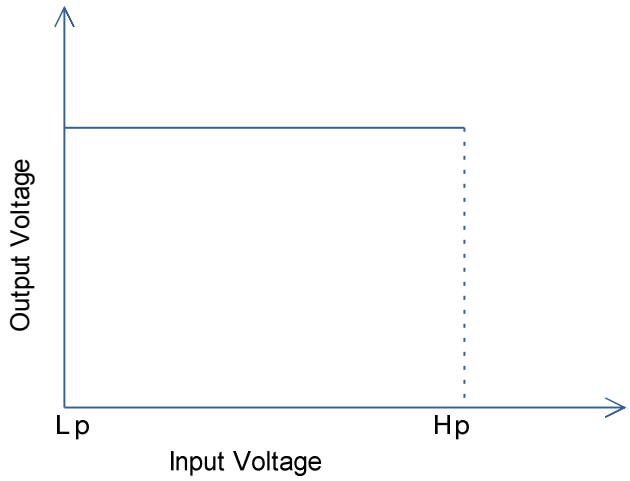

Figure 5.6. Input voltage vs. output voltage of classical load modulation.

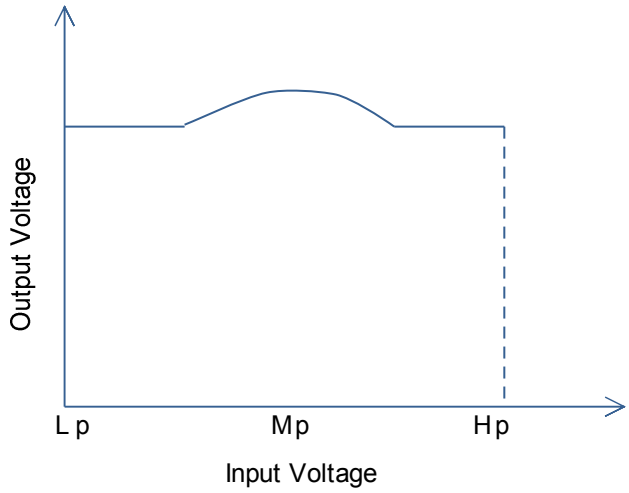

Figure 5.7. Input voltage vs. output voltage of three-stage load modulation.

5.3 Circuit Prototype and results

The three-stage load modulation RF power amplifier utilises the FPD1500S0T89 device. It has been designed using TOM3 large signal model and FPD1500 transistor. The FPD1500SOT89 is a packaged depletion model AIGaAs/InGaAs pHEMT. It contains double recessed gate structure which minimises parasitic and optimise performance.

In this chapter, the bias circuit for the carrier amplifier was designed based on class B mode and the two peaking amplifiers were based on class C mode. The decision to use class B mode as a carrier amplifier instead of class AB mode, which is widely adopted in the combination of Doherty amplifier, was taken in order to improve the efficiency of the entire design. The conduction angle of class B amplifier remains at 180-degree and is independent of the input signal level. However, the class B amplifier DC quiescent

current is at threshold that means the quiescent current is theoretically zero. But in this design, the quiescent current was increased to an order of 8% of the peak drain current which resulted to 0.046mA. The motive behind this is to minimise crossover distortion and increase the efficiency. The peak drain current of FPD1500 transistor is 0.587mA when the gate bias voltage is at (0V) and the drain bias voltage at (5V). The 5V was chosen for the drain bias voltage because it's located between the cut-off and saturation point of the FPD1500 transistor. The carrier amplifier gate bias voltage should be set to (-0.9V) to establish the carrier amplifier quiescent current at (0.046mA) which is the 8% of the peak drain current of the transistor. The gate bias voltage versus drain current of class B is depicted in Figure 5.8.

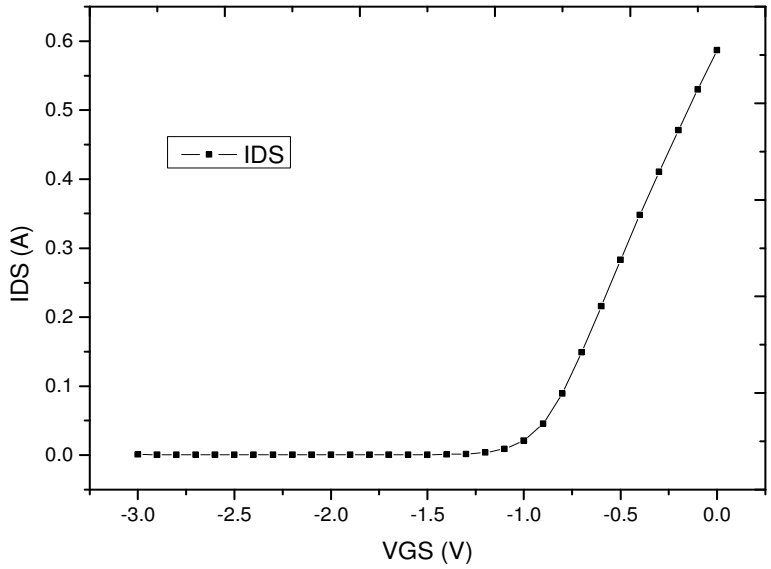

Figure 5.8. The Threshold of the Drain Current of Class B

The two peaking amplifiers are biased to turn on only when the carrier amplifier reaches the saturation level. The peaking1 and peaking2 amplifiers are biased in class C mode

that is below threshold. They can only turn on when the input drive reaches a predetermined level, because class C mode is absolutely dependent on the input drive level. The peaking1 and peaking2 amplifiers gate bias voltage should be set to (-1.1V) to properly work in class C mode. The two peaking amplifiers quiescent current is (0.004mA).

To this point, we have in fact biased both the carrier and the two peaking amplifiers, where the bias condition for the carrier amplifier is V_{gs} = -0.9V (I_{ds} = 46 mA), and for the peaking1 and peaking2 amplifiers is V_{gs} = -1.1V (I_{ds} = 4 mA). The drain bias voltage for both amplifiers is (V_{ds}=5V). The splitter at the input, the carrier amplifier, the peaking1 amplifier, the peaking2 amplifier, and the impedance transformer with phase compensation at the output, are combined to form a single three-stage load modulation RF power amplifier. Figure 5.9, shows the prototype diagram of the proposed three-stage load modulation RF power amplifier.

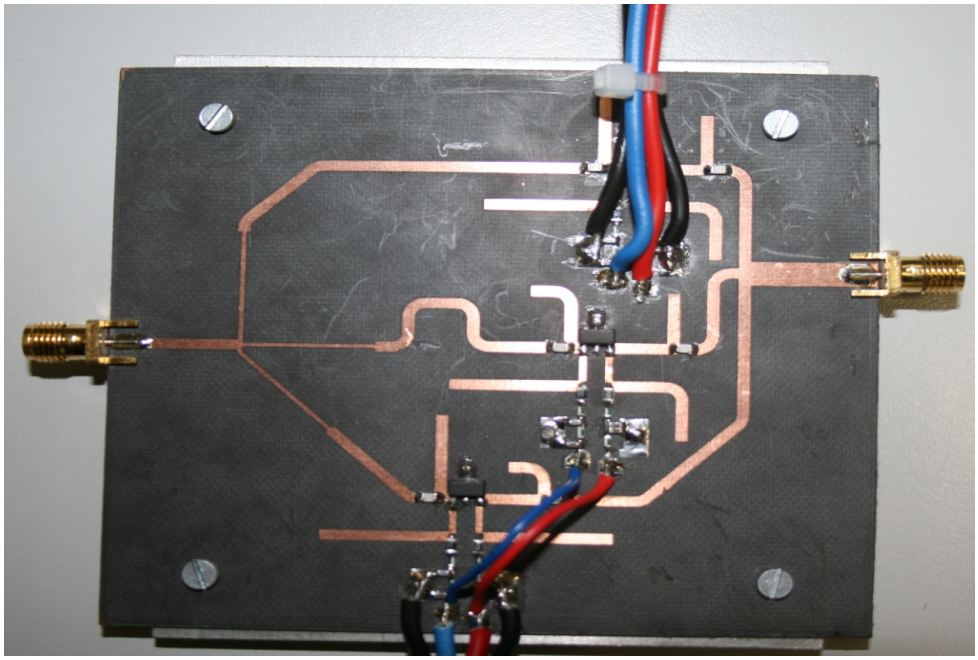

Figure 5.9. Prototype of the three-stage load modulation RF power amplifier.

The three-stage load modulation RF power amplifier is initially characterised for AM-AM and AM-PM responses, as well as for output power and efficiency. The performance comparisons between the three-stage load modulation amplifier and the classical load modulation amplifier were performed, where the output power increased to 30dBm at the 1dB compression point while the efficiency increased to 67%.

Figure 5.10 represents the variation and comparison of the input power versus output power for the three-stage load modulation and classical load modulation amplifiers. It clearly shows that the 30dBm output power is at the edge of the linear region of the amplifier, and this was achieved due to the characteristic of the overall gain as a product of the three-stage load modulation, which preserves its constant nature throughout the range up to 30dBm. The peaking 1 and peaking 2 amplifiers late gain expansion can compensate the carrier amplifier gain compression. Figure 5.11 shows the comparison of AM-PM characteristics of the two different topologies.

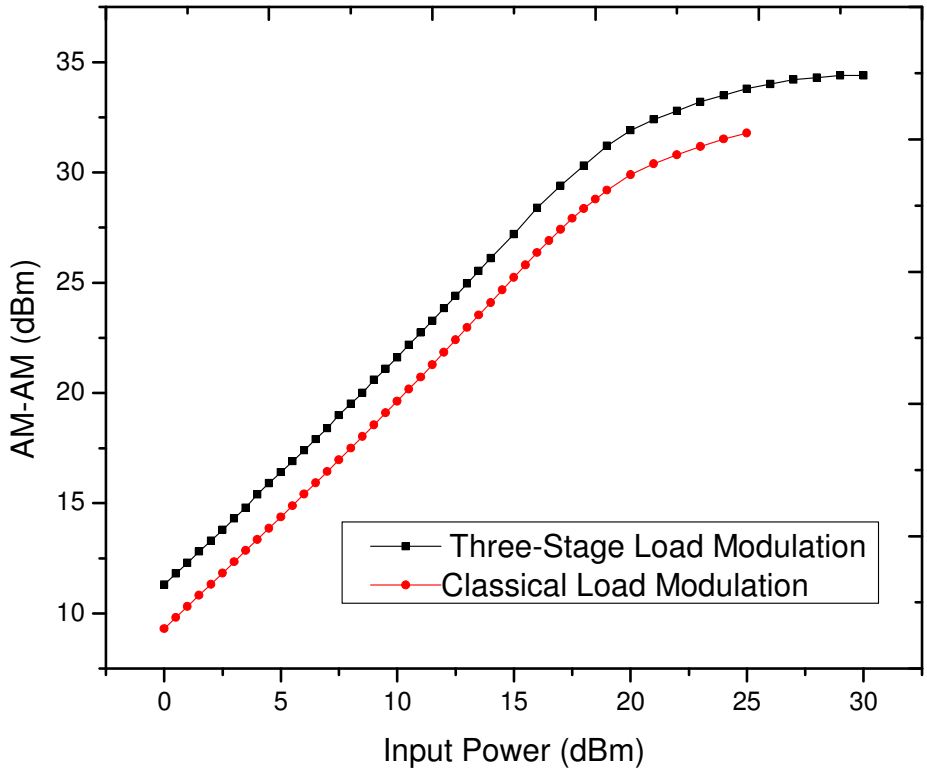

Figure 5.10. AM-AM characteristics of three-stage load modulation.

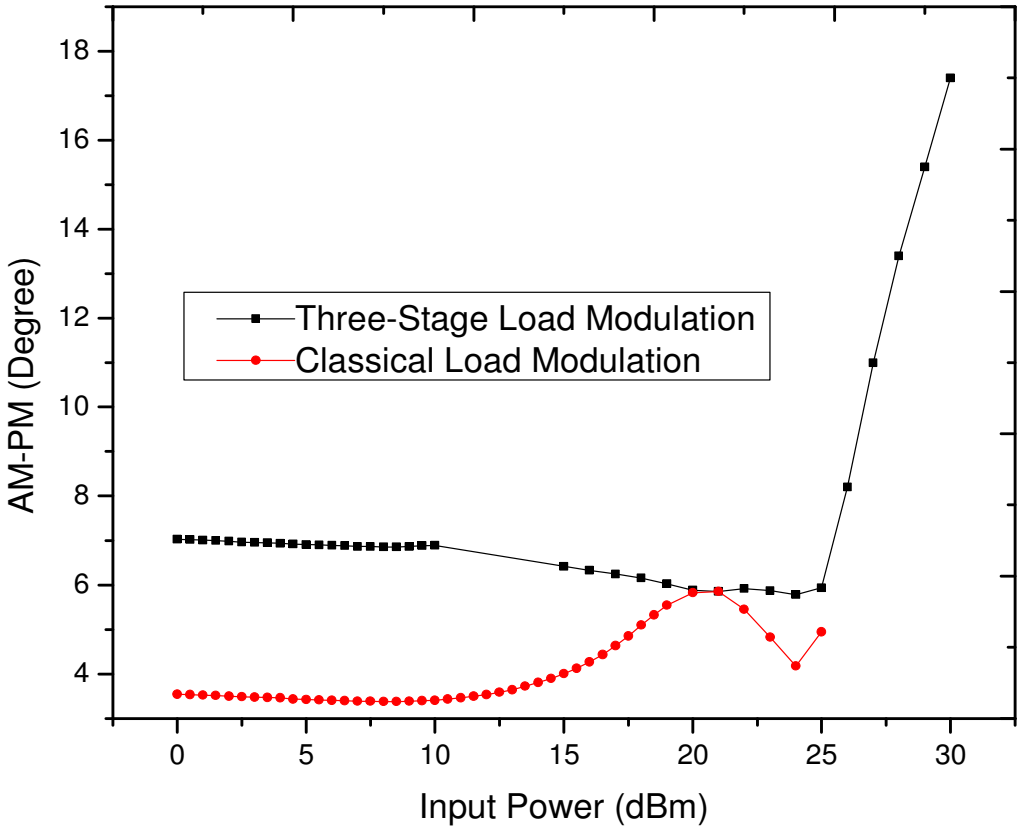

Figure 5.11. AM-PM characteristics of three-stage load modulation.

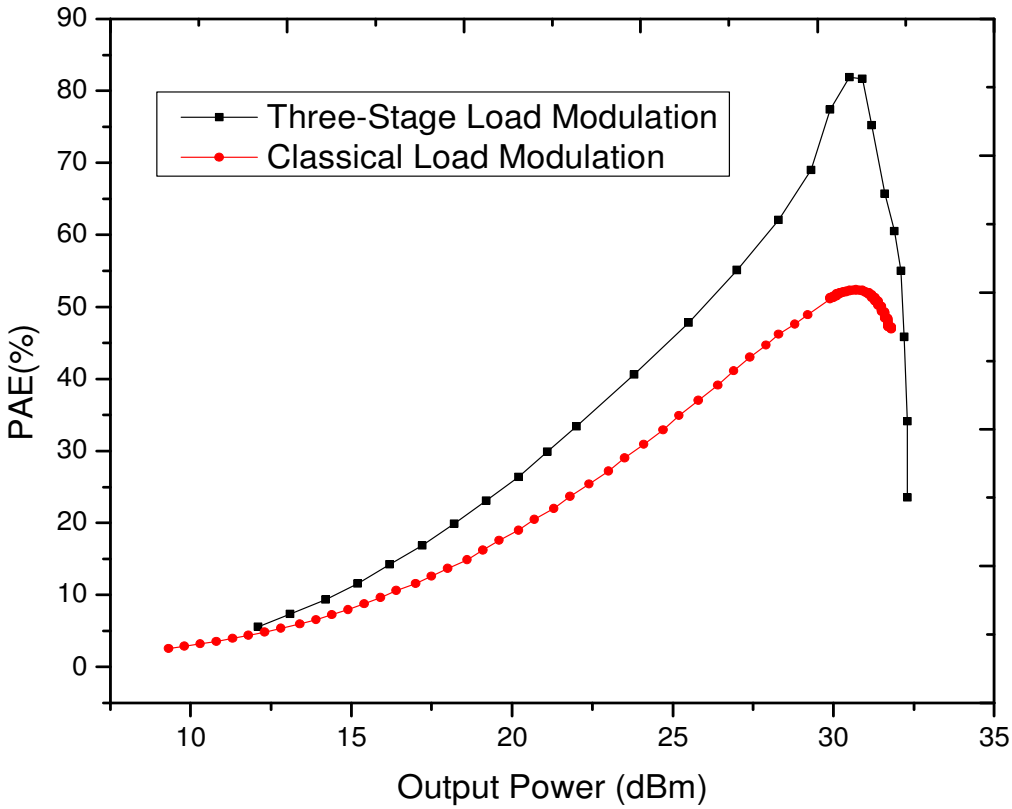

Figure 5.12. Power-Added Efficiency.

The power added efficiency versus output power is shown in Figure 5.12. The three-stage load modulation amplifier has higher efficiency over the range of output power levels compared to the classical load modulation amplifier.

The two-tone characterisation with 5MHz tone spacing was performed and was concentrated on achieving acceptable IMD3 and IMD5. Figure 5.13 and Figure 5.14 shows the performance comparisons between the three-stage load modulation amplifier and the classical load modulation amplifier for the IMD3 and IMD5 as a function of output power.

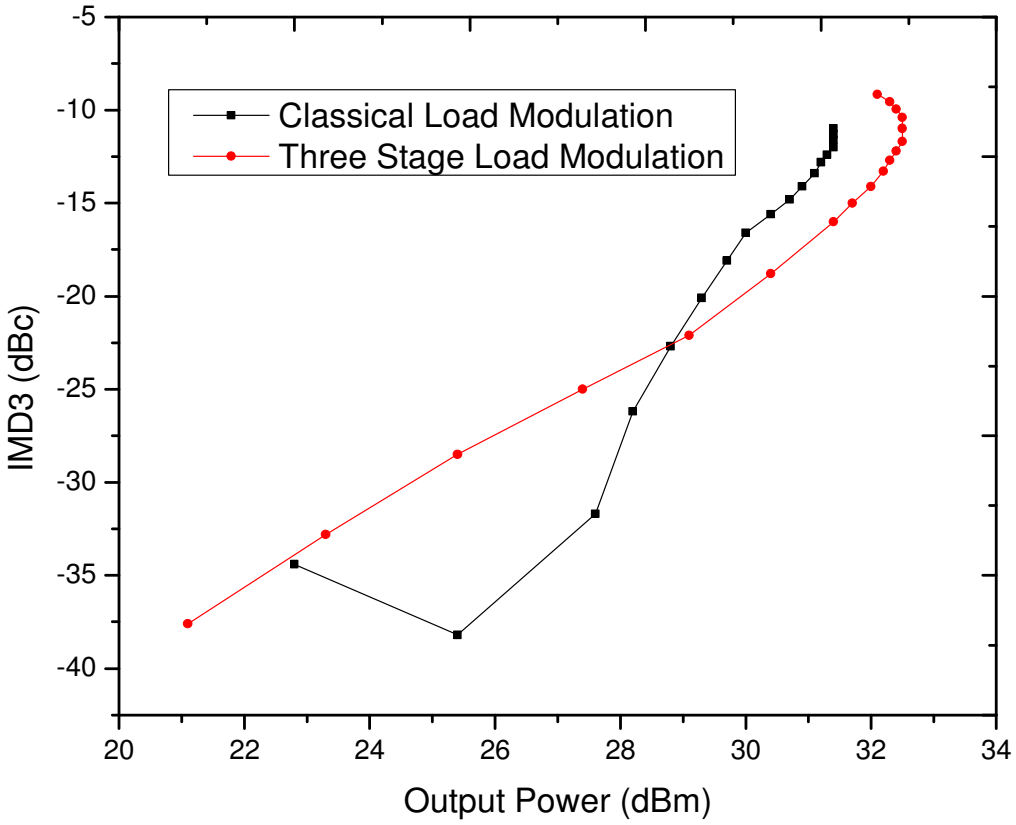

Figure 5.13. Two-tone characterisation (IMD3).

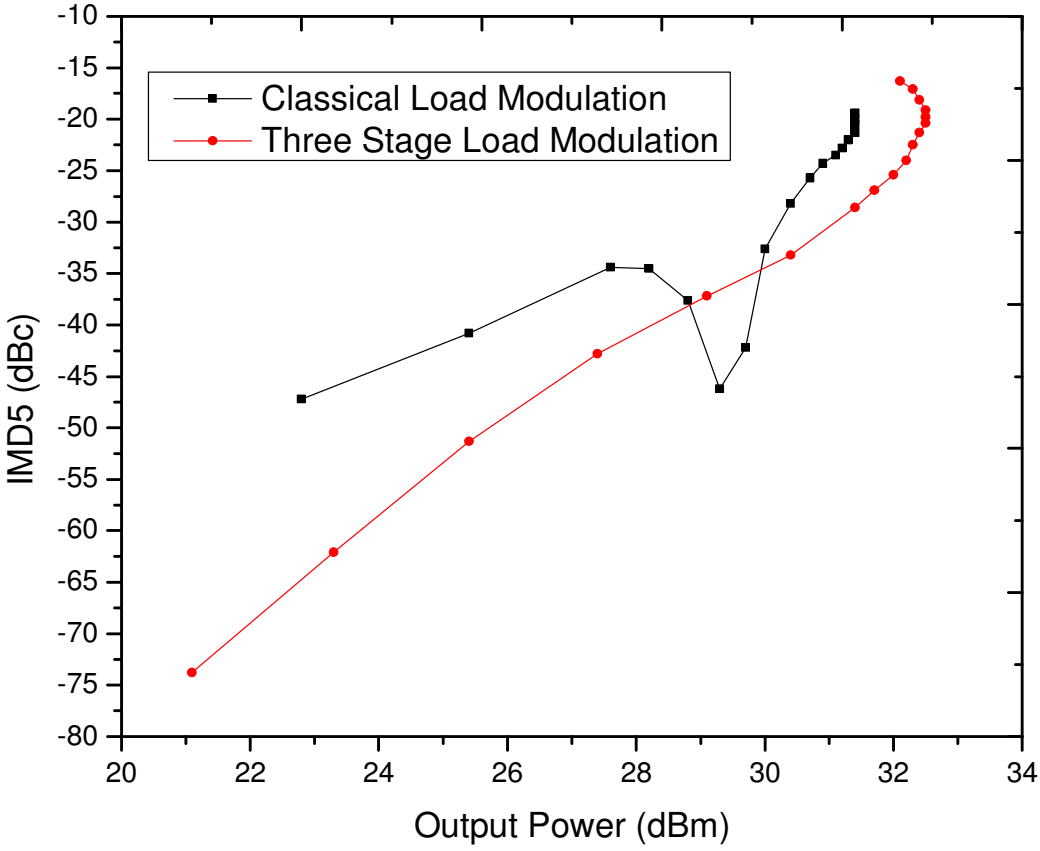

Figure 5.14. Two-tone characterisation (IMD5).

These results show that the IMD3 and IMD5 tone response of a three-stage load modulation have been improved significantly over the IMD3 and IMD5 of the classical load modulation. The three-stage load modulation power amplifier was also tested with the modulated mobile WiMAX signal. The modulated 64-QAM OFDM signal with 10MHz bandwidth was used and a result of less than 5% EVM was obtained.

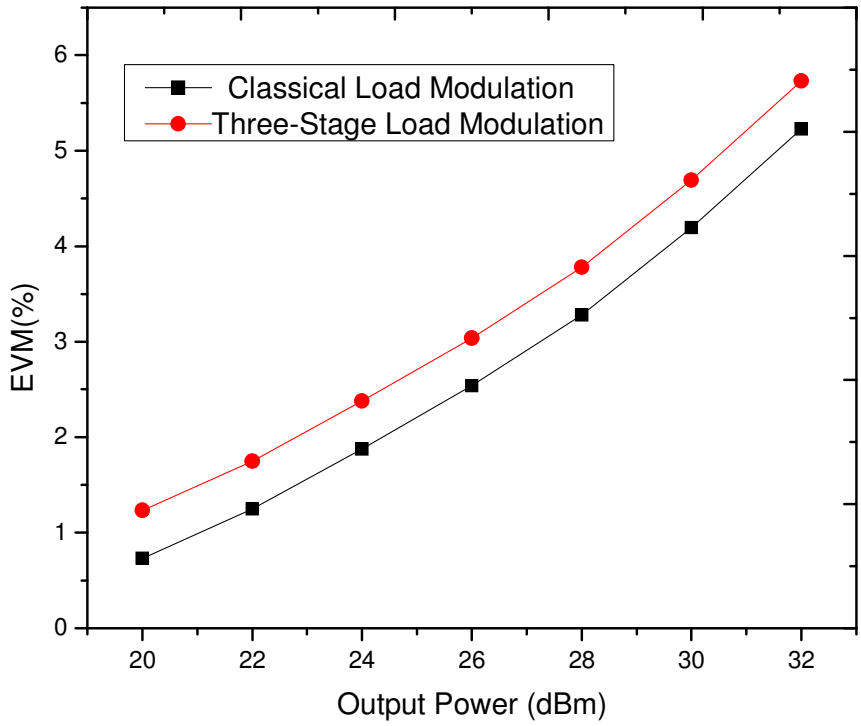

Figure 5.15: Error vector magnitude (EVM) characterisation.

Figure 5.16 shows the comparison of the linearity performance of a three-stage load modulation with the classical load modulation fed by a modulated mobile WiMAX signal, and it can be seen that the spectrum mask of the mobile WiMAX requirement are satisfied. EVM for the three stage load modulation is generally poorer than classical load modulation.

5.4 Conclusion

This chapter five has presented the design and implementation of the three-stage load modulation RF power amplifier for mobile WiMAX application. The amplifier was characterised using single tone, two-tone and the mobile WiMAX modulated input signals. The achieved results have shown good efficiency, power performances, and satisfy the linearity requirement for mobile WiMAX. The proper phasing of the splitter at the input, and the proper design of the impedance transformer with phase compensation at the output can effectively contribute to the total efficiency of the system. The operation of this design was strongly influenced by the coupling factor of the splitter, the biasing of the carrier amplifier, and the biasing of the peaking 1 and the peaking 2 amplifiers. The turn–on of the two peaking amplifiers are dependent on the input signal. The performance of the 3-stage load modulation RF power amplifier has compared with the legacy 2-stage load modulation RF power amplifier technique. The experimental results show that 30% PAE can be achieved at 23dBm average output power, and that 30dBm peak output power can be achieved with 67% PAE, which represent a 14% improvement over current state of the art system while meeting the power output requirements for mobile WiMAX. The results have shown that the proposed three-stage load modulation RF power amplifier can be suitable candidate for the mobile WiMAX application.

References

[1] W. H. Doherty, “A New High Efficiency Power Amplifier for Modulated Wave”, Proc. IRE, Vol. 24, No. 9, PP. 1163 – 1182, September, 1936.

[2] S.C. Cripps Advanced Techniques in RF Power Amplifier Design, Norwood, MA: Artech House, 2002.

[3] S.C.Cripps, RF Power Amplifier for Wireless Communications, Norwood, MA: Artech House, 1999.

[4] F. H. Raab, “Efficiency of Doherty RF Power Amplifier System”, IEEE Trans. Broadcasting, Vol. BC-33, No 3, PP. 77-83, September, 1987.

[5] Raab, F.H.; Asbeck, P.; Cripps, S.; Kenington, P.B.; Popovic, Z.B.; Pothecary, N.; Sevic, J.F.; Sokal, N.O.;,“Power amplifiers and transmitters for RF and microwave”, IEEE Transactions on Microwave Theory and Techniques, Vol. 50, No 3, PP. 814 – 826, March, 2002.

[6] Srirattana, N.; Raghavan, A.; Heo, D.; Allen, P.E.; Laskar, J.; “Analysis and design of a high-efficiency multistage Doherty power amplifier for wireless communications”., IEEE Transactions on Microwave Theory and Techniques, Vol. 53, No 3, Part 1, PP. 852 – 860, March, 2005.

[7] Abubakar Sadiq Hussaini, Bashir A. L. Gwandu, Raed Abd-Alhameed, Jonathan Rodriguez, “The Beyond 3G Energy Efficient Power Amplifier for Mobile Communications” Proc. of the 26th WWRF Meeting, Doha, Qatar, 11th-13th April 2011, Paper No. WWRF25-WG4-9.

[8] Abubakar Sadiq Hussaini, Raed Abd-Alhameed, Jonathan Rodriguez, "Design of Energy Efficient Power Amplifier for 4G User Terminals", 17th IEEE International Conference on Electronics, Circuits, and Systems (ICECS 2010), Athens, Greece 12-15 December 2010, Paper No. 533, pp. 617-620.

[9] Abubakar Sadiq Hussaini, Raed Abd-Alhameed, Jonathan Rodriguez, "Green Radio: Approach Towards Energy Efficient Power Amplifier for 4G Communications", Proc. of the 25th WWRF Meeting, Kingston-upon-Thames, UK, 16th-18th November 2010, Paper No. WWRF25-WG4-12.

[10] Abubakar Sadiq Hussaini, Bashir A. L. Gwandu, Raed Abd-Alhameed, Jonathan Rodriguez, "Design of Power Efficient Power Amplifier for B3G Base Stations", 9th IEEE International Symposium on Electronics and Telecommunications (ISETC 2010), Timisoara, Romania, 11-12 November 2010, Paper No. 103, pp. 89-92.

[11] Abubakar Sadiq Hussaini, Tahereh Sadeghpour, Raed Abd-Alhameed, Mark Child, Nazar Ali, Jonathan Rodriguez, “Design of Doherty RFPA for Mobile WiMAX Base Stations”, 6th International ICST Conference on Mobile Multimedia Communications, EERT-3, Lisbon, Portugal, 6-8 September 2010, Paper No. 3, pp. 1-8.

[12] Wang, F.; Kimball, D.; Popp, J.; Yang, A.; Lie, D.Y.C.; Asbeck, P.; Larson, L.;, “Wideband envelope elimination and restoration power amplifier with high efficiency wideband envelope amplifier for WLAN 802.11g applications”, Microwave Symposium Digest, 2005 IEEE MTT-S International, PP. 4, June, 2005.

[13] Kimball, D.F.; Jeong, J.; Hsia, C.; Draxler, P.; Lanfranco, S.; Nagy, W.; Linthicum, K.; Larson, L.E.; Asbeck, P.M.; “High-Efficiency Envelope-Tracking W-CDMA Base-Station Amplifier Using GaN HFETs”, IEEE Transactions on Microwave Theory and Techniques, Vol. 54, No. 11 PP. 3848 – 3856, November, 2006.

[14] Feipeng Wang; Ojo, A.; Kimball, D.; Asbeck, P.; Larson, L.;, "Envelope tracking power amplifier with pre-distortion linearization for WLAN 802.11g", Microwave Symposium Digest, 2004 IEEE MTT-S International, Vol. 3, PP. 1543–1546, June, 2004.

[15] Junghwan Moon; Jangheon Kim; Ildu Kim; Jungjoon Kim; Bumman Kim;, "A Wideband Envelope Tracking Doherty Amplifier for WiMAX Systems", Microwave and Wireless Components Letters, IEEE, Vol. 18, No 1, PP. 49 – 51, January, 2008.

[16] H. Chireix, "High Power Outphasing Modulation", Proceedings of the IRE, Vol. 23, No 11, PP. 1370– 1392, November, 1935.

[17] Raab, F, "Efficiency of Outphasing RF Power-Amplifier Systems", IEEE Transactions on Communications, Vol. 33, No 10, PP. 1094– 1099, October, 1985.

[18] Kahn, L.R.;, "Comparison of Linear Single-Sideband Transmitters with Envelope Elimination and Restoration Single Sideband Transmitters", Proceedings of the IRE, Vol. 44, No 12, PP. 1706 - 1712, December, 1956.

CHAPTER SIX

6. Conclusion and future work

6.1 Summary of Thesis

The performance comparisons between all the designs have been presented. The research work explores the emerging area of optimising efficiency as well as linearity in RF power amplifier design, as part of the green RF front end. The efficiency enhancement technique applied by Doherty technique has been implemented in the linear region of the RF power amplifier to achieve higher efficiency at a low-level input signal.

We have highlighted energy consumption and linearity as two important design requirements that should be addressed if we are to have effective RF power amplification in tomorrow's handsets and base stations.

The original achievement of the present work can be summarised as follows:

In chapter 2, the overview and the concept of signal amplification and feature of power amplifiers have been reviewed. Amplifiers are classified according to their circuit configurations and methods of operation into different classes, such of these are A, B, AB, C, and F. These classes are based on conduction angle ($2\theta_c$).

Moreover in the chapter 2, it presents widely used figures of merit to evaluate the linearity or the impact of nonlinearity of RF power amplifiers. These have shown the classes of RF power amplifier from highly linear to the less linear. It is well known that power amplifiers cannot operate efficiently when used for linear amplification.

The classes A, B and AB are considered linear amplifiers and have been used for GSM and AM broadcasting. High data transfer, leads to the development of multilevel modulations, which causes non-constant envelope and wide envelope frequency, and are significantly sensitive to nonlinear distortion, usually caused by RF power amplifier. Therefore, linear or linearisation RF power amplifier is needed for high data transfer.

Chapter 3 unfolds and describes the characterisation and design of energy efficient user terminal transceiver power amplifier. The design comprised several design steps for which the optimisation is applied to each in order to obtain global high performances of the entire system. Initially, the design of carrier and peak amplifiers, input signal 3dB 90-degree hybrid coupler designs, Output 90 degree offset line and impedance transformer designs were performed.

The chapter 3 has presented two different topologies. Topology one (combination of class B and class C) is even Doherty in which the results are compared with classical class B. The even Doherty has better efficiency and output power than class B but still it has some limitation, which doesn't allow utilising all the efficiency. Doherty techniques are based on load modulation and when two transistors are applied, the second transistor should be able to pull the load presented to the first transistor to achieve high efficiency. However, it is impossible for class C to deliver the same output power as

class B because, class C used part of the input signal to turn on and for this reason class C will never pull the load presented to class B for peak efficiency. With this reason we decided to designed uneven Doherty RF power amplifier with uneven signal splitter, which is to allow more input signal to class C amplifier than class B amplifier. The trade-off between efficiency and linearity in load modulation power amplifier has been presented. The achieved results of the proposed design process have shown an excellent efficiency and power performances. The proper phasing of 3dB quadrature splitter effectively contributed to the total efficiency of the system. The operation of this design was strongly influenced by the coupling factor of the splitter, biasing of class B and C amplifiers. In addition, the turn–on of the class C amplifier was dependent on the gate bias voltage and the input signal.

Chapter 4 covers the proposed base stations efficient RF power amplifiers design and its implementations. The aim of this chapter was the design process of the base station load modulation RF power amplifier and balance RF power amplifier. The conventional balance amplifier was first proposed to improve power efficiency of 3G base station, is designed to work over a given dynamic range where the amplifier should work linearly. Conventional balanced amplifier was a commercially successful to 2G/3G base station front end power amplifier. However, there are some problems that limit the balanced amplifier for use as power amplifier for 4G communications.

Three different topologies of RF power amplifiers (Doherty, Conventional Balanced, and Uneven Load modulation) have been designed with custom-made even and uneven signal splitters that have been tested and compared, and both of them are for the base station applications. The presented designs can be summarised separately as follows:

In section 4.1, the Doherty RF power amplifier was designed using Freescale N-Channel Enhancement-Mode Lateral MOSFET transistor, the achieved results of the Doherty were compared with conventional Class AB amplifier, and Doherty exhibited a PAE of 66% at peak output power of 43 dBm close to 1dB compression point. And exhibited a PAE of 40% at average output power of 37 dBm back off. The Class AB, Class C, input signal splitter and output transformer were adjusted to optimise the design under Doherty operation. The Doherty RF power amplifier can make a good concession between the cost, linearity, efficiency, and output power. The proper phasing of 3dB quadrature splitter effectively contributed to the total efficiency of the system. In addition, the turn–on of the class C amplifier was dependent on the gate bias voltage and the input signal.

Section 4.4 presents the performance comparisons between load modulation power amplifier and conventional balanced power amplifier. The achieved results of the proposed design process have shown an excellent efficiency and power performances. Load modulation achieved a PAE of 66% at peak output power of 43 dBm close to 1dB compression point. And exhibited a PAE of 40% at average output power of 37 dBm back off., while conventional balanced achieved a PAE of 50% at peak output power of 42 dBm and achieved a PAE of 15% at average output power of 37 dBm back off . Load modulation has 16% peak PAE achievement over conventional balanced RF power amplifier.

The proper phasing of input signal splitter effectively contributed to the total efficiency of the system. The load modulation amplifier offers improved efficiency over wide range of output power compared to conventional balanced amplifier. The load

modulation has less gain compared to balanced amplifier due the arrangement of lower biasing of Class C peaking transistor of load modulation. The operation of this design was strongly influenced by the coupling factor of the splitter, biasing of class AB and C amplifiers.

In section 4.6 the performance comparisons between uneven load modulation RF power amplifier and load modulation RF power amplifier are presented. As we have seen, the operation of the second amplifier has been forced to operate in Class C, typically Class C have lower gain than Class AB amplifier, and it is impossible for Class C to deliver the same output power as Class AB because, Class C used part of the input signal to turn on and for this reason Class C will never pull out the load presented to Class AB for peak efficiency. To achieve the maximum output power and overall performance, one solution is to supply more input power to Class C amplifier than Class AB. With this one should be able to achieve maximum output power without creating AM-AM distortion.

The operation of this design was strongly influenced by the coupling factor of the splitter, biasing of class AB and C amplifiers. The achieved results of the proposed design process have shown an excellent efficiency and power performances. The uneven load modulation RF power amplifier achieved a PAE of 66% at peak output power of 45 dBm close to 1dB compression point. And exhibited a PAE of 25% at average output power of 39 dBm back off.

Chapter 5 describes the proposed Multi-stage Load Modulation circuit architecture; section 5.1 explains the current drive analysis for the three stage load modulation

circuit; circuit prototype and results are given by section 5.2. This chapter six has presented the design and implementation of the three-stage load modulation RF power amplifier for mobile WiMAX application. The amplifier was characterised using single tone, two-tone and the mobile WiMAX modulated input signals. The achieved results have shown good efficiency, power performances, and satisfy the linearity requirement for mobile WiMAX. The proper phasing of the splitter at the input, and the proper design of the impedance transformer with phase compensation at the output can effectively contribute to the total efficiency of the system. The operation of this design was strongly influenced by the coupling factor of the splitter, the biasing of the carrier amplifier, and the biasing of the peaking 1 and the peaking 2 amplifiers. The turn–on of the two peaking amplifiers are dependent on the input signal. The performance of the 3-stage load modulation RF power amplifier has compared with the legacy 2-stage load modulation RF power amplifier technique. The experimental results show that 30% PAE can be achieved at 23dBm average output power, and that 30dBm peak output power can be achieved with 67% PAE.

6.2 Conclusion

Five different topologies of RF power amplifiers have been designed with custom-made even and uneven signal splitters that have been tested and compared, two for the user terminal and three for the base station applications. The design core of the Doherty technique is based on the combinations of a class B power amplifier, class AB and a class C power amplifier, which also includes 90-degree 2-way power splitter at the input and a quarter wavelength transformer at the output, which performs the load impedance transformation and combines the two output signals. Moreover, the 3-stage

load modulation RF power amplifier has been designed with the proposed new output power combiner. The 3-stage load modulation RF power amplifier is a new design, which provides high output power and better efficiency together with reduction in power consumption and power dissipations over the legacy 2-stage load modulation RF power amplifier. The design core is based on the combinations of a Class B power amplifier and two Class C power amplifiers, which includes 180-degree 3-way power splitter at the input and a quarter wavelength transformer at the output. However, the designs are to operate in the 3.4 - 3.6GHz frequency band of Europe mobile WiMAX. The performances of the designs were compared and analysed. The experimental results show that 30% PAE can be achieved at 23dBm average output power, and that 30dBm peak output power can be achieved with 67% PAE, for the user terminal and 25% PAE can be achieved at 39dBm average output power and 66% PAE at 45dBm peak output powervfor base stations which marks the peak 14% and 11% respectively, improvement over current state-of-the-art systems, while meeting the power output requirements for mobile WiMAX applications. The beyond 3G mobile communication systems will accommodate multiple wireless standards (2G, 2.5G, 3G, Mobile WiMAX, LTE, and LTE-A) and both mobile's and base station's devices will be asking for more and high efficient power amplifier with the aim to prolong their operation time and avoid active cooling in the base station. However, it is impossible to achieved higher efficiency and high linearity with single stage traditional power amplifier. Therefore, there is need to adapt an external technique to improve the efficiency of the transceiver while at the same time maintaining the linearity for the signal with high PAPR. Moreover, we will have to acknowledge and mention it here, there are various techniques that are used to mitigate or to reduce the PAPR: these techniques if succeeded in mitigating the PAPR of OFDM will enable the power amplifier to be operated in a more efficient region with

OFDM signals and will also relax the stringent linearity requirements of power amplifier design. Various techniques such as: Clipping; Selective Mapping; Coding; Wave Form Shaping; Scrambling; Partial IFFT; Interleaving Technique; Tone Reservation Technique; Tone Injection Technique; Active Constellation Extension Technique, are available and most of have computation complexity and/or causing another distortion. Our research focuses on energy efficient Doherty RF power amplifier for B3G transceivers applications. Applying load modulation technique can significantly reduce the CO2 footprint and power consumption in the transceiver.

6.3 Recommendation for future work

After improving the RF power amplifier transceiver's performance in term of battery lifetime/talk time of battery-powered devices and energy consumptions of base station, with the aim to prolong their operational time and avoid active cooling in the base station. The recommended future work is to design a frequency reconfigurable RF front ends (multi-standard) by using RF MEMS technology.

The first part of the design should focus on RF MEMS matching network for the reconfiguration of RF power amplifier to cover more than six frequency bands (a tunable RF power amplifier). And the second part of the design would address the RF MEMS Filters.

Without a holistic design and fabrication approach, future wireless communication devices would be extremely large in size to accommodate multiple RATs compared to

today's more conventional mono-mode devices. Typically multiple RAT devices will be comprised of multiple RF power amplifiers, LNA, RF band pass filters, modulators and demodulators; one for each wireless technology. Obviously, this will increase the complexity of the circuit design and will cover a large part of the circuit space leading to power hungry devices. RF-MEMS can be good candidate for innovative RF front end devices since it is reconfigurable features in nature therefore allowing a reduction in the number of external components in a single device for the use of multiple RATs.

The future mobile multimedia handset and base station devices will accommodate multiple wireless standards (2G, 2.5G, 3G, WiMAX, Mobile WiMAX, LTE, and LTE-A). This will require multiple RF power amplifiers, LNAs, RF band pass filters, modulators and demodulators since all of these standards work on different frequency bands. If we were to upgrade these mobile devices to support future standards, this indeed would entail adding another set of customised RF front end devices leading to extra complexity and power consumption. If were not to take any preventive measure towards reducing energy consumption on the mobile device, this means that users could eventually fall victim to the energy trap: users will be restricted to the nearest power socket instead of having the flexibility to roam freely between different networks. Therefore, future design requirements dictate the need for reconfigure handsets so as to reduce the number of duplicated circuits, and hence the energy consumption, and from a business perspective, to introduce the handsets to the market at a very low cost. Therefore the design process requires a reconfigurable/tunable RF front end structural design with high energy efficiency, high tuning speed, and excellent linearity that have to deal with the wide frequency range, low loss/or high-Q circuits. Therefore tunable

power amplifiers, tunable antennas, tunable band pass filters, and tunable matching networks are the key building blocks for reconfigurable RF front-end systems.

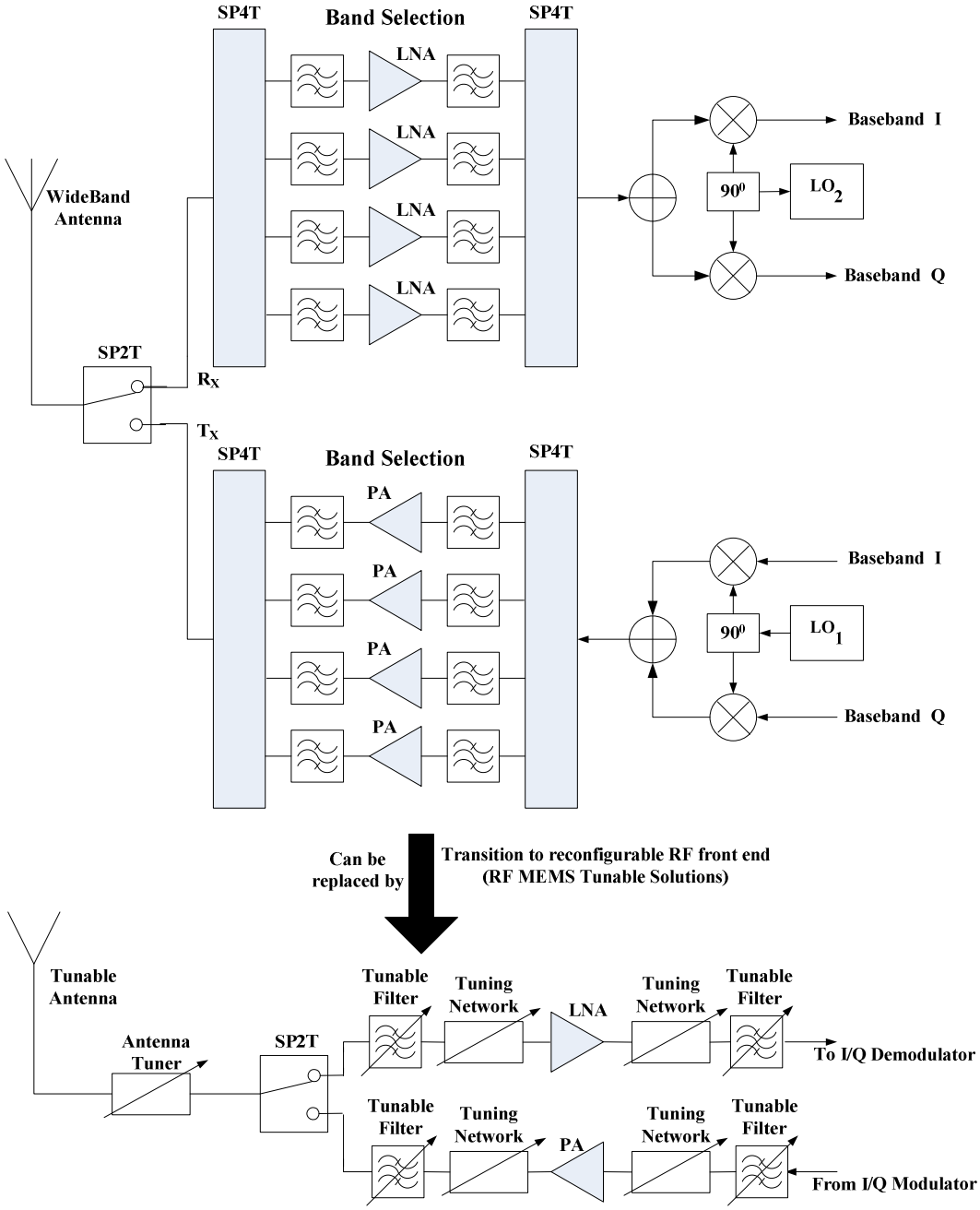

Figure 6.1: Block diagrams of multi-standard wireless systems showing the transistion to reconfigurable solutions

References

[1] J. Helszajn, YIG Resonators & Filters, John Wiley & Sons New York: 1985.

[2] YIG Tuned Filters, Micro Lambda Inc., Fremont, CA, USA.

[3] W. J. Keane, "YIG filters aid wide open receivers," Microwave J., vol. 17, no. 8, Sept. 1980.

[4] H. Tanbakuchi et al, "A broadband tracking YIG-tuned mixer for a state of the art spectrum analyser" European Microwave Conference Dig., pp. 482-490, Sept. 1987.

[5] R. F. Fjerstad, "Some design considerations and realisations of iris-coupled YIG-tuned filters in the 12-40 GHz region," IEEE Trans. Microwave Theory Tech, vol. 18, pp. 205–212, Apr. 1970.

[6] A. Tombak, J.-P. Maria, F. T. Ayguavives, Z. Jin, G. T. Stauf, A. I. Kingon, and A. Mortazawi, "Voltage-controlled RF filters employing thin-film barium-strontium-titanate tunable capacitors," IEEE Trans. Microwave Theory & Tech., vol. 51, no. 2, pp. 462–467, Feb. 2003.

[7] B. H. Moekley and Y. Zhang, "Struntium titanate thin films for tunable Y Ba2Cu3O7 microwave filters," IEEE Trans. Appl. Superconduct., vol. 11, pp. 450–453, Mar. 2001.

[8] S. R. Chandler, I. C. Hunter, and J. C. Gardiner,"Active varactor tunable bandpass filters," IEEE Microwave Guided Wave Lett., vol. 3, pp. 70-71, March 1993.

[9] A. R. Brown and G. M. Rebeiz, "A varactor-tuned RF filter," IEEE Trans. Microwave Theory & Tech., vol. 48, no. 7, pp. 1157–1160, July 2000.

[10] I. C. Hunter and J. D. Rhodes, "Electronically tunable microwave bandpass filters," IEEE Trans. Microwave Theory & Tech., vol. 30, no. 9, pp. 1354–1360, Sept. 1982.

[11] G. M. Rebeiz, RF MEMS Theory, Design, and Technology.New York, USA: Wiley, 2003.

[12] K. Entesari and G. M. Rebeiz, "A differential 4-bit 6.5-10 GHz RF MEMS tunable filter," IEEE Trans. Microwave Theory & Tech., vol. 53, no. 3, pp. 1103–1110, Mar. 2005.

[13] L. Dussopt and G. M. Rebeiz, "Intermodulation distortion and power handling in RF MEMS switches, varators, and tunable filters," IEEE Trans. Microwave Theory & Tech., vol. 51, no. 4, pp. 1247–1256, Apr. 2003.

[14] L. Dussopt and G. M. Rebeiz, "High-Q millimeter-wave MEMS varactors," IEEE MTT-S Int. Microwave Symp. Dig., pp. 1205–1208, June 2000.

[15] A. Pothier, J.-C. Orlianges, G. Zheng, C. Champeaux, A. Catherinot, P. B. D. Cros, and J. Papapolymerou, "Low-loss 2-bit tunable bandpass filters using MEMS DC contact switches," IEEE Trans. Microwave Theory & Tech., vol. 53, no. 1, pp. 354–360, Jan. 2005.

[16] J.-M. Kim, S. Lee, J.-H. Park, J.-M. Kim, C.-W. Baek, Y. Kwon, and Y.-K. Kim, "Dig- itally frequency-controllable dual-band WLAN filters using micromachined frequency- tuning elements," in 19th IEEE MEMS 2006 Conf., Istanbul, Turkey, Jan. 2006, pp. 158–161.

[17] S. Duffy, C. Bozler, S. Rabe, J. Knecht, L. Travis, P. Wyatt, C. Keast, and M. Gouker, "MEMS microswitches for reconfigurable microwave circuitry," IEEE Microw. Wireless Compon. Lett., vol. 11, no. 3, pp. 106–108, Mar. 2001.

[18] R. M. Young, J. D. Adam, C. R. Vale, T. T. Braggins, S. V. Krishnaswamy, C. E. Milton, D. W. Bever, L. G. Chorosinski, L.-S. Chen, D. E. Crockett, C. B. Freidhoff, S. H. Talisa, E. Capelle, R. Tranchini, J. R. Fende, J. M. Lorthioir, and A. R. Tories, "Low-loss bandpass RF filter using MEMS capacitance

switches to achieve a one-octave tuning range and independently variable bandwidth," in IEEE MTT-S International Microwave Symposium Digest, Philadelphia, PA, June 2003, pp. 1781–1784.

[19] A. Grichener, B. Lakshminarayanan, and G. M. Rebeiz, "High-Q RF MEMS capacitor with digital/analog tuning capabilities," IEEE MTT-S Int. Microwave Symp. Dig., June 2008.

[20] H. Joshi, H. H. Sigmarsson, D. Peroulis, and W. J. Chappell, "Highly loaded evanescent cavities for widely tunable high-Q filters," in IEEE MTT-S Int. Microwave Symp. Dig., Honolulu, Hawaii USA, June 2007, pp. 2133–2136.

[21] J. Brank, J. Yao, M. Eberly, A. Malczewski, K. Varian, and C. L. Goldsmith, "RF MEMS-based tunable filters," Int. J. RF Microwave CAE, vol. 11, pp. 276–284, Sept. 2001.

[22] B. Lakshminarayanan and T. Weller, "Tunable bandpass filter using distributed MEMS transmission lines," in IEEE MTT-S Int. Microwave Symp. Dig., Philadelphia, PA USA, June 2003, pp. 1789–1792.

[23] R. M. Young, J. D. Adam, C. R. Vale, T. T. Braggins, S. V. Krishnaswamy, C. E. Milton, D. W. Bever, L. G. Chorosinski, L.-S. Chen, D. E. Crockett, C. B. Freidhoff, S. H. Talisa, E. Capelle, R. Tranchini, J. R. Fende, J. M. Lorthioir, and A. R. Tories, "Low-loss bandpass RF filter using MEMS capacitance switches to achieve a one-octave tuning range and independently variable bandwidth," in IEEE MTT-S International Microwave Symposium Digest, Philadelphia, PA, June 2003, pp. 1781–1784.

[24] A. Abbaspour-Tamijani, L. Dussopt, and G. M. Rebeiz, "Miniature and tunable filters using MEMS capacitors," IEEE Trans. Microwave Theory & Tech., vol. 51, no. 7, pp. 1878–1885, July 2003.

[25] C. D. Nordquist, A. Muyshondt, M. V. Pack, P. S. Finnegan, C. W. Dyck, I. C. Reines, G. M. Kraus, T. A. Plut, G. R. Sloan, C. L. Goldsmith, and C. T. Sullivan, "An x- band to Ku-band RF MEMS switched coplanar strip filter," IEEE Microw. Wireless Compon. Lett., vol. 14, no. 9, pp. 425–427, Sept. 2004.

[26] B. Pillans, A. Malczewski, R. Allison, and J. Brank, "6-15 GHz RF MEMS tunable filters," in IEEE MTT-S Int. Microwave Symp. Dig., Long Beach, CA USA, June 2005, pp. 919–922.

[27] C. L. Goldsmith, Z. Yao, S. Eshelman, and D. Denniston, "Performance of low-loss RF MEMS capacitive switches," IEEE Microw. Guided Wave. Lett., vol. 11, no. 3, pp. 106–108, Mar. 2001.

AUTHOR'S PUBLICATION RECORD

LIST OF PUBLICATIONS

JOURNAL ARTICLES

[1] **A .S. Hussaini**, I. T . E . Elfergani, J. Rodriguez, and R. Abd-Alhameed **"Efficient Multi-Stage Load Modulation RF Power Amplifier for Green RF Front End",** IET Science, Measurement & Technology, May 2012, Volume 6, Issue 3, p.117–124.

[2] I.T. E. Elfergani, **Abubakar Sadiq Hussaini**, T. Sadeghpour, R.A. Abd-Alhameed and J. Rodriguez "**A Design Procedure of Mobile Handsets Reconfigurable Antenna and Harmonics Suppression Method**" IET Microwave, Antennas & Propagation, July 2012, Vol. 6, Iss. 9, pp. 990–999.

[3] R.A. Abd-Alhameed, P.S. Excell, J. Rodriguez, and **A.S. Hussaini**, Editorial: **"Energy Efficient Reconfigurable Transceivers"**, IET Science, Measurements and Technology, May 2012, Vol. 6, Iss. 3, pp. 113–116.

CONFERENCES AND WORKSHOPS

[1] **Abubakar Sadiq Hussaini**, Raed Abd-Alhameed, Jonathan Rodriguez, **"Tunable RF Filters: survey and beyond"**, 18th IEEE International Conference on Electronics, Circuits, and Systems (ICECS 2011), Beirut, Lebanon, 11-14 December 2011.

[2] **A. S. Hussaini,** T. Sadeghpour, R. Abd-Alhameed, B. A. L. Gwandu, J. Rodriguez, **"Energy Conservation and CO2 Reduction by Improved Power Amplifier Design"**, Proc. of the 2012 IEEE Topical Symposium on Power Amplifiers for Wireless Communications, Tempe, Arizona, USA, November, 2011.

[3] **Abubakar Sadiq Hussaini**, Issa T. E. Elfergani, Bashir A. L. Gwandu, Raed Abd-Alhameed, Jonathan Rodriguez, **"Load Pull Characterisation for High Power And High Energy Efficient Active amplifying device"**, 4th International Conferences On Internet Technologies and Applications (ITA 11), Glyndwr University, Wrexham, North Wales, UK, 6-9 September 2011.

[4] **Abubakar Sadiq Hussaini**, Bashir A. L. Gwandu, Raed Abd-Alhameed, Jonathan Rodriguez, **"The Beyond 3G Energy Efficient Power Amplifier for Mobile Communications"** Proc. of the 26th WWRF Meeting, Doha, Qatar, 11th-13th April 2011, Paper No. WWRF25-WG4-9.

[5] **Abubakar Sadiq Hussaini**, Raed Abd-Alhameed, Jonathan Rodriguez, **"Design of Energy Efficient Power Amplifier for 4G User Terminals"**, 17th IEEE International Conference on Electronics, Circuits, and Systems (ICECS 2010), Athens, Greece 12-15 December 2010, Paper No. 533, pp. 617-620, ISBN: 978-1-4244-8156-9.

[6] **Abubakar Sadiq Hussaini**, Raed Abd-Alhameed, Jonathan Rodriguez**, "Green Radio: Approach Towards Energy Efficient Power Amplifier for 4G Communications"**, Proc. of the 25th WWRF Meeting, Kingston-upon-Thames, UK, 16th-18th November 2010, Paper No. WWRF25-WG4-12.

[7] **Abubakar Sadiq Hussaini**, Bashir A. L. Gwandu, Raed Abd-Alhameed, Jonathan Rodriguez, **"Design of Power Efficient Power Amplifier for B3G Base Stations"**, 9th IEEE International Symposium on Electronics and Telecommunications (ISETC 2010), Timisoara, Romania, 11-12 November 2010, Paper No. 103, pp. 89-92, ISBN: 978-1-4244-8458-4.

[8] **Abubakar Sadiq Hussaini**, Tahereh Sadeghpour, Raed Abd-Alhameed, Mark Child, Nazar Ali, Jonathan Rodriguez, **"Design of Doherty RFPA for Mobile WiMAX Base Stations"**, 6th International ICST Conference on Mobile Multimedia Communications, EERT-3, Lisbon, Portugal, 6-8 September 2010, Paper No. 3, pp. 1-8, ISBN: 978-963-9799-98-1.

[9] **A. S. Hussaini,** R. A. Abd-Alhameed, J. Rodriguez, **"Implementation of Efficiency Enhancement Techniques in the Linear Region of Operations of Power Amplifier"**, 7th Conference on Telecommunications 2009 (Conftele 2009) Santa Maria de Feira, Portugal, 3- 5 May 2009, Paper No. 103, pp. 105-108.

[10] I.T.E. Elfergani, **Abubakar Sadiq Hussaini**, R.A. Abd-Alhameed, , M.B. Child, S.M.R. Jones and Jonathan Rodriguez, **" Tunable PIFA Slot Antenna for Mobile Handset and WLAN Applications "**, 6th IEEE European Conference on Antennas and Propagation: EuCAP 2012, Prague, Czech Republic, 25-30 March 2012.

[11] I.T.E. Elfergani, **Abubakar Sadiq Hussaini**, R.A. Abd-Alhameed, , M.B. Child, S.M.R. Jones and Jonathan Rodriguez, **" Tunable PIFA Slot Antenna for Mobile Handset and WLAN Applications "**, 6th IEEE European Conference on Antennas and Propagation: EuCAP 2012, Prague, Czech Republic, 25-30 March 2012.

[12] Y. A. S. Dama, **A. S. Hussaini,** R. A. Abd-Alhameed, S. M. R. Jones, N. J. McEwan, T. Sadeghpour, and J. Rodriguez, **"Envelope correlation formula for (N, N) MIMO antenna array including power losses,"** 18th IEEE International Conference on Electronics, Circuits, and Systems (ICECS 2011), Beirut, Lebanon, 11-14 December 2011, pp. 508-511.

[13] I.T.E. Elfergani, **Abubakar Sadiq Hussaini**, R.A. Abd-Alhameed, C.H. See, H.I. Hraga, M.S.Bin-Melha, P.S.Excell and Jonathan Rodriguez, **"A Dual-Band Frequency Tunable Planar Inverted F Antenna"**, 5th IEEE European Conference on Antennas and Propagation: EuCAP 2011, Rome, Italy, pp. 235-239, 11-15 April 2011.

[14] Issa T. E. Elfergani, **Abubakar Sadiq Hussaini**, Raed A. Abd-Alhameed, Chan H. See, Musa M. Abusitta, Hmeda I. Hraga, A. G. Alhaddad, and Jonathan Rodriguez **"Frequency Tuned Planar Inverted F Antenna with L Shaped Slit Design for Wide Frequency Range"** 29th Progress in Electromagnetics Research Symposium (PIERS 2011), Marrakesh, MOROCCO 20-23 March 2011, Proceedings, 443 - 447, ISSN: 1559 – 9450.

[15] Nazar Ali, **Abubakar Sadiq Hussaini,** Raed Abd-Alhameed, Neil McEwan, Mark Child, E. Khazmi, Jonathan Rodriguez, **"Explanation of DC/RF Loci for Active Patch Antennas"**, 6th International ICST Conference on Mobile Multimedia Communications, EERT-3, Lisbon, Portugal, 6-8 September 2010, Paper No. 2, pp. 1-8, ISBN: 978-963-9799-98-1.

[16] T. Sadeghpour, **A. S. Hussaini**, A. Ghorbani, R. Abd-Alhameed, J. Rodriguez, **"Behavioral Modeling and Compensation Procedure of OFDM Transmitters"**, Proc. of the 9th IEEE Malaysia International Conference on Communications (MICC 2009), Kuala Lumpur, Malaysia, 14 – 17 December 2009.

[17] T. Sadeghpour, **A. S. Hussaini**, R. Abd-Alhameed, A. Ghorbani, J. Rodriguez, **"Behavior Modeling and Compensation Procedure of Wideband RF Transmitters Exhibiting Memory Effects",** Proc. of the 2009 IEEE Topical Symposium on Power Amplifiers for Wireless Communications, San Diego, USA, September 2009.

www.ietdl.org

Published in IET Science, Measurement and Technology
Received on 28th June 2011
Revised on 6th January 2012
doi: 10.1049/iet-smt.2011.0127

ISSN 1751-8822

Efficient multi-stage load modulation radio frequency power amplifier for green radio frequency front end

A.S. Hussaini[1,2] *I.T.E. Elfergani*[1] *J. Rodriguez*[2] *R.A. Abd-Alhameed*[1]

[1]*School of Engineering, Design and Technology, University of Bradford, Bradford, UK*
[2]*Instituto de Telecomunicações, Aveiro, Portugal*
E-mail: i.t.e.elfergani@bradford.ac.uk

Abstract: The road towards the reduction in the carbon footprint associated with power-hungry wireless communication devices will require a holistic design approach to ensure that energy saving can be achieved throughout the entire system. The information and communication technology today accounted for 3 and 2% global power consumption and global CO_2 emissions, respectively, where a significant portion is a result of the power consumption in the radio frequency (RF) power amplifier device. Moreover, tomorrow amplifiers will need to be reconfigurable and host a plethora of modulated signals to support effective signal processing. Therefore performance metrics such as linearity, power efficiency and their trade-off should be at the forefront of the RF power amplifier design. This study proposes an energy-efficient power amplifier design based on the Doherty configuration as part of a green RF front end for mobile WiMAX. The authors extend the classical Doherty to incorporate a three-stage load modulation design with a proposed new output power combiner. The performance of the three-stage load modulation RF power amplifier is compared with the legacy two-stage load modulation technique. The experimental results show that 30 dBm output power can be achieved with 67% power-added efficiency, which represents a 14% improvement over the current state-of-the-art system while meeting the power output requirements for mobile WiMAX.

1 Introduction

The future accelerated growth of mobile traffic coupled with the need for broadband applications have increased the complexity and design requirements of radio frequency (RF) front end, especially the RF power amplifier design. Beyond third-generation (3G) communication paradigms the end user is envisaged as living in a pervasive and ubiquitous wireless world having the freedom of access to internet services on any device or any network at anytime. The flexibility to be connected to any network implies that future handsets will become fully virtualised and support multiple air-interfaces using reconfigurable hardware- and software-defined radio. These two enabling technologies will interact in synergy to allow the mobile device to scan and synchronise to the available radios, and to connect in a seamless fashion to the best available network. This means that the power amplifier needs to effectively support a whole host of modulation schemes, and frequencies. The most commonly used modulation technique in legacy and future emerging technologies is orthogonal frequency division multiplexing (OFDM). This is a multicarrier modulation technique that can provide high data rate and significantly overcome multipath interference that leads to signal degradation. However, this modulation technique, unlike legacy 2G modulation techniques, has a high crest factor enforcing linear amplification over a large dynamic range. If this were to be done with existing power amplifier techniques, this would result in poor efficiency and output power.

A rising concern in today's green society is the energy consumption and the carbon footprint emitted by ICT (information and communication technology) devices. In fact, the whole ICT sector has been estimated to account for only 2 per cent of global CO_2 emissions; this percentage is comparable to the emissions caused by global aviation. Therefore energy saving should be at the forefront of any communication system design. Moreover, there is a continuously increasing gap between the energy requirements of power-hungry radio devices, and what can actually be delivered by new battery technology. Without new approaches to energy saving, there is significant concern that future mobile users will be searching for power outlets rather than for network access which stands in complete irony to the beyond-3G philosophy. In typical mobile terminals for cellular systems, up to half of the power consumptions come from communications-related functions, such as baseband processing, RF and connectivity functions. Therefore any reduction in the power consumption of the power amplifier device will have a substantial impact on carbon footprint and prolong battery lifetime.

We have highlighted energy consumption and linearity as two important design requirements that should be addressed if we are to have effective RF power amplification in tomorrow's handsets. The state-of-the-art on energy-efficient RF power amplifier design techniques include the Chireix out-phasing [1], Doherty configuration [2], envelope tracking and Kahn envelope elimination and

restoration [3], which involve a complex circuit design and require the use of external circuit control and signal processing making their practical implementation challenging. However, the Doherty amplifier, which has self-managing characteristics, is considered to be the most attractive design and is considered here as the baseline for the proposed three-stage design. The proposed Doherty configuration will be designed for the mobile WiMAX frequency band, where we focus on the 3.4–3.6 GHz range which is the band being used in Europe.

This paper has the following outline: Section 2 addresses the RF power amplifier's linearity and output power requirement; Section 3 describes the proposed multi-stage load modulation circuit architecture; Section 4 explains the current drive analysis for the three-stage load modulation circuit; circuit prototype and then results are given in Section 5, and finally summarised conclusions are presented in Section 6.

2 RF power amplifier's linearity and output power requirement

The envelope variation of an OFDM signal clearly requires a linear radio frequency power amplifier). It should be noted that the IEEE 802.16e/Mobile WiMAX standard does not specify the minimal required intermodulation distortion (IMD) of the user terminal PA (Power Amplifier), but exploits the system-level requirement to describe the maximal allowable distortion. These system-level requirements include the spectral mask and the error vector magnitude (EVM) [4]. The spectral mask is specified at the PA output, and ensures that the user terminal transmitter does not corrupt or block the spectrum from adjacent channels. The error vector ($E(s)$) is the difference between the actual transmitted ($A(s)$) and ideal ($H(s)$) constellation point. EVM is specified after reception and demodulation by an ideal receiver, and is a measure of performance within the channel. The EVM of a symbol S is defined as

$$\mathrm{EVM} = \sqrt{\frac{|E(s)|^2}{(1/N)\sum_S |H(s)|^2}} \tag{1}$$

where N is the level of the modulation.

To obtain EVM as a percentage, the RMS value is used; this is a useful system-level figure of merit for the accuracy of the OFDM signal

$$\mathrm{EVM}\ (\%) = \sqrt{\frac{P_{\mathrm{error}}}{P_{\mathrm{ref}}}} \times 100\% \tag{2}$$

And can also be measured in (dB)

$$\mathrm{EVM}\ (\mathrm{dB}) = 10\log_{10}\left(\frac{P_{\mathrm{error}}}{P_{\mathrm{reference}}}\right) \tag{3}$$

where P_{error} is the RMS power of the error vector, and P_{ref} for single-carrier modulation is the power of the outermost point in the reference constellation and for multi-carrier modulations, is defined as the reference constellation average power. The spectral mask and EVM for mobile WiMAX are comparatively rigorous among existing standards.

3 Multi-stage load modulation circuit architecture

The classical load modulation RF power amplifier, shown in Fig. 1, has two amplifiers with the same output power capability arranged in parallel, but different in biasing. The two amplifiers are the carrier amplifier stage, which operates in class AB and the peaking amplifier stage that operates in class C. The input signal is divided equally in amplitude by a splitter with 90° phase difference, so as to drive the class AB carrier amplifier stage and the class C peaking amplifier stage, and their outputs are connected by a transformer coupler which combines the output signals [5–11].

The classical load modulation RF power amplifier achieves a significantly higher efficiency at some point of output power back-off over the traditional stand-alone RF power amplifier. However, with OFDM wireless signals that have high peak-to-average power ratios, the efficiency of the classical load modulation RF power amplifier can be improved further by extending configuration to a three-stage design.

The proposed three-stage load modulation RF power amplifier, shown in Fig. 3, has three power amplifiers with the same out power capability and are arranged in parallel; two have the same bias point whereas the other has its own different bias point. The three amplifiers are carrier amplifier stage, which operates in class B mode whereas the two peaking amplifiers operate in class C mode. Furthermore, for proper load modulation, the input signal is divided equally in amplitude, but with phase differences. The phase difference between carrier amplifier and peaking 1 amplifier is 90°, and the phase difference between carrier amplifier and peaking 2 amplifier is 180°. The signal splitter was designed independently and tested in terms of the frequency response and the operational bandwidth, before integrating it into the whole design. This was done because the operation is strongly influenced by the coupling factor of the input splitter.

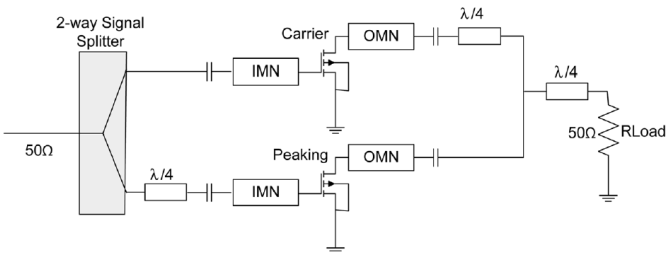

Fig. 1 *Schematic diagram of a classical load modulation power amplifier*

IET Sci. Meas. Technol., pp. 1–8
doi: 10.1049/iet-smt.2011.0127

In this design, the class B mode was chosen to act as the carrier amplifier stage, instead of the class AB mode which is widely used in the classical load modulation power amplifier design. The selection of the class B mode as the carrier amplifier stage would significantly increase the efficiency of the whole design.

According to [9] and Fig. 2, the output of the carrier amplifier and the output of the peaking 1 amplifier require a quarter-wavelength transmission line, which is also applied to the output of peaking 1 amplifier and the output of peaking 2 amplifier. Obviously, this will increase the complexity of the design and increase the circuit space, and if not properly designed can significantly reduce the efficiency and linearity of the whole design.

In this paper, as shown in Fig. 3, we considered a simple summing network at the output of the three-stage load modulation power amplifier. The summing network also acts as a phase difference compensator which adds the signal from each amplifier to the output load constructively. The quarter-wavelength transmission line was implemented between the output of the carrier amplifier and the output of the peaking 1 amplifier; then the output of the peaking 2 amplifier was directly connected to the output of the peaking 1 amplifier without adding any quarter-wavelength transmission line. This summing network will allow a proper load modulation operation. The operation is also strongly influenced by the quarter-wavelength at the output of the carrier amplifier. However, the peaking 1 and the peaking 2 amplifiers can pull out the load presented to the carrier amplifier for peak efficiency and output power.

4 Current drive analysis of a three-stage load modulation circuit

For the transmission line, the relationship between input voltage $\boldsymbol{V}_{\text{in}}$ and input current $\boldsymbol{I}_{\text{in}}$ to the output voltage $\boldsymbol{V}_{\text{out}}$ and output current $\boldsymbol{I}_{\text{out}}$ is given in matrix form [4, 5]

$$\begin{bmatrix} \boldsymbol{V}_{\text{in}} \\ \boldsymbol{I}_{\text{in}} \end{bmatrix} = \begin{bmatrix} \cos \pi/2 & jZ_{\text{o}} \sin \pi/2 \\ jY_{\text{o}} \sin \pi/2 & \cos \pi/2 \end{bmatrix} \begin{bmatrix} \boldsymbol{V}_{\text{out}} \\ \boldsymbol{I}_{\text{out}} \end{bmatrix} \tag{4}$$

$Z_{\text{in}} = \boldsymbol{V}_{\text{in}}/\boldsymbol{I}_{\text{in}}$ is the source impedance, Z_{o} is the characteristic impedance of the transmission line, and Z_{L} is the load impedance and is given as $Z_{\text{L}} = \boldsymbol{V}_{\text{out}}/\boldsymbol{I}_{\text{out}}$.

Z_{in} becomes

$$Z_{\text{in}} = \frac{Z_L \cos \pi/2 + jZ_0 \sin \pi/2}{j(Z_L/Z_0) \sin \pi/2 + \cos \pi/2} \tag{5}$$

For the quarter-wavelength transmission line, $\cos \pi/2 = 0 = 0$ and $\sin \pi/2 = 1$, then Z_{in} will become

$$Z_{\text{in}} = \frac{Z_0}{Z_{\text{L}}/Z_0}, \quad Z_{\text{in}} = \frac{Z_0^2}{Z_{\text{L}}} \tag{6}$$

Fig. 4 shows the analysis diagram for a three-stage current. The quarter wavelength at the output of carrier amplifier acts as a load modulation coupler which causes the resistive impedance seen by the carrier amplifier to go high when two peaking amplifiers are in off-state and to go low when the two peaking amplifiers are in on-state.

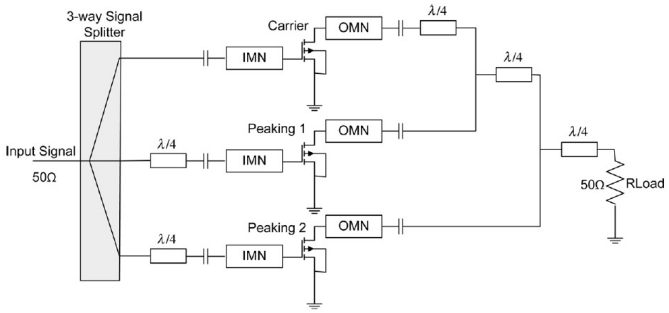

Fig. 2 *Schematic diagram of a three-stage load modulation power amplifier*

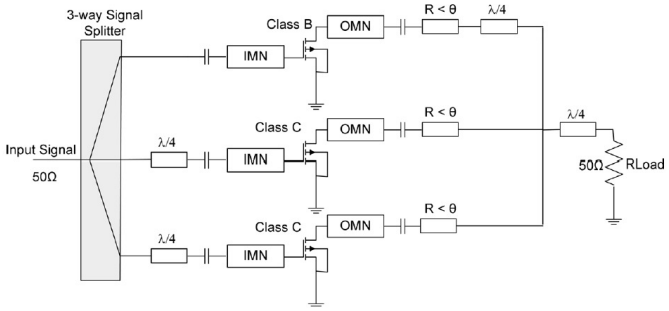

Fig. 3 *Schematic diagram of the proposed three-stage load modulation power amplifier*

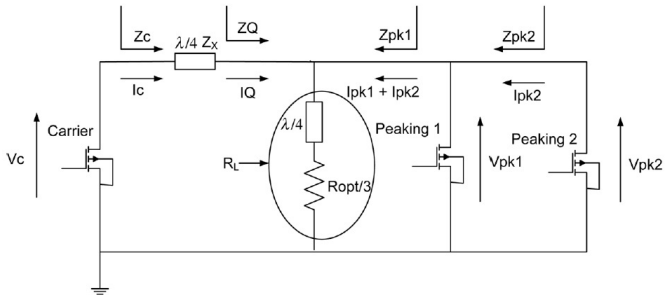

Fig. 4 *Analysis diagram for three-stage current*

The phase output current of carrier amplifier (I_c) must lead that of the output current of peaking 1 and peaking 2 amplifiers (I_{pk1}, I_{pk2}) by 90 and 180°, respectively. However, the operational principle of a three-stage load modulation RF power amplifier can be best described by dividing the level of input drive into low-level drive (carrier is turned ON and peaking 1 and peaking 2 are turned OFF), medium-level drive (carrier and peaking 1 are turned ON and peaking 2 is turned OFF) and high-level drive (where both amplifiers are turned ON). At high input signal, both the carrier and the two peaking amplifiers are in on-state and their RF current envelopes can be written as follows

$$I_C = \frac{I_{max}}{6}(1+x) \tag{7}$$

$$I_{PK1} = \frac{I_{max}}{3}x \tag{8}$$

$$I_{PK2} = \frac{I_{max}}{3}x(x-0.5) \tag{9}$$

where x has a value of 0 at low-level drive, a value of 0.5 at medium-level drive and a value of 1 at high-level drive.

The effective impedance with load pulling effect, on each amplifier can be given by

$$Z_Q = R_L\left(1+\frac{I_{PK1}+I_{PK2}}{I_Q}S\right) \tag{10}$$

$$Z_{PK1} = R_L\left(1+\frac{I_Q}{I_{PK1}+I_{PK2}}\right) \tag{11}$$

$$Z_{PK2} = R_L\left(1+\frac{I_Q+I_{PK1}}{I_{PK2}}\right) \tag{12}$$

From (3), and in Fig. 5, the quarter wavelength at the output of the carrier amplifier acts as a load modulation coupler where the resistive impedance seen by the carrier amplifier goes high when the two peaking amplifiers are in off-state and goes low when they are in on-state.

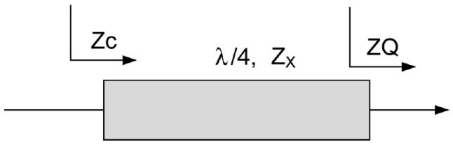

Fig. 5 *Quarter-wavelength transmission line*

The transformation of the input, output and characteristic impedance of a quarter-wavelength transmission line is given as

$$Z_C = \frac{Z_X^2}{Z_Q} \tag{13}$$

Equation (10) is the output impedance seen by the carrier amplifier and when substituting Z_Q in (10), the output impedance becomes

$$Z_C = \frac{Z_X^2}{Z_Q} = \frac{Z_X^2}{R_L(1+(I_{PK1}+I_{PK2}/I_Q))} \tag{14}$$

V_c is the output voltage of carrier amplifier and is given as

$$V_C = Z_C * I_C = \frac{Z_X^2}{R_L(1+(I_{PK1}+I_{PK2}/I_Q))} * I_C$$

$$I_Q = \frac{V_C}{Z_X} \tag{15}$$

$$V_C = \frac{Z_X^2 * I_C}{R_L(1+(I_{PK1}+I_{PK2}/V_C/Z_X))} \tag{16}$$

After substituting I_C, I_{PK1} and I_{PK1} into Z_C, Z_C becomes

$$V_C = \left(\frac{Z_X}{6R_L}\right)(I_{MAX})(Z_X(1+X) - 4R_L X^2 + 2R_L X$$

$$R_L = \frac{R_{opt}}{3}) \tag{17}$$

$$V_C = \frac{Z_X}{R_{opt}}\left(\frac{I_{max}}{2}\right) \times \left(Z_X(1+X) - 4\frac{R_{opt}}{3}X^2 + 2\frac{R_{opt}}{3}X\right) \tag{18}$$

$$Z_X = R_{opt}$$

$$V_C = \frac{R_{opt}+I_{max}}{2}\left(-\frac{4}{3}X^2 + \frac{5}{3}X + 1\right) \tag{19}$$

From the above equation, the output voltage remains approximately constant only at low-level drive where only the carrier is in on-state and high-level drive (where both amplifiers are in on-state), at medium-level drive, the output voltage of the carrier amplifier increases by the factor

doi: 10.1049/iet-smt.2011.0127

3/2 (1.5). Figs. 6 and 7 show input voltage against output voltage of classical and three-stage load modulation, respectively.

5 Circuit prototype and results

The three-stage load modulation RF power amplifier utilises the FPD1500S0T89 device. It has been designed using a TOM3 large signal model and an FPD1500 transistor. The FPD1500SOT89 is a packaged depletion model AlGaAs/InGaAs pseudomorphic high electron mobility transistor. It contains double recessed gate structure, which minimises parasitic and optimise performance.

In this paper, the bias circuit for the carrier amplifier was designed based on class B mode and the two peaking amplifiers were based on class C mode. The decision to use class B mode as a carrier amplifier instead of class AB mode, which is widely adopted in the combination of Doherty amplifier, was taken in order to improve the efficiency of the entire design. The conduction angle of class B amplifier remains at 180° and is independent of the input signal level. However, the class B amplifier DC quiescent current is at the threshold that means the quiescent current is theoretically zero. But in this design, the quiescent current was increased to an order of 8% of the peak drain current which resulted to 0.046 mA. The motive behind this is to minimise crossover distortion and increase the efficiency. The peak drain current of FPD1500 transistor is 0.587 mA when the gate bias voltage is at (0 V) and the drain bias voltage at (5 V). The 5 V was chosen for the drain bias voltage because it is located between the cut-off and saturation point of the FPD1500 transistor. The carrier amplifier gate bias voltage should be set to (−0.9 V) to establish the carrier amplifier quiescent current at (0.046 mA) which is 8% of the peak drain current of the transistor. The gate bias voltage against drain current of class B is depicted in Fig. 8.

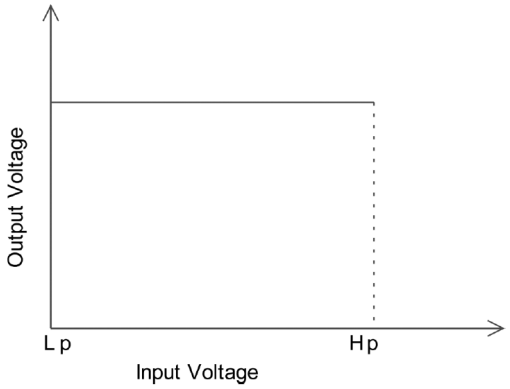

Fig. 6 *Input voltage against output voltage of classical load modulation*

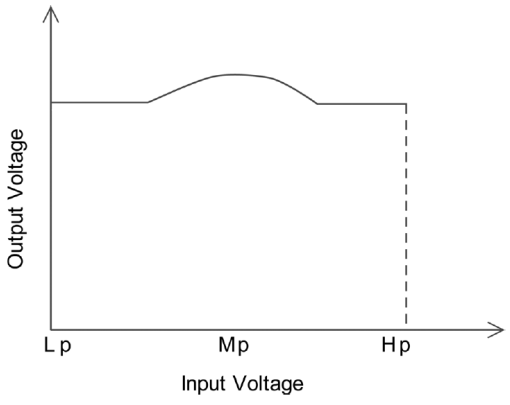

Fig. 7 *Input voltage against output voltage of three-stage load modulation*

The two peaking amplifiers are biased to turn on only when the carrier amplifier reaches the saturation level. The peaking 1 and peaking 2 amplifiers are biased in the class C mode that is below the threshold. They can only turn on when the input drive reaches a predetermined level, because class C mode is absolutely dependent on the input drive level. The peaking 1 and peaking 2 amplifiers' gate bias voltage should be set to (−1.1 V) to properly work in the class C mode. The two peaking amplifiers quiescent current is (0.004 mA).

To this point, we have in fact biased both the carrier and the two peaking amplifiers, where the bias condition for the carrier amplifier is $V_{gs} = -0.9$ V ($I_{ds} = 46$ mA), and for the peaking 1 and peaking 2 amplifiers is $V_{gs} = -1.1$ V ($I_{ds} = 4$ mA). The drain bias voltage for both amplifiers is ($V_{ds} = 5$ V). The splitter at the input, the carrier amplifier, the peaking 1 amplifier, the peaking 2 amplifier and the impedance transformer with phase compensation at the output are combined to form a single three-stage load modulation RF power amplifier. Fig. 9 shows the prototype diagram of the proposed three-stage load modulation RF power amplifier.

The three-stage load modulation RF power amplifier is initially characterised for AM–AM and AM–PM responses, as well as for output power and efficiency. The performance comparisons between the three-stage load modulation amplifier and the classical load modulation amplifier were performed, where the output power increased to 30 dBm at the 1 dB compression point whereas the efficiency increased to 67%. Fig. 10 represents the variation and comparison of the input power against output power for the three-stage load modulation and classical load modulation amplifiers. It clearly shows that the 30 dBm output power is at the edge of the linear region of the amplifier, and this was achieved due to the characteristic of

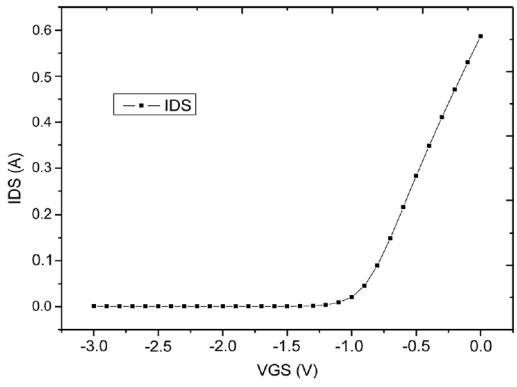

Fig. 8 *Threshold of the drain current of class B*

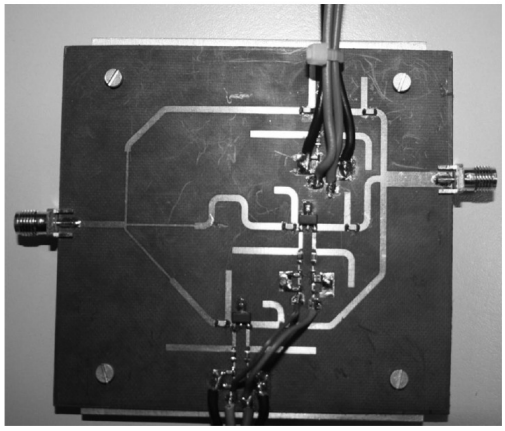

Fig. 9 *Prototype of the three-stage load modulation RF power amplifier*

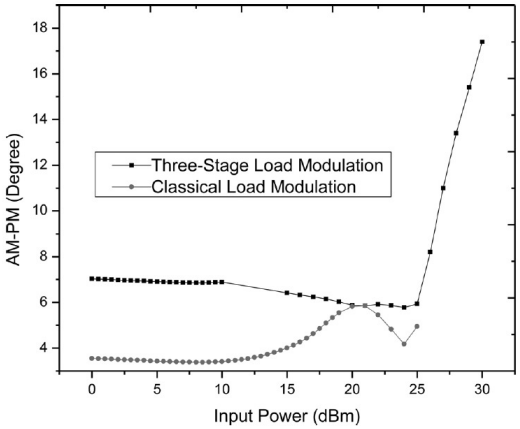

Fig. 11 *AM–PM characteristics of three-stage load modulation*

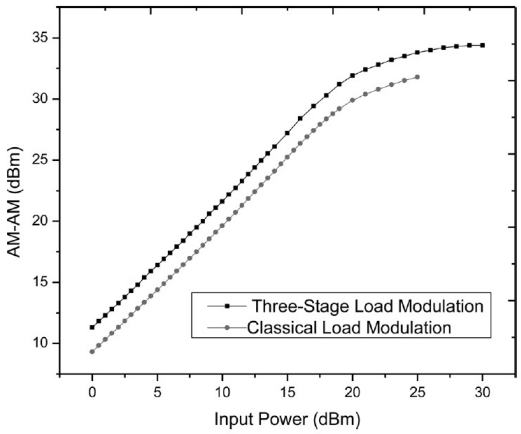

Fig. 10 *AM–AM characteristics of three-stage load modulation*

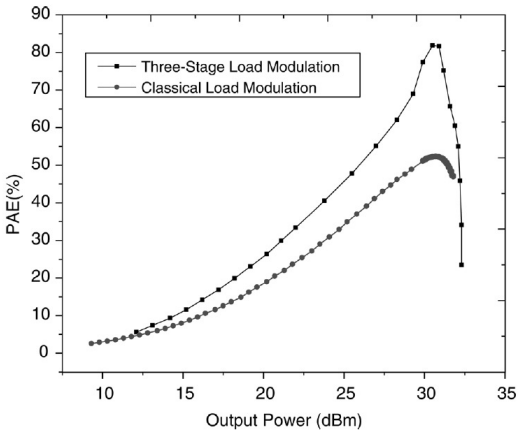

Fig. 12 *Power-added efficiency*

the overall gain as a product of the three-stage load modulation, which preserves its constant nature throughout the range up to 30 dBm. The peaking 1 and peaking 2 amplifiers late gain expansion can compensate for the carrier amplifier gain compression. Fig. 11 shows the comparison of AM–PM characteristics of the two different topologies.

The power-added efficiency against output power is shown in Fig. 12. The three-stage load modulation amplifier has higher efficiency over the range of output power levels compared to the classical load modulation amplifier.

The two-tone characterisation with 5 MHz tone spacing was performed and was concentrated on achieving acceptable IMD3 and IMD5. Figs. 13 and 14 shows the performance comparisons between the three-stage load modulation amplifier and the classical load modulation amplifier for the IMD3 and IMD5 as a function of output power.

These results show that the IMD3 and IMD5 tone response of a three-stage load modulation have been improved significantly over the IMD3 and IMD5 of the classical load modulation.

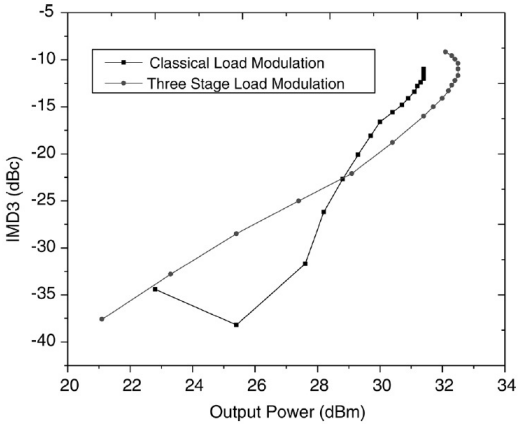

Fig. 13 *Two-tone characterisation (IMD3)*

doi: 10.1049/iet-smt.2011.0127

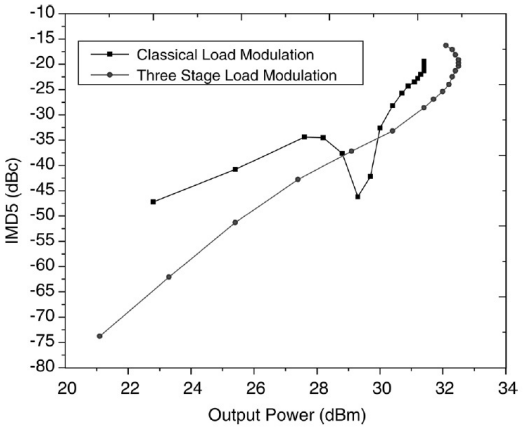

Fig. 14 *Two-tone characterisation (IMD5)*

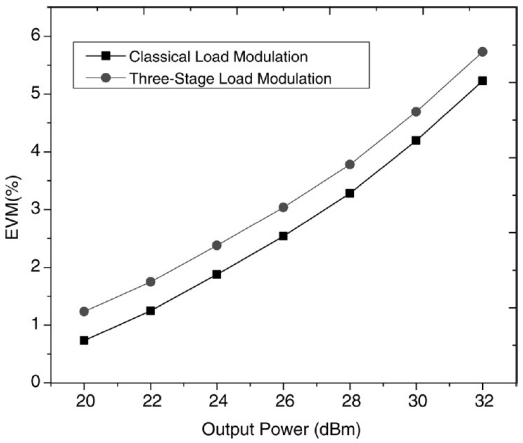

Fig. 15 *EVM characterisation*

The three-stage load modulation power amplifier was also tested with the modulated mobile WiMAX signal. The modulated 64-QAM OFDM signal with 10 MHz bandwidth was used and a result of less than 5% EVM was obtained. Fig. 15 shows the comparison of the linearity performance of a three-stage load modulation with the classical load modulation fed by a modulated mobile WiMAX signal, and it can be seen that the spectrum mask of the mobile WiMAX requirement are satisfied. EVM for the three-stage load modulation is generally poorer than classical load modulation.

6 Conclusion

This paper has presented the design and implementation of the three-stage load modulation RF power amplifier for mobile WiMAX application. The amplifier was characterised using single-tone, two-tone and the mobile WiMAX-modulated input signals. The achieved results have shown good efficiency, power performances and satisfy the linearity requirement for mobile WiMAX. The proper phasing of the splitter at the input, and the proper design of the impedance transformer with phase compensation at the output can effectively contribute to the total efficiency of the system. The operation of this design was strongly influenced by the coupling factor of the splitter, the biasing of the carrier amplifier and the biasing of the peaking 1 and the peaking 2 amplifiers. The turn-on of the two peaking amplifiers are dependent on the input signal. The performance of the three-stage load modulation RF power amplifier has compared with the legacy two-stage load modulation RF power amplifier technique. The experimental results show that 30 dBm output power can be achieved with 67% power-added efficiency, which represent a 14% improvement over the current state-of-the-art system while meeting the power output requirements for mobile WiMAX. The results have shown that the proposed three-stage load modulation RF power amplifier can be a suitable candidate for the mobile WiMAX application.

7 Acknowledgments

This work has been performed in the framework of the C2POWER project (FP7/2007-2013) under the European Community, funded through the Seventh Framework programme (project no. 248577).

8 References

1 Chireix, H.: 'High power outphasing modulation, *Proc. IRE*, 1935, **23** (11), pp. 1370–1392
2 Doherty, W.H.: 'A new high efficiency power amplifier for modulated wave', *Proc. IRE*, 1936, **24**, (9), pp. 1163–1182
3 Kahn, L.R.: 'Comparison of linear single-sideband transmitters with envelope elimination and restoration single sideband transmitters', *Proc. IRE*, 1956, **44**, (12), pp. 1706–1712
4 Cripps, S.C.: 'Advanced techniques in RF power amplifier design' (Artech House, Norwood, MA, 2002)
5 Cripps, S.C.: 'RF power amplifier for wireless communications' (Artech House, Norwood, MA, 1999)
6 Raab, F.: 'Efficiency of outphasing RF power-amplifier systems', *IEEE Trans. Commun.*, 1985, **33**, (10), pp. 1094–1099
7 Raab, F.H.: 'Efficiency of Doherty RF power amplifier system', *IEEE Trans. Broadcast.*, 1987, **BC-33**, (3), pp. 77–83
8 Raab, F.H., Asbeck, P., Cripps, S., *et al.*: 'Power amplifiers and transmitters for RF and microwave', *IEEE Trans. Microw. Theory Tech.*, 2002, **50**, (3), pp. 814–826
9 Srirattana, N., Raghavan, A., Heo, D., Allen, P.E., Laskar, J.: 'Analysis and design of a high-efficiency multistage Doherty power amplifier for wireless communications', *IEEE Trans. Microw. Theory Tech.*, 2005, **53**, (3), Part 1, pp. 852–860
10 Hussaini, A.S., Gwandu, B.A.L., Abd-Alhameed, R., Rodriguez, J.: 'The beyond 3G energy efficient power amplifier for mobile communications'. Proc. 26th WWRF Meeting, Doha, Qatar, 11–13 April 2011, Paper No. WWRF25-WG4-9
11 Hussaini, A.S., Abd-Alhameed, R., Rodriguez, J.: 'Design of energy efficient power amplifier for 4G user terminals'. Seventeenth IEEE Int. Conf. on Electronics, Circuits, and Systems (ICECS 2010), Athens, Greece, 12–15 December 2010, Paper No. 533, pp. 617–620
12 Hussaini, A.S., Abd-Alhameed, R., Rodriguez, J.: 'Green radio: approach towards energy efficient power amplifier for 4 G communications'. Proc. 25th WWRF Meeting, Kingston-upon-Thames, UK, 16–18 November 2010, Paper No. WWRF25-WG4-12
13 Hussaini, A.S., Gwandu, B.A.L., Abd-Alhameed, R., Rodriguez, J.: 'Design of power efficient power amplifier for B3G base stations'. Nineth IEEE Int. Symp. on Electronics and Telecommunications (ISETC 2010), Timisoara, 11–12 November 2010 (Romania) Paper No. 103, pp. 89–92
14 Hussaini, A.S., Sadeghpour, T., Abd-Alhameed, R., Child, M., Ali, N., Rodriguez, J.: 'Design of Doherty RFPA for mobile WiMAX base stations'. Sixth Int. ICST Conf. on Mobile Multimedia Communications, EERT-3, Lisbon, Portugal, 6–8 September 2010, Paper No. 3, pp. 1–8
15 Wang, F., Kimball, D., Popp, J., *et al.*: 'Wideband envelope elimination and restoration power amplifier with high efficiency wideband envelope amplifier for WLAN 802.11 g applications'. 2005 IEEE MTT-S Int. Microwave Symp. on Digest, June 2005, p. 4

16 Kimball, D.F., Jeong, J., Hsia, C., *et al.*: 'High-efficiency envelope-tracking W-CDMA base-station amplifier using GaN HFETs', *IEEE Trans. Microw. Theory Tech.*, 2006, **54**, (11), pp. 3848–3856
17 Wang, F., Ojo, A., Kimball, D., Asbeck, P., Larson, L.: 'Envelope tracking power amplifier with pre-distortion linearization for WLAN 802.11 g'. Microwave Symp. Digest, 2004 IEEE MTT-S International, June 2004, vol. 3, pp. 1543–1546
18 Moon, J., Kim, J., Kim, I., Kim, J., Kim, B.: 'A wideband envelope tracking Doherty amplifier for WiMAX systems', *IEEE Microw. Wirel. Compon. Lett.*, 2008, **18**, (1), pp. 49–51

IET Sci. Meas. Technol., pp. 1–8
doi: 10.1049/iet-smt.2011.0127

Reconfigurable Antenna Design for Mobile Handsets Including Harmonic Radiation Measurements

I.T.E. Elfergani[1], A.S. Hussaini[1, 2], T. Sadeghpour[1], R.A. Abd-Alhameed[1], J.M. Noras[1], S.M.R. Jones[1] and J. Rodriguez[2]

[1]Mobile and Satellite Communications Research Centre, University of Bradford, Bradford, UK
[2]Instituto de Telecomunicações, Aveiro, Portugal

ABSTRACT

A reconfigurable antenna with high efficiency, good load matching and covering a wide frequency range presents a practical design challenge when the antenna size is tightly constrained. A procedure is presented for the design of a reconfigurable mobile antenna, which overcomes the antenna size limitations. Tuning is achieved by placing a varactor diode at a specific position across a slot in the radiator conducting surface. The fabricated antenna is designed to cover a wide band, between 1700 MHz and 2040 MHz, at a return loss better than than 10 dB. The radiation of harmonics generated due to the varactor nonlinearities are simulated and measured. The experimental setup insures that the low levels of radiated harmonics are reliably validated. The experimental results show a good agreement with that computed using the Friis equation.

Index Terms— Reconfigurable antenna, Harmonics, Antenna radiation, Varactor.

1. INTRODUCTION

Small antennas are widely implemented in mobile terminals, e.g. PIFA and patch antennas [1-3]. The pursuit of greater compactness yields antennas that strongly resonate around the service frequencies. This limits both the bandwidth for multiband design and adaptability to environmental detuning. An efficient method to achieve wider effective bandwidth and to compensate for environmental impact is to tune dynamically the resonant frequency of such antennas, through tuneable reactive loadings [4, 5]. Varactors offer promise in such applications, bringing the possibility of simple voltage control and integration into the antenna conducting surfaces [5-15]. By implementing similar design principles as described in [8,9,13,14,15], this paper documents a tuneable slot antenna for mobile handset applications, but achieves both a size reduction and improved performance by comparison. The antenna occupies an envelope size of 50 x 80 x 1.6 mm^3, small enough for potential integration in a commercial handset or mobile user terminal. Furthermore, this antenna design has the benefit of a simpler geometrical structure than the above.

However, varactors exhibit voltage-dependent capacitance, sensitive not only to DC voltages, but also to induced RF voltages. The RF voltage across the varactor can generate high-order harmonic currents, with resulting radiative harmonics, especially when a varactor loaded antenna is stimulated near to resonance.

To overcome this problem, it is necessary to control the input impedance of the patch antenna at the harmonic frequencies and to keep in mind acceptable antenna gain across the operating bandwidth. Several methods have been used in practice to suppress harmonic resonances and to avoid spurious radiation [16-22]. Future systems employing active antennas will require

very low levels of harmonic radiation in order to meet electromagnetic compatibility specifications. Active antennas introduce nonlinear devices directly into the antenna and thus can exhibit high levels of harmonic radiation. Moreover, due to size constraints, filters cannot easily be added, as in conventional systems. The harmonic reception problem can be reduced in the case of active receiving antennas, by suppressing the harmonic resonances of the antenna [23-24]. However, due to the interdependence of the active device and patch, the solution to the problem of harmonic radiation for typical patch antennas is more complex. It may be approached in two ways. Firstly, out-of-band radiation from the active integrated antenna can be minimized at the design stage by control of the impedance presented by the antenna to the oscillator. Secondly, it may be controlled once the device has been constructed by the use of frequency-selective surfaces [25]. Many papers have described active patch antennas for transmitting applications. Such antennas may be defined as an active device very closely integrated with a passive radiating structure and with little or no intervening circuitry [26]. They divide into the general classes of self-oscillating antennas and radiating power amplifiers.

In radio frequency power amplifiers, operation with significant non-linearity will generally be needed for good efficiency. Load impedances at harmonic frequencies are frequently optimised to improve the maximum efficiency [16], [27]. In an active transmitting antenna, harmonic load impedances also influence the radiation of harmonics and the interference they may cause to other systems. Therefore, preventing power being lost to harmonic radiation is likely to increase efficiency, besides helping to improve system operation.

This paper concentrates on two approaches. Firstly, a new tuneable antenna is developed, which gives the designer insight into the application of the tuning technique. Secondly, a

reliable method for measuring output power from the resultant tuned antenna, at fundamental and harmonic frequencies, has been devised in order to prove that the harmonics have been successfully suppressed. A measurement setup is used to evaluate the power received by an antenna at its fundamental and harmonic frequencies, for which the results are found to be in good agreement with calculations.

The paper is organized as follows. The antenna design concept is presented in section 2, whereas section 3 investigates the simulated and the measured results of the proposed design. Analysis of the harmonics is discussed in section 4 and finally the conclusions summarise what has been achieved.

2. ANTENNA DESIGN STRUCTURE

As the aim is to devise a frequency-tuneable microstrip antenna having wide tuning range, with a single feed, the underlying passive antenna design is vital. The design must ensure good matching below −10 dB (i.e. return losses better than 10 dB) for resonant mode, even when the frequencies are strongly shifted by applying a reverse DC voltage. The radiator is fed by a 67 mm × 3 mm, 50 Ω standard microstrip line. FR4 epoxy is used as the substrate throughout the module, with a thickness of 1.6 mm, and the dielectric constant (ε_r) is assumed to be uniformly 4.4, with a loss tangent of 0.02 over the target frequency range. The PCB has a width (W_{board}) of 50 mm and a length (L_{board}) of 80 mm, as shown in Fig. 1. The optimised antenna dimensions are 13 mm in width (L_P) and 50 mm in length; the metal etching is located on the top side of the substrate, and slotted in a shape as shown, again, in Fig. 1b. The length of the ground plane is 80 mm with a 50 mm × 13 mm clearance below the antenna layout as shown in Fig. 1b. The layout of the antenna with varactor and passive components

are depicted in Fig.1c. Analysis and optimisation were carried out using Ansoft HFSS [28]. The selected slot dimensions were as follows: L_1 = 32 mm, L_2 = 7 mm, L_3 = 22 mm, and L_S = 7 mm, with a trace width (L_T) of 1 mm.

2.1 UNLOADED ANTENNA RESULTS

Fundamentally, the first step is to fabricate the antenna without the inclusion of varactor or lumped capacitor then perform the required test and measurements in order to find out if it does radiate as expected. It is interesting to note that the unloaded antenna resonates at 1.4 GHz as shown in Fig. 2. Both the simulation results generated by using HFFS software package and the measurement achieved from the network analyzer (NA) show fairly good agreement.

2.2 A CAPACITOR-LOADED PRINTED ANTENNA

In this section the frequency tuneability of this printed antenna is investigated by loading a lumped ceramic capacitor in place of a varactor diode. Hence, the DC bias circuit parasitic effects are excluded. The intent is to determine how the loaded capacitor affects the antenna performance and to find the optimized location on the antenna radiation arm. The antenna exhibits a reasonable frequency range from 1.65 to 2.05 GHz by varying the value of the capacitor loaded on the long arm from 0.4pF to 10 pF, while the capacitor on short arm remains constant at 2pF. One can observe that the resonant frequency would not be shifted down to less than 1.65GHz even when the capacitance is increased up to 10 pF as shown in Fig. 3. Therefore, 1.8 pF was selected to be the highest capacitance value in this study. First, the actual prototype in Fig. 4 is fabricated and tested, without any bias circuit. By varying the

value of the capacitor mounted on the 'long-arm' in the range (0.4, 0.8, 1.3, and 1.8 pF), one at a time and keeping the 'short-arm' capacitance unchanged at 2 pF, the tuneabilty is found to cover the frequency range from 1.7 to 2.04 GHz as indicated in Fig. 5. As can very clearly be seen, a higher band corresponds to a lower capacitance value. From the examination of Fig. 5, it can be concluded that both the computed and measured results obtained by adding lumped capacitors exhibit good impedance matching (below -10 dB) as well as being in satisfactory agreement with each other. The bandwidth obtained by simulation and measurement for each capacitor value is detailed in Table I. The antenna could be used for DCS1800, PCS1900, and UMTS applications. The small discrepancy noted between the measured and simulated results can be attributed to misalignment of the capacitor in the antenna assembly.

2.3 VARACTOR AND THE DC BIAS CIRCUITS OF PRINTED ANTENNAS

The feasibility of frequency tuning using a varactor-loaded uniplanar printed antenna with a DC bias circuit was explored. The tuning circuit exploits the diode package (MMBV3102), the bias connection being de-coupled via 100 nH inductors, and a 100 Ω resistor. The diode junction capacitance as a function of reverse bias voltage is shown in Fig. 6.

The loaded uni-planar antenna prototype PCB complete with DC bias circuit is shown in Fig. 7. The simulation results for reflection coefficient and isolation are shown in Fig. 8 for four different capacitance values (0.4, 0.8, 1.3 and 1.8 pF). One can observe that a progressive shift of resonant frequency from 1.7 to 2.04 GHz with acceptable bandwidth was accomplished, as shown in Fig. 8.

It can be seen from the measurement results that by varying the 'long-arm' varactor DC bias from 0 V, through 5V, 9 V and 15 V, whilst keeping the 'short-arm' bias unchanged at 2 pF, the antenna may be tuned through the range 1.7 GHz to 2.04 GHz as shown in Fig. 8.

Both predicted results and those obtained from measurements with the biased varactor are plainly in close agreement with one another shown in Fig. 8. The variation between the predicted and measured results may be due to inaccuracies in the fabricated prototype (i.e. dimensional tolerancing) as well as the effect of varactor diode and other passive components. Moreover, it can be observed that the bandwidth is enhanced in the case when the DC voltage is applied to the varactor, as indicated in Table I.

The reflection coefficient of the proposed antenna is shown in Fig. 9. It is apparent that this antenna resonates at 1.7, 1.8, 1.9 and 2.04 GHz with DC voltages of 0, 5, 9 and 15V respectively, and suppresses higher harmonics for each single band including, in particular: 3.4 and 5.1 GHz for the 1.7 GHz band; 3.6 and 5.4 GHz for the 1.8 GHz band; 3.8 and 5.7 GHz for the 1.9 GHz band; and finally 4.08 and 6.16 GHz for the 2.04 GHz band, (corresponding to the second and third harmonic frequencies). Also, from Fig. 10, it is observed that the input impedances at antenna harmonic frequencies are almost reactively terminated over all capacitance values.

The predicted (HFSS) and measured radiation patterns are given in Fig. 11, at 1.7GHz, 1.8 GHz, 1.9 GHz, and 2.05 GHz, with DC bias voltages of 0 V, 5V, 9 V and 15 V, respectively. These radiation patterns are approximately omni-directional, and measurements were made in an anechoic chamber using a calibrated EMCO type 3115 broadband horn as the reference antenna. Two pattern cuts (H-plane and E-plane) were taken at operating frequencies which cover the aggregate bandwidth required for this study. The simulated patterns were generated

from HFSS for the same cut planes. The patterns were normalized for ease of comparison and presented in Fig. 11. The results indicate a notable agreement between simulated and measured radiation patterns at all the designated frequencies.

Measured and simulated gains at fundamental resonance frequencies are reported in Fig. 12. The maximum gains achieved across the tuning range at the spot frequencies 1.7 GHz, 1.8 GHz, 1.9 GHz and 2.04 GHz were 2.9 dBi (3.4 dBi), 3.5 dBi (3.17 dBi), 2.38 dBi (2.51 dBi) and 1.55 dBi (2.42 dBi) with DC voltages of 0, 5, 9 and 15V for the measured one and capacitance value of 0.4, 0.8, 1.3 and 1.8 pF for the simulated one, respectively, (the simulation figures are in parentheses).

3. TRANSCEIVER HARMONICS ANALYSIS

In general, the power radiated by the tuneable antenna at the target design frequencies and harmonics can be computed using simulation and the Friis transmission equation, and the modelling then validated by performing the measurement inside the anechoic chamber [29]. In this work, the Friis transmission equation has been applied to reconfigurable printed antennas at their fundamental frequencies and harmonics up to third order. To yield the impedance of the varactor diode at the working frequency bands of the antenna structure the equivalent circuit model of the nonlinear device is used for S-parameter simulation and large signal analysis in a harmonic balance solver e.g. Advanced design System (ADS). The circuit model and simulation results are illustrated in Fig.13a and 13b and Table II. Fig. 13.b represents the power levels of fundamental, second- and third-order harmonics of varactor diode acquired from a harmonic balance simulation for a bias point of 9 V at 1.8 GHz. The varactor capacitance in the antenna structure in the HFSS simulator is then replaced by the

voltage source holding the power level values according to the measurement of harmonic frequencies shown in Fig. 13.b and the series impedance of the varactor represented in Table II. Next, the S-parameter simulation results are applied to the Friis equation to find the power incident on the receiver. According to the test set up illustrated in Fig. 14, the available power at the input of the antenna structure, P_{in} can be given as follows:

$$P_{in} = L_{cable}.G_{amplifier}\,L_{filters}.L_{Iso}.P_{SG} \quad (1)$$

where $G_{amplifier}$ and P_{SG} are the gain of the amplifier and output power of signal generator respectively. L_{cable} , $L_{filters}$ *and* L_{Iso} are the losses due to the cables, filters and isolators as measured by a network analyser.

Thus the transmitted power by the structure is given by:

$$P_t = P_{in}.(1- s_{11}{}^2) \quad (2)$$

where s_{11} is the return loss of the tuneable antenna at the target frequencies and harmonics achieved from simulations. The path-loss, L, is given by:

$$L = \frac{\lambda}{4\pi r}{}^2 \quad (3)$$

where λ is the wavelength and r is the separation between the standard horn antenna and tuneable antenna. If the gains of the horn and active antenna are denoted by G_H and G_{VD} respectively, the power received by the horn, P_H is given by:

$$P_H = \eta . L . G_H . P_t . G_{VD} \quad (4)$$

where η is the radiation efficiency of the antenna. Thus, the accepted power for the horn is defined as follows:

$$P_{acc\_H} = P_H(1 - s_{11h}{}^2) \quad (5)$$

where s_{11h} is the horn return loss. Finally, the power received by spectrum analyser is:

$$P_R = L_{cable} . P_{acc\_H} \quad (6)$$

The calculation results are given in Table III for each frequency and its harmonics, with different power levels applied.

The test setup illustrated in Fig. 14 is used in an anechoic chamber to validate the antenna performance for the frequency bands of interest. An RF signal from a signal generator is fed through a high-power amplifier and then passes through two isolators as well as two tuneable band-pass filters. The isolators are used to remove standing waves from the circuit, and the two band-pass filters are used to suppress harmonics generated by the amplifier nonlinearity. To ensure that in-band distortion due to the power amplifier nonlinear characteristic functions, AM/AM and AM/PM, is not a factor, the power amplifier is well backed-off from its nonlinear region. The power amplifier used in this work was a wideband amplifier with 26 dB gain whose response is illustrated in Fig. 15. The tuneable filters are adjusted at each resonant frequency (1.7, 1.8, 1.9 and 2.04 GHz) to remove the generated harmonics while the varactor capacitance of the active patch is set to specific values namely; 0, 5, 9, and 15 V

accordingly, to configure the signal at the target frequency. The power transmitted by the tunable antenna and the power accepted by the standard horn antenna over all frequency components were measured using a spectrum analyser (HEWLETT PACKARD 8510C) for three selected positions of the transmitter antenna that are equivalent for three orthogonal planes.

As can be seen from the calculated values and measured values in Tables III and IV respectively or equivalently from the graphs of Fig. 16, there is reasonable agreement between measurements and values calculated using the Friis equation for the fundamental frequencies and harmonics.

4. CONCLUSIONS

A design procedure for a printed antenna for mobile handsets has been presented. The antenna is reconfigurable over a wide frequency range to cover DCS, PCS and UMTS bands by controlling the DC bias voltage of a varactor diode. Good matching is maintained at the target frequencies and harmonic radiation is suppressed. In order to validate the suppression of the harmonics, it is critical to avoid harmonics being generated by the source generator. Thus two tuneable band-pass filters were inserted in the transmitter chain to suppress any harmonic content in the signal input to the antenna. Calculated values for received power and measured ones were in reasonable agreement. Both show suppression of the second and third harmonic radiation. Therefore, the proposed antenna can usefully improve multiband system performance.

Authors Affiliations:

I.T.E.Elfergani, T. Sadeghpour, R. A. Alhameed, J.M. Noras and S.M.R. Jones are with School of Engineering, Design and Technology, Bradford University Bradford, BD7 1DP, UK;

Email:
i.t.e.elfergani@bradford.ac.uk,tsadeghp@brad.ac.uk,r.a.a.abd@bradford.ac.uk,
j.m.noras@bradford.ac.uk, m.r.jones@bradford.ac.uk

A.S. Hussaini and J. Rodriguez with Instituto de Telecomunicações, Aveiro, Portugal
E-mail: ash@av.it.pt, jonathan@av.it.pt

REFERENCES

[1] W.-J. Liao, S.-H. Chang, and L.-K. Li "A compact Planar Multiband Antenna for Integrated Mobile Devices" Progress In Electromagnetics Research Letters, *Vol. 109, pp. 1-16, 2010.*

[2] C. W. Chiu and F. L. Lin, "Compact dual-band PIFA with multi resonators," Electron. Lett., vol. 38, no. 12, pp. 538–540, Jun. 2002.

[3] Gandara, T. and C. Peixeiro, "Compact double U-slotted microstrip patch antenna element for GSM1800, UMTS and HIPERLAN2," IEEE Antennas and Propagation Society International Symposium, Vol. 2, pp. 1459–1462, 2004.

[4] Bhartia.P, Bahl, I. J., "Frequency agile microstrip antennas", *Microw.* 37, pp. 1136 1139, 1982.

[5] P.K. Panayi, M.O. AI-Nuaimi, I.P. Ivrissimtzis,"Tuning techniques for planar inverted-F antenna," *Electron. Lett., 37,* (16), pp.l003-1004, 2001.

[6] P.S. Hall, S. Kapoulas, R. Chauhan, and C. Kalialakis, "Microstrip antennas with adaptive integrated tuning," *Proc. Int. ConI On Antennas and Propagation,* pp. 501-504, 1997.

[7] Virga k.L., Samii y.R.: '*Low-profile enhanced-bandwidth PIFA antennas for wireless communications packaging*', IEEE Trans. Microw. Theory Tech., 2002, 45, pp. 1879–1888.

[8] N. Behdad, and K. Sarabandi, "*Dual-band reconfigurable antenna with a very wide tenability range,"* IEEE Trans. Antennas Propagat., Vol. 54, pp. 409-416, February 2006.

[9] A. F. Sheta, and M. Alkanhal, "*Compact Dual-Band Tunable Microstrip Antenna for GSM/DCS 1800 Applications*," IET Microwave Antenna and Propagation, Vol. 2, No. 3, pp. 274-280, 2008.

[10] Ollikainen J., Kivekas O., Vainikainen P.: '*Low loss tuning circuits for frequency-tunable small resonant antennas*'. IEEE PIMRC, 2002, pp. 1882–1887.

[11] Peroulis D., Sarabandi K., Katehi l.: '*Design of reconfigurable slot antennas*', IEEE Trans. Antennas Propag., 2005, 53, pp. 645–654.

[12] Behdad N., Sarabandi K.: '*A varactor-tuned dual-band slot antenna*', IEEE Trans. Antennas Propag., 2006, 54, pp. 401–408.

[13] Okabe H., Takei K.: '*Tunable antenna system for 1.9 GHz PCS handsets*'. Proc. IEEE AP-Symp., 2001, pp. 166–169

[14] M. S. Nishamol, V. P. Sarin, D. Tony, C. K. Aanandan, P. Mohanan, K. Vasudevan "Design of Frequency and Polarization Tunable Microstrip Antenna " Microwave Review - Vol. 16, No.2,pp.22-18, December 2010.

[15] S. S. Yang, A. A. Kishk, and K. F. Lee, "Frequency reconfigurable U-slot microstrip patch antenna," *IEEE Antennas Wireless Propag. Lett.*, vol. 7, pp. 127–129, 2008.

[16] V. Radisic, Y. Qian, and T. Itoh, "Broadband power amplifier integrated with slot antenna and novel harmonic tuning structure", in 1998 IEEE MTT-S Dig, 1998, pp. 1895-1898.

[17] Y. Horii and M. Tsutsumi, "Harmonic Control by Photonic Bandgap on Microstrip Patch Antenna", IEEE Microwaves and Guided Wave Letters, vol 9, n°1, January 1999.

[18] Y.J. Sung and Y.S. Kim, "An Improved Design of Microstrip Patch Antennas Using Photonic Bandgap Structure",IEEE Transactions on Antennas and Propagation, vol 53, no 5, may 2005, pp. 1794-1804.

[19] V. Radisic, Y. Qian, and T. Itoh, "Novel architectures for high-efficiency amplifiers for wireless applications," *IEEE Trans. Microwave Theory Tech.*, vol. 46, pp. 1901–1909, Nov. 1998.

[20] A. F. Sheta and S. F. Mahmoud, "A novel H-shaped patch antenna," in *IEEE APS Int. Symp. Dig.*, vol. 2, July 2001, pp. 720–723.

[21] S. Kwon, H. K. Yoon, and Y. J. Yoon, "Harmonic tuning antennas using slots and short-pins," in *IEEE APS Int. Symp. Dig.*, vol. 1, July 2001, pp. 118–121.

[22] Kalialakis, C., Gardner, P., and Hall, P.S.: "Harmonic radiation from varactor-loaded microstrip antennas". 31st Europ. Microw. Conf. Proc., 2001, vol. 2, pp. 133–136.

[23] E. Elkhazmi, N. J. McEwan, and J. Moustafa, "Control of harmonic radiation from an active microstrip patch antenna," *J. Int. Nice Sur Les Antennas*, pp. 313–316, Nov. 1996.

[24] V. Radisic, Y. Qian, and T. Itoh, "Class F power amplifier integrated with circular sector microstrip antenna," in *IEEE MTT-S Int. Microwave Symp. Dig.*, Denver, CO, June 1997, pp. 687–690.

[25] A. Henderson, A. A. Abdulaziz, and J. R. James, "Microstrip planar array with interference suppression radome," *Electron. Lett.*, vol. 28, pp. 1465–1466, July 1992.

[26] Y. Qian and T. Itoh, "Progress in active integrated antennas and their applications," *IEEE Trans. Microwave Theory Tech.*, vol. 46, pp.1891–1900, Nov. 1998.

[27] M. Maeda, H. Takehara, and M. Nakamura, "A high power and high efficiency amplifier with controlled second-harmonic source impedance", IEEE MTT-S Dig. April 1995, pp 579-582.

[28] Ansoft High Frequency Structure Simulator v10 Uses Guide, CA, USA.

[29] Balanis, C. A., *Antenna Theory: Analysis and Design*, 3rd edition, 94-96, John Wiley & Sons Inc., 2005.

Tables and Figures Captions:

Table I: The bandwidth at each operating frequency band for the proposed design.

Table II: Varactor diode equivalent circuit impedances at fundamental and harmonics frequencies applying different bias level

Table III: Received power at fundamentals and harmonics for different power levels achieved from calculation.

Table IV: Received power at fundamentals and harmonics for different power levels achieved from measurement.

Figure 1: Basic antenna structure; (a) Top view (b) Bottom view (c) Schematic view.

Figure 2: Measured and simulated reflection coefficients $|S_{11}|$ of unloaded antenna.

Figure 3: Simulated reflection coefficients $|S_{11}|$ of the antenna with variable capacitor (from 0.4 to 10 pF) loading

Figure 4: Prototype of the capacitor-loaded version of the proposed antenna.

Figure 5: Measured and simulated reflection coefficients $|S_{11}|$ of capacitor- loaded antenna.

Figure 6: Varactor junction capacitance versus reverse bias voltage at 2GHz operating frequency.

Figure 7: Prototype of the varactor -loaded version of the antenna.

Figure 8: Measured and simulated reflection coefficients $|S_{11}|$ of varactor-loaded antenna.

Figure 9: Measured reflection coefficients $|S_{11}|$ of varactor-loaded antenna at fundamental and harmonic frequencies for (a) 0v, (b) 5v, (c) 9v (d) 15v.

Figure 10: Input impedance of the antenna for (a) 0v, (b) 5v, (c) 9v (d) 15v.

Figure 11: Simulated vs. Measured normalised antenna radiation patterns for two planes (left: xz, right: xy) at 1700MHz, 1800MHz, 1900MHz, 2050MHz.

'xxxx' simulated cross-polarization 'oooo' simulated co-polarization

'------' measured cross-polarization'——' measured co-polarization

Figure 12: Measured and simulated antenna gains.

Figure 13(a): Varactor diode equivalent circuit model used in harmonic balance solver.

Figure 13(b): Power level at fundamental and harmonics versus input power level at bias voltage of 9 V at 1.8 GHz achieved from harmonic balance simulation.

Figure 14: Experimental test set up in anechoic chamber.

Figure 15: Power amplifier gain characteristic function.

Figure 16: Measured and **c**alculated results for received power at (a) fundamental, (b) 2^{nd} harmonics (c) 3^{rd} harmonics.

Table I:

Fre. GHz	C values	Relative Simulated Bandwidth in % using C values	Relative Measured Bandwidth in % using C values	Applied DC voltages across the varactor diode	Relative Measured Bandwidth in % using the varactor diode
1.7	1.8pf	5	3.2	0V	5.5
1.8	1.3pf	5	3.2	5V	5.5
1.9	0.8pf	6	4	9V	4.2
2.04	0.4pf	6.5	5.5	15V	7

Table II:

Freq (GHz)	Zin @ Vbias=0V	**Freq (GHz)**	Zin @ Vbias=5 V	**Freq (GHz)**	Zin @ Vbias=9 V	**Freq (GHz)**	Zin @ Vbias=15 V
1.7	6.167 ∠ -77.181	**1.8**	38.514 ∠ -88.922	**1.9**	53.051 ∠ -89.49	**2.04**	60.489∠-89.689
3.4	30.449 ∠ 84.025	**3.6**	2.606 ∠ -57.556	**3.8**	15.462 ∠ -86.93	**4.08**	22.189 ∠ -88.559
5.1	429.108 ∠67.08	**5.4**	73.330 ∠ 81.204	**5.7**	26.755 ∠ 81.04	**6.12**	9.037 ∠ 75.402

Table III:

Frequency (GHz)	Signal generator power (dBm)	Input power at transmitter antenna (dBm)	Received power at fundamental (dBm)	Received power at 2nd harmonic (dBm)	Received power at 3rd harmonic (dBm)
1.7	-30	-7	-49.402	-105.2	-103
	-20	3.5	-38.9	-93.2	-98
	-10	13.5	-28.23	-75.25	-92
	-5	18	-23.57	-67.28	-85
	0	21	-20.73	-54.5	-75
1.8	-30	-7	-50	-105	-107
	-20	3.5	-40	-93.25	-99
	-10	14.7	-28.7	-75.7	-95
	-5	18.83	-25	-67.75	-87
	0	21.67	-21.8	-54.25	-76
1.9	-30	-7	-47.10	-105.3	-106.2
	-20	3.5	-36.60	-93.3	-100.25
	-10	14.17	-25.94	-75.03	-95
	-5	18.83	-21.27	-67.25	-87
	0	21.67	-18.43	-54.25	-77
2.04	-30	-7	-50.2	-105	-106
	-20	3.5	-39.4	-93.25	-99
	-10	14	-28.5	-75.9	-94
	-5	18.83	-23.15	-68.9	-89
	0	21.67	-19.318	-54.9	-78

Table IV:

Frequency (GHz)	Signal generator power (dBm)	Input power at transmitter antenna (dBm)	Received power at fundamental (dBm)	Received power at 2nd harmonic (dBm)	Received power at 3rd harmonic (dBm)
1.7	-30	-7	-49.25	-100	-100
	-20	3.5	-39.25	-90	-97
	-10	13.5	-29	-73.25	-93
	-5	18	-25.25	-65	-87
	0	21	-21.75	-56.5	-75.8
1.8	-30	-7	-50.6	-100	-100
	-20	3.5	-40.25	-91.25	-97
	-10	14.7	-29	-74.5	-95
	-5	18.83	-25.4	-65.25	-88
	0	21.67	-21.5	-57.25	-77.2
1.9	-30	-7	-48.5	-100	-100
	-20	3.5	-38.75	-91.25	-99
	-10	14.17	-28.25	-73	-93
	-5	18.83	-22	-64.25	-89
	0	21.67	-19.75	-56.25	-79
2.04	-30	-7	-50.75	-100	-100
	-20	3.5	-39.5	-92	-97
	-10	14	-29.1	-76.25	-93.5
	-5	18.83	-24	-67.25	-91
	0	21.67	-20.1	-55.75	-79

Figure 1:

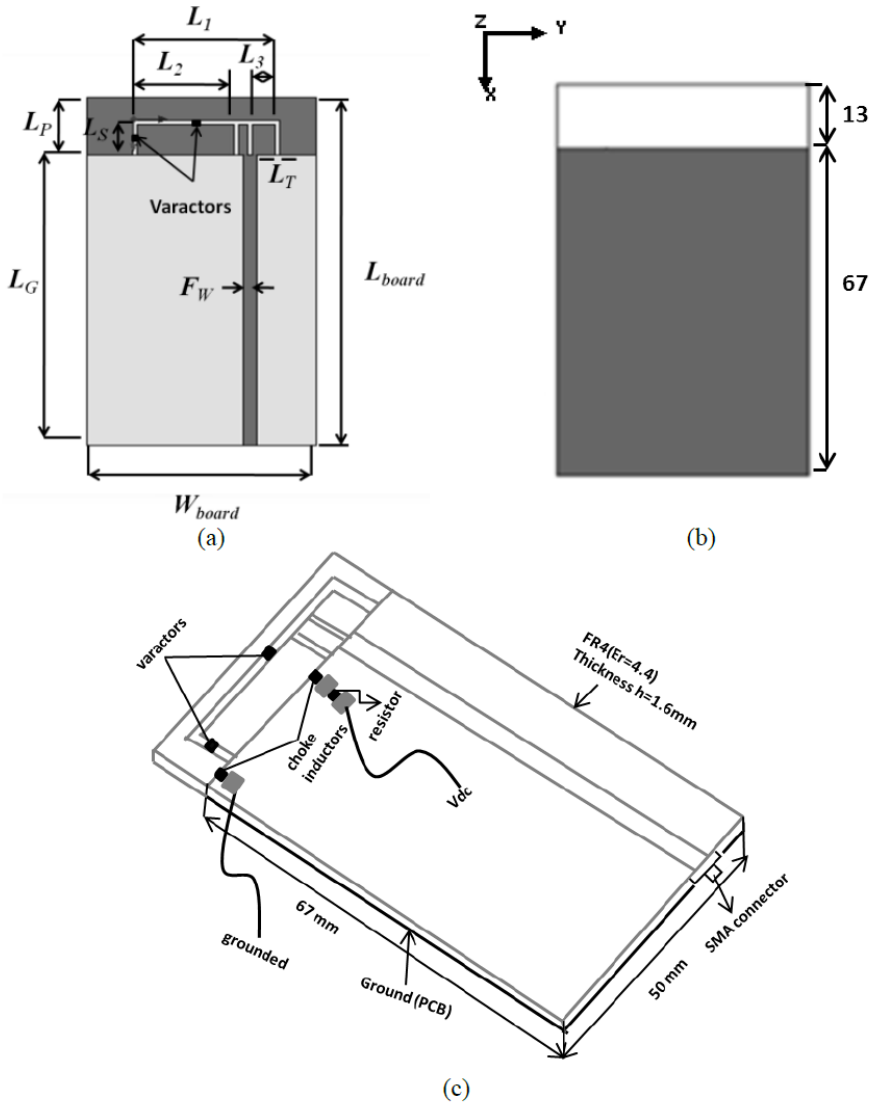
L_1
L_2
L_3
L_P
L_S
L_T
Varactors
L_G
F_W
L_{board}
W_{board}
(a)
Z
Y
X
13
67
(b)
Varactors
FR4(Er=4.4)
Thickness h=1.6mm
choke inductors
resistor
Vdc
67 mm
grounded
Ground (PCB)
50 mm
SMA connector
(c)

Figure 2:

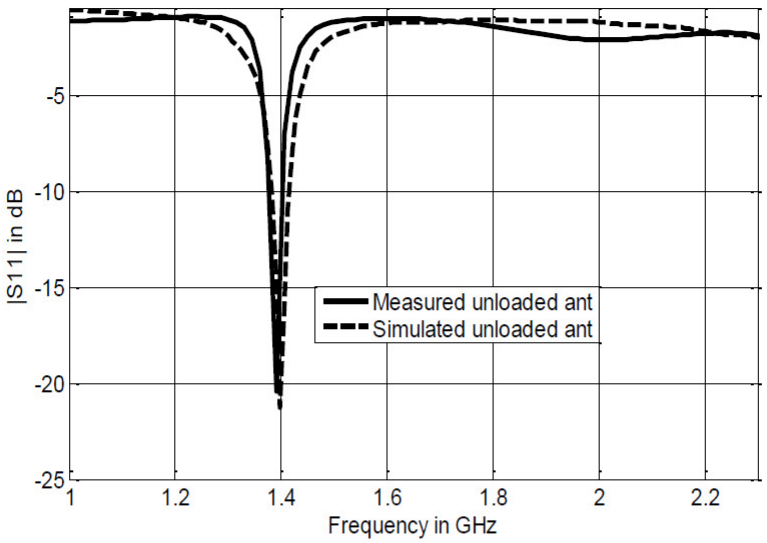

Figure 3:

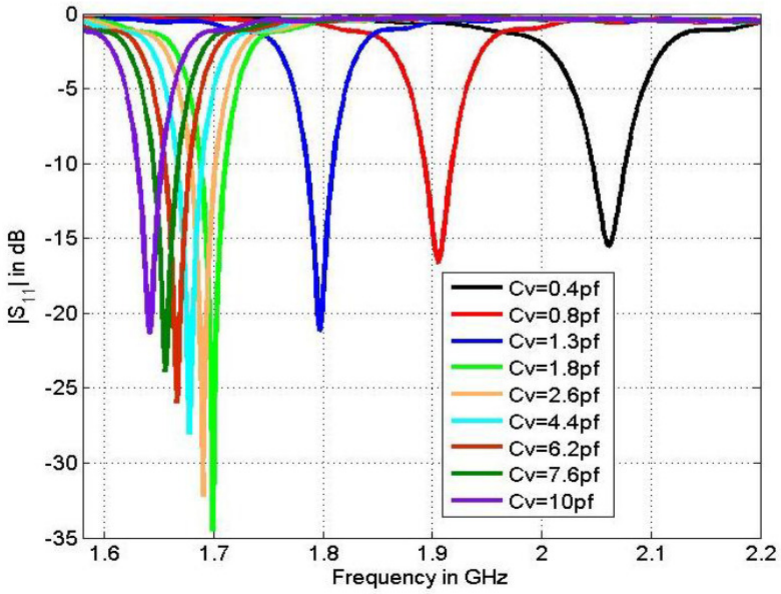

Figure 4:

Figure 5:

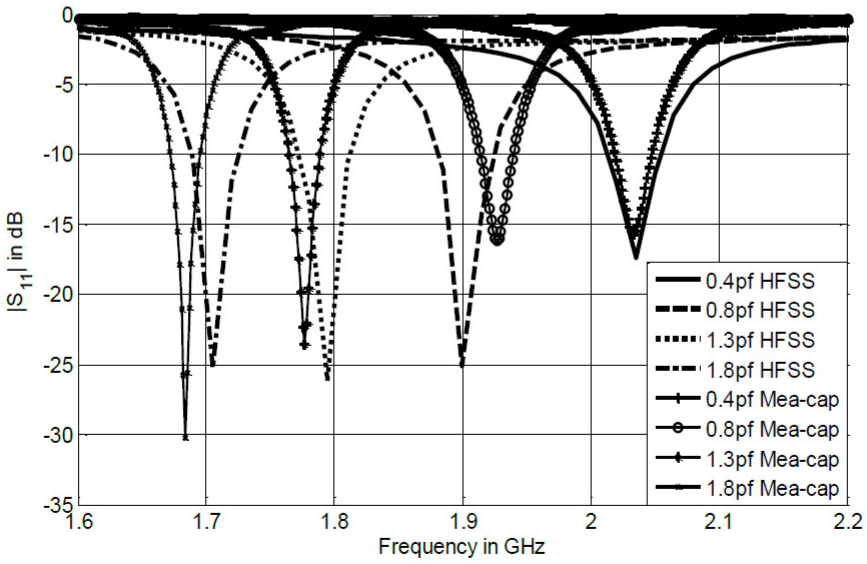

Figure 6:

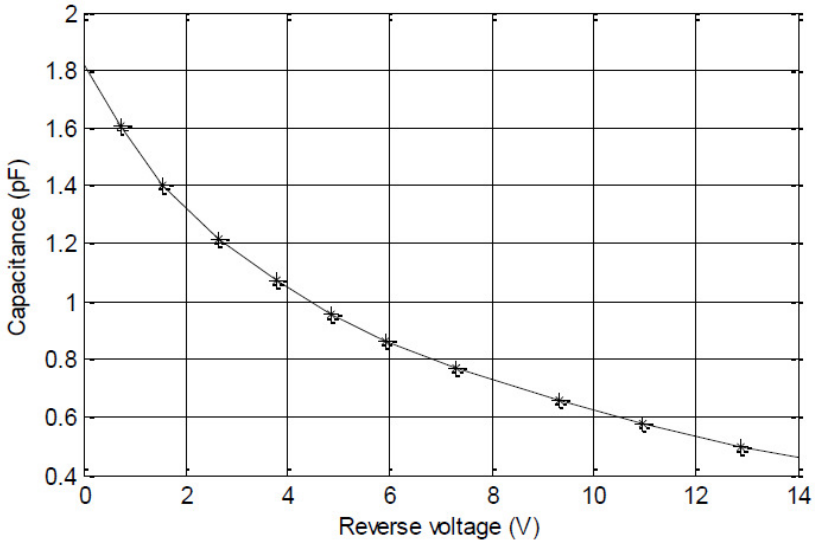

Figure 7

Figure 8:

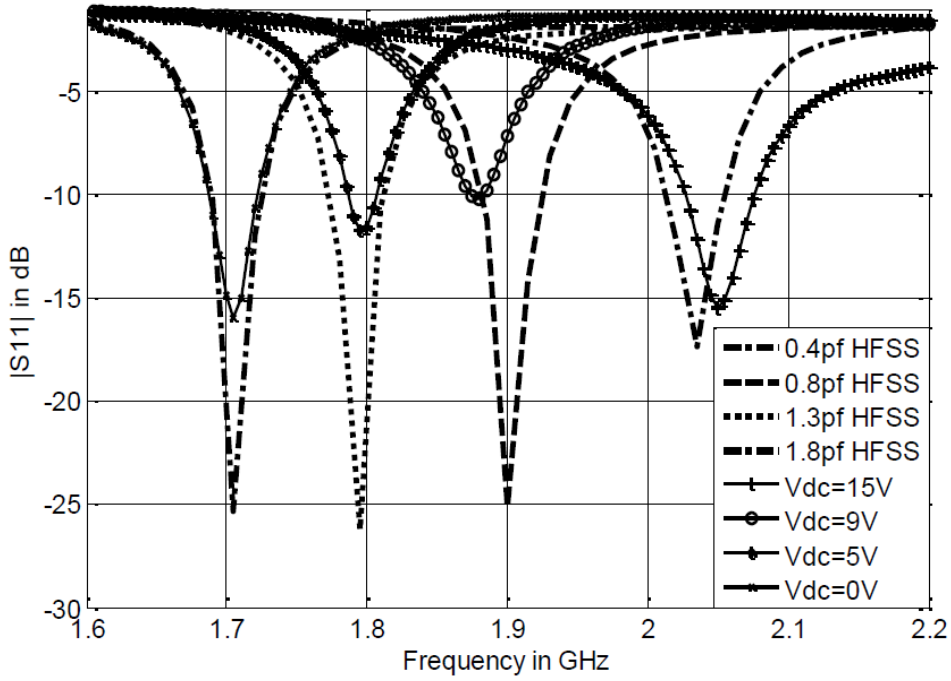
-5
-10
-15
-20
-25
-30
|S11| in dB
1.6
1.7
1.8
1.9
2
2.1
2.2
Frequency in GHz
0.4pf HFSS
0.8pf HFSS
1.3pf HFSS
1.8pf HFSS
Vdc=15V
Vdc=9V
Vdc=5V
Vdc=0V

Figure 9:

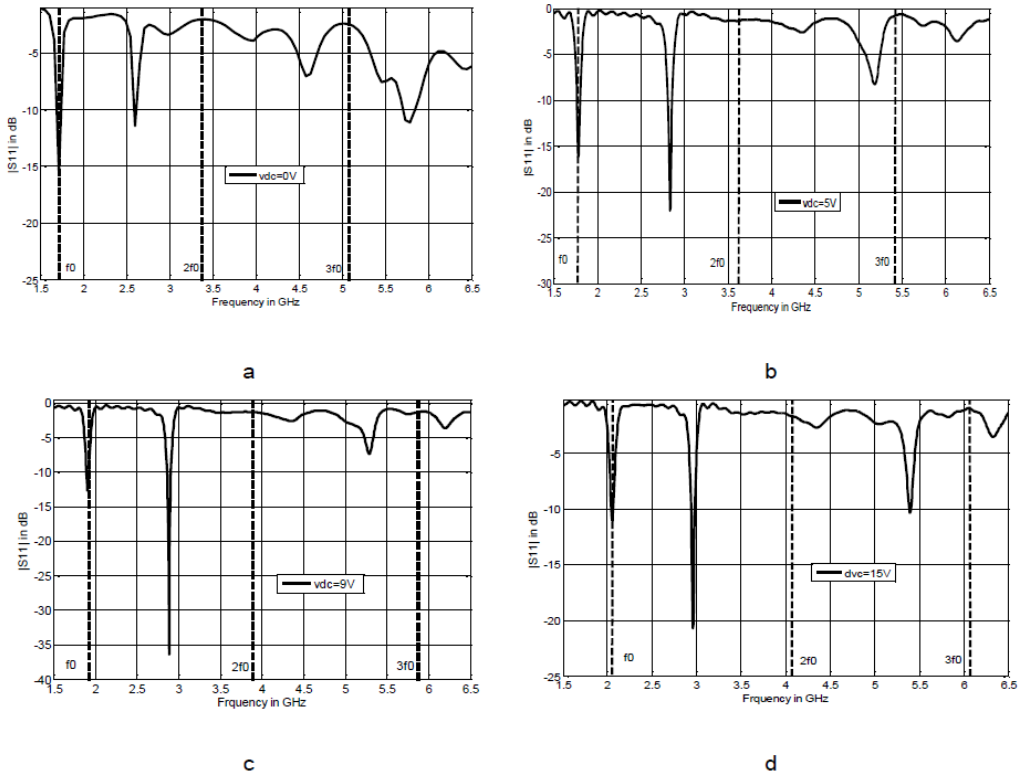
|S11| in dB
Frequency in GHz
vdc=0V
f0
2f0
3f0
a
vdc=5V
b
vdc=9V
Frquency in GHz
c
dvc=15V
d

Figure 10:

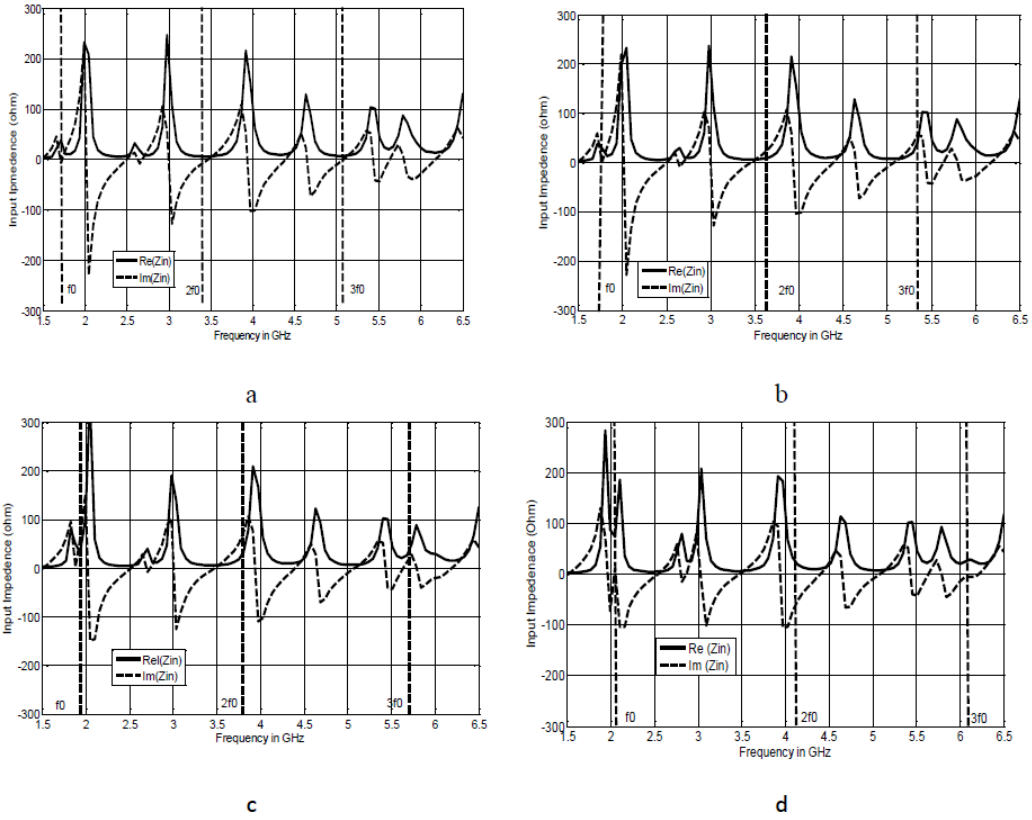
Input Ipmedence (ohm)
Frequency in GHz
Re(Zin)
Im(Zin)
f0
2f0
3f0
a
Input Impedence (ohm)
Frequency in GHz
Re(Zin)
Im(Zin)
f0
2f0
3f0
b
Input Impedence (ohm)
Frequency in GHz
Rel(Zin)
Im(Zin)
f0
2f0
3f0
c
Input Impedenace (Ohm)
Frequency in GHz
Re (Zin)
Im (Zin)
f0
2f0
3f0
d

Figure 11:

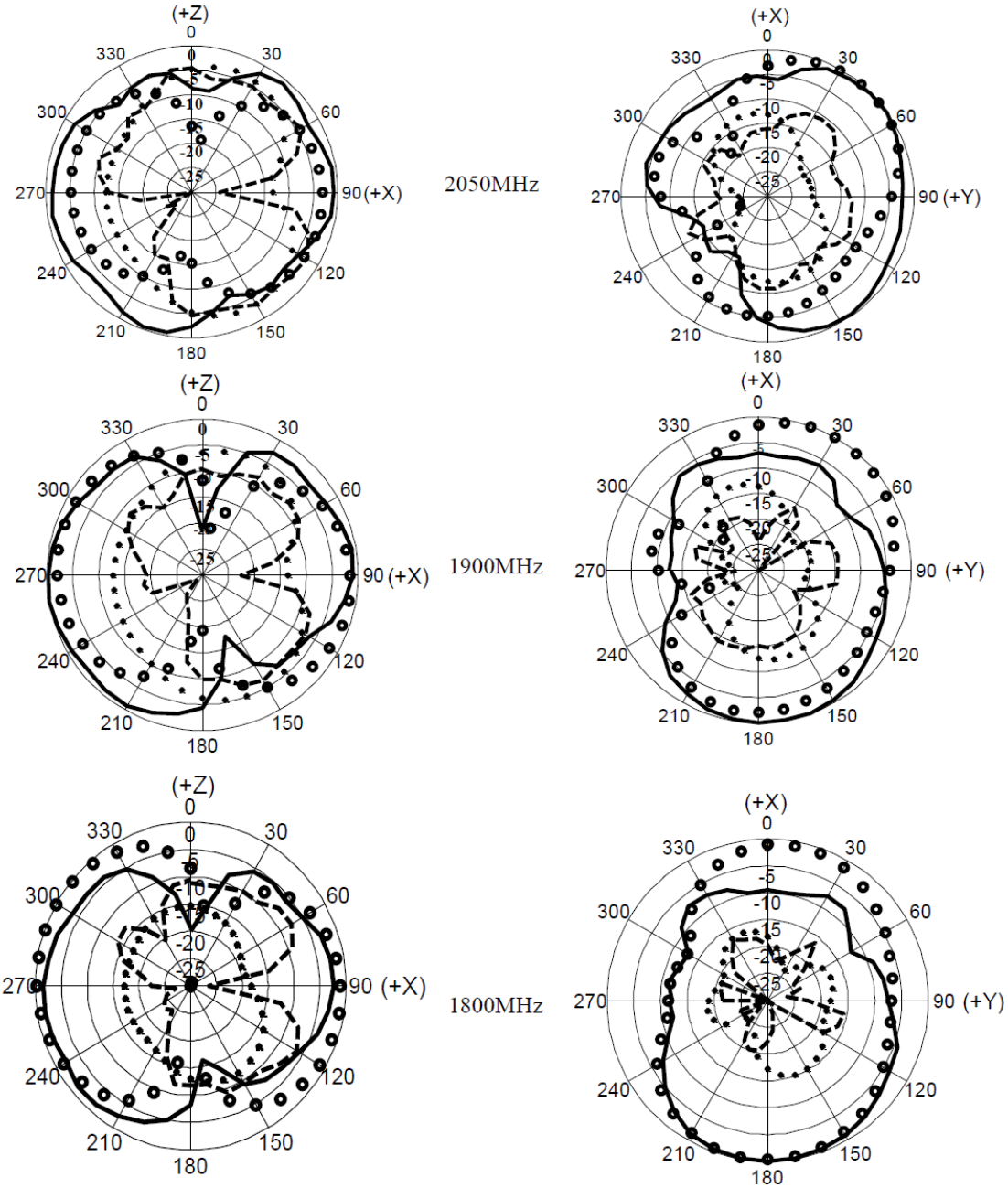

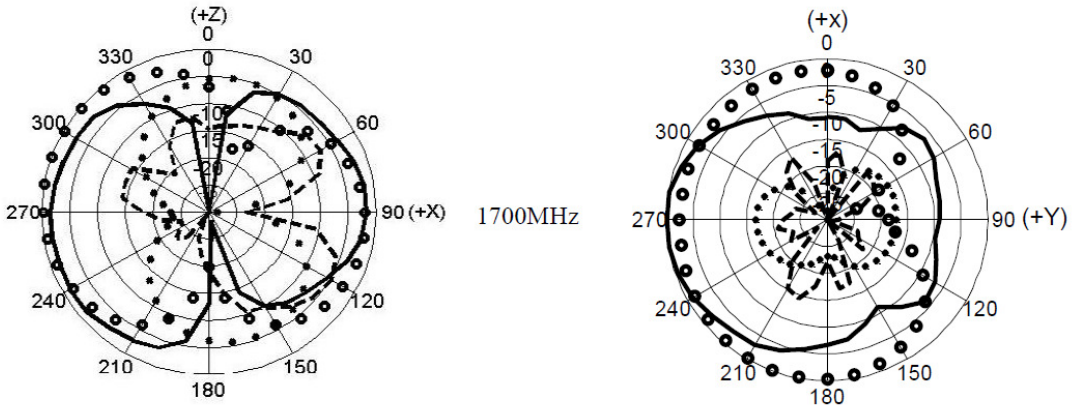
(+Z)
0
30
60
90 (+X)
120
150
180
210
240
270
300
330
1700MHz
(+X)
0
30
60
90 (+Y)
120
150
180
210
240
270
300
330

Figure 12:

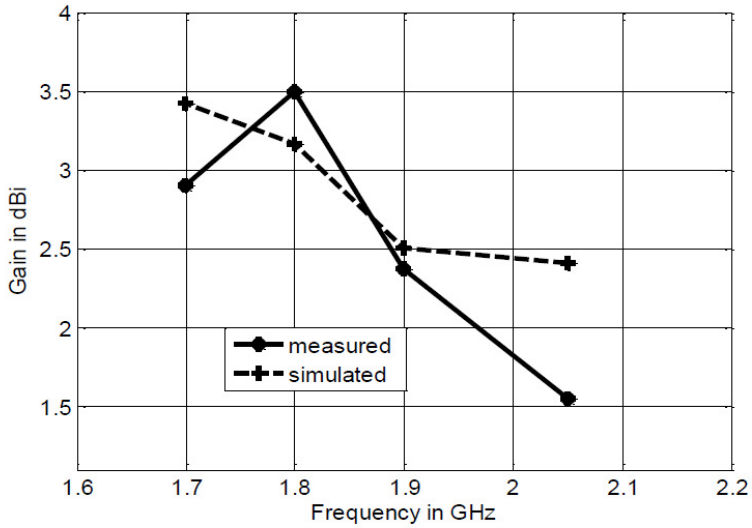
Gain in dBi
Frequency in GHz
measured
simulated
4
3.5
3
2.5
2
1.5
1.6
1.7
1.8
1.9
2
2.1
2.2

Figure 13 (a):

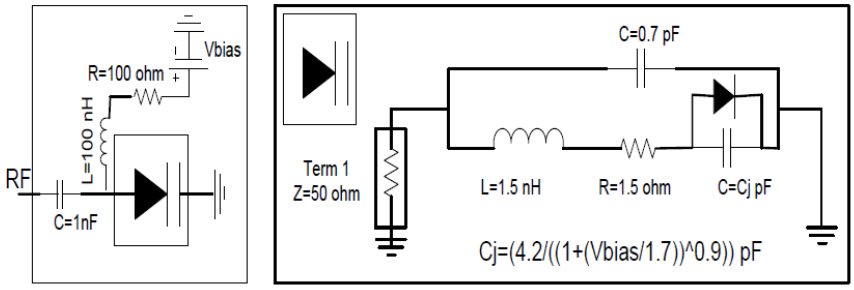

Figure 13 (b):

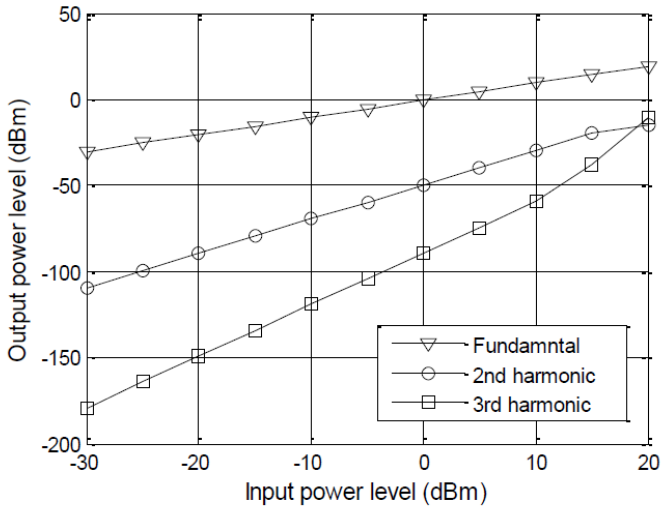

Figure 14:

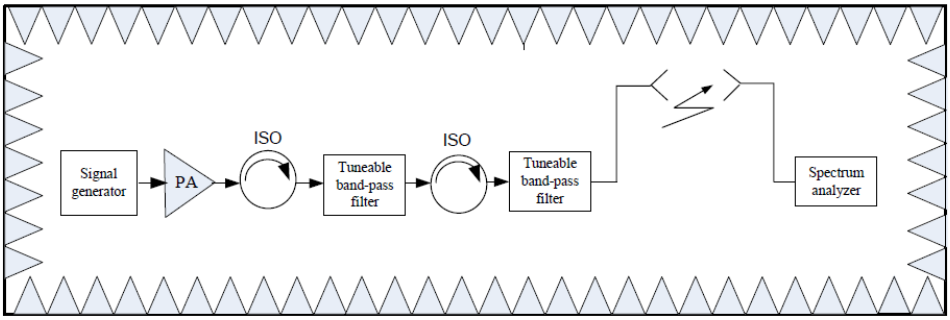

Figure 15:

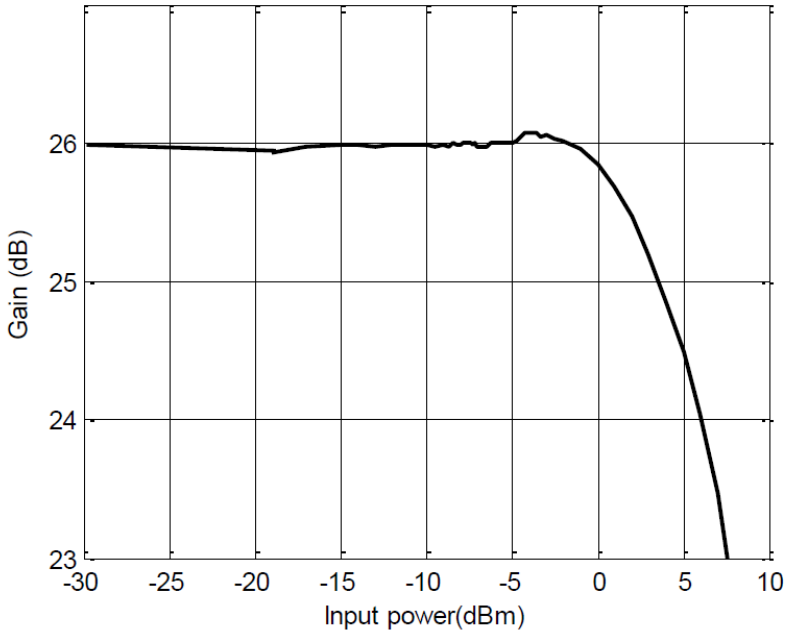

Figure 16:

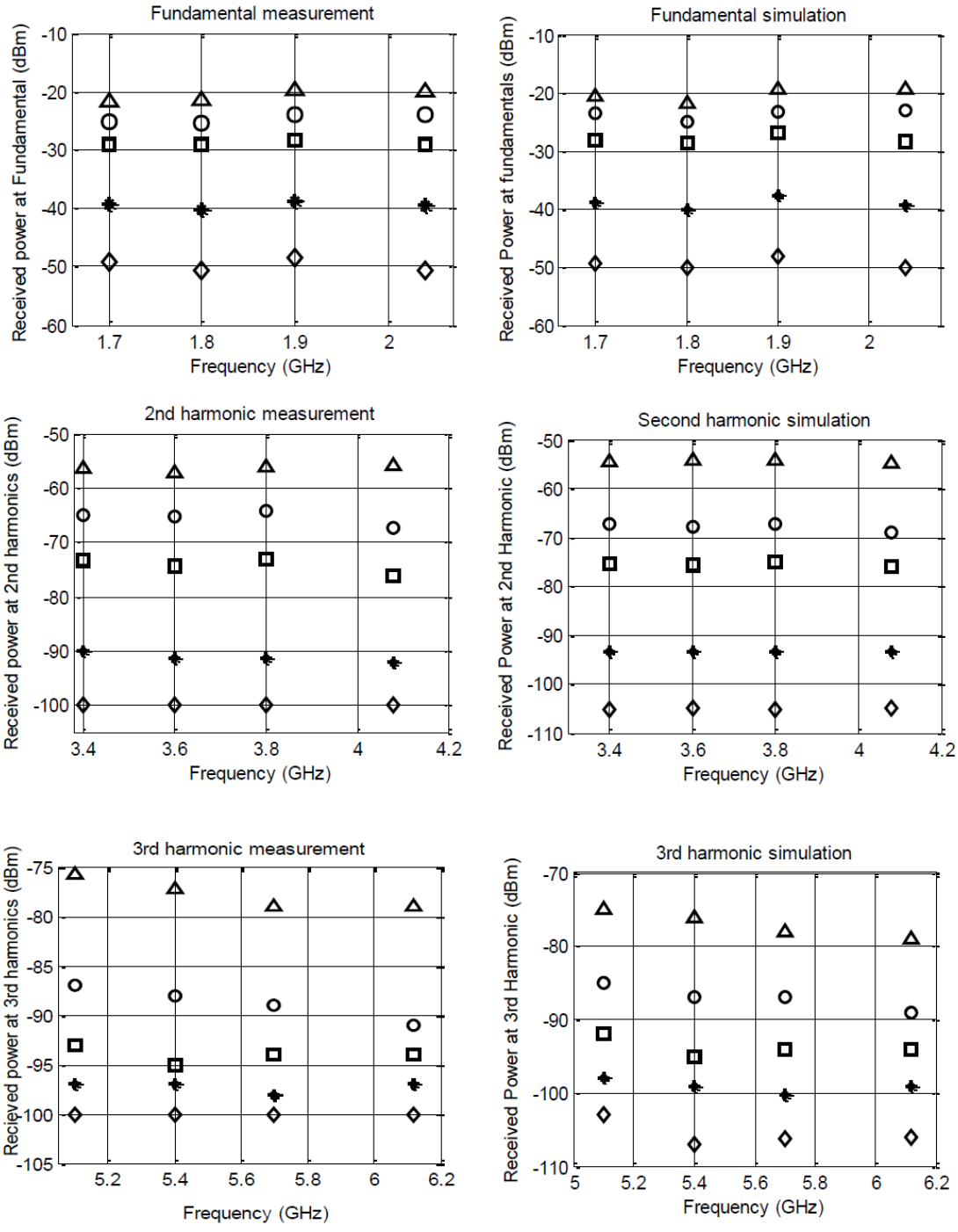
Fundamental measurement
Received power at Fundamental (dBm)
-10
-20
-30
-40
-50
-60
1.7
1.8
1.9
2
Frequency (GHz)
Fundamental simulation
Received Power at fundamentals (dBm)
-10
-20
-30
-40
-50
-60
1.7
1.8
1.9
2
Frequency (GHz)
2nd harmonic measurement
Received power at 2nd harmonics (dBm)
-50
-60
-70
-80
-90
-100
3.4
3.6
3.8
4
4.2
Frequency (GHz)
Second harmonic simulation
Received Power at 2nd Harmonic (dBm)
-50
-60
-70
-80
-90
-100
-110
3.4
3.6
3.8
4
4.2
Frequency (GHz)
3rd harmonic measurement
Recieved power at 3rd harmonics (dBm)
-75
-80
-85
-90
-95
-100
-105
5.2
5.4
5.6
5.8
6
6.2
Frequency (GHz)
3rd harmonic simulation
Received Power at 3rd Harmonic (dBm)
-70
-80
-90
-100
-110
5
5.2
5.4
5.6
5.8
6
6.2
Frequency (GHz)

www.ietdl.org

Published in IET Science, Measurement and Technology
doi: 10.1049/iet-smt.2012.0027

Special Issue on Energy Efficient Reconfigurable Transceivers

ISSN 1751-8822

Editorial

Special Issue on Energy Efficient Reconfigurable Transceivers

Throughout the global community, wireless communications have had a profound social and economic impact, enriching our daily lives with a plethora of services from media entertainment to more sensitive applications such as e-commerce. Looking towards the future, although voice and SMS are still major sources of revenue, richer mobile traffic will account for a large chunk of the internet highway. To cope with this increased demand, operators will be required to invest more in core infrastructure, and deploy more advanced technologies. In fact, already in todaýs market, operators are deploying over 120,000 new Base Stations (BSs) on a yearly basis across the world. Moreover, the rapid evolution of mobile technologies, from 3rd Generation (3G) supporting 384 kb/s downlink in 2001 to the Long Term Evolution (LTE) supporting 300 Mb/s downlink in 2010, is further increasing the cost for network operators. However, although the data throughput per user is rapidly growing, the revenue per Mb is continuously dropping such that resorting to advanced spectral efficiency technology alone appears insufficient to maintain a profitable business. Consequently, service providers – and infrastructure vendors – are increasing their focus on cost reductions.

The increasing demand for data and voice services is not the only cause for concern since energy management and conservation now is at the forefront of the political agenda. The vision of Europe 2020 is to become a smart, sustainable and inclusive economy, and as part of these priorities the EU have set forth the 20:20:20 targets, whereby greenhouse gas emissions and energy consumption should be reduced by 20% while energy from renewables should be increased by 20%. In fact, in todaýs energy-conscious society, Information and Communication Technology (ICT) accounts for 2% of global CO_2 emissions: for example, a medium-sized cellular network uses as much energy as 170,000 homes; further, the cost of powering the existing BSs accounts for a staggering 50% of a service provider's overall expenses. Therefore new solutions are required whereby operators can accommodate this additional traffic volume whilst reducing their investment in new infrastructure, and beyond that significantly reduce their energy bill. Moreover, the EU political agenda, in unison with expected growth in mobile data, has identified cost and energy per bit reduction as a stringent design requirement for mobile networks of the future.

In the future communications will be pervasive in nature, such that a user will be able to attain any service, at any time, on any device. This requires a future handset that is multi-mode in nature, with multiple air-interfaces, continuously scanning for available networks and establishing new connections in a seamless manner. This Beyond-3G application paradigm has spurred extensive research into reconfigurable transceivers, and software-defined radios; two terms that go hand-in-hand to create a truly portable, ergonomically feasible and energy friendly mobile terminal. However, practical implementations of future handsets are still in their infancy and significant research challenges still lie ahead in terms of complete multi-standard integration in the baseband and RF front-end. The IST C2POWER project, is a prime example of a European initiative that is leading research on this area.

This Special Issue targets some high quality research and practical case studies in the very active field of green communications and reconfigurable transceivers to provide design recommendations for tomorrow's ICT networks that will support a whole host of future services and e-applications with minimised energy cost. The scientific works presented here provide a step further toward overcoming the so called energy trap, which is seen by many as the next stumbling block in the migration towards Beyond-3G systems. We present eleven leading works that will allow the IET readership to go beyond state-of-the-art on these topics, and perhaps establish new bridges towards further innovation in green communications.

The first article by Elfergani *et al.* entitled 'Efficient Multi-Stage Load Modulation RF Power Amplifier for Green RF Front End' explores the trade-off between optimising efficiency and linearity in RF power amplifier design as an integral part of the green RF front end. The 3-stage load modulation RF power amplifier was proposed, based on Doherty configuration, to operate in the 3.4–3.6GHz mobile WiMAX frequency band. The experimental results show that 30 dBm output power can be achieved with 67% added efficiency, which represents a 14% improvement over current state of the art 2-stage load modulation while meeting the power output requirements for mobile WiMAX.

The contribution by Sadeghpour *et al.* entitled 'Compensation of Transmission Nonlinearity Distortion with Memory Effect for WLAN802.11a Transmitter' investigates

the effect of nonlinearity caused by a typical radio frequency high-power amplifier front-end on the performance of an OFDM signal for the 802.11a standard. To overcome the non-linear distortion, the authors propose an adaptive baseband predistorter based on the Hammerstein system with a new parameter estimation technique. The performance of the predistorter is assessed using a transmitter which includes an S-band lateral MOSFET transistor amplifier producing 40 dBm peak envelope power. The experimental results show that an accurate prediction of PA nonlinearity with memory effect is achieved, and the new proposed algorithm yields a useful trade-off between accuracy and convergence speed in the reduction of linear and nonlinear distortion, as well as good suppression of spectrum re-growth.

'Generic Load-Pull Based Design Methodology for Performance Optimisation of Doherty Amplifiers' by Darraji *et al.* proposes a systematic design methodology to optimise the operation of Doherty power amplifiers (PAs). The approach makes use of two sets of load-pull data to enhance the performance of Doherty PAs at low- and high-power drive levels. To assess its effectiveness, the proposed methodology is applied to the design of three Doherty PAs optimised for power efficiency, linearity and gain, respectively. Around the Doherty turn-on point, these circuits achieved up to 9% efficiency improvement, up to 10 dB inter-modulation reduction and up to 2 dB gain improvement, respectively.

A pivotal theme is this Special Issue considers reconfigurability, a design attribute that proliferates from the transceiver to the network to provide a virtualised platform for the delivery of future internet services. To address this topic, the contribution by Vázquez-Gallego *et al.* entitled 'OpenMAC: A New Reconfigurable Experimental Platform for Energy-Efficient Medium Access Control Protocols' considers an innovative reconfigurable open MAC platform which overcomes the limitations of state-of-the-art experimental tools to test Medium Access Control (MAC) protocols. The purpose of the so called 'OpenMAC' platform is to simplify the prototyping process by enabling the implementation of MAC protocols designed in C++, relieving the protocol designer from the hardware and timing aspects, and thus avoiding the need to code optimised C/assembler or Hardware Description Language (HDL). For this purpose, the OpenMAC platform introduces an innovative hardware/software partitioning concept for MAC protocol implementation which is based on a shared-memory architecture. Measurements carried out on an FPGA board demonstrate that this platform meets the Short Inter-Frame Space (SIFS) specification of the IEEE 802.11 Standard, hence enabling field testing of prototyped MAC protocols.

Tsimenidis *et al.* contribute the work entitled 'Adaptive Resource Allocation for Single-Cell Downlink OFDMA Systems' that proposes a cross-layer resource allocation strategy entitled 'Joint bit and power allocation' (JBPA) for orthogonal frequency division multiple access (OFDMA) systems based on adaptive modulation and coding (AMC). The JBPA strategy takes into account the total transmission power constraints and the related channel state information (CSI) in order to select the most suitable modulation and coding scheme (MCS) for each sub-channel. The performance in terms of average throughput of the proposed strategy is examined and compared with those of the conventional resource allocation approaches for AMC-OFDMA systems in the context of WiMAX technology. The simulation results show that the proposed JBPA strategy significantly outperforms the conventional approaches.

The article 'Analysis of effect of high power amplifier modelling on the performance of OFDM orthogonal frequency division multiplexing transceiver for wireless communications' by Madani *et al.* presents a theoretical analysis of performance degradation in orthogonal frequency division multiplexing systems when the signal, including phase noise, is passed through a dynamic nonlinear circuit such as a high power amplifier (HPA). The HPA is modelled by use of a memory polynomial model. The results show that the dynamic nonlinear circuit introduces phase noise expansion that is relative to the memory length of the nonlinear device and this causes higher degradation in OFDM signals. This analysis allows designers to choose optimum design parameters including the operating point of the HPA for a desired OFDM transceiver performance, allowing for savings in energy consumption.

The next article 'Receiver-Aided Predistortion of Power Amplifier Nonlinearities in Cellular Networks' by Zeleny *et al.* proposes a system architecture that encompasses the estimation of nonlinearities at the receiver based on a training sequence, and sent back to the transmitter to apply predistortion. The proposed architecture achieves efficient compensation of power amplifier nonlinearities for WiMAX and LTE standards without introducing extra hardware. The results show that the suggested architecture can be applied for high data rate systems at base stations, relay stations and mobile stations.

The work of Athanasopoulos *et al.* entitled 'Performance Verification of a Prototype WiMAX Relay Station' presents the performance of a prototype WiMAX Relay Station which has been developed in the framework of the FP7 ICT REWIND project. The prototype operates in the 3.5 GHz frequency band and supports both networking and operational features that are currently being specified in the evolving IEEE802.16j standard. Performance field tests that are presented verify that the introduction of the prototype within the network provides extension of the base station coverage area, while, in parallel, it provides significant improvement in terms of throughput and signal-to-noise ratio.

The final article, by Kwan *et al.* entitled 'LUT-based Digital Predistorter Implementation for FPGAs using LTE signals with 60 MHz Bandwidth' discusses the implementation of a digital predistorter to linearise RF power amplifiers using signals with 60 MHz bandwidth. The digital predistorter characterisation is performed on a digital signal processor using a memory polynomial modelling technique with QR-RLS as the extraction procedure. Linearisation results are shown for a LDMOS-based PA biased in class AB operation with a three carrier LTE-TDD input signal. Combining both the optimised predistortion coefficient extraction and predistorter implementation gives over 20 dBc improvement in the adjacent channel.

Overall, the papers presented here represent a cross-section of leading-edge work across a range of topics relevant to the theme of the Special Issue, drawn from a broad spread of international contributors, and giving clear indicators of the way in which work to address the green communications agenda is progressing. We would like to thank all authors who submitted manuscripts to this Special Issue and for the reviewers that assisted the guest editors to select the best articles for publication. Our gratitude also extends to the

IET Sci. Meas. Technol., 2012, Vol. 6, Iss. 3, pp. 113–116
doi: 10.1049/iet-smt.2012.0027

2010 edition of the EERT workshop and the FP7 C2POWER (248577) project that provided the launch pad for this Special Issue.

RAED A. ABD-ALHAMEED
University of Bradford, UK
r.a.a.abd@bradford.ac.uk

PETER S. EXCELL
Glyndŵr University, Wrexham, UK
p.excell@glyndwr.ac.uk

JONATHAN RODRIGUEZ
Inst. Telecomunicações, Portugal
jonathan@av.it.pt

ABUBAKAR SADIQ HUSSAINI
Inst. Telecomunicações, Portugal
ash@av.it.pt

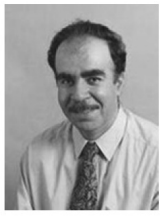

Prof Raed Abd-Alhameed is the Professor of Electromagnetic and RF Engineering, in the School of Engineering, Design and Technology at the University of Bradford. He has over 20 years research experience in the areas of RF, antennas, electromagnetic computational techniques, biological cell modelling and has published over 380 academic journals and referred conference papers. This research has produced new antenna design configurations and computational techniques for various wireless communications applications. In particular his work has produced highly realistic analysis of antenna design processes in the presence of large multi-layer scatterers, using the Bradford-developed hybrid modelling techniques (MoM and FDTD methods). He is the head of RF, Antennas and Computational Electromagnetics and leader of the Communications research group. He was the Principal Investigator for an EPSRC-funded project 'Multi-Band Balanced Antennas with Enhanced Stability and Performance for Mobile Handsets'. He has also been a co-investigator in several funded research projects including: (i) Nonlinear and demodulation mechanisms in biological tissue (Dept. of Health, Mobile Telecommunications & Health Research Programme) and (ii) Assessment of the Potential Direct Effects of Cellular Phones on the Nervous System (EU). In addition he has managed four KTP projects that focussed on advanced RF and antenna design and so has experience in working closely with industry. He is a Fellow of the Institution of Engineering and Technology, Fellow of the Higher Education Academy and a Chartered Engineer.

Prof Peter Excell joined Glyndwr University in 2007. He was previously Associate Dean for Research in the School of Informatics at the University of Bradford, UK, where he had worked since 1971. He obtained a BSc in Engineering Science from Reading University in 1970 and was awarded his PhD from Bradford University in 1980 for research in electromagnetic hazards. His long-standing research interests have been in the applications and computation of high-frequency electromagnetic fields. These have led to numerous research grants, contracts and patents in the areas of antennas, electromagnetic hazards, electromagnetic compatibility and field computation. His principal recent work has been in the computation and measurement of electromagnetic fields due to mobile communications terminals. This led to significant advances in the development of the hybrid field computation method and novel designs for mobile communications antennas. His current work includes studies of advanced methods for electromagnetic field computation (including the use of high performance computing), the effect of electromagnetic fields on biological cells, advanced antenna designs for mobile communications, and consideration of usage scenarios for future mobile communications devices. He is a Fellow of the Institution of Engineering & Technology, the British Computer Society and the Higher Education Academy, a Chartered Engineer and Chartered IT Professional, a Senior Member of the Institute of Electronics and Electrical Engineers, an Associate Fellow of the Remote Sensing and Photogrammetry Society, and a member of the Association for Computing Machinery, the Applied Computational Electromagnetics Society, and the Bioelectromagnetics Society.

Dr Jonathan Rodriguez received his Masters degree and his Ph.D in Electronic and Electrical Engineering from the University of Surrey (UK), in 1998 and 2004 respectively. In 2002, he became a Research Fellow at the Centre for Communication Systems Research and was responsible for coordinating Surrey's involvement in European research projects under Framework Programmes 5 and 6. Since 2005, he has been a Senior Researcher at the Instituto de Telecomunicações (Portugal), and founded the 4TELL Wireless Communication Research Group in 2008. The 4TELL group currently comprises 25 researchers with a project portfolio that includes 10 ongoing European collaborative research projects. He is currently the project coordinator for the Seventh Framework C2POWER project, and technical manager for COGEU. He is author of more than 100 scientific publications, served as general chair for several prestigious conferences and workshops, and has carried out consultancy for major manufacturers participating in DVB-T/H and HS-UPA standardisation. His research interests include green communications, cognitive radio cooperative strategies, radio resource management cross-layer design and baseband digital signal processing.

Abubakar Sadiq Hussaini received his Diploma in Electrical and Electronic Engineering from the Bayero University (Nigeria) in 2003 with a specialisation in Microwave/RF power amplifier design and tunable filters; and he received his MSc in Radio Frequency Communication Engineering from the University of Bradford (UK) in 2007. Since 2009,

he has been a researcher at the Instituto de Telecomunicações – Aveiro, in Portugal. He is a member of the IEEE, IET, and Optical Society of America; and involved in several European Framework 7 and CELTIC research projects. He has chaired several workshops and special sessions in major international conferences, and is author of 20 scientific works in his field. His research interests include radio frequency system design and high-performance RF-MEMS tunable filters, with specific emphasis on energy efficiency and linearity.

IET Sci. Meas. Technol., 2012, Vol. 6, Iss. 3, pp. 113–116
doi: 10.1049/iet-smt.2012.0027

Design of Energy Efficient Power Amplifier for 4G User Terminals

Abubakar Sadiq Hussaini[#**1], Raed Abd-Alhameed[#2]
[#]School of Engineering, Design and Technology
University of Bradford, UK
{[1]ashussa2, [2]r.a.a.abd}@brad.ac.uk

Jonathan Rodriguez[**3]
[**]Instituto de Telecomunicações
Aveiro, Portugal
{[1]ash, [3]jonathan}@av.it.pt

Abstract—**This paper describes the characterization and design of energy efficient user terminal transceiver power amplifier. To reduce the design of bulky external circuitry, the load modulation technique is employed. The design core is based on the combination of Class B and Class C that includes quarter wavelength transformer at the output to perform the load modulation. The handset transceiver for this power amplifier is designed to operate over the frequency range of 3.4GHz to 3.6GHz mobile WiMAX band. The performances of the load modulation amplifier are compared with conventional Class B amplifier. The results of 30dBm output power and 53% power added efficiency are achieved.**

Keywords-Class B; load modulation RF power amplifier; OFDM; mobile WiMAX

I. INTRODUCTION

The performance of the 4G handset transceiver depends primarily on the performance of RF power amplifier. However due the thirst high data rate of the 4G communications, it adopts OFDM modulation scheme. Certainly this scheme offers high data rate but is critically dependent on linearity of transceiver power amplifier due to its high crest factor. As a result of this phenomenon, the power amplifier mostly operates at the back off region and thus the resultant efficiency degrades dramatically. To boost the efficiency and keep the same margin for high crest factor signal, load modulation techniques with new offset line are employed.

A load modulation technique was proposed in 1936 [1] to work with AM broadcasting transmitter but at that time nobody adopted it. This was mainly because the signals of AM transmitter were around 0dBm crest factor. However, until recently beyond 2G where the transmission signals contains 8 to 12dBm crest factor and the load modulation becoming widely adopted. The concept of load modulation technique has been fully explained by the present authors of their previous work in [2]. The work involves the use of two or more power amplifiers with quarter wave transmission line coupler as an impedance inverting network. The resultant linear power amplifier achieved a higher efficiency at the outputs below peak output power (PEP) than conventional class B linear power amplifier [3], [4]. The technique essentially makes use of a Class C amplifier to adapt the load impedance at the Class AB amplifier for optimum efficiency over a wide range of output power. The quarter- wave transformers based on a transmission line structure are served as the power-coupling element between the two amplifier paths.

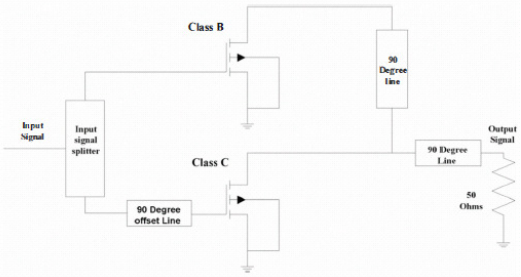

Figure 1. The schematic diagram of load modulation power amplifier

There are ten frequency bands defined in the WiMAX standard, the 3.5 GHz is the mobile WiMAX band and being the most common in Europe. This band has a range of frequency from 3.4GHz to 3.6GHz (Uplink: 3400MHz – 3500MHz, Downlink: 3500MHz – 3600MHz).

In this paper, the efficiency and the output power of the load modulation amplifier has been achieved by 1) Proposed additional of 32mm offset lines at the output and input matching network for which it prevents power leakage at the output junction between the output impedance transformer and peaking Class C amplifier, 2) The optimum design of Class B amplifier with proposed circuitry increases the quiescent current to an order of 8% of the peak drain current of the transistor, 3) The optimum design of the input signal of 3dB 90 degree splitter, and RF-DC blocking circuit proposed as an open short circuits are added to right angle of the RF blocking transmission lines. The schematic diagram is presented in Figure 1.

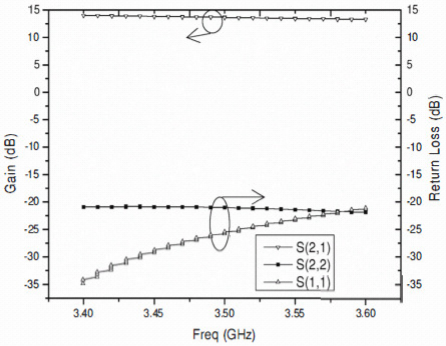

Figure 2. Linear simulation: Flat gain & return loss

II. CIRCUIT DESING

A 3.5GHz, 30dBm Mobile WiMAX handset load modulation RF power amplifier, has been designed using the TOM3 large signal model and FPD1500 transistor. The FPD1500SOT89 is a packaged depletion model AlGaAs/InGaAs pseudomorphic High Electron Mobility Transistor (pHEMT). It contains double recessed gate structure which minimizes parasitic and optimize performance.

This design comprised several design steps for which the optimization is applied to each in order to obtain global high performances of the entire load modulation RF power amplifier. Initially, the design of carrier and peak amplifiers, input 3dB 90 degree hybrid coupler designs, Output 90 degree offset line and impedance transformer designs were performed.

However, it is important to note that in the designing of carrier and peak amplifiers, the DC simulation should be done first in order to find the optimal bias point and bias network based on the class of operation and power requirements. In this paper the bias circuit was designed based on Class B and Class C of the carrier peaks. We decided to use class B to improve the efficiency and linearity instead of Class AB which is widely used in the combination of Doherty amplifier. The DC quiescent current for Class B is at threshold while for Class C is below the threshold. In theory the quiescent current of Class B is zero but for the current work, we increased the quiescent current to an order of 8% of the peak drain current that is resulting in 0.046mA. The reason for this is to minimize crossover distortion and increases the efficiency. The peak drain current is 0.587mA when the VGS is at 0V and VDS is 5V. 5V was chosen for VDS since it is located between cut-off and saturation of the transistor. 0.046mA is 8% of the peaks drain current which gave the VGS of -0.9V while the overall power consumption is 0.228Watts. Moreover, the same supplied power applied to class C but the drain current was 0.004mA and the power consumption was 0.019Watts.

Having obtained the DC quiescent current, the next step is to determine the load line impedance to design the output and input matching of Class B amplifier, to obtain the performance regarding the output power and efficiency. The output matching network was designed for optimum output power performance with load pull technique based on input matching S-parameters.

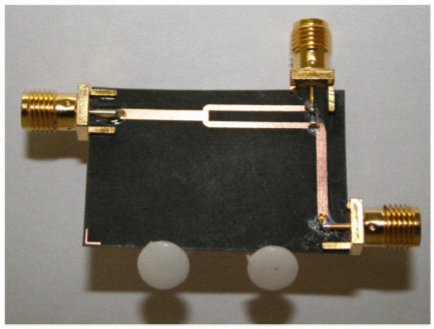

Figure 3. Power splitter

The transistor parasitic elements are included in the load-pull analysis in order to optimize the output matching network. The results obtained from the load pull simulation showed that the transistor needs to see an impedance of 20.492 + j3.775 at the output. Therefore the target of the matching network was to transform the impedance from 49.393 – j1.776 to 20.492 + j3.775. This impedance was the optimal load value which compromised the efficiency 40.39% and 27.05dBm output power at 1dB compression point of single Class B alone. The load reflection coefficient was used to design the output matching network while for the input matching network S-parameter was employed and conjugated the input reflection coefficient for maximum power transfer. Figure 2 shows the linear results obtained from matched Class B power amplifier, the gain is flat over the range of 3.4GHz to 3.6GHz with excellent matching at the input and output return losses.

The non-linear simulation of Class B was performed and the performance of the design in terms of output power and efficiency was observed. The 26.98dBm output power was achieved at 1dB compression point and 39% efficiency. From this nonlinear simulation, the result shows a clear compromise with the load pull measurement values. The same was applied to Class C but with different bias point.

A 3dB quadrature splitter is part of load modulation and if properly can contribute a lot to the total efficiency of the system. Our investigation shows that the operation of this technique is strongly influenced by the coupling factor of the input splitter. In fact, in this research 3dB quadrature splitter have been designed (Figure 3) and tested in terms the operated frequency and bandwidth, and this showed good results as appeared in Figures 4, and 5. It should be noted that, this splitter is at the input of amplifier will divides the input signal equally between the carrier and peaking amplifiers. The splitter, the Carrier Class B, the peaking Class C, and impedance transformer at the output are combined to form a load modulation RF power amplifier.

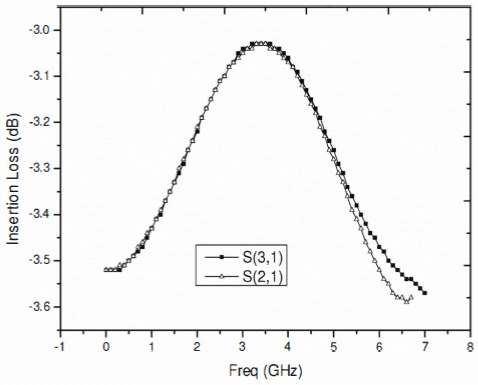

Figure 4. Insertion Loss

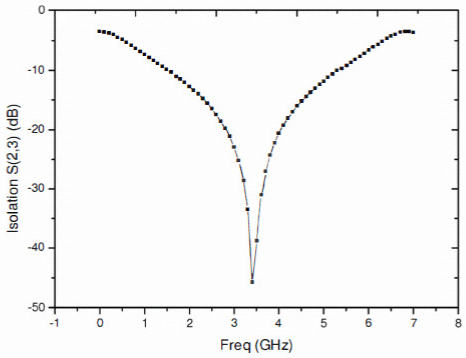

Figure 5. Isolation

III. Implementation & Results

Figure 6, shows the prototype diagram of the proposed load modulation RF power amplifier with offset transmission line at both output and input circuit which maximize the overall system's efficiency with the configuration of Class B amplifier. The FPD1500SOT89 transistor with 27.5dBm output power was used for both Class B and Class C amplifiers and produce a load modulation amplifier with 30dBm and Efficiency of 53%. Table 1 summarizes the recommended bias setting. The bias condition for the Class B carrier amplifier are Vgs = -0.9V (Ids = 46 mA), and for the Class C peaking amplifier, Vgs = -1.1V (Ids = 4 mA). Both of the amplifiers use the same drain voltage (5V)

The load modulation initially characterized for AM-AM and AM-PM responses as well as output power and efficiency. The performance comparisons between the load modulation amplifier and Class B amplifier are performed and the output power increased to 30dBm at 1dB compression point while the efficiency increased to 53%. Figure 7 represent the variation of the input power versus output power of the load modulation. It clearly shows that 30dBm output power is at linear region of the amplifier and this was achieved due to the characteristic of gain compression and expression of the load modulation. The peaking amplifier Class C late gain expansion can compensate the carrier Class B amplifier gain compression. Figure 9 represent the gain characteristic versus output power, the graph shows the power gain of load modulation amplifier is degraded drastically compared to Class B due to the arrangement of lower biasing.

Figure 10 shows the power added efficiency versus output power. The load modulation amplifier have higher efficiency over the range of wide output power levels compared to Class B amplifier.

Table 1: Bias point setting for load modulation

Drain Voltage	Carrier VGS	Peaking VGS
5V	-0.9V	-1.1V

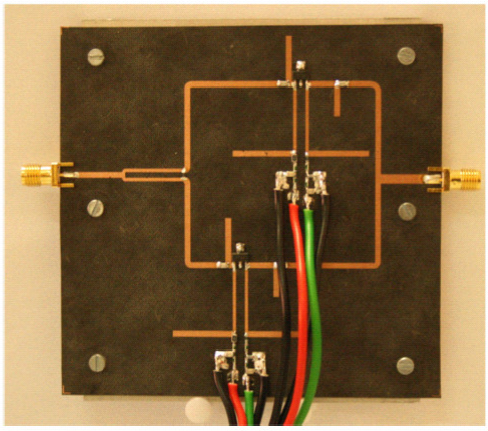

Figure 6. Implemented prototype of energy efficient 4G load modulation power amplifier

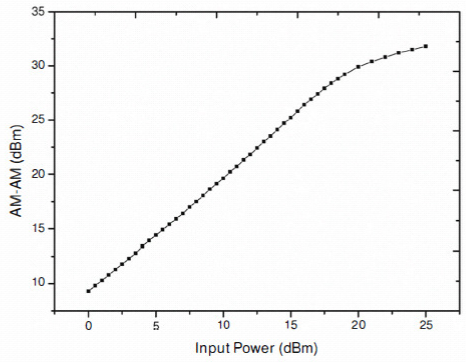

Figure 7. AM-AM characteristics of load modulation amplifier

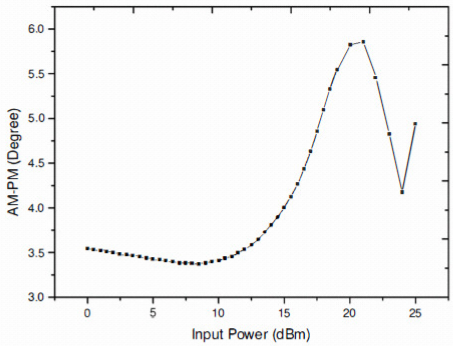

Figure 8. AM-PM characteristics of load modulation amplifier

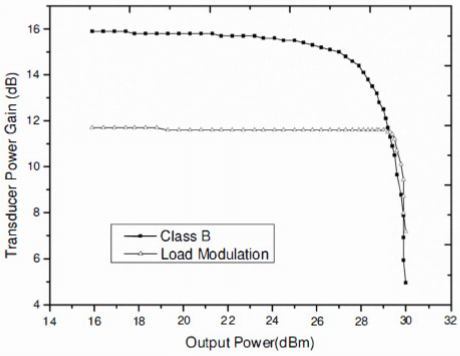

Figure 9. Gain characteristics

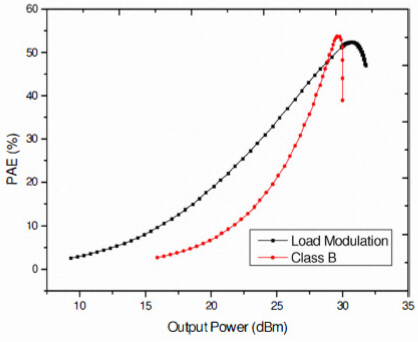

Figure 10. Power-Added Efficiency

Table 2: Comparison performance of Class B and Load modulation at Pout 1dB compression point

Amplifier	Gain (dB)	Pout (dBm) at 1dB	PAE (%) at P1dB
Class B amplifier	15.4dB	27.5dBm	37%
Load modulation	11.8dB	30dBm	53%

IV. CONCLUSION

The trade-off between efficiency and linearity in load modulation power amplifier has been presented. The achieved results of the proposed design process have shown an excellent efficiency and power performances. The proper phasing of 3dB quadrature splitter effectively contributed to the total efficiency of the system. The operation of this design was strongly influenced by the coupling factor of the splitter, biasing of class B and C amplifiers. In addition, the turn–on of the class C amplifier was dependent on the gate bias voltage and the input signal. The self-managing characteristic of the load modulation amplifier has made its implementation more attractive.

ACKNOWLEDGMENT

This work has been performed in the framework of the MOBILIA project (CP5-016) under the Eureka Celtic Framework, funded through the QREN Framework – PO Centro (project n. 5555).

REFERENCES

[1] W. H. Doherty, "A New High Efficiency Power Amplifier for Modulated Wave", Proc. IRE, Vol. 24, No. 9, PP. 1163– 1182, September, 1936.

[2] A. S. Huusaini, R. Abd-Alhameed, J. Rodriguez, "Implementation of Efficiency Enhancement Techniques in the Linear Region of Operations of Power Amplifier", IT 7th Conference on Telecommunications, No 103, PP. 105 – 108, May, 2009.

[3] F. H. Raab, "Efficiency of Doherty RF Power Amplifier System", IEEE Trans. Broadcasting, Vol. BC-33, No 3, PP. 77-83, September, 1987.

[4] S.C.Cripps, RF Power Amplifier for Wireless Communications, Norwood, MA: Artech House, 1999.

[5] Raab F.H., Asbeck P., Cripps S., Kenington P.B., Popovic Z.B., Pothecary N., Sevic J.F., Sokal N.O., "Power amplifiers and transmitters for RF and microwave", IEEE Transactions on Microwave Theory and Techniques, Vol. 50, No 3, PP. 814 – 826, March, 2002.

[6] J. Groe, "Polar transmitters for wireless communications", IEEE Communications Mag., Vol. 45, No 9, PP. 58 – 63, Sept. 2007.

[7] P. B. Kenington, High- Linearity RF Amplifier Design, Norwood, MA: Artech House, 2000.

[8] D. M. Upton and P. R. Massey, "A New Circuit Topology to Realize High Efficiency, High Linearity and High Power Microwave Amplifiers", RAWCON '98 Proceedings, PP. 317– 320, August, 1998.

Design of Power Efficient Power Amplifier for B3G Base Stations

Abubakar Sadiq Hussaini[#*], Bashir A. L. Gwandu[†], Raed Abd-Alhameed[#], Jonathan Rodriguez[*]
[#]School of Engineering, Design and Technology, University of Bradford, UK
[†]Nigerian Communications Commission (NCC), Abuja, Nigeria
[*]Instituto de Telecomunicações , Aveiro, Portugal
ash@av.it.pt, Gwandu@ncc.gov.ng, r.a.a.abd@brad.ac.uk, jonathan@av.it.pt

Abstract— **Fourth generation systems require the use of both amplitude and phase modulation to efficiently utilize the available spectrum and to obtain high data rates, hence imposing stringent requirements on the power amplifier in terms of efficiency and linearity and requires the power amplifier to operate linearly and efficiently. The B3G base station transceiver Doherty power amplifier was designed to operate over the frequency range of 3.47GHz to 3.53GHz mobile WiMAX band using Freescale's N-Channel Enhancement-Mode Lateral MOSFET Transistor, MRF7S38010HR3; The performances of the Doherty amplifier are compared with that of the conventional Class AB amplifier. The results of 43 dBm output power and 66% power added efficiency are achieved.**

Keywords-Class AB; 4G; Doherty RF power amplifier; OFDM; mobile WiMAX; 3.5GHz band, base station

I. INTRODUCTION

The Beyond 3G (B3G) wireless communications adopts OFDM modulation scheme. This scheme offers high data rate but on the other hand has a high crest factor. The beyond 3G base stations require the transceiver to operate linearly and efficiently. Linearity is needed in order to preserve the information, and transmit the signal without error, while efficiency of the base station transceiver is an important attribute that leads to decreased power consumption and active cooling of the base station. All these depend primarily on the performance of the RF power amplifier of the transceiver. As a result of this phenomenon, the power amplifier mostly operates at the back-off region and thus the resultant efficiency degrades dramatically. Power amplifier design has becomes more compound in terms of contending multi dimensional necessities of power output, linearity and efficiency performances. There is a trade-off between power per cost versus efficiency and linearity. To enhance the efficiency and keep the same periphery for high crest factor signal, Doherty techniques with 15mm offset line are employed.

The Doherty configuration was proposed in 1936 [1] to work with AM broadcasting transmitter, but at that time nobody adopted it. This was mainly because the signals of the AM transmitter were around 0dBm crest factor. However, the onset of 2G system has led to the widespread adoption of the Doherty techniques, where the signal crest factor is between 8 to 12dB. The concept of Doherty technique has been fully explained by the present authors in their previously reported work [2]. The Doherty amplifier consists of Class AB carrier and Class C peaking amplifiers connected by a quarter wave transmission line coupler. The resultant linear power amplifier achieved a higher efficiency at the outputs below peak output power (PEP) than conventional class B linear power amplifier [3], [4]. The technique essentially makes use of a Class C amplifier to adapt the load impedance at the Class AB amplifier for optimum efficiency over a wide range of output power. The quarter- wave transformers based on a transmission line structure are served as the power-coupling element between the two amplifier paths.

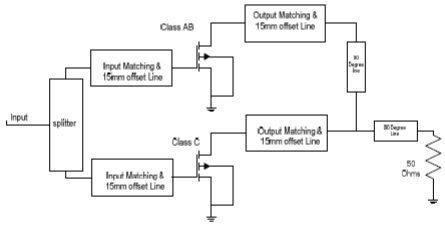

Figure 1. The proposed block diagram of Doherty RF power amplifier

In this paper, the efficiency and the output power of the Doherty RF power amplifier has been achieved by two identical 33dBm, 15dB gain, 30V devices for 3400 – 3600MHz configured as Class AB and Class C respectively, with the proposed additional of 15mm offset lines at the output matching to adopt to the Doherty configuration and prevents the power leakage at the output junction between the output impedance transformer and peaking Class C amplifier. The 15mm length of micro strip line was obtained by using "LineCalc" from ADS simulator with RT 5880 substrates' parameters Er = 2.2, H= 0.5mm, Zo = 50 Ohms, T= 35um, TanD= 0.017. The 50 Ohm 90 degree open short circuits were added to right angle of the RF blocking transmission lines. The proposed schematic diagram of this kind of amplifier is presented in Fig. 1.

978-1-4244-8460-7/10/$26.00 ©2010 IEEE

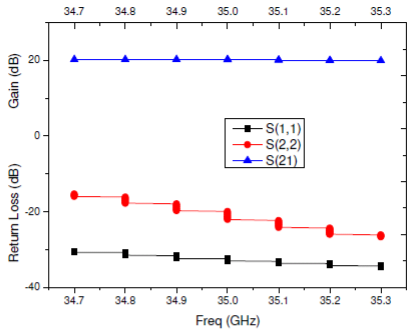

Figure 2. Linear simulation: Flat gain & return loss

II. CIRCUIT DESING

A 43dBm output power beyond 3G base station Doherty RF power amplifier have been designed using the Freescale N-Channel Enhancement-Mode Lateral MOSFET MRF7S38010HR3. The 50Ω quarter wavelength transmission line impedance inverter is used to provide a dynamic load adaptation. This also includes the optimized biases, and operation classes of carrier and peaking amplifier using a large signal harmonic balance simulation to offer improvements in efficiency. The design comprises several design steps for which the optimization is applied to each in order to obtain high performances of the entire Doherty RF power amplifier.

However, it is important to note that in the design of the Doherty RF power amplifier, the DC simulation should be carried out first in order to find the optimal bias point and bias network based on the class of operation and power requirements. In this paper the bias circuit was designed based on Class AB carrier and Class C peaking amplifiers. In Class AB, the transistor is biased just at the start of conduction, about 300mA while Class C is biased in the pinch off region and conducts as the input signal increases.

Having obtained the selected DC quiescent current to maximally cancel the signal distortions, the next step is to determine the design of Class AB amplifier and to obtain the performance regarding the output power and efficiency before incorporating into Doherty design. The output and input impedance was internally matched to 50 ohm impedance microstrip transmission lines, the 15mm offset lines is added to the input side before the input matching network and another 15mm offset line was added to the output side after the output matching network. The Class AB in this design will serve as a carrier amplifier in which the Doherty configuration and the quarter wavelength line will enable it to see high output impedance which leads to its saturation and keeps it maximum voltage at constant condition.

Figure 2 shows the linear results obtained from the matched Class AB power amplifier, the gain is flat in the range of 3.47 to 3.6GHz with excellent matching at the input and output return losses.

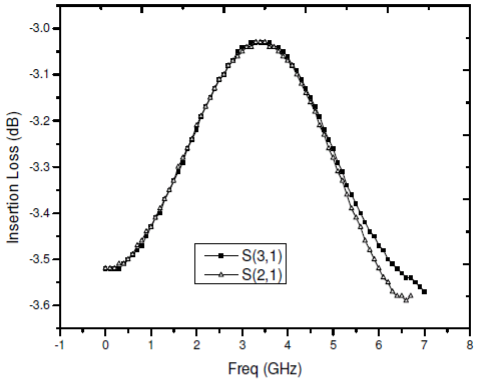

Figure 3. Insertion Loss

The non-linear simulation of Class AB was performed and the performance of the design in terms of output power and efficiency was observed. The 38dBm output power was achieved at 1dB compression point and 32% efficiency. The same was applied to Class C, but with different bias point.

3dB quadrature splitters in the past were very expensive and difficult to design for wide bandwidths and at low frequencies are bulky in nature. The power input splitter is part of the Doherty configurations and if properly designed can contribute to the total efficiency of the system. Our investigation shows that the operation of this technique is strongly influenced by the coupling factor of the input splitter. In fact, in this research the splitters have been designed and tested in terms of operation frequency and bandwidth, and showed good results as seen in Figures 3, 4, and 5. It should be noted that this splitter, at the input of amplifier, divides the input signal equally, but 90 degree phase difference between the carrier and peaking amplifiers. The splitter, the Carrier Class AB, the peaking Class C, and impedance transformer at the output are combined to form the Doherty RF power amplifier.

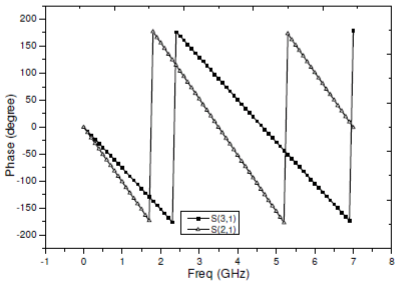

Figure 4. Phase Difference

III. IMPLEMENTATION & RESULTS

Figure 6, shows the prototype diagram of the proposed Doherty RF power amplifier with offset transmission lines at both output and input circuit which maximize the overall system's efficiency with the configuration of Class AB and Class C amplifiers. The Freescale N-Channel Enhancement-Mode Lateral MOSFET, MRF7S38010HR3 transistor with 33dBm output power was used for both Class AB and Class C amplifiers and produce a Doherty RF power amplifier with 43dBm output power and efficiency of 66%. The bias conditions used in this experiment are: class AB as carrier amplifier was set at Vgs = 3.0V (Ids =300 mA) and class C as the peaking amplifier was set at Vgs = 2.4V (Ids = 1 mA). Both amplifiers use the same drain voltage (30V).

The non-linear simulations of Doherty RF power amplifier was achieved through the Advance Design Systems (ADS) simulator. The following results are based on simulations and were initially characterized for AM-AM and AM-PM responses, as well as output power and efficiency. The performance comparisons between the Doherty amplifier and Class AB amplifier were performed. The output power of Class AB power amplifier standalone was 37.5dBm and with Doherty configuration, the output power was increased to 43dBm at 1dB compression point, while the efficiency increased to 66%. Figure 7 represent the variation of the input power in relation to output power of the Doherty amplifier. It clearly shows that 43dBm output power is achieved at linear region of the amplifier, and this was achieved due to the characteristic of gain compression and expression of the Doherty amplifier. The peaking amplifier Class C late gain expansion compensated the carrier Class AB amplifier gain compression. Figure 8 represent the AM-PM data and the graph shows the phase can vary approximately 40 to 47 degree at the 1dB compression point. Figure 9 represent the gain in relation to output power, the graph shows the power gain of Doherty amplifier degraded severely compared to Class AB amplifier due to the arrangement of lower biasing.

Figure 10 shows the power added efficiency versus output power. The Doherty RF power amplifier has higher efficiency over the range of wide output power levels compared to Class AB RF power amplifier.

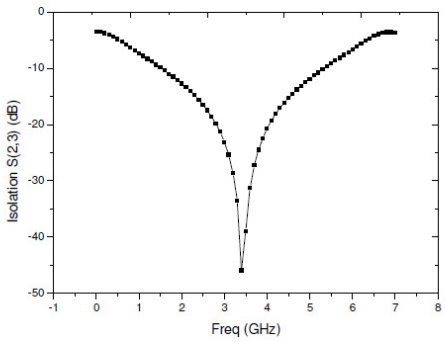

Figure 5. Isolation

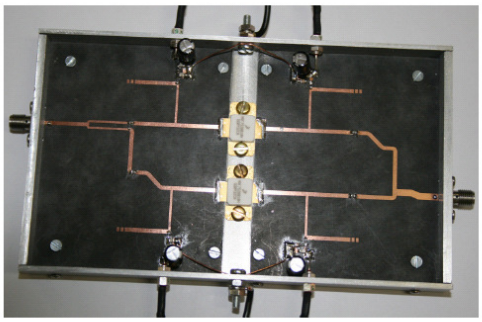

Figure 6. Implemented prototype of proposed power efficient power amplifier

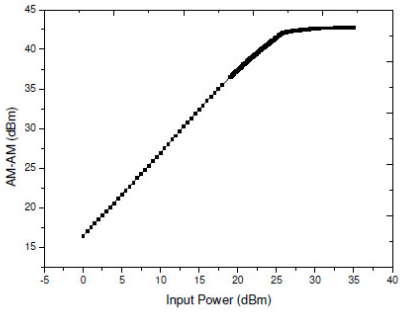

Figure 7. AM-AM characteristics of load modulation amplifier

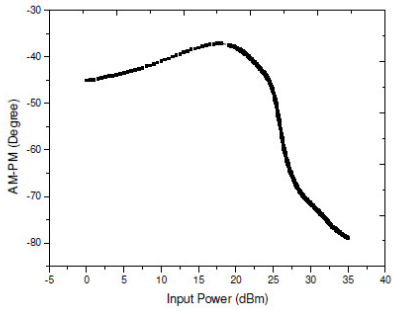

Figure 8. AM-PM characteristics of load modulation amplifier

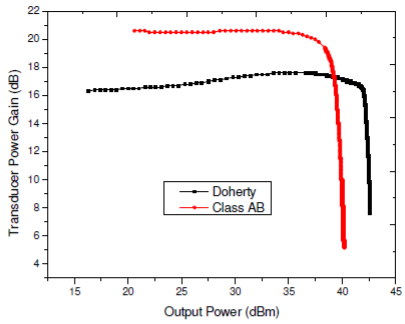

Figure 9. Gain characteristics

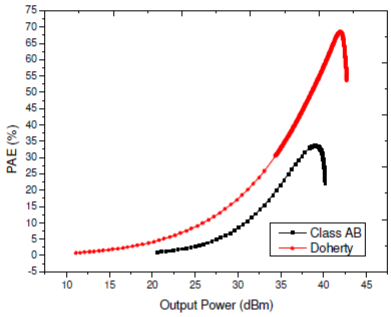

Figure 10. Power-Added Efficiency

IV. CONCLUSION

The Doherty RF power amplifier was designed using Freescale N-Channel Enhancement-Mode Lateral MOSFET transistor, the achieved results of the Doherty were compared with conventional Class AB amplifier, and it exhibited a power added efficiency of 66% for 43dBm output power. The Class AB, Class C, input signal splitter and output transformer were adjusted to optimize the design under Doherty operation. The Doherty RF power amplifier can make a good concession between the cost, linearity, efficiency, and output power. The proper phasing of 3dB quadrature splitter effectively contributed to the total efficiency of the system. In addition, the turn–on of the class C amplifier was dependent on the gate bias voltage and the input signal. The self-managing characteristic of the Doherty RF power amplifier has made its implementation more attractive.

ACKNOWLEDGMENT

This work has been performed in the framework of the MOBILIA project (CP5-016) under the Eureka Celtic Framework, funded through the QREN Framework – PO Centro (project n. 5555).

REFERENCES

[1] W. H. Doherty, "A New High Efficiency Power Amplifier for Modulated Wave", Proc. IRE, Vol. 24, No. 9, PP. 1163– 1182, September, 1936.

[2] A. S. Hussaini, R. A. Abd-Alhameed, J. Rodriguez, "Implementation of Efficiency Enhancement Techniques in the Linear Region of Operations of Power Amplifier", 7th Conference on Telecommunications (Conftele2009), pp. 105-108, Santa Maria de Feira, Portugal, May 2009. [LINK: http://www.av.it.pt/conftele2009/Papers/103.pdf]

[3] F. H. Raab, "Efficiency of Doherty RF Power Amplifier System", IEEE Trans. Broadcasting, Vol. BC-33, No 3, PP. 77-83, September, 1987.

[4] S.C. Cripps, Advanced Techniques in RF Power Amplifier Design, Norwood, MA: Artech House, 2002.

[5] S.C.Cripps, RF Power Amplifier for Wireless Communications, Norwood, MA: Artech House, 1999.

[6] D. M. Upton, P. R. Massey, "A New Circuit Topology to Realize High Efficiency, High Linearity and High Power Microwave Amplifiers", RAWCON '98 Proceedings, PP. 317– 320, August, 1998.

[7] S. M. Wood, R.S. Pengelly, M. Suto, "A high power, high efficiency UMTS amplifier using novel Doherty Configuration," in Proc. IEEE Radio Wireless Conf., Boston, MA, Aug. 2003, pp. 329-332.

[8] Y. Zhao, M. Iwamoto, L. E. Larson, P. M. Asbeck, "Doherty amplifier with DSP control to improve performance in CDMA operation", in IEEE MTT-S Int. Microwave Symp. Dig., 2003, pp. 687-690

[9] C. T. Burns, A. Chang, D. W. Runton, "A 900 MHz, 500 W Doherty power amplifier using optimized output matched Si LDMOS power transistors", IEEE MTT-S Int. Microw. Theory Tech., Symp. Dig., PP. 1557 – 1580, June, 2007.

[10] Raab F.H., Asbeck P., Cripps S., Kenington P.B., Popovic Z.B., Pothecary N., Sevic J.F., Sokal N.O., "Power amplifiers and transmitters for RF and microwave", IEEE Transactions on Microwave Theory and Techniques, Vol. 50, No 3, PP. 814 – 826, March, 2002.

[11] K. J. Cho, J-H. Kim, and S. P. Stapleton, "A Highly Efficient Doherty Feed-Forward Linear Power Amplifier for W-CDMA Base-Station Applications," IEEE Trans. on MTT, Vol. 53, pp. 292 - 300, Jan. 2005.J. Groe, "Polar transmitters for wireless communications", IEEE Communications Mag., Vol. 45, No 9, PP. 58 – 63, Sept. 2007.

[12] P. B. Kenington, High- Linearity RF Amplifier Design, Norwood, MA: Artech House, 2000.

Approach Towards Energy Efficient Power Amplifier for 4G Communications

Abubakar Sadiq Hussaini[#*1], Raed Abd-Alhameed[#2], Jonathan Rodriguez[*3]

[#]School of Engineering, Design and Technology, University of Bradford, UK
Email: [1]ashussaini2@bradford.ac.uk, [2]r.a.a.abd@bradford.ac.uk

[*]Instituto de Telecomunicações – Aveiro, Portugal
Email: [1]ash@av.it.pt, [3]jonathan@av.it.pt

***Abstract*—The biggest challenge for future 4G systems is the need to limit the energy consumptions of battery-powered and base station devices, with the aim to prolong their operational time and avoid active cooling in the base station. The green wireless communications requires research in areas such as energy efficient RF front end, MAC protocol, networking, deployment, operation, and also the integration of base station with renewable power supply. In this paper, the design concept of energy efficient RF front end is considered in terms of RF power amplifiers at which it represents the workhorse of modern wireless communication systems and inherently nonlinear. The approach of output power back off is to amplify the signal at the linear region to avoid distortion, but this approach suffers from significant reduction in efficiency and power output. To boost the efficiency at wide range of output power and keep the same margin for signal with high crest factor, the load modulation technique with new offset line are employed to operate over the frequency range of 3.4GHz to 3.6GHz band. The performances of load modulation power amplifier are compared with balanced amplifier. The results of 42dBm output power and 62% power added efficiency are achieved.**

***Index Terms*— Balanced amplifier; load modulation RF power amplifier; OFDM; 4G**

I. Introduction

The approach towards energy conservation and CO_2 reduction in 4G communications will require a lot of effort form physical layer to upper layers. As of today information and communication technology accounted for 3% and 2% global power consumption and global CO_2 emissions respectively. Corporate social responsibility for international efforts against climate change, targets set to reduce carbon emissions and environmental impacts of networks. Therefore, there's need at both terminal and base station, to take a more holistic approach for improving or achieving green communications, right from radio operation, functionality, up to the implementation. 4G devices should be reconfigurable for multi-standard radios; that will scan the available spectrum and change its network parameters (frequency, bandwidth, modulation) for maximum data transfer, highly integrated, power efficient, and low cost. The 4G networks will provide mobility and connectivity at all the time, putting the priority of data over voice; as a result of this it needs higher modulation scheme to accommodate data. However, 4G adopts Orthogonal Frequency Division Multiplexing (OFDM), with modulations from QPSK to 64-QAM, and has crest factor around 9dB-12dB. This wideband digital modulation scheme offers high data rates and resilience to multipath effects. However, the scheme is critically dependent on linearity in the hardware system due to its inherently high crest factor and also affects the RF power amplifier efficiency. To support the proposed data services, the base station and the user terminal itself must be able to handle higher data rates. Achieving high efficiency and good linearity simultaneously in power amplifier design are the most challenging task.

The 4G offers a higher data rate but unfortunately at the expense of more power consumption. The transmitted power of base station increase exponentially as the data rate increase, from the baseband unit, the radio and the feeder network, the radio consumes more than 75% energy of the base station's energy need and 60% consumed by power amplifier alone. The power amplifier consumes the highest power at the base station and converts more than 50% of what it consumed into heat as a waste. This paper explores the energy efficient power amplifier. The efficiency and the output power of the load modulation power amplifier have been achieved and the results show significant improvement over balanced RF power amplifier.

II. Conventional Balanced and Load Modulation Circuit Architecture

The conventional balance and load modulation amplifiers exploit the Freescale N-Channel Enhancement-Mode Lateral MOSFET MRF7S38010HR3 transistor. The balanced amplifier was first proposed to improve efficiency of 3G base station, is designed to work over a given dynamic range where the amplifier should behave linearly. Conventional balanced amplifier was commercially successful 2G/3G base station amplifiers. However, there are some problems that limit the balanced amplifier for use as power amplifier for 4G communications. Balanced amplifier can be realized by combining two class AB amplifiers as shown in Figure 1. The splitter divides the input signal equally with 90 degree phase-shift, after the input matching circuitry the signals are fed to the transistors' gates. With the proper biasing of VGS both class AB amplifiers are set to conduct in the positive cycles, the signals from the drain of the transistors are also

90 degree in phase and feed into the combiner and at the output, combiner combines the signals un-phase-shift, and full sine wave. While load modulation can be realized by combining carrier class AB and peaking class C amplifiers as shown in Figure 2. The splitter divides the input signal into two equal magnitude but 90 degree phase difference. At the output a microstrip quarter wave impedance inverter combines the signals. The concept of load modulation technique has been fully explained by the present authors of their previous work in [2]. Load modulation power amplifier improves the efficiency and the linearity by complementing the saturation class AB amplifier with the turn on characteristic of class C amplifier.

The design comprises of step-by-step procedure for the optimum design of energy efficient power amplifier, the proposed additional of 90 degree offset lines at the output and input matching network for which will prevents power leakage at the output junction between the output impedance transformer and peaking Class C amplifier. The gate biases and the individually matchings of class AB and class C amplifiers are further optimized to achieve high efficiency, linearity and wideband characteristics. The peaking amplifier allows the load modulation amplifier to respond to the high input levels of short duration, by amplifying the signal peaks, and to dynamically change the load impedance of the main class AB amplifier.

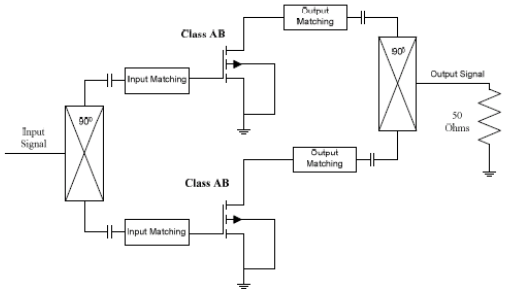

Figure 1. Balanced amplifier configuration

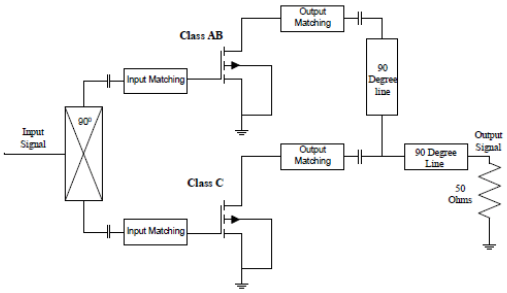

Figure 2. load modulation amplifier configuration

III. Design Layout and Results

The conventional balanced and load modulation amplifiers are fabricated with RT 5880 substrates, H=0.5mm and relative permittivity of 2.2. Figure 3 and 4 shows the layout of conventional balanced amplifier and load modulation amplifier respectively. Figure 5 and 6 shows the simulated linear performance of the balance and load modulation amplifier respectively, the gain is flat in the range of 3.47 to 3.53 GHz with excellent input and out put return losses.

The non-linear simulations and the comparisons of conventional balanced and load modulation amplifiers are performed. The bias conditions used in this experiment are shows in table 1, for balanced amplifier while in table 2; represent that of load modulation amplifier. The drain bias voltage VDS = 30V for both two transistors of balanced and their gate voltage is VGS = 3V. The drain bias voltage of load modulation amplifier is VDS = 30V for both carrier and the peak transistors, while their respective gate bias voltages are VGS (Carrier) = 3V and VGS (Peaking) = 2.2V. Figure 7 represent the comparison of the variation of the input power versus output power of both balanced and load modulation amplifiers. It clearly shows that 42dBm output power is achieved at the linear region of both amplifiers. Figure 9 represent the transducer power gain versus output power. The load modulation has less gain compared to balanced amplifier; this is due to the fact that the peaking amplifier of load modulation is biased in Class C mode. Figure 10 shows the power added efficiency (PAE) versus output power of balanced and load modulation amplifier. From the graph one can be seen that the load modulation amplifier has a higher efficiency over the wide range of output power than conventional balanced amplifier. The PAE of 62% is obtained at 1dB compression point of 42dBm output power of load modulation amplifier while the PAE of 50% is obtained at 1dB compression point of 42dBm output power of conventional balanced amplifier.

The load modulation offers improved efficiency at the whole range of output power compared to conventional balanced amplifier. The heart of the load modulation is the load modulation output combiner and that is the fascinating part of the design, while the input behaves the same as a conventional balanced amplifier.

Table 1: Bias point setting for balanced amplifier

Drain Voltage (V)	Class AB 1 VGS (V)	Class AB 2 VGS (V)
30	3.0	3.0

Table 2: Bias point setting for load modulation

Drain Voltage (V)	Carrier VGS (V)	Peaking VGS (V)
30	3.0	2.2

Table 3: Performances of load modulation and balanced amplifiers

	Gain (dB)	PAE (%)
Balanced	19.5	50
Load Modulation	16.5	62

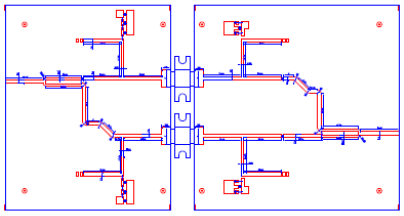

Figure 3. Design layout of Balance amplifier

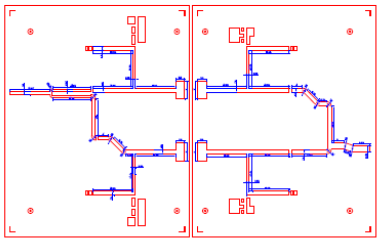

Figure 4. Design layout of load modulation amplifier

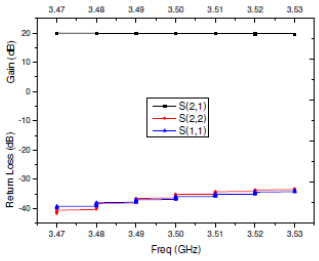

Figure 5. Linear similation of Balance amplifier

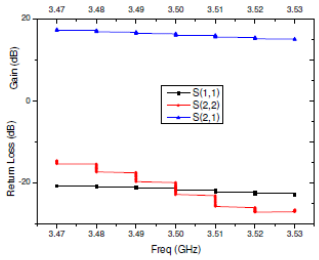

Figure 6. Linear simulation of load modulation amplifier

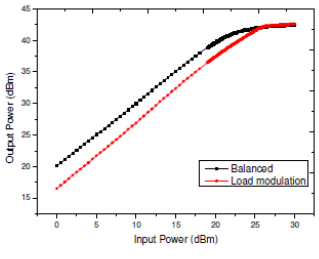

Figure 7. AM-AM responses

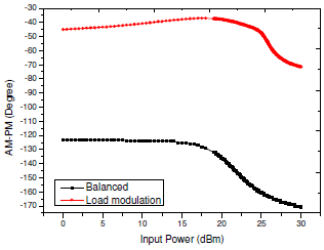

Figure 8. AM-PM responses

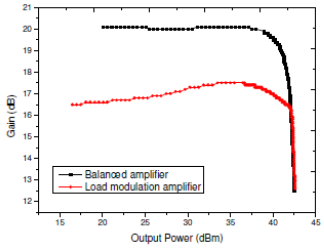

Figure 9. Transducer power gain

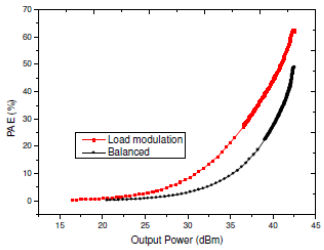

Figure 10. Power-Added Efficiency

IV. Conclusion

The performance comparisons between load modulation power amplifier and conventional balanced power amplifier are performed. The achieved results of the proposed design process have shown an excellent efficiency and power performances. The proper phasing of input signal splitter effectively contributed to the total efficiency of the system. The load modulation amplifier offers improved efficiency over wide range of output power compared to conventional balanced amplifier. The load modulation has less gain compared to balanced amplifier due the arrangement of lower biasing of Class C peaking transistor of load modulation. The operation of this design was strongly influenced by the coupling factor of the splitter, biasing of class AB and C amplifiers. Applying load modulation technique can significantly reduce the CO_2 emission and power consumption in the transceiver. The self-managing characteristic of the load modulation power amplifier has made its implementation more attractive.

ACKNOWLEDGMENT

This work has been performed in the framework of the C2POWER project (FP7/2007-2013) under the European Community, funded through the Seventh Framework programme (project n. 248577) and MOBILIA project (CP5-016) under the Eureka Celtic Framework, funded through the QREN Framework – PO Centro (project n. 5555).

REFERENCES

[1] W. H. Doherty, "A New High Efficiency Power Amplifier for Modulated Wave", Proc. IRE, Vol. 24, No. 9, PP. 1163– 1182, September, 1936.

[2] A. S. Hussaini, R. A. Abd-Alhameed, J. Rodriguez, "Implementation of Efficiency Enhancement Techniques in the Linear Region of Operations of Power Amplifier", 7th Conference on Telecommunications (Conftele2009), pp. 105-108, Santa Maria de Feira, Portugal, May 2009.
[LINK: http://www.av.it.pt/conftele2009/Papers/103.pdf]

[3] F. H. Raab, "Efficiency of Doherty RF Power Amplifier System", IEEE Trans. Broadcasting, Vol. BC-33, No 3, PP. 77-83, September, 1987.

[4] S.C. Cripps, Advanced Techniques in RF Power Amplifier Design, Norwood, MA: Artech House, 2002.

[5] S.C.Cripps, RF Power Amplifier for Wireless Communications, Norwood, MA: Artech House, 1999.

[6] D. M. Upton, P. R. Massey, "A New Circuit Topology to Realize High Efficiency, High Linearity and High Power Microwave Amplifiers", RAWCON '98 Proceedings, PP. 317– 320, August, 1998.

[7] S. M. Wood, R.S. Pengelly, M. Suto, "A high power, high efficiency UMTS amplifier using novel Doherty Configuration," in Proc. IEEE Radio Wireless Conf., Boston, MA, Aug. 2003, pp. 329-332.

[8] Y. Zhao, M. Iwamoto, L. E. Larson, P. M. Asbeck, "Doherty amplifier with DSP control to improve performance in CDMA operation", in IEEE MTT-S Int. Microwave Symp. Dig., 2003, pp. 687-690

[9] C. T. Burns, A. Chang, D. W. Runton, "A 900 MHz, 500 W Doherty power amplifier using optimized output matched Si LDMOS power transistors", IEEE MTT-S Int. Microw. Theory Tech., Symp. Dig., PP. 1557 – 1580, June, 2007.

[10] Raab F.H., Asbeck P., Cripps S., Kenington P.B., Popovic Z.B., Pothecary N., Sevic J.F., Sokal N.O., "Power amplifiers and transmitters for RF and microwave", IEEE Transactions on Microwave Theory and Techniques, Vol. 50, No 3, PP. 814 – 826, March, 2002.

[11] K. J. Cho, J-H. Kim, and S. P. Stapleton, "A Highly Efficient Doherty Feed-Forward Linear Power Amplifier for W-CDMA Base-Station Applications," IEEE Trans. on MTT, Vol. 53, pp. 292 - 300, Jan. 2005.J. Groe, "Polar transmitters for wireless communications", IEEE Communications Mag., Vol. 45, No 9, PP. 58 – 63, Sept. 2007.

[12] P. B. Kenington, High- Linearity RF Amplifier Design, Norwood, MA: Artech House, 2000.

[13] C. F. Campbell, "A fully integrated Ku-band Doherty amplifier MMIC," IEEE Microw. Wireless Compon. Lett., vol. 9, no. 3, pp. 114–116, Mar. 1999.

Abubakar Sadiq Hussaini (S'05) Research Scientist / PhD in view: Instituto de Telecomunicações - Pólo de Aveiro / University of Bradford, United Kingdom; MSc in Radio Frequency Communication Engineering, University of Bradford, United Kingdom, 2007; Post Graduate in Electrical/Electronic Engineering, Bayero University, Kano, Nigeria 2003; Specialization in Microwave/RF power amplifiers design and Tunable Filters.
Technical Education: SDH Network Configuration Siemens (Information and Communication Network Training Institution Siemens), 2002; Telecomm Engineer, Nigerian Telecommunications Limited, Abuja, 2000; where I was responsible for the operations and maintenance of SRT 1F, SRT 1S, SRT 1 (Siemens Radio), Planning and implementing the provision and utilization of microwave radio transmission systems. Contribute article to numerous publications.
Award: Best Student, Newton Institute, Jos, 1993; Nominated in the 26th Edition of Who's Who in the World 2009; Member: Senate Committee of the University of Bradford-2007, IEEE, IET, Optical Society of America (OSA); Involved in European and CELTIC research projects. His research interests include Radio Frequency System Design and High-Performance RF-MEMS Tunable Filters with specific emphasis on energy efficiency and linearity.
Achievements: participation in process to produce energy efficient Power Amplifier at 3.5GHz (Mobile WiMAX Frequency); Designed and developed "Radio over Fiber" Optical transmitter and Optical Receiver (1550nm Wavelength) where investigated radio over fiber technology in which the frequency limitations of quantum well lasers in direct RF to Light transponding was investigated.

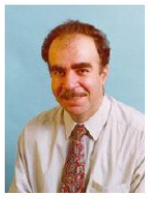

Professor Raed A. Abd-Alhameed received his PhD from Electrical and Electronic Engineering, Bradford University, UK, in 1997. From 1997 to 1999 he was a Postdoctoral Research Fellow at the University of Bradford, specialisation in computational modelling of electromagnetic field problems, microwave nonlinear circuit simulation, signal processing of preadaption filters for adaptive antenna arrays and simulation of active inductance. From 2000 to 2003 he has been a lecturer in the University of Bradford. In August 2003 he was appointed as a senior lecturer in applied Electromagnetics and then Sept 2005 to a Reader in Radio Frequency Engineering at the same University. Since Nov 2007 he was appointed as Professor of Electromagnetics and Radio Frequency Engineering in the school of Engineering, Design and technology, Bradford University. Abd-Alhameed is the Director of Mobile and Satellite Communications Research Centre, Leader of Communications Research group, and the head of the Radio Frequency, Antennas, Propagations and Computational Electromagnetiscs Research group including his appointment as a research visitor for Wrexham University, Wales, UK since 2009. He has worked on several funded projects from EPSRC, Dept. of Health, Mobile Telecommunications and Health Research Programme, EU FP5 and a number of industrial KTPs. He has published over 300 technical Journal and Conference papers including several book chapters. In addition, he holds two patents work on RF antenna designs. He has invited as keynote speaker for ITA 09, Mobimedia 2010, and he chaired the 1st EERT 2010 workshop and several sessions at many international conferences. He is also appointed as guest editor for IET SMT Journal special issue on EERT for 2011. In addition, he is invited to several IEEE, IET and International Journals for his successful research in radio frequency engineering. His current research interests include hybrid electromagnetic computational techniques, EMC, antenna design, low SAR antennas for mobile handset, bioelectromagnetics, RF mixers, active antennas and MIMO antenna systems. Prof Abd-Alhameed is Fellow of the Institution of Engineering and Technology, a Chartered Engineers and Fellow of Higher Education Academy.

Jonathan Rodriguez (M' 04) received his Masters degree in Electronic and Electrical Engineering and Ph.D from the University of Surrey (UK), in 1998 and 2004 respectively. In 2002, he became a Research Fellow at the Centre for Communication Systems Research at Surrey and responsible for managing the system level research component in the IST MATRICE, 4MORE and MAGNET projects. Since 2005, he is a Senior Researcher at the Instituto de Telecomunicações, Pólo de Aveiro (Portugal), where he is the project coordinator for the C2POWER project, technical manager of COGEU and technical workpackage leader in WHERE, HURRICANE, PEACE and MOBILIA. He was also the project coordinator of the Celtic LOOP Project. He is leading the 4TELL Wireless Communication Research Team at IT, author of several conference and journal publications, and has carried out consultancy for major manufacturers participating in DVB-T/H and HS-UPA standardisation. His research interests include Radio Access Networks for current and beyond3G systems with specific emphasis on Radio Resource Management, Digital Signal Processing and PHY/MAC optimization strategies.

The Beyond 3G Energy Efficient Power Amplifier for Mobile Communications

Abubakar Sadiq Hussaini[#*1], Bashir A. L. Gwandu[¥2], Raed Abd-Alhameed[#3], Jonathan Rodriguez[*4]

[#]School of Engineering, Design and Technology, University of Bradford, UK
Email: [1]ashussaini2@bradford.ac.uk, [3]r.a.a.abd@bradford.ac.uk

[¥]Nigerian Communications Commission (NCC), Abuja, Nigeria
Email: [2]Gwandu@ncc.gov.ng

[*]Instituto de Telecomunicações – Aveiro, Portugal
Email: [1]ash@av.it.pt, [4]jonathan@av.it.pt

***Abstract*—The beyond 3G mobile communication systems will accommodate multiple wireless standards (2G, 2.5G, 3G, Mobile WiMAX, LTE, and LTE-A) and both mobile's and base station's devices will be asking for more and high efficient power amplifier with the aim to prolong their operation time and avoid active cooling in the base station. However, it is impossible to achieved higher efficiency and high linearity with single stage traditional power amplifier. Therefore, there is need to adapt an external techniques to improve the efficiency of the transceiver while at the same time maintaining the linearity for the signal with high Peak-to-Average Power Ratio (PAPR). Our research focuses on energy efficient Doherty RF power amplifier for B3G transceivers applications. In this paper, the authors' presents an innovative uneven load modulation RF power amplifier for the applications of B3G base station whose operating frequency covers 3.4GHz to 3.6GHz band. The performances of uneven load modulation RF power amplifier have been compared with the load modulation RF power amplifier. The results of 45dBm output power and 66% power added efficiency have been achieved.**

***Index Terms*— Uneven load modulation RF power amplifier; even load modulation RF power amplifier; B3G; efficiency; linearity; OFDM**

I. Introduction

Energy efficiency and linearity are the main requirements that are driving present's and future's transmitter designs and are the top concerns of vendors for B3G communications while trying to give more priority to data over voice, thus driving the need for higher modulation scheme and the need for linear and efficient power amplifiers. The B3G is an OFDM based technology; OFDM is a multicarrier digital modulation scheme offers high data rates and resilience to multipath effects and is widely adopted. Thus is critical and more sensitive to non linear distortions of power amplifier due to its inherently high Peak-to-Average Power Ratio (PAPR) of about 9dB-12dB and also critical and sensitive to frequency offsets which cause by oscillators mismatch. Therefore, there's need at both mobile and base station, to take a more holistic approach for improving energy efficiency, right from radio operation, functionality, up to the implementation. Transceiver consumes more than 70% of the total power supply to the base station and 50% consumed by power amplifier alone. The power amplifier consumes the highest power at the base station and converts more than 50% of what it consumed into heat as a waste. This paper describes approach to optimize the output power and efficiency of RF power amplifier for B3G base station applications. The efficiency and the output power of the uneven load modulation RF power amplifier have been achieved and the results show significant improvement over the classical load modulation RF power amplifier.

II. Uneven Load Modulation Circuit Design

This work is an improvement of load modulation RF power amplifier which uses identical transistors but differ only in biasing (Class AB power amplifier and Class C power amplifier). Load modulation RF power amplifiers are base on load modulation techniques and when using two transistors, the second transistor should be able to pull the load presented to the first transistor for high output power and efficiency. However, it is impossible for Class C to deliver the same output power as Class AB because, Class C used part of the input signal to turn on and for this reason Class C will never pull out the load presented to Class AB for peak efficiency. Therefore, to solve this problem, uneven load modulation RF power amplifier with uneven signal splitter at the input has been designed, and this will allow more input signal to pass through Class C amplifier than Class AB amplifier. The proposed diagram of this kind of amplifier is presented in fig 1.

The bias and biasing networks are very important in controlling bias current and voltage for the operation of uneven load modulation RF power amplifier. The DC quiescent current for Class AB is in the region between the cut-off point/pinch-off and the Class A bias point, typically at 10 to 15 percent of Ids while for Class C is below the threshold. With this arrangement, and at the low level of input signal looking at Figure 2, the Class C will act as open circuit, because at low level input signal, the signal is too small to turn on the Class C amplifier and as a result of this, the quarter wavelength transmission line present in front of Class AB will enable Class AB amplifier to see high output

impedance which leads to its saturation and keeps it at maximum voltage constant condition.

The transformation of input, output and characteristic impedance of a quarter wave transmission line is given as:

$$Z_1 = Z_O^2 / Z_2 \quad (1)$$

Z_1 and Z_2 are the input and output impedance respectively and Z_o is the characteristic impedance of the transmission line. However, with the increased of input signal and the saturation of Class AB, the suitable bias of Class C will enable it to turn on automatically and start sending current and the same time increasing the impedance of Z_O. With the increase of impedance of Z_O results in decrease of impedance of Z_1, which is the impedance seen by Class AB. At this stage, both Class AB and Class C amplifiers will see a terminating impedance of $2R_L$, while Class C amplifier also reaches its saturation. This means that both Class AB and Class C amplifiers contributed the same amount of power to the load Figure 1 i.e $I_0 = I_2$, and Z_1 and Z_2 becomes:

$$Z_1 = Z_O^2 / 2R_L \quad (2)$$

$$Z_2 = 2R_L \quad (3)$$

As we have seen, the operation of the second amplifier has been forced to operate in Class C, and as we all know that, the DC quiescent current of Class C amplifier is below the threshold, typically have lower gain than Class AB amplifier. Therefore to achieve the maximum output power and overall performance, one solution is to supply more input power to Class C amplifier than Class AB amplifier. With this solution, one should be able to achieve maximum output power without creating AM-AM distortion

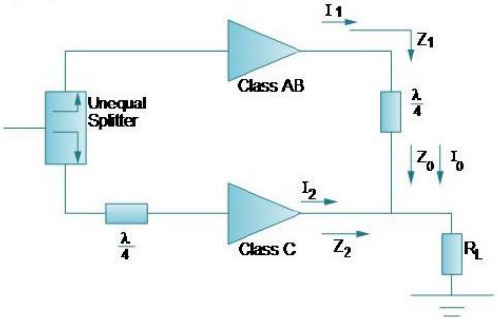

Figure 1. Uneven load modulation at high level input signal

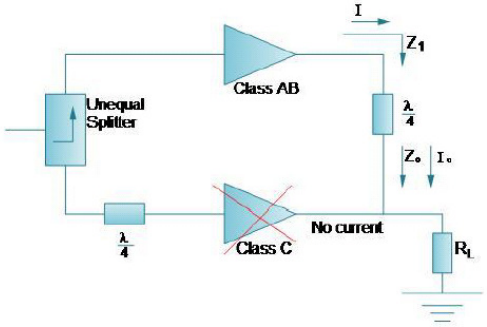

Figure 2. Uneven load modulation at low level input signal

III. Design Prototype and Results

An unequal splitter is part of an uneven load modulation RF power amplifier and if design properly can contribute a lot to the total efficiency of the system. Our investigation shows that the operation of this technique is strongly influenced by the coupling factor of the input splitter. In fact, in this work unequal splitter have been designed (Figure 3) and tested in terms of operating frequency and bandwidth, and this showed good results as appeared in Figures 4 insertion loss, and Figure 5 isolation. It should be noted that, the unequal splitter is at the input of amplifier and divides the input signal unequally between the carrier class AB amplifier and peaking class C amplifier. An unequal splitter, the Carrier Class AB, the peaking Class C, and impedance transformer at the output are combined to form an uneven load modulation RF power amplifier.

Figure 6 shows the implemented prototype of uneven load modulation RF power amplifier which fabricated with RT 5880 substrates, H=0.5mm and relative permittivity of 2.2 and covers the range of frequency from 3.4GHz to 3.6GHz, with excellent input and out put return losses.

The comparisons of uneven load modulation RF power amplifier and load modulation RF amplifier have been performed. The bias conditions used in this experiment are: The drain bias voltage VDS for all transistors is 30V and the gate bias voltage VGS for both Class AB is 3.0V and for Class C is 2.4V. Figure 7 represent the comparison of the variation of the input power versus output power for both uneven load modulation RF power amplifier and load modulation RF power amplifier. It clearly shows that there's an increase of 2dB more in compared with load modulation, this shows that with uneven splitter you can able to pull more output power than with equal splitter. The 45dBm output power was achieved at the linear region of uneven load modulation. Figure 9 represent the transducer power gain versus output power. The uneven load modulation has more gain compared to load modulation; this is due to the fact that we provided more input power to Class C than Class AB in the uneven configuration, while in the load modulation configuration, the input signal are equally divided.

Figure 10 shows the power added efficiency (PAE) versus output power of uneven load modulation RF power amplifier and load modulation amplifier. From the graph one can be seen that uneven load modulation amplifier has a higher efficiency. The PAE of 66% is obtained at 1dB compression point of 45dBm output power of uneven load modulation RF power amplifier while the PAE of 62% is obtained at 1dB compression point of 42dBm output power of load modulation RF power amplifier. The heart of uneven load modulation and the load modulation is the load modulation output combiner, and that is the fascinating part of the design.

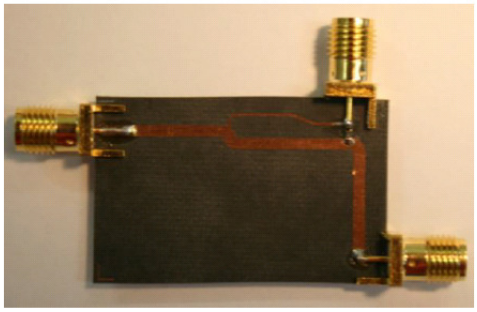

Figure 3. Unequal splitter

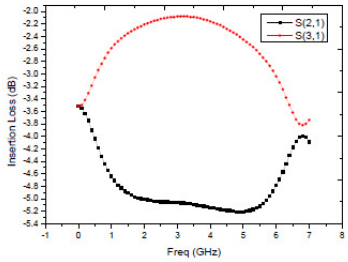

Figure 4. Insertion loss

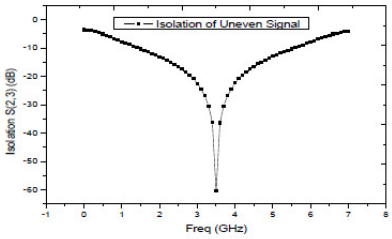

Figure 5. Isolation

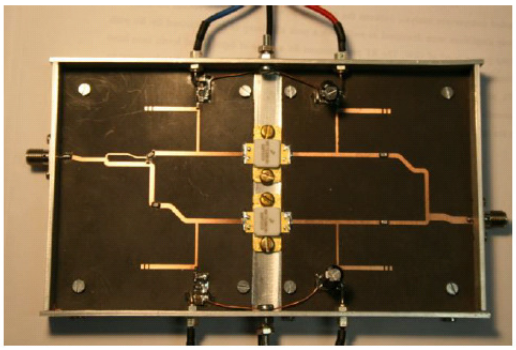

Figure 6. Prototype of uneven load modulation RF power amplifier

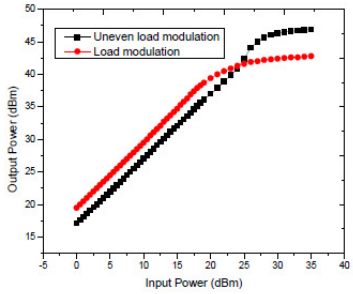

Figure 7. AM-AM responses

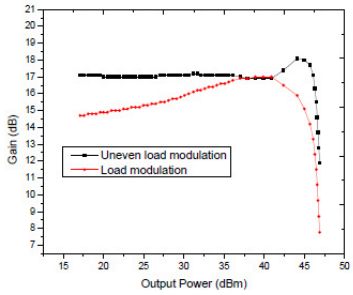

Figure 8. Transducer power gain

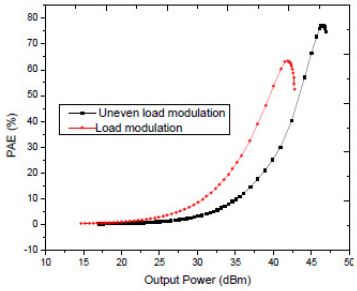

Figure 9. Power-Added Efficiency

IV. CONCLUSION

The performance comparisons between uneven load modulation RF power amplifier and load modulation RF power amplifier are presented. As we have seen, the operation of the second amplifier has been forced to operate in Class C, typically Class C have lower gain than Class AB amplifier, and it is impossible for Class C to deliver the same output power as Class AB because, Class C used part of the input signal to turn on and for this reason Class C will never pull out the load presented to Class AB for peak efficiency. To achieve the maximum output power and overall performance, one solution is to supply more input power to Class C amplifier than Class AB. With this one should be able to achieve maximum output power without creating AM-AM distortion

The operation of this design was strongly influenced by the coupling factor of the splitter, biasing of class AB and C amplifiers. The achieved results of the proposed design process have shown an excellent efficiency and power performances.

ACKNOWLEDGMENT

I would like to acknowledge WWRF for the grant; many thanks go to Dr. Angeliki Alexiou, Dr. Vino Vinodrai, Lisbete Simões, and Paulo Gonçalves of IT-Portugal. I would also like to acknowledge C2POWER project (FP7/2007-2013) under the European Community, funded through the Seventh Framework programme (project n. 248577).

REFERENCES

[1] The W. H. Doherty, "A New High Efficiency Power Amplifier for Modulated Wave", Proc. IRE, Vol. 24, No. 9, PP. 1163– 1182, September, 1936.

[2] F. H. Raab, "Efficiency of Doherty RF Power Amplifier System", IEEE Trans. Broadcasting, Vol. BC-33, No 3, PP. 77-83, September, 1987.

[3] S.C. Cripps, Advanced Techniques in RF Power Amplifier Design,Norwood, MA: Artech House, 2002.

[4] S.C.Cripps, RF Power Amplifier for Wireless Communications, Norwood, MA: Artech House, 1999.

[5] A. S. Huusaini, R. Abd-Alhameed, J. Rodriguez, "Implementation of Efficiency Enhancement Techniques in the Linear Region of Operations of Power Amplifier", IT 7th Conference on Telecommunications, No 103, PP. 105 – 108, May, 2009.

[6] Abubakar Sadiq Hussaini, Bashir A. L. Gwandu, Raed Abd-Alhameed, Jonathan Rodriguez, "Design of Power Efficient Power Amplifier for B3G Base Stations", 9th International Symposium on Electronics and Telecommunications (ISETC 2010) , Timisoara, Romania 11-12 November 2010, Paper No. 103, pp. 89-92, ISBN: 978-1-4244-8458-4

[7] Abubakar Sadiq Hussaini, R. Abd-Alhameed, J. Rodriguez, "Green Radio: Approach Towards Energy Efficient Power Amplifier for 4G Communications", Proc. of the 25th WWRF Meeting, Kingston-upon-Thames, UK, 16th-18th November 2010.

[8] Abubakar Sadiq Hussaini, Raed Abd-Alhameed, Jonathan Rodriguez, "Design of Energy Efficient Power Amplifier for 4G User Terminals", 17th IEEE International Conference on Electronics, Circuits, and Systems (ICECS 2010), Athens, Greece 12-15 December 2010, Paper No. 533, pp. 617-620, ISBN: 978-1-4244-8156-9

[9] C. T. Burns, A. Chang, D. W. Runton, "A 900 MHz, 500 W Doherty power amplifier using optimized output matched Si LDMOS power transistors", IEEE MTT-S Int. Microw. Theory Tech., Symp. Dig., PP. 1557 – 1580, June, 2007.

[10] Raab F.H., Asbeck P., Cripps S., Kenington P.B., Popovic Z.B., Pothecary N., Sevic J.F., Sokal N.O., "Power amplifiers and transmitters for RF and microwave", IEEE Transactions on Microwave Theory and Techniques, Vol. 50, No 3, PP. 814 – 826, March, 2002.

[11] K. J. Cho, J-H. Kim, and S. P. Stapleton, "A Highly Efficient Doherty Feed-Forward Linear Power Amplifier for W-CDMA Base-Station Applications," IEEE Trans. on MTT, Vol. 53, pp. 292 - 300, Jan. 2005.J. Groe, "Polar transmitters for wireless communications", IEEE Communications Mag., Vol. 45, No 9, PP. 58 – 63, Sept. 2007.

[12] P. B. Kenington, High- Linearity RF Amplifier Design, Norwood, MA: Artech House, 2000.

[13] C. F. Campbell, "A fully integrated Ku-band Doherty amplifier MMIC," IEEE Microw. Wireless Compon. Lett., vol. 9, no. 3, pp. 114–116, Mar. 1999.

Abubakar Sadiq Hussaini (S'05) Research Scientist / PhD in view: Instituto de Telecomunicações - Pólo de Aveiro / University of Bradford, United Kingdom; MSc in Radio Frequency Communication Engineering, University of Bradford, United Kingdom, 2007; Post Graduate in Electrical/Electronic Engineering, Bayero University, Kano, Nigeria 2003; Specialization in Microwave/RF power amplifiers design and Tunable Filters.

Technical Education: SDH Network Configuration Siemens (Information and Communication Network Training Institution Siemens), 2002; Telecomm Engineer, Nigerian Telecommunications Limited, Abuja, 2000; where I was responsible for the operations and maintenance of SRT 1F, SRT 1S, SRT 1 (Siemens Radio), Planning and implementing the provision and utilization of microwave radio transmission systems. Contribute article to numerous publications.

Award: Best Student, Newton Institute, Jos, 1993; Nominated in the 26th Edition of Who's Who in the World 2009; Member: Senate Committee of the University of Bradford-2007, IEEE, IET, Optical Society of America (OSA); Involved in European and CELTIC research projects. His research interests include Radio Frequency System Design and High-Performance RF-MEMS Tunable Filters with specific emphasis on energy efficiency and linearity.

Achievements: participation in process to produce energy efficient Power Amplifier at 3.5GHz (Mobile WiMAX Frequency); Designed and developed "Radio over Fiber" Optical transmitter and Optical Receiver (1550nm Wavelength) where radio over fiber technology in which the frequency limitations of quantum well lasers in direct RF to Light transponding was investigated.

Dr Bashir Gwandu is the Executive Commissioner (Technical Services) of the Nigerian Communications Commission (NCC) and was the Acting Vice Chairman/CEO of the NCC from June to July 2010. After receiving his BSc in Physics from Usman Danfodiyo University, Sokoto and an MSc in Applied Physics from the University of Jos, in addition to a brief Engineering service at the Tactical Air-command, Makurdi and lecturing at Usman Danfodiyo University, Sokoto, he proceeded to the United Kingdom where he attended MSc Courses in Power Electronics and Drives and MSc courses in Communications Engineering; he further obtained an MPhil degree in Electrical/Electronic Engineering, all from the University of Birmingham. He returned briefly to Usman Danfodiyo University, Sokoto to lecture before going back to the UK to study for a PhD in Electronic/Electrical Engineering at Aston University and subsequently undertook an MBA Finance course at the Birmingham Business School.

Dr Gwandu was the Head, Physics Department of Usman Danfodiyo University until December 1991. He has designed many devices that are used in the telecom industry some of which have been patented in Europe and United States. He is a Chartered Electrical Engineer, and a full member of the 3 main International Electrical Engineering Institutes, i.e. The IEE UK, IEEE USA, and IEICE Japan and has published over 36 Electronic and Electrical Engineering Research papers in world-class Electrical Engineering journals and conference proceedings. Since 2002, Dr Bashir Gwandu has been involved in research work on Regulation of Utilities. He was also one of the engineers invited as part of the Institution of Electrical Engineers (IEE) team to outline policy issues for the UK Energy White-paper. He was also a regular contributor to IEE/Ofcom consultation on spectrum management issues.

Dr Gwandu is currently the Executive Commissioner for Engineering and Technical Standards at the Nigerian Communications Commission (NCC); supervising Spectrum planning and management, Quality of Service Monitoring and Network Optimization, Equipment Type-approval, Numbering Plan, Allocation and Management. He was the Executive Commissioner in Charge of Licensing and Consumer Affairs of the NCC until Jun 07. Dr Gwandu was part of the Launch Committee of the recently Launched Nigerian Communications Satellite (NigComsat-1), has represented Nigeria in many Forums on Telecoms Regulations, and was until recently on the Board of the NigComSat Ltd, and the Board of Digital Bridge Institute. Dr Gwandu having skills in diverse areas of Engineering, Accounting, Finance, the Art of Regulation and Administration; the key competences required of a utility regulator, is currently on the Board of NCC.

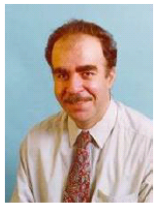

Professor Raed A. Abd-Alhameed received his PhD from Electrical and Electronic Engineering, Bradford University, UK, in 1997. From 1997 to 1999 he was a Postdoctoral Research Fellow at the University of Bradford, specialisation in computational modelling of electromagnetic field problems, microwave nonlinear circuit simulation, signal processing of preadaption filters for adaptive antenna arrays and simulation of active inductance. From 2000 to 2003 he has been a lecturer in the University of Bradford. In August 2003 he was appointed as a senior lecturer in applied Electromagnetics and then Sept 2005 to a Reader in Radio Frequency Engineering at the same

University. Since Nov 2007 he was appointed as Professor of Electromagnetics and Radio Frequency Engineering in the school of Engineering, Design and technology, Bradford University. Abd-Alhameed is the Director of Mobile and Satellite Communications Research Centre, Leader of Communications Research group, and the head of the Radio Frequency, Antennas, Propagations and Computational Electromagnetiscs Research group including his appointment as a research visitor for Wrexham University, Wales, UK since 2009. He has worked on several funded projects from EPSRC, Dept. of Health, Mobile Telecommunications and Health Research Programme, EU FP5 and a number of industrial KTPs. He has published over 300 technical Journal and Conference papers including several book chapters. In addition, he holds two patents work on RF antenna designs. He has invited as keynote speaker for ITA 09, Mobimedia 2010, and he chaired the 1st EERT 2010 workshop and several sessions at many international conferences. He is also appointed as guest editor for IET SMT Journal special issue on EERT for 2011. In addition, he is invited to several IEEE, IET and International Journals for his successful research in radio frequency engineering. His current research interests include hybrid electromagnetic computational techniques, EMC, antenna design, low SAR antennas for mobile handset, bioelectromagnetics, RF mixers, active antennas and MIMO antenna systems. Prof Abd-Alhameed is Fellow of the Institution of Engineering and Technology, a Chartered Engineers and Fellow of Higher Education Academy.

Jonathan Rodriguez (M' 04) received his Masters degree in Electronic and Electrical Engineering and Ph.D from the University of Surrey (UK), in 1998 and 2004 respectively. In 2002, he became a Research Fellow at the Centre for Communication Systems Research at Surrey and responsible for managing the system level research component in the IST MATRICE, 4MORE and MAGNET projects. Since 2005, he is a Senior Researcher at the Instituto de Telecomunicações, Pólo de Aveiro (Portugal), where he is the project coordinator for the C2POWER project, technical manager of COGEU and technical workpackage leader in WHERE, HURRICANE, PEACE and MOBILIA. He was also the project coordinator of the Celtic LOOP Project. He is leading the 4TELL Wireless Communication Research Team at IT, author of several conference and journal publications, and has carried out consultancy for major manufacturers participating in DVB-T/H and HS-UPA standardisation. His research interests include Radio Access Networks for current and beyond3G systems with specific emphasis on Radio Resource Management, Digital Signal Processing and PHY/MAC optimization strategies.

Optimum Design of Doherty RFPA for Mobile WiMAX Base Stations.

Abubakar Sadiq Hussaini[1], Tahereh Sadeghpour[2], Raed Abd-Alhameed[2], Mark B. Child[2], N. T Ali[3] and Jonathan Rodriguez[1].

[1]Instituto de Telecomunicações – Aveiro, Portugal.
[2]Mobile & Satellite Communications Research Centre, University of Bradford, Bradford, United Kingdom, BD7 1DP.
[3]Khalifa University, Sharjah, PO Box 573, United Arab Emirates.
{ash,jonathan}@av.it.pt
{tsadeghp,r.a.a.abd,m.b.child}@bradford.ac.uk
{ntali}@kustar.ac.ae

Abstract. RF power amplifiers in mobile WiMAX transceivers operate in an inherently nonlinear manner. It is possible to amplify the signal in the linear region, and avoid distortion, using output power back-off; however, this approach may suffer significant reduction in efficiency and power output. This paper investigates the use of Doherty techniques instead of back-off, to simultaneously achieve good efficiency and acceptable linearity. A 3.5 GHz Doherty RFPA has been designed and optimized using a large signal model simulation of the active device, and performance analysis under different drive levels. However, the Doherty EVM is generally poor for mobile WiMAX. Linearity may be improved by further digital pre-distortion, and a simple pre-distortion method using forward and reverse AM-AM and AM-PM modeling. Measurements on the realized amplifier show that this approach satisfies the EVM requirements for WiMAX base stations. It exhibits a PAE over 60%, and increases the maximum linear output power to 43 dB_m, whilst improving the EVM.

Keywords: Doherty, RFPA, linearity, digital pre-distortion, OFDM.

1 Introduction

A linear power amplifier (PA) with a high efficiency across a wide range of output power is very important for mobile WiMAX, and general mobile applications that utilize power control. The PA should also have acceptable linearity with respect to a non-constant envelope signal. This is due to the fact that when amplifying such a signal, a nonlinear PA might cause and generate distortion, dramatically affecting the

dynamic range of the system dominated by the maximum signal levels [1]. The resulting output signal might be combined by the intermodulation distortion (IMD). This would be undesirable since it falls in-band, and typically in adjacent channels.
Mobile WiMAX adopts Orthogonal Frequency Division Multiplexing (OFDM), with modulations from QPSK to 64-QAM, and has crest factor around 9dB-12dB. This wideband digital modulation scheme offers high data rates and has resilience to multipath effects. However, the scheme is critically dependent on linearity in the hardware system due to its inherently high crest factor [2]. Mobile WiMAX strives to reach a 100Mbps data rate. To support the proposed data services, the base station and the user terminal itself must be able to handle higher data rates. Achieving high efficiency and good linearity simultaneously in power amplifier design are the most challenging task. The error vector magnitude (EVM) is critical for a given rated output power. This indicates which PA is capable of meeting the system requirements. Mobile WiMAX power amplifiers must not exceed 5% EVM for 16-QAM and 2.5% for 64QAM OFDM modulation. There are ten frequency bands defined in the WiMAX standard, the 3.5 GHz band being the most common in Europe, this band has a range of frequency from 3.4GHz to 3.6GHz (Uplink: 3400MHz – 3500MHz, Downlink: 3500MHz – 3600MHz).

In this paper, the performance of a Doherty amplifier is investigated and discussed in terms the coupling factor of the input splitter, the gate bias voltage, and the adjustment of output matching of the peaking amplifier. This adjustment was introduced by using an extra quarter wavelength section of transmission line. The gate bias and the output matching of the peaking amplifier are optimized. The peaking amplifier allows the Doherty amplifier to respond to the high input levels of short duration, by amplifying the signal peaks, and to dynamically change the load impedance of the main amplifier. For linearity a baseband digital pre-distorter has been applied. Results in terms of efficiency and linearity have been achieved.

2 Mobile WiMAX: linearity and output power requirements.

The envelope variation of an OFDM signal clearly requires a linear RFPA. It should be noted that the IEEE 802.16e/Mobile WiMAX standard doesn't specify the minimal required intermodulation distortion (IMD) of the user terminal PA, but it uses system level requirement to describe the maximal allowable distortion. These system level requirements are: Spectral Mask (SM) and Error Vector Magnitude (EVM) [3], [4]. The spectral mask is specified at the PA output, and ensures that the user terminal transmitter does not corrupt or block the spectrum from adjacent channels. The error vector (E(s)) is the difference between the actual transmitted (A(s)) and ideal (H(s)) constellation point. EVM is specified after reception and demodulation by an ideal receiver and ensures a correct transmission within the channel. The EVM of a symbol S is defined as,

$$EVM = \sqrt{\frac{|E(s)|^2}{\frac{1}{N}\sum_S |H(s)|^2}}$$

To obtain EVM as a percentage, the RMS value is used, this is a useful systems level figure of merit for the accuracy of the OFDM signal,

$$EVM(\%) = \sqrt{\frac{P_{error}}{P_{ref}}} \cdot 100\%$$

where P_{error} is the RMS power of the error vector, and P_{ref} is the power of the outermost point in the reference constellation. The spectral mask and EVM targets for mobile WiMAX comparatively rigorous among existing standards.

3 Doherty RF PA design for Mobile WiMAX.

This section explored the Doherty configurations. In 1936 W.H Doherty, from Bell Telephone Laboratories Inc, proposed the high efficiency power Amplifier called Doherty Amplifier [5]. The concept of the Doherty power amplifier configuration, have narrated in our previous paper [6], involves the use of two or more power amplifiers and the quarter wave transmission line coupler or impedance inverting network. The resultant linear power amplifier achieves a higher efficiency at the outputs below peak output power (PEP) than conventional class B linear power amplifier [7], [8]. The basic block diagram of this kind of amplifier can be seen in Fig.1.

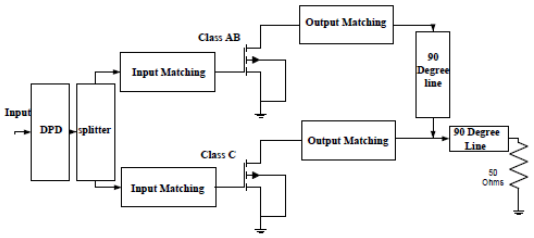

Fig. 1 Block diagram of a mobile WiMAX Doherty power amplifier

The Doherty PA configuration was introduced at Bell Labs in 1936 [5], and has received fresh attention in modern radio design. The Doherty approach uses two or more PA and a quarter wave transmission line coupler, or impedance inverter, as shown in Fig. 1. The resulting sub-system is capable of achieving a higher efficiency at the outputs below the peak output power than a conventional Class B PA [6].

The Doherty PA in this study uses the load modulation technique, and the linearity was enforced by further digital pre-distortion. The Freescale N-channel Enhancement-Mode Lateral MOSFET MRF7S38010HR3 was used throughout. The dynamic load adaptation is provided by a 50Ω transmission line impedance inverter, the passive sub-system also includes a 90° hybrid splitter. The design also includes the optimized bias and class of operation for the carrier and peaking amplifiers, this was obtained from a large signal harmonic balance analysis. The bias condition for the Class AB carrier amplifier are V_{gs} = 3.0V (I_{ds} =300 mA), and for the Class C peaking amplifier, V_{gs} = 2.4V (I_{ds} = 1 mA). Both of the amplifiers use the same drain voltage (30V). The performance of this design is strongly influenced by the coupling factor of the hybrid splitter, and the Class AB and Class C biasing. Furthermore, the turn–on of the class C amplifier was dependent on the gate bias voltage, and the input signal, which in turn fixes the low efficiency and peak values of the configuration.

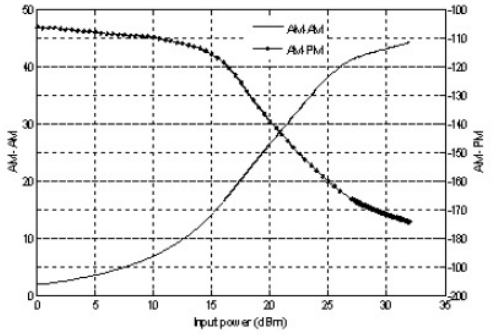

Fig. 2 AM/AM and AM/PM characteristics

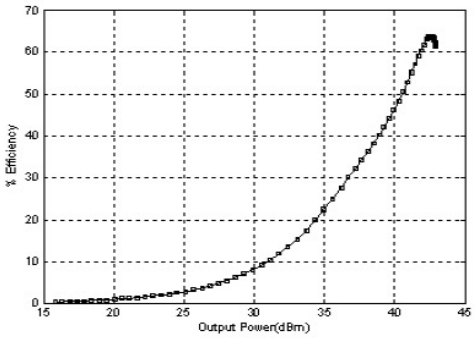

Fig. 3 % Efficiency of Doherty PA

The amplifier has been tested with one tone test characterizing the AM-AM and AM-PM responses (Fig. 2), two tone test, and 802.16e signal (10MHz bandwidth 16-QAM OFDM modulation signal and crest factor of 10dB). Comparing with a conventional Class AB design, there is an improvement from 20% to 25% efficiency; and the

design is capable of delivering 15 W of RF power with a 60% workable efficiency. The IMR[1] value is -22.5 dB for IMD3 and -40 dB for IMD5 (for the 1 dB compression point), the input and output IP3 values are 26 dBm and 46 dBm, respectively.

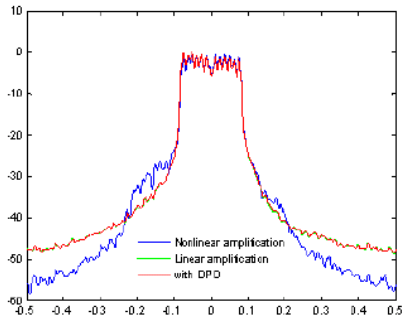

Fig. 4 Nonlinear amplification of OFDM signal

The nonlinear amplification of OFDM signal is given in Figure 4. Spectral re-growth is observed as the result of nonlinearity. The improvement of the linearity has been achieved by means of baseband digital pre-distortion, where the multicarrier input signal is pre-distorted in such a manner that the overall system becomes approximately linear. Figure 4 shows the measurement performance of amplification of an 802.16e signal in an OFDM power amplifier applying the pre-distortion. For two-tone excitation, the Doherty amplifier showed both better ACPR and PAE at the same time than the conventional class AB type amplifier. An ACPR performance of -40dBc was achieved using this pre-distortion method. This results show that the Doherty power amplifier and digital pre-distortion method can be a promising combination to enhance the efficiency and linearity for 4G communication systems.

4 Conclusions.

The results show that the implementation of a Doherty configuration can provide efficient RF power transmission. It demonstrates a significant improvement in power added efficiency (PAE) in the low power region, compared to a traditional design. It has exhibited a PAE of 60% for 15 W output power, and by applying a digital pre-distorter, the maximum output power EVM has improved. The operation of this design was strongly influenced by the coupling factor of the splitter, and biasing of the Class AB/C amplifiers. In addition, the turn–on of the class C amplifier depends on the gate bias voltage and the input signal. The self-managing characteristic of the Doherty amplifier has made its implementation more attractive.

[1] The difference between the fundamental power (dBm) and the IMD power (dBm).

Acknowledgement

The Instituto de Telecomunicações (Aveiro) contribution to this work has been supported through the Eureka Celtic Framework, under Mobilia Contract CP5-016.

References

1. S.C. Cripps, Advanced Techniques in RF Power Amplifier Design, Norwood, MA: Artech House, 2002.

2. Tahereh Sadeghpour, Abubakar S. Hussaini, Ayaz Ghorbani, Raed Abd-Alhameed, Jonathan Rodriguez, "Behavioral Modeling and Compensation Procedure of OFDM Transmitters", 9th IEEE Malaysia International Conference on Communications (MICC 2009), Kuala Lumpur, Malaysia, 14 – 17 December, 2009.

3. J. Groe, "Polar transmitters for wireless communications", IEEE Communications Mag., Vol. 45, No 9, PP. 58 – 63, Sept. 2007.

4. P. B. Kenington, High- Linearity RF Amplifier Design, Norwood, MA: Artech House, 2000.

5. W. H. Doherty, "A New High Efficiency Power Amplifier for Modulated Wave", Proc. IRE, Vol. 24, No. 9, PP. 1163– 1182, September, 1936.

6. A. S. Huusaini, R. Abd-Alhameed, J. Rodriguez, "Implementation of Efficiency Enhancement Techniques in the Linear Region of Operations of Power Amplifier", IT 7th Conference on Telecommunications, No 103, PP. 105 – 108, May, 2009.

7. F. H. Raab, "Efficiency of Doherty RF Power Amplifier System", IEEE Trans. Broadcasting, Vol. BC-33, No 3, PP. 77-83, September, 1987.

8. C. T. Burns, A. Chang, and D. W. Runton, "A 900 MHz, 500 W Doherty power amplifier using optimized output matched Si LDMOS power transistors", IEEE MTT-S Int. Microw. Theory Tech., Symp. Dig., PP. 1557 – 1580, June, 2007.

Tunable RF Filters: survey and beyond

Abubakar Sadiq Hussaini[#*], Raed Abd-Alhameed[#], Jonathan Rodriguez[*]
[#]School of Engineering, Design and Technology, University of Bradford, UK
[*]Instituto de Telecomunicações, Aveiro, Portugal
ash@av.it.pt, r.a.a.abd@brad.ac.uk, jonathan@av.it.pt

Abstract—**Without a holistic design and fabrication approach, future wireless communication devices would be extremely large in size to accommodate multiple radio access technologies (RATs) compared to today's more conventional mono-mode devices. Typically multiple RAT devices will be comprised of multiple RF power amplifiers, low noise amplifiers (LNA), RF band pass filters, modulators and demodulators; one for each wireless technology. Obviously, this will increase the complexity of the circuit design and will cover a large part of the circuit space leading to power hungry devices. Radio frequency microelectromechanical systems (RF-MEMS) can be good candidate for innovative RF front end devices since it is reconfigurable features in nature therefore allowing a reduction in the number of external components in a single device for the use of multiple RATs. This paper discusses the history, state of the art of tunable RF filter and beyond..**

Keywords- RF MEMS filter; yttrium-iron-garnet (YIG) filter; barium strontium titanate (BST) filter; varactor filter

I. INTRODUCTION

The future mobile multimedia handset and base station devices will accommodate multiple wireless standards (2G, 2.5G, 3G, WiMAX, Mobile WiMAX, LTE, and LTE-A). This will require multiple RF power amplifiers, low noise amplifiers (LNAs), RF band pass filters, modulators and demodulators since all of these standards work on different frequency bands. If we were to upgrade this mobile devices to support future standards, this indeed would entail adding another set of customized RF front end devices leading to extra complexity and power consumption. If were not to take any preventive measure towards reducing energy consumption on the mobile device, this means that users could eventually fall victim to the energy trap: users will be restricted to the nearest power socket instead of having the flexibility to roam freely between different networks. Therefore, future design requirements dictate the need for reconfigure handsets so as to reduce the number of duplicated circuits, and hence the energy consumption, and from a business perspective, to introduce the handsets to the market at a very low cost. Therefore the design process requires a reconfigurable/tunable RF front end structural design with high energy efficiency, high tuning speed, and excellent linearity that have to deal with the wide frequency range, low loss/or high-Q circuits. Therefore tunable power amplifiers, tunable antennas, tunable band pass filters, and tunable matching networks are the key building blocks for reconfigurable RF front-end systems.

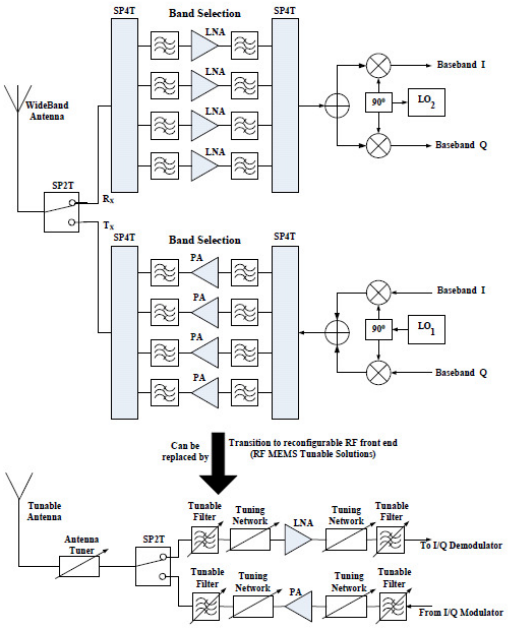

Figure 1. Block diagrams of multi-standard wireless systems showing the transistion to reconfigurable solutions

The aim of this paper is to provide a survey on tunable RF filters, and to identify the path ahead with applications towards beyond 3G multimode devices. In the last decades, several tuning techniques have been developed to design tunable filters, including electrical, mechanical, and magnetic tuning techniques. However, among those techniques, only mechanical techniques provide enhanced quality factor, good linearity, very good power handling capability, and excellent insertion loss, but their drawbacks are bulky in size and very low tuning speed. Mechanical tunable filters have been used since the development of radar, but because they are very big in size and low tuning speed, their applications were somewhat restricted. In the past towards the present moment, several approaches and technologies have been considered to realize RF tunable filters for wireless communication systems

978-1-4577-1846-5/11/$26.00 ©2011 IEEE

applications, such as Yttrium-Iron-Garnet (YIG) filters, Barium Strontium Titanate (BST) filters, Varactors filters, and RF MEMS filters. Most of them have limiting factors such as power handling capability (power consumption), nonlinearities, size, tuning speed, and weight. An exception are the RF MEMS filters which have good linearity, low power consumption, size reduction, and also have high level of integration.

II. Yttrium-Iron-Garnet (YIG) Filters

Yttrium-Iron-Garnet (YIG) filters, was first developed in 1958 for military radar communications and tracking receivers [1]. Their resonators contain crystal Yttrium-Iron-Garnet (YIG). Yttrium-Iron-Garnet (YIG) is a ferrimagnetic material which contain sort of synthetic garnet, their chemical composition is $Y3Fe2(FeO_4)_3$, or $Y_3Fe_5O_1$. These are substance materials, which the YIG filter resonator depend on, and allow it to act as a tunable filter [1-5]. This filter has high Q factor, which is roughly around 10,000, has high performance with excellent linearity and low loss; however, it is normally applicable to the range of frequency between 0.5GHz to 40GHz. The tuning of this type of filter is accomplished by varying the current of magnetic bias applied to a resonator that is an integral part of the YIG filter. The resonance frequency is directly proportional to the force of the applied magnetic field.

Like silicon crystal, YIG crystal is in the form of cubed like shapes and normally was normally placed inside a tumbler to shape the YIG cube shape into sphere shape. This would obtain uniform coupling in a resonator circuit which allow the current to generate magnetic field, and also for the magnetic field to generate current [2]. Figure 1 shows a typical coupling of YIG band pass filter. This type of filter have been use in Radar communication, but it's size, weight, power consumption, and tuning speed are the factors that limit it's use in mobile communications devices.

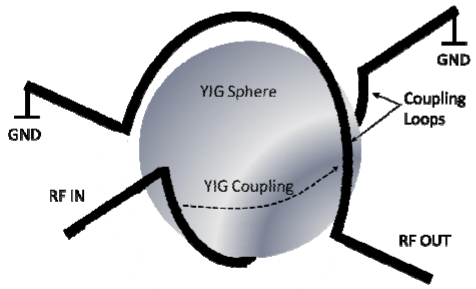

Figure 2. Single stage bandpass filter coupling structure (courtesy of Micro lambda wireless, Inc)

III. Barium Strontium Titanate (BST) Filters

Barium Strontium Titanate (BST) tunable filter, is a another form of tunable filter that uses barium strontium titanate thin films material with chemical composition of (Ba0.6Sr0.4)TiO3 for tuning devices [6]. It has a dependent electric field permittivity that enables it's use as a tunable dielectric constant in a voltage tunable capacitor or varactor. Barium strontium titanate is one of the two most popular types of ferroelectrics thin films, and is the best amongst the two in terms of integration with CMOS active devices, and exhibits high tunability at room temperature. While the second type of thin films is Strntium Titante (STO) and has the chemical composition (SrTiO3), that exhibits very little tunability at room temperature and is very difficult to integrate with system active devices [7]. BST has a very good power handling capability, has a high Q-factor, and allow the fabrication of several parts simultaneously.

BST is a complex dielectric material though it has the ability to hold a large amount of electrical charge due to its high dielectric constant, and also has the ability to change the dielectric constant with applied DC voltage [8]. The material makes a structure phase change at a certain Curie temperature from paraelectric phase (polar phase) to ferroelectric phase (nonpolar phase), which are the two phases of operations of ferroelectric thin film tunable capacitors. However, in the paraelectric phase, which is the nonpolar phase, allows a 2-5V DC bias of the electrically tunable capacitor, and also maintains a very large dielectric constant (approximately 300) , and tunability with applied electric field. The BST capacitors are suitable for high power, but have a very poor linearity. The nonlinearity and cost of the capacitor, and associated difficulty in producing high-quality thin films are the biggest factors that limits its use in mobile communications.

IV. Varactor Filters

This is an electrical tunable filter, which is used as a special PN junction diode called a varactor diode or variable capacitance diode [9-11]. Every PN junction diode has a depletion region and the width depends on applied voltage. When the PN junction diode is forward bias the width of the depletion get smaller, and when it has reverse bias the width of the depletion region get wider. Once the reverse bias voltage is applied to the PN junction diode no current will flow, and the reverse resistance is almost infinity acting as a capacitance. With the reverse bias voltage, the width of depletion region will increase and thus decreasing in capacitance. This is what makes it a special diode, since the capacitance can be controlled depending on the reverse bias voltage. As the magnitude of the reverse bias voltage increases the capacitance decreases. This is the properties of varactor diode whose variations between maximum to minimal is significant, the capacitance of the varactor diode has been designed to vary with applied voltage. The tuning of the filter is achieved by changing the bias of the varactor diode. The varactor filters have very high tuning speed and very small in size, making it a better choice over the conventional YIG and BTS, for integrated RF front ends in wireless communication

devices. There's another diode which has similar characteristics to the varactor diode called the schottky diode, whose capacitance variations between maximum to minimal is significant, and has a delay time of the order of nanaseconds. The schottky diode is not a semiconductor silicon diode like the varactor, it is metal and semiconductor in nature and has a forward bias voltage which varies from 0.1V to 0.3V. The Schottky diode will start conducting much earlier than the varactor diode since it has a smaller cutting voltage than the varactor diode, which varies from 0.5V to O.7V. The schottky diode is closer to the ideal diode in the forward characteristics than the varactor and conventional diode. Figure 3, represents the characteristics of the two special diodes in comparison to the conventional diode, and clearly shows that the capacitance variations between maximum to minimal of the schottky and varactors diodes are significant, as the magnitude of the reverse bias voltage increases. However, both schottky and varactor diodes are highly non-linear, have poor power handling capabilities and low Q factor at high frequencies, making them difficult for use in future mobile handsets. Though there's a lot of ongoing research towards how to model the non-linearity and how to increase the Q factor.

Future mobile handsets will become more sophisticated, providing user centric broadband applications and full mobility within a plethora of wireless access systems. This will lead to power hungry devices and towards a reduction in battery lifetime< and eventually having a global impact on the of CO2 footprint. Therefore, the varactor diode is not a key enabling technology for a reconfigurable radio front ends that promises to deliver new paradigms in RF system design.

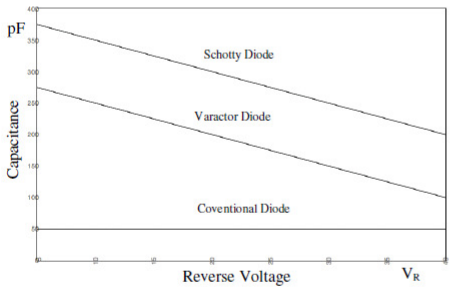

Figure 3. Capacitance verses reverse voltage

V. RF MEMS FILTERS

MEMS or micro-electro-mechanical systems (a.ka. microsystems technology or micromachines), are electrical-mechanical devices, which are made from micro fabrication and was first developed in the 1970s [12-28]. There are several applications of MEMS; they include biotechnology, medicine, communication and inertial sensing. However, this paper discusses the application of MEMS in communication and one such application is the RF filter, which is called RF MEMS filter. RF MEMS or Radio frequency micro-electro-mechanical systems mean the design and fabrication of micro-electro-mechanical systems for radio frequency IC circuits. Unlike conventional RF filter, RF MEMS filters depend also on the mechanical properties and can be integrated and fabricated in batch directly.

RF MEMS filters are designed using RF MEMS components (RF MEMS capacitors) and are classified according to their actuation method (piezoelectric, electro-thermal, electro-static, magneto-static), clamp configuration (fixed-fixed beam, cantilever), circuit configuration (series, shunt), axis of deflection (vertical, lateral) and contact interface (ohmic, capacitive) [12]. The tuning of the RF MEMS filter is achieved with variable MEMS capacitor and its capacitance value is able to change with applied dc voltage.

RF-MEMS is a key enabling technology for reconfigurable radio frequency front ends that promises to enable new paradigms in radio frequency system, due to its superior functionality, integration and performance. RF MEMS have very good linearity, low power consumption, size reduction, and have a high integration-level. The challenges facing RF MEMS technology is regarding the fabrication and packaging of RF MEMS filters. The RF MEMS filters fabrication process requires the ability to deposit thin films of material on a substrate, which will start by wafers, deposition, lithography, etching and lastly to have a full fabricated chip.

VI. CONCLUSION

This paper provided a survey on tunable RF filters and beyond. In order to realize a multi-standard RF front end transceiver requires a customized RF device that includes power amplifiers, low noise amplifiers, band pass filters to be integrated for each standard in order to cover all the different frequency bands. However, using conventional RF design processes, this would lead to hot and power hungry mobile devices. Therefore, there is a need for reconfigurable handsets in order to reduce the number of duplicated circuits, and to be able to introduce the handets to the market at low cost. Furthermore, it is a necessity that the reconfigurable/tunable RF front end structural design has high energy efficiency, high tuning speed, and excellent linearity that have to deal with the wide frequency range, and low loss/or high-Q circuits. The paper discussed several approaches and technologies for RF tunable filters such as Yttrium-Iron-Garnet (YIG) filters, Barium Strontium Titanate (BST) filters, Varactors filters, and RF MEMS filters. Most of them have limiting factors such as power handling capability (power consumption), nonlinearities, size, tuning speed, and weight. An exception are the RF MEMS filters which have good linearity, low power consumption, size reduction, and support a have high level of integration.

ACKNOWLEDGMENT

This research has received funding from the European Community's Seventh Framework Programme ARTEMOS project under work programme ENIAC JU 2010 and FCT (Fundação para a Ciência e Tecnologia).

REFERENCES

[1] J. Helszajn, YIG Resonators & Filters, John Wiley & Sons New York: 1985.

[2] YIG Tuned Filters, Micro Lambda Inc., Fremont, CA, USA.

[3] W. J. Keane, "YIG filters aid wide open receivers," Microwave J., vol. 17, no. 8, Sept. 1980.

[4] H. Tanbakuchi et al, "A broadband tracking YIG-tuned mixer for a state of the art spectrum analyzer" European Microwave Conference Dig., pp. 482-490, Sept. 1987.

[5] R. F. Fjerstad, "Some design considerations and realizations of iris-coupled YIG-tuned filters in the 12-40 ghz region," IEEE Trans. Microwave Theory Tech, vol. 18, pp. 205–212, Apr. 1970.

[6] A. Tombak, J.-P. Maria, F. T. Ayguavives, Z. Jin, G. T. Stauf, A. I. Kingon, and A. Mortazawi, "Voltage-controlled RF filters employing thin-film barium-strontium-titanate tunable capacitors," IEEE Trans. Microwave Theory & Tech., vol. 51, no. 2, pp. 462–467, Feb. 2003.

[7] B. H. Moekley and Y. Zhang, "Struntium titanate thin films for tunable Y Ba2Cu3O7 microwave filters," IEEE Trans. Appl. Superconduct., vol. 11, pp. 450–453, Mar. 2001.

[8] www.ngimat.com/pdfs/RF_Wireless_Tunable_Filters.pdf

[9] S. R. Chandler, I. C. Hunter, and J. C. Gardiner,"Active varactor tunable bandpass filters," IEEE Microwave Guided Wave Lett., vol. 3, pp. 70-71, March 1993.

[10] A. R. Brown and G. M. Rebeiz, "A varactor-tuned RF filter," IEEE Trans. Microwave Theory & Tech., vol. 48, no. 7, pp. 1157–1160, July 2000.

[11] I. C. Hunter and J. D. Rhodes, "Electronically tunable microwave bandpass filters," IEEE Trans. Microwave Theory & Tech., vol. 30, no. 9, pp. 1354–1360, Sept. 1982.

[12] G. M. Rebeiz, RF MEMS Theory, Design, and Technology.New York, USA: Wiley, 2003.

[13] K. Entesari and G. M. Rebeiz, "A differential 4-bit 6.5-10 GHz RF MEMS tunable filter," IEEE Trans. Microwave Theory & Tech., vol. 53, no. 3, pp. 1103–1110, Mar. 2005.

[14] L. Dussopt and G. M. Rebeiz, "Intermodulation distortion and power handling in RF MEMS switches, varators, and tunable filters," IEEE Trans. Microwave Theory & Tech., vol. 51, no. 4, pp. 1247–1256, Apr. 2003.

[15] L. Dussopt and G. M. Rebeiz, "High-Q millimeter-wave MEMS varactors," IEEE MTT-S Int. Microwave Symp. Dig., pp. 1205–1208, June 2000.

[16] A. Pothier, J.-C. Orlianges, G. Zheng, C. Champeaux, A. Catherinot, P. B. D. Cros, and J. Papapolymerou, "Low-loss 2-bit tunable bandpass filters using MEMS DC contact switches," IEEE Trans. Microwave Theory & Tech., vol. 53, no. 1, pp. 354–360, Jan. 2005.

[17] J.-M. Kim, S. Lee, J.-H. Park, J.-M. Kim, C.-W. Baek, Y. Kwon, and Y.-K. Kim, "Dig- itally frequency-controllable dual-band WLAN filters using micromachined frequency- tuning elements," in 19th IEEE MEMS 2006 Conf., Istanbul, Turkey, Jan. 2006, pp. 158–161.

[18] S. Duffy, C. Bozler, S. Rabe, J. Knecht, L. Travis, P. Wyatt, C. Keast, and M. Gouker, "MEMS microswitches for reconfigurable microwave circuitry," IEEE Microw. Wireless Compon. Lett., vol. 11, no. 3, pp. 106–108, Mar. 2001.

[19] R. M. Young, J. D. Adam, C. R. Vale, T. T. Braggins, S. V. Krishnaswamy, C. E. Milton, D. W. Bever, L. G. Chorosinski, L.-S. Chen, D. E. Crockett, C. B. Freidhoff, S. H. Talisa, E. Capelle, R. Tranchini, J. R. Fende, J. M. Lorthioir, and A. R. Tories, "Low-loss bandpass RF filter using MEMS capacitance switches to achieve a one-octave tuning range and independently variable bandwidth," in IEEE MTT-S International Microwave Symposium Digest, Philadelphia, PA, June 2003, pp. 1781–1784.

[20] A. Grichener, B. Lakshminarayanan, and G. M. Rebeiz, "High-Q RF MEMS capacitor with digital/analog tuning capabilities," IEEE MTT-S Int. Microwave Symp. Dig., June 2008.

[21] H. Joshi, H. H. Sigmarsson, D. Peroulis, and W. J. Chappell, "Highly loaded evanescent cavities for widely tunable high-Q filters," in IEEE MTT-S Int. Microwave Symp. Dig., Honolulu, Hawaii USA, June 2007, pp. 2133–2136.

[22] J. Brank, J. Yao, M. Eberly, A. Malczewski, K. Varian, and C. L. Goldsmith, "RF MEMS-based tunable filters," Int. J. RF Microwave CAE, vol. 11, pp. 276–284, Sept. 2001.

[23] B. Lakshminarayanan and T. Weller, "Tunable bandpass filter using distributed MEMS transmission lines," in IEEE MTT-S Int. Microwave Symp. Dig., Philadelphia, PA USA, June 2003, pp. 1789–1792.

[24] R. M. Young, J. D. Adam, C. R. Vale, T. T. Braggins, S. V. Krishnaswamy, C. E. Milton, D. W. Bever, L. G. Chorosinski, L.-S. Chen, D. E. Crockett, C. B. Freidhoff, S. H. Talisa, E. Capelle, R. Tranchini, J. R. Fende, J. M. Lorthioir, and A. R. Tories, "Low-loss bandpass RF filter using MEMS capacitance switches to achieve a one-octave tuning range and independently variable bandwidth," in IEEE MTT-S International Microwave Symposium Digest, Philadelphia, PA, June 2003, pp. 1781–1784.

[25] A. Abbaspour-Tamijani, L. Dussopt, and G. M. Rebeiz, "Miniature and tunable filters using MEMS capacitors," IEEE Trans. Microwave Theory & Tech., vol. 51, no. 7, pp. 1878–1885, July 2003.

[26] C. D. Nordquist, A. Muyshondt, M. V. Pack, P. S. Finnegan, C. W. Dyck, I. C. Reines, G. M. Kraus, T. A. Plut, G. R. Sloan, C. L. Goldsmith, and C. T. Sullivan, "An x- band to Ku-band RF MEMS switched coplanar strip filter," IEEE Microw. Wireless Compon. Lett., vol. 14, no. 9, pp. 425–427, Sept. 2004.

[27] B. Pillans, A. Malczewski, R. Allison, and J. Brank, "6-15 GHz RF MEMS tunable filters," in IEEE MTT-S Int. Microwave Symp. Dig., Long Beach, CA USA, June 2005, pp. 919–922.

[28] C. L. Goldsmith, Z. Yao, S. Eshelman, and D. Denniston, "Performance of low-loss RF MEMS capacitive switches," IEEE Microw. Guided Wave. Lett., vol. 11, no. 3, pp. 106–108, Mar. 2001.